UNIVERSITY OF SOUTHAMPTON

FACULTY OF NATURAL AND ENVIRONMENTAL SCIENCES

Chemistry

The Stepwise Modification of Carbon Electrodes Using Electrochemical and Solid Phase Synthesis for Covalent Binding of Proteins

by

Emma Jane Wright

Thesis for the degree of Doctor of Philosophy

January_2014

UNIVERSITY OF SOUTHAMPTON

ABSTRACT

FACULTY OF NATURAL AND ENVIRONMENTAL SCIENCES

Chemistry

Thesis for the degree of Doctor of Philosophy

THE STEPWISE MODIFICATION OF CARBON ELECTRODES USING ELECTROCHEMICAL AND SOLID PHASE SYNTHESIS FOR COVALENT BINDING OF PROTEINS

Emma Jane Wright

The chemical and electrochemical functionalisation of surfaces is of great importance in the construction of electrodes modified with biomolecules. Besides fundamental investigations, research is driven by numerous important applications including biosensing, biofuel cells or molecular electronics.

While significant developments have been made some key problems remain, particularly the stability, orientation and electrical communication of the immobilised biomolecule with the conducting support. In order to address these issues a modular approach to electrode modification has been developed, allowing simple variation of the key elements of the tether (Figure 1)

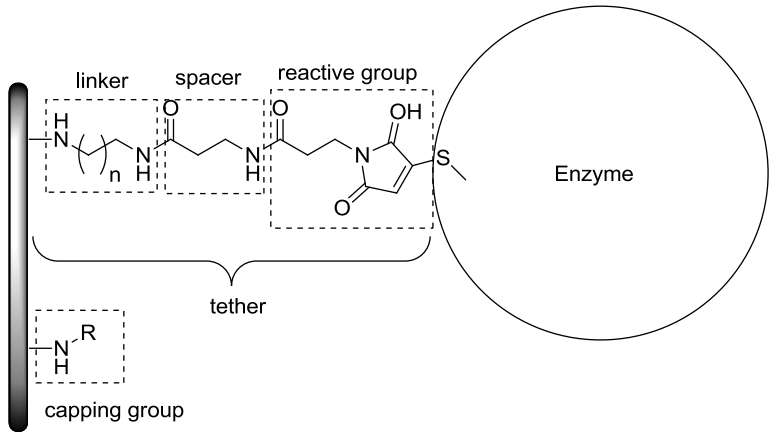

Figure 1 – Modular approach to electrode modification

After electrochemical attachment of a mono-Boc-protected diamine linker, deprotection followed by amide coupling can be used to introduce a spacer to control the length of the structure. A reactive group may then be introduced and the enzyme coupled.

In this work the reactive group chosen was maleimide. A maleimide group will react 1000 times faster with a thiol than an amine at neutral pH, allowing selective attachment to a free cysteine residue in a biomolecule.

The initial modification of the electrode surface with linker has been modified to create a partial coverage of the linker on the electrode surface The oxidation of a mixture of amines, using a Boc-protected diamine and a capping group allowed the Boc amine to be spaced out on the surface for optimal enzyme attachment.

The developed methods have been used to successfully couple Cytochrome C and two engineered variants of glucose dehydrogenase from *Glomerella cingulate* to modified electrodes.

Contents

List of tables

List of figures

DECLARATION OF AUTHORSHIP

I, Emma Jane Wright declare that the thesis entitled

"The Stepwise Modification of Carbon Electrodes Using Electrochemical and Solid Phase Synthesis for Covalent Binding of Proteins"

and the work presented in the thesis are both my own, and have been generated by me as the result of my own original research. I confirm that:

- this work was done wholly or mainly while in candidature for a research degree at this University;
- where any part of this thesis has previously been submitted for a degree or any other qualification at this University or any other institution, this has been clearly stated;
- where I have consulted the published work of others, this is always clearly attributed;
- where I have quoted from the work of others, the source is always given. With the exception of such quotations, this thesis is entirely my own work;
- I have acknowledged all main sources of help;
- where the thesis is based on work done by myself jointly with others, I have made clear exactly what was done by others and what I have contributed myself;
- none of this work has been published before submission, or [delete as appropriate] parts of this work have been published as: [please list references]

Signed: ……..

Date:……

Acknowledgements

There are a large number of people who I wish to thank for help, and without which it would not be possible for me to have got this far.

Firstly I would like to thank my supervisors, Jeremy and Phil for their support, advice and knowledge.

Thanks also go to Maciek, who had to put up with a lot of my frustration when things were just not working. Also for the great introduction to electrochemistry, a very different lab and helping with so many questions. Thanks also go to Sally for her help on the other half of my project, the synthesis side.

I would also like to thank other Kilburn group members for their support and technical assistance, Aleks for her project knowledge and help with my first electrodes, Will and Biniam for their organic and lab help. Thanks to Boris for being the other remaining student in Jeremy's lab and all the help! Thanks to all for the 'coffee' (tea for me), sometimes a break was just what I needed! Of course thanks to all other Kilburn group members I had the pleasure of meeting and working with. Thanks also to the Bartlett group, past and present, in particular Thomas, David, Rob and Charlie who have all put up with many a question and kept me company in the lab.

Another set of people to thank are my research consortium, who gave me so much knowledge I would not have gained otherwise. It was an amazing project to be a part of and I hope that one day we will see the long term goals realised.

Thanks to my students Beth and Thomas who helped me get things done and sneakily gave me teaching experience too. Thanks also to the level 5 teaching lab staff and students.

Another lot of thanks go to the many required services, without which I wouldn't have had the equipment or data to do what I did! Thanks to stores, Karl, Clive and Keith – not only did I get what I needed but often was a little entertained too. Thanks to Neil in NMR and John and Julie (and Chrissie) in Mass Spec for help getting the right spectra! I would also like to thank to Sally Dady for always helping me sort out the forms and papers.

On a more personal note I would like to thank my family, my parents and sisters for their endless support. Thanks for listening and telling me I can do it, I know I must have been quite a pain at times.

Last, but definitely not least I would like to thank the friends I have made (Jo, Chrissie, Laura, Sophie and Becky) for so, so much help. Thanks for the support, advice and friendship – not sure what I would have done without it.

Abbreviations

Ag/AgCl	Silver/silver chloride reference electrode
Boc-EDA	*N*-Boc-ethylenediamine
$CDCl_3$	Deuterated chloroform
CV	Cyclic voltammetry
DCIP	2,6-dichlorophenolindophenol
DCM	dichloromethane
DET	Direct electron transfer
DMF	N, N-dimethylformamide
$DMSO_{d6}$	deuterated dimethylsulphoxide
EDA	1,2-ethylenediamine
FAD	Flavin adenine dinucleotide
GC	glassy carbon
GDH	Glucose dehydrogenase
GOX	Glucose oxidase
HBTU	O-(benzotriazol-1-yl)-N,N,N',N'- tetramethylammonium hexafluorophosphate
HDA	1,6-hexanediamine
HOPG	highly oriented pyrolytic graphite
HRMS	High resolution mass spectrometry
LRMS	Low resolution mass spectrometry
mCPBA	*meta*chloroperoxybenzoic acid
MET	Mediated electron transfer
NTA	Nitrilotriacetic acid
PDB	Protein data bank
SAM	Self-Assembled monolayer
SCE	Saturated calomel reference electrode
TBATFB	*tert*butyl ammonium tetrafluoroborate salt
TEATFB	*Tetra*ethyl ammonium tetrafluoroborate salt
XPS	X-Ray Photoelectron spectroscopy

1. Introduction

1.1 Modification of electrode surfaces

The functionalization of electrode surfaces is an important area of chemistry as it can both provide insight into mechanisms of electron transfer[1] and surfaces of interest for a range of applications including catalysis[2]. Over 30 years ago Murray stated that this area of research would lead to surfaces with unusual analytical, chemical, catalytic and optical properties[3]. Since then modified electrodes have been used for sensors[4] and molecular and bio electronics[5].
In order to fulfil the desire for tailor-made electrodes, designed with properties for a particular use, new methods of electrode modification[6] with the ability to create stable, selective and reproducible electrodes were required. In order to achieve this kind of modification the methods developed must allow a great degree of control, with the physical and (electro)chemical properties of the target molecule to be attached retained once it is on the surface.

1.2 Aim of the project

The aim of the project is to develop surface modification chemistry to allow the modification of electrodes with functional groups to enable the attachment of enzymes to the electrode. The attachment of enzymes to electrodes is of use in many areas including sensors[4] and biofuel cells[7].

Although there have already been many developments in this area of chemistry some key problems remain. The enzyme is often only randomly distributed on the surface of the electrode and not orientated correctly for direct electron transfer, in addition to this there is poor communication between the electrode and bioelement, leading to poor efficiency[8]. In order to address these issues there are several important considerations to take into account; key variables include the choice of electrode and bioelement, the distance and the method of linkage between the two. In addition to this it is important to develop chemistry which is adaptable, allowing simple variation of the key elements to form comparable surfaces.

Therefore this project aims to use a controlled and modular approach to electrode modification (Figure 2).

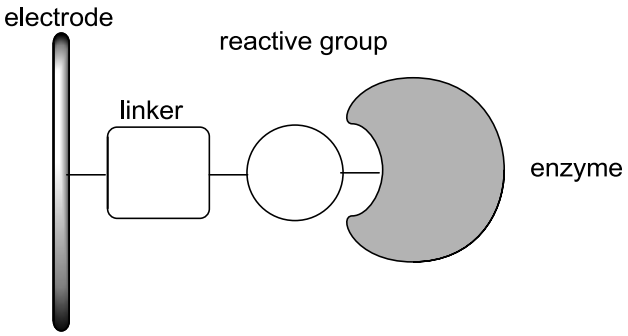

Figure 2 – Modular approach to enzyme modification

The electrode surface is first modified with a linker; a reactive group can then be coupled to the linker which can then be reacted with the enzyme. By variation of the different elements the effect on the coverage and activity of the enzyme can be investigated.

1.3 Chemically modified electrodes

The modification of electrodes may be executed by two main means: chemisorption and physisorption. Physisorption is a much simpler interaction; a weak non-specific physical force is used to hold the substrate onto the surface. Spontaneous physisorption is fairly common, for example physisorption of large aromatic adsorbates such as porphyrin onto carbon for use in oxygen reduction[9]. On the other hand chemisorption uses strong chemical forces to hold a substrate onto the surface, resulting in a firm attachment to the surface. While both chemisorption and physisorption result in modified electrodes the strength of the interaction between the adsorbate and surface is varied, with physisorption a much weaker interaction which may be removed relatively easily from the surface, chemisorption is a strong interaction and often used to modify the behaviour of the electrode surface[10].

The first chemically modified electrodes were developed in 1973 when Hubbard adsorbed olefins on platinum[1]. The first goal was to investigate electron transfer reactions; this idea prompted the development and growth of a new field of electrochemistry – chemically modified electrodes.

The first examples of modification were based on chemisorption, electron density was shared between the surface and target molecule. Although these methods had been used before, Hubbard was the first to state a purpose for

the modification. Aromatic systems were later adsorbed onto the surface of carbon electrodes by Anson[11] using π stacking interactions. Using this method it was assumed the greatest possible coverage would be a monolayer, as a contact between the adsorbed molecule and surface is required. In addition to this the adsorbed molecules slowly desorb from the surface and leach into the solution.

Self-assembled monolayers (SAMs) were the next development, over 20 years ago, formed by immersing a solid substrate into a solution which would spontaneously attach to the surface to form a monolayer[12]. This simple procedure allowed a high degree of control over the surface composition allowing a variety of applications. It was found that when a gold electrode was immersed in a dilute solution of thiol a densely packed monolayer of the thiol formed on the surface[13] (Figure 3). A number of reviews have since been completed on the topic of SAMs[12, 14].

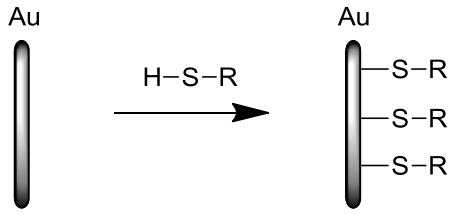

Figure 3 – Formation of a SAM on gold

It has been demonstrated that in addition to using gold as a solid substrate, monolayers of organosulphur species will form on other transition metals such as silver[15] , copper[15b, 15c, 16], iron[17] and platinum[18]. However gold is favoured as it does not have a stable surface oxide[19] and only very slowly becomes contaminated.

Although the formation is simple the layer formed has been shown to have limited stability[20] as the bonds between gold and sulphur are susceptible to cleavage and rearrangement on the surface[19]. In addition to this the long chains required to give a dense monolayer decrease the rate of electron transfer and electrochemical signal.

The second form of modification was developed in the mid-late 1970s, the formation of a covalent bond between a functional group on the surface and

the target molecule was developed. Murray found that silanes would react with hydroxide groups on the surface of electrodes such as SnO_2, RuO_2, TiO_2, Pt and Au[21].

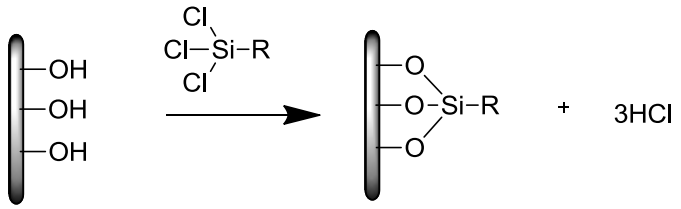

Figure 4 – reaction of trichlorosilane with hydroxide groups on the surface.

Though three bonds are shown it is unlikely that they all bond, if water is present then the silane hydrolises and forms a polymer which attaches to the surface, allowing the formation of a multi-layered modification.

Another method of covalent modification was developed by Miller, who used thionyl chloride to activate surface carboxylic acid functionalities and then coupled amines with these[2]. This method was also used later to create multilayers by adding monolayers in sequence[22].

Polymer films have also been used as a method of modification since 1978 when both Bard [23] and Miller [24] developed the chemistry to do this. Since then it has become widely used since it provides a simple method to modify the surface with some control over the thickness and the ability to tailor the properties and functionality by preparation of polymers with different composition. A number of methods have been developed to attach the polymer to the electrode surface [25] including dipping, drop casting, electrochemical deposition and spin coating. Nafion films in particular have been widely used[26].

1.4 Modification of Carbon surfaces

The use of carbon as an electrode material later became very popular due to the low cost, wide potential window and suitability for use in both aqueous and organic solvents. Carbon materials of note include graphite, carbon fibres, glassy carbon and carbon black[27].

Electrochemical modification of carbon surfaces has been widely reported since the 1990s, although there are a range of methods the majority are based on the formation of radicals in solution which then couple onto the surface. A review by A. Downard in 2000[28] reported the modification of carbon electrodes by 4 key methods; the oxidation of primary and secondary amines, the

reduction of diazonium salts, the oxidation of arylacetates and oxidation in the presence of alcohols. The methods reported all formed a robust linkage to the surface, allowing the surface to be functionalized with a range of functional groups available for further reactions.

1.4.1 Oxidation of amines

Barbier *et al.* first reported the electrochemical oxidation of diamines onto carbon fibre surfaces for use in the aerospace industry[29]. The oxidation of amines onto the surface (Figure 5) was developed to introduce more variation to the surface compared to previous methods which were largely limited to the introduction of oxygen functionalities by oxidation. Diamines were used to allow one amine to bind to the surface and another to be free for further chemical reaction, forming a link to the surface. Though the diamines were useful to allow further reactions it was found that some of the diamines were attached to the surface by both amines, forming a 'bridge' structure and preventing further reactions.

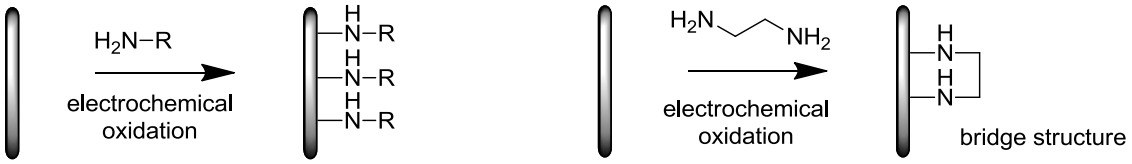

Figure 5 – Electrochemical oxidation of amines

Upon electrochemical oxidation by cyclic voltammetry a single oxidation peak was observed, with no reduction wave, suggesting the amine had undergone a chemical reaction. The second cycle of the cyclic voltammetry showed that the surface had been passivated by ethylenediamine. XPS (X-Ray Photoelectron Spectroscopy) confirmed the attachment of EDA (ethylenediamine) to the carbon fibres, only on fibres which had been oxidised in EDA, not those immersed in EDA without cyclic voltammetry[29].

The method was later used on GC electrodes[30], the immobilisation primary, secondary and tertiary amines was investigated and the direct coupling of dopamine or biotin to the surface. The stability of the surfaces formed were also tested by cycling (100 cycles, 0.2 to 0.8 V) prepared electrodes in perchloric acid (0.1 M), butylamine modified electrode had ~10 % decrease in

coverage and a dopamine modified electrode had ~ 23 % decrease in coverage. The greatest coverage was obtained from the oxidation of primary amines, secondary amines did bond to the surface, however no oxidation was observed for tertiary amines and this was attributed to steric hindrance.

The mechanism of the reaction was investigated in 2004 by Adenier *et al.*[31] who oxidised primary, secondary and tertiary amines. They found that following the formation of the cation radical a proton was lost before attachment to the surface. The primary amine radical cation was found to have a lifetime shorter than 0.2 ms, due to instability.

1.4.2 Reduction of diazonium salts

The first modification of carbon surfaces by the reduction of diazonium salts was reported in 1992 by Pinson *et al.*[32]. The reduction method used was reported to be non-corrosive and a good alternative to the harsh oxidative conditions previously used to form oxygen functionalities on the surface. The electrochemical reduction of aromatic diazonium salts has since been shown to be a general and versatile method for the modification of carbon surfaces[33]. The layer formed has been demonstrated to be strongly bound to the surface and mechanical abrasion is required to remove the attached compounds, suggesting the formation of a covalent bond[34]. The mechanism of the reaction was proposed as the attachment of the aryl radical formed from the 1 electron reduction of the diazonium salt[32] (Figure 6).

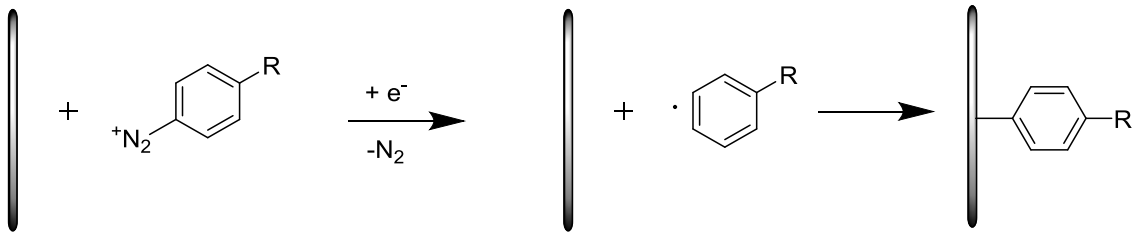

Figure 6 – Proposed method of diazonium salt attachment.

The use of diazonium salts is of particular interest not only due to the range of diazonium salts available, but also because it can be used on a range of electrode materials. It has been used to modify, a range of carbon surfaces

(including GC[33, 35], HOPG[36], carbon fibres[35] and carbon nanotubes[37]), Au, silicon[36a] and metals[38].

In addition to the simple synthetic methods to prepare diazonium salts they have been prepared *in situ* from the corresponding amine to react directly with the electrode of interest[38c]. The generation of the diazonium salt *in situ* removed the need to isolate and purify the synthesized salt, the corresponding amine was dissolved in a solution of $NaNO_2$ in aqueous HCl, in the electrochemical cell[39]. The electrochemistry of diazonium salts prepared *in situ* is very similar to the corresponding isolated and purified diazonium salts[40], however the layers prepared from aqueous solution were determined to be thinner by cyclic voltammetry in $[Fe(CN)_6]^{3-/4-}$.

Though diazonium salts are useful for the functionalization of surfaces, there are limitations in the control of layer thickness. The layer formed from attachment of the diazonium is not always a monolayer thickness and though desirable in some applications[36b] the control of surface structure to a monolayer or less is desirable in the preparation of bioelectrodes[38b].

1.4.3 Electrochemical and Solid Phase Synthesis

Previous work in Southampton developed a procedure for the attachment of mono-Boc protected diamines to GC electrodes by electrochemical oxidation of the free amine. The Boc group was then removed to allow further modification of the electrode by solid phase synthesis. A range of 7 linkers were covalently attached to GC electrodes which were then reacted with anthraquinone or nitrobenzene.

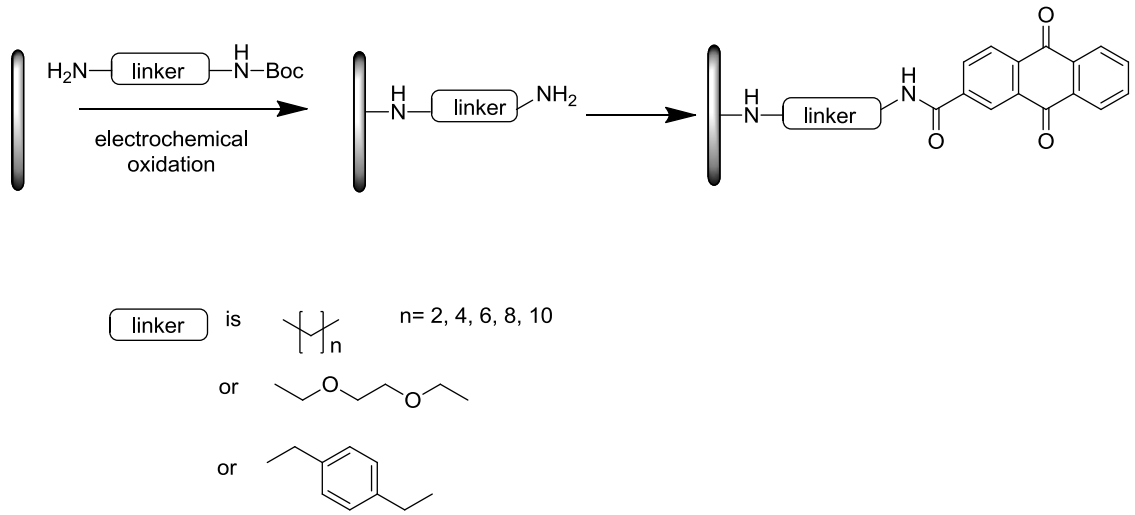

Figure 7 – Previous work by Bartlett *et al.* [41].

The surface coverage of anthraquinone was found to decrease as linker length increased, however for nitrobenzene there was no significant difference in surface coverage[41]. The synthetic procedure developed allowed the attachment of a range of molecules simply, without the need for the synthesis of unstable diazonium salts. The use of mono-Boc protected diamines prevented the formation of bridge or multilayer structures on the surface, usually formed when using diamines, allowing much greater control of the modification. Using the same methods the electrodes were modified with 'spacers' composed of aliphatic and aromatic small organic molecules. Following coupling of the spacers anthraquinone was coupled and the electrode properties were investigated[42]. The long term stability of the anthraquinone modified electrodes was also found to be good with only a 23% gradual decline in coverage over 20 days. In work following on from this, electrodes were modified with 2 or more functionalities using different coupling conditions. The functionalities were added both sequentially and simultaneously[43]. Anthraquinone-modified electrodes prepared using these methods have been used to bind laccase from *Trametes hirsuta*[44]. The methods have also been used to prepare electrodes for the oxidation of NADH using dihydroxybenzene[45] and metal complexes[46] as mediators.

1.5 Bioelectrochemistry

The future of applied electrochemistry was said to be dependent on the growth of photo- and bioelectrochemistry back in 1990[6]. Enzyme-modified electrodes have become of great importance in modern society and are the key elements of both biofuel cells and biosensors[47]. Enzymes are powerful catalysts and can convert 10,000 substrate molecules per second[48], in addition they are also able to respond to very small overpotentials which makes them highly efficient electrocatalysts[49] .

1.5.1 Biofuel Cells

Biofuel cells have been an attractive concept for a number of years and articles on the subject date as far back as the 1980s, however, in more recent years, research and publications in this area have increased dramatically. In the modern world a great number of devices are becoming smaller and with that comes a desire to create small power sources. There is vast research in this field, aiming to commercialise a microfuel cell[8f].

The development of biofuel cells able to produce current comparable to that of traditional fuel cells in ambient conditions and the immobilisation of enzymes on electrodes has brought about interest in their development for implantable devices. Enzymes immobilised on an electrode surface are able to catalyse reactions such as the reduction of oxygen to water[50]. However it is important to consider the linkage carefully as it is possible that during immobilisation the kinetic performance may be hindered or that the enzyme will be denatured[51].

Enzyme based biofuel cells enable the generation of electrical power from biomass or biofuel substrates meaning that biological fluids may be used as a fuel source in implantable medical devices. The glucose and oxygen content in the body tissues could be sufficient enough to power small devices such as hearing aids, pacemakers or miniature pumps. It is also possible to power biosensor/transmitter devices, allowing alerts of glucose concentration or infection following operations[8c].

While traditional metal catalysts are often poisoned by physiological conditions, enzymes have evolved to survive and function in these conditions,

making them ideal for use in implantable biofuel cells. In addition to this, the cell design is simplified and compacted due to the selective nature of enzymes as there is no need to separate the fuel and oxidants of the fuel cell[8c].

In order to produce such devices, there are many important considerations including the choice of electrode material, enzyme and connection between the two. The research in this area requires new, reproducible methods of electrode modification to allow control over the surface modification. Without these methods there is limited scope for successful attachment of enzymes which remain stable and active on the surface of the electrode.

1.5.2 Biosensors

Biosensors are a method of detecting pathogens and other metabolites which may be important to human health. They do not require reagents and are therefore a simple method to use[52]. Biosensor requirements include the immobilization and retention of an active biomolecule on the surface. In addition the response must be reproducible and resist interference and fouling in complex solutions.

Biosensors are of particular interest in the detection and monitoring of blood glucose levels. Approximately 5% of the world's population are diabetic and require blood glucose monitoring and consequently blood glucose assays are one of the most common assays[53].

Initial research into biosensors began in 1970s-80s when glucose biosensors emerged. The first generation of electrochemical glucose biosensors started with the use of GOx (glucose oxidase) and was reliant on the detection of the produced hydrogen peroxide[53]. The main drawback of this method was the high potential required for the oxidation of hydrogen peroxide at ~600 mV vs SCE at Pt electrodes. The use of such a high potential meant that a number of other compounds, including ascorbate and urate, were also oxidized.

The next generation of biosensors involved the use of redox mediators such as derivatives of ferrocene and quinones, these artificial compounds allowed fast electron transfer between the electrode and enzyme, acting as an alternative electron acceptor to oxygen. As the potential which the mediators were

oxidized at was lower than oxygen there was less interference and therefore the biosensors were more efficient. Simple and inexpensive sensors were prepared by a simple mixture of either GOx or GDH (glucose dehydrogenase), mediator and carbon paste[53].

There is now desire for a third generation of biosensors, based on the direct electron transfer between the enzyme and electrode, disposing of the need for a mediator.

As biosensors become more advanced there is a desire for greater control over the composition of the surface. SAMs are a favoured surface modification method as they provide the closest thing to a molecular level of control of the surface composition, allowing the best control over interaction with biomolecules[54].

1.6 Immobilisation of bioelements

There are a number of important considerations in the immbilisation of bioelements on electrode surfaces. These include electrode material, binding methods and materials, enzyme variant and, if desired, an electron transfer mediator. The immobilisation step is considered one of the key steps in determining the effectiveness of enzyme modified electrodes[47]. In the case of proteins the active site must be orientated towards the electrode surface, in order to enable electron transfer. In addition the protein must not denature in contact with the electrode, or the activity would be lost.

A number of methods have been used to bind enzymes to electrode surfaces to date[47], with the methods being split into either covalent or non-covalent interactions.

1.6.1 Non Covalent Immobilisation

The non-covalent attachment of proteins is reliant upon the use of interactions such as electrostatic, hydrophobic or hydrophilic interactions between the protein and the surface[52]. The simplest method is adsorption of the desired enzyme onto the surface of the conducting support. Disposable biosensors can be made by screen printing a mixture of carbon powder and enzyme in a solution of binder[55].

The use of positively charged ammonium ions and negatively charged carboxylate groups is an alternative, and has been used for immobilization of proteins such as Cytochrome C[56]. Though the method is similar to natural protein-protein interactions and rarely deactivates the protein, it is dependent on the pH of solutions used for immobilization and testing, resulting in very limited scope for variation.

Enzymes may also be entrapped into porous materials, such as polymers and membranes[57] with the adsorption is often aided by electrostatic interactions. Though the immobilization method is simple the enzyme is only weakly bound and liable to desorb from the surface during testing. An alternative is the entrapping of enzyme into an electrodeposited polymer layer[55, 58], which may be pre-deposited onto the electrode or grown around an enzyme on the surface.

The orientation of proteins is very important in bioelectrochemistry, particularly the orientation of the protein, distance from the surface and access to the active site. Without appropriate orientation electron transfer between the protein and electrode would not occur or would be slow, similarly the distance and access to the active site may also prevent electron transfer. Therefore the modification of proteins to allow site specific orientation is desirable. One method of ensuring the correct orientation of proteins is the use of histidine tags, which are commonly used to immobilise proteins by chelating to metal ions such as Ni^{2+}, Cu^{2+}, Zn^{2+}, Co^{2+}. The metal ion can be immobilized on the electrode surface as a complex with NTA (nitrilotriaceticacid)[59] introduced by a variety of means.

Other interactions explored include the avidin-biotin interaction which has frequently been used[52]. Avidin and similar forms streptavidin and neutravidin are glycoproteins and biotin is a vitamin found in all living cells. The avidin is tetrameric and therefore able to bind up to 4 biotin molecules; the bond is formed rapidly and is one of the strongest non-covalent interactions possible.

1.6.2 Covalent attachment

The covalent attachment of proteins to electrode surfaces is made possible by the reaction between groups on the protein surface and an electrode functionalised with reactive groups.

The reaction between carboxylic acids and amines is commonly used for the immobilisation of proteins on an electrode surface[55]. The procedure usually uses an amine-functionalised surface to react with aspartic or glutamic acid side chains on the protein surface. Carbodiimide reagents can be used to increase the reactivity of the carboxyl groups, though the reagents are susceptible to hydrolysis and may cause crosslinking between groups on the protein surface[60].

A number of groups have used polymers with varying functional groups to bind to the enzyme. The polymer containing amine groups was coated on the electrode surface and used to couple to carboxylic acids on the enzyme[61]. The polymer used could also incorporate an electron transfer mediator into the structure. An alternative to the use of polymers is the use of a SAM to introduce the desired functional groups to bind the enzyme. As SAMS are often well-defined layers they provide a good basis for formation of a bioelectrode, with control over the orientation and accessibility of the biomolecule[52].

There is a vast array of alternative coupling methods that have been used to couple proteins to electrodes including; nucleophilic substitution, click chemistry, Diels Alder reactions and palladium-catalysed cross-coupling [52].

Although a lot of research has been done and is ongoing in this area, there are still limitations, including possible side reactions, or the use of non-targeted approaches. For example the use of amino acid side chains for coupling is not generally specific; there is often more than one amino acid in the protein which would react with the functionalized electrode. The result is that the protein may be incorrectly orientated on the surface, which can cause problems with electron transfer. In addition the active site may become blocked by the attachment or the structure may be changed by the attachment to the surface. For this reason it is also important to consider the use of engineered enzymes with specific target groups to allow a more targeted approach.

2. Model Synthesis

2.1 Aims of the work

The main aim of this part of the work was to build up a structure on the electrode surface to enable the coupling of enzymes onto the electrode. Depending on the enzyme used the bioelectrode synthesised could then have a range of applications including as a biosensor or biofuel cell.

In order to create an optimal surface we set out to achieve a great deal of control over the surface composition. We also wanted to be able to vary the surface in order to find an electrode that functions well for its given purpose. Therefore a key aspect of this work was not only to attach the enzyme to the surface but also to create a surface with a number of variable elements which could be achieved by building up the structure of the surface in a stepwise manner, allowing the key elements of the construction to be simply varied (Figure 8).

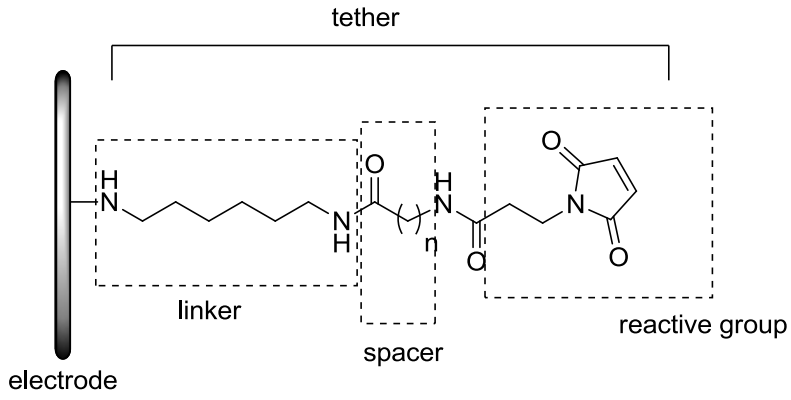

Figure 8 – Surface structure, key elements of the composition

Our work builds on previous work by Bartlett, Kilburn *et al*, where methods have been developed to create an amine functionalised surface using electrochemical oxidation of diamine linkers[41-43], followed by the use of solid phase synthesis to couple various redox groups with carboxylic acid functionalities. We planned to use this method as a basis for the initial functionalization of the surface, followed by coupling of molecules to allow further adaptation of the structure on the surface. The key elements in this

case are the electrode, linker, spacer and reactive group, each of which can be modified to introduce variation onto the surface Figure 8.

Our main focus is on using carbon as the electrode material is carbon as it is a relatively cheap and widely available material which has been widely used in disposable biosensors. However in addition to commonly used glassy carbon other types of carbon could be investigated such as HOPG (highly ordered pyrolitic graphite) edge and basal plane and carbon nanotubes.

The linker is used to create a link between the electrode surface and the rest of the tether, and a mono-Boc protected diamine was used for this purpose. Electrochemical oxidation of the amine enables the formation of a bond to the surface (Figure 9), an amine functionalised surface is then created on removal of the Boc group.

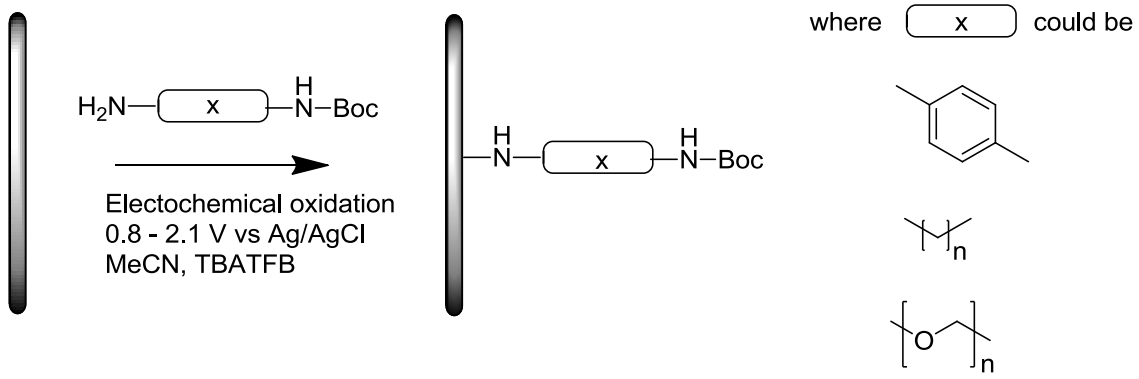

Figure 9 – Electrochemical oxidation of amine linker

The middle part of the linker used could be an alkyl chain of varying length or could incorporate other functional groups such as aromatic rings or ethers (Figure 9).

A spacer (Figure 8) could then be coupled to the linker using amide chemistry. Simple alkyl chains could be used to increase the length of tether, or other functionalities could be used.

Finally a reactive group (Figure 8) can then be coupled to the spacer (or linker if a spacer is not used) to allow coupling of the enzyme to the tether. In our work the reactive group chosen was a maleimide which has been widely used to bind biomolecules[62] in electrochemistry[63] and as a label for proteins in biochemistry[64]. In addition maleimide reacts selectively with sulfhydryl groups

at pH 7[60], allowing targeted attachment to cysteine groups in proteins in the presence of more abundant lysine residues.

Using this building block approach and simple variation of the composition the effect on protein attachment could be monitored and optimised.

2.2 Solution based synthesis

Previously in our group the attachment of enzymes using maleimide had been attempted as shown in Scheme 1. An amine modified surface was reacted with 3-maleimido propionic acid (**1**).

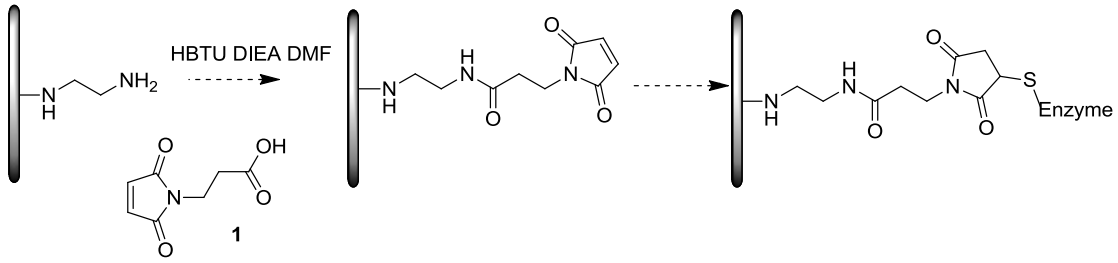

Scheme 1 – Direct attachment of maleimide on the surface

This method appeared to be unsuccessful, and it was not clear which stage of the synthesis had failed. Therefore a new approach was taken in order to avoid possible side reactions during the coupling. Instead of coupling **1** directly the maleimide was masked using thiophenol to create a thioether, which could later be eliminated (Scheme 2). The preparation of maleimide from thioethers has been used in organic synthesis for many years[65]. The thioether can be oxidised using *meta*chloroperoxybenzoic acid (*m*CPBA)[65] and the sulphoxide can then be eliminated by heating to reform the double bond of the maleimide.

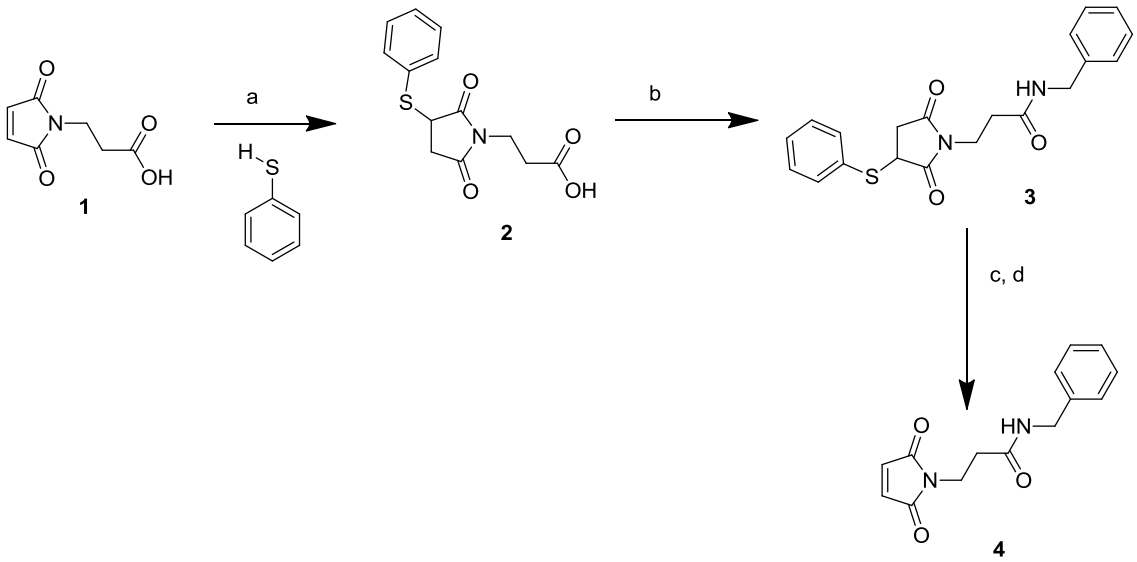

Scheme 2 - Solution model of preparing maleimide on the surface. a) acetonitrile, water b) HBTU, DIEA, DMF 16 h c) mCPBA 0°C 1 hour, d) toluene, reflux 2 h

As this was a multistep reaction which had not been tested on the surface, it was decided to first follow the course of the reaction in solution. Initially the maleimide **1** was reacted with thiolphenol to give the thioether **2** in a quantative yield. Benzylamine was used as a simple amine model for the amine functionalized surface, and coupled with **2** to give **3** in 54% yield**.** The thioether was then eliminated by oxidation followed by heating to give **4** in 49% yield. Although these yields are not high the chemistry was to be transferred onto the electrode surface where the conditions would be different so it would need to be optimized again anyway. When the amide coupling is carried out on the surface the carboxylic acid is usually in a large excess, however a 1:1 ratio was used in solution, so the reaction would be pushed to completion on the surface.

2.3 Model on the surface

Once the reactions had been successfully completed in solution the chemistry needed to be tested on the electrode surface, where the process needed to be refined. The electrode was modified first with a linker. Boc-ethylenediamine (Boc-EDA) was chosen as it had previously given the greatest surface coverage out of a range of linkers investigated on glassy carbon electrodes, amine linkers were electrochemically oxidised onto the surface and coupled with

anthraquinone [41]. Following the addition of Boc-EDA to the surface the amine was deprotected and coupled with **2**, the thioether was then eliminated using the same method as in solution (Scheme 3).

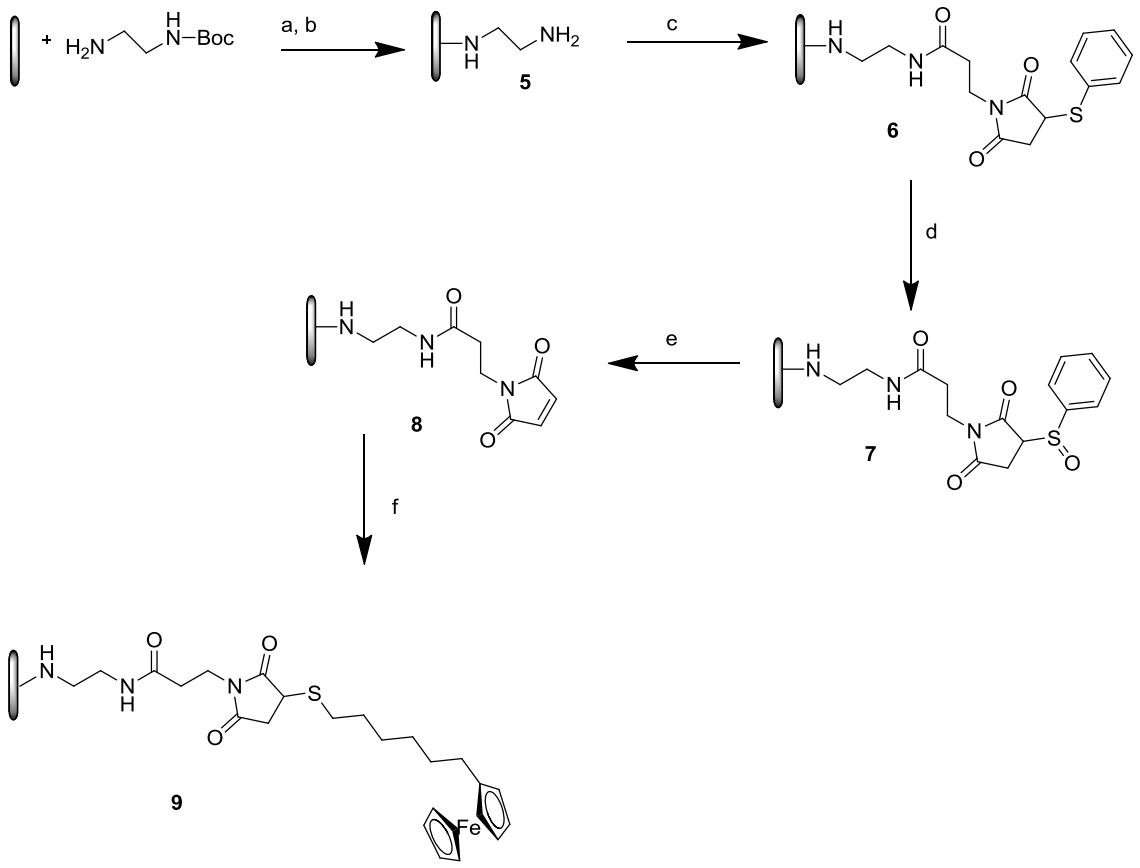

Scheme 3 – model on the surface. a) 0.8 – 2.1V vs Ag/AgCl, 5 cycles b) 4 M HCl in dioxane, 1 h c) **2,** HBTU, DIEA, DMF, 16 h d) mCPBA in acetonitrile, 0°C, 1 h, e) Δ f) ferrocenyl hexanethiol in acetonitrile, 2.5 hours.

The first modification of the electrode surface was completed by oxidation of Boc-EDA onto the surface using cyclic voltammetry (CV). Glassy carbon (GC) electrodes were polished on wet 1200 grade silicon carbide paper then wet 5 µm alumina lapping film then 1 µm and 0.3 µm alumina slurries before washing with water and drying in a stream of argon. Electrodes were prepared in duplicate immersed in a degassed solution of Boc-EDA in acetonitrile with electrolyte and the potential was cycled from 0.8 to 2.1 V vs Ag/AgCl (Figure 10) at 50 mV s^{-1} for 5 cycles. The irreversible attachment was almost complete after the first cycle, after which the oxidation peak had almost disappeared and

after 5 cycles the current had drastically decreased which suggested that the surface had been blocked with the Boc-amine.

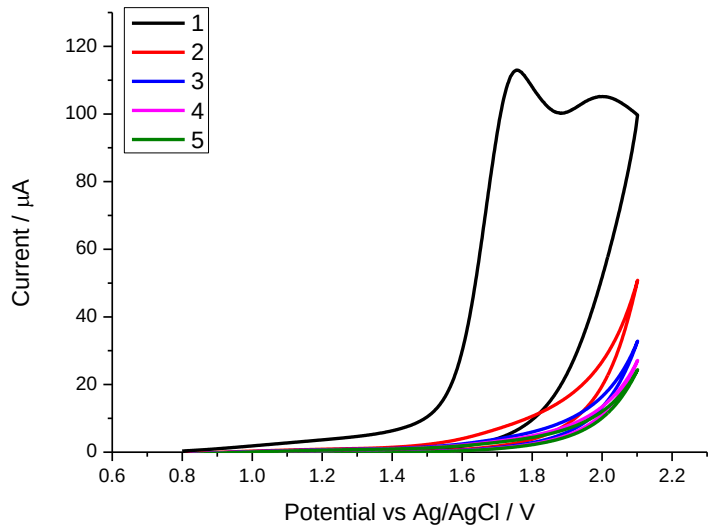

Figure 10 - Boc-EDA attachment to electrode, preparation of 5, CV at 50 mV/s in acetonitrile with 150 mM TBATFB and 10 mM Boc-EDA, electrode area 0.0707 cm^2

After the attachment of Boc-EDA the Boc group was removed with 4M HCl in dioxane to give an amine functionalized surface. The thioether (**2**) was coupled and oxidized with mCPBA to the sulphoxide and then heated to eliminate the sulphoxide, ferrocene hexane thiol was then coupled as a simple thiol model for an enzyme. As none of the tether intermediates (**5-8,** Scheme 3) were electrochemically active it was hard to monitor the progress of the synthesis until the last stage when the ferrocene, which is redox active, was attached.

Once the ferrocene electrodes had been prepared they were evaluated by CV (Figure 11) in acetonitrile with TBATFB as an electrolyte. Electrodes were cycled from 0 to 1.1 V vs Ag/AgCl for an initial 10 cycles at 100 mV s^{-1}. Initially a very large peak was observed at 0.74 V vs Ag/AgCl, the current then significantly decreased and became constant.

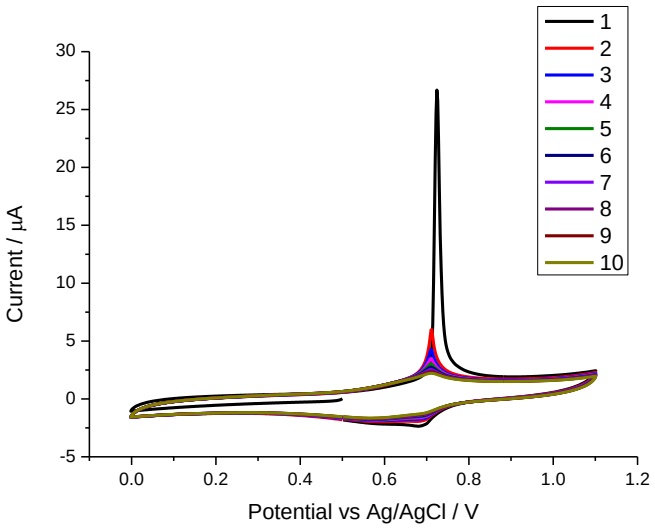

Figure 11 – CV of **9** (Scheme 3), CV at 100 mV/s in acetonitrile with 100 mM TBATFB first 10 cycles shown, electrode area 0.0707 cm^2

This initially large current, not seen in the reverse scan appears to be loosely bound ferrocene which desorbs from the surface quickly. On closer inspection the peaks also appear broad and shouldered, suggesting the presence of different ferrocene species, also suggesting non-specific adsorption to be a factor in the initial large currents. A control sample, **8** was prepared and tested without ferrocene and no peaks were seen by CV.

The synthesis (Scheme 3) was repeated with an increased amount of washing before electrochemical testing. This washing appeared to improve the consistency of the cycles (Figure 12), with the initial current being much closer to the steady current after cycling and less shouldered peaks.

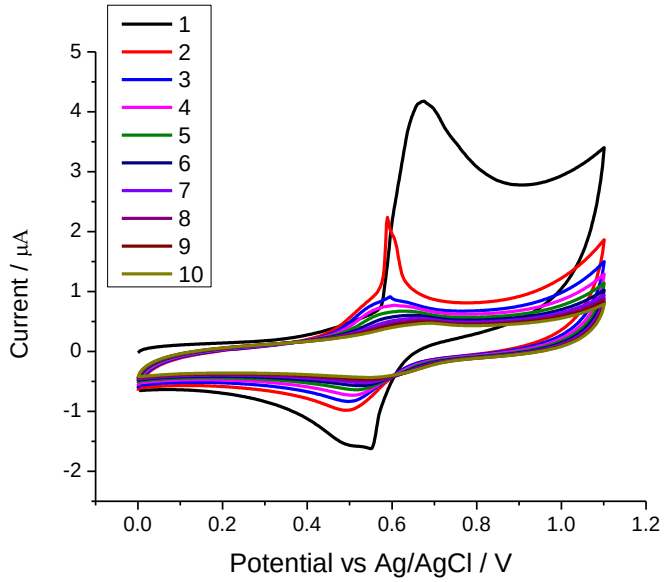

Figure 12 – CV of **9 (**Scheme 3**)** in acetonitrile with 100 mM TBATFB at 100 mV/s initial 10 cycles, electrode area 0.0707 cm^2.

The CV may also be used to calculate the amount of ferrocene on the surface. The coverage of the electroactive ferrocene on the surface is directly proportional to the charge seen by CV and this may be used to calculate the coverage using Faradays law (Equation 1):

$$\Gamma = Q/nFA\rho \qquad \text{(Equation 1)}$$

where Γ is the surface coverage, Q is the charge under the oxidation or reduction peak, n is the number of electrons transferred (in this case 1), F is the Faraday constant, A is the geometric area of the electrode (0.0707 cm^2) and ρ is the roughness factor. In this case a roughness factor was not used, as previous work used by Jaegfeldt[66] who calculated roughness factors of between 2 and 5 for graphite electrodes polished using 600 grit paper, having used electron microscopy to evaluate defects. As the present work uses much less abrasive polishing methods, finishing with a slurry of 0.3 µm alumina to give a smooth mirror like finish it is reasonable to use a roughness factor of less than 2. However, it should be noted that it is likely that in reality the roughness of the electrodes is most likely greater than this, however it is very difficult to say the precise roughness for a carbon based electrode and in this work the geometrical area of electrodes was used.

The coverage of ferrocene was calculated from the final (10th) cycle of the initial test as the current continued to decrease, however by the 10th cycle in all cases the CV was constant. Both anodic and cathodic peaks were integrated and an average of the two was taken for calculation of the surface coverage. An average coverage of 1.41 x 10^{-10} mol cm^{-2} was calculated, a 31% coverage using a close packed monolayer value of 4.5 x 10^{-10} mol cm^{-2} [67] However Brozik *et al.* obtained a coverage of 1.9 x 10^{-10} mol cm^{-2}, 42% of a close packed monolayer, after coupling the same ferrocene to a maleimide layer[67b]. Using this experimental value as a full monolayer the coverage obtained in our work (1.41 x 10^{-10} mol cm^{-2}) is 73%.

While the coverage obtained is reasonable the procedure needed optimization to achieve ferrocene coverage closer to 100%. The synthesis procedure used had 5 steps, with only the first and last steps monitored electrochemically and thus it was difficult to know which step or steps were limiting. The method of coupling of carboxylic acids to amine modified surface has been used by Bartlett, Kilburn *et al* to successfully prepare close packed monolayers[41-42] previously which suggested that it was the removal of the thioether or addition of the ferrocenenyl hexane thiol to the electrode that was limiting the coverage.

The addition of thiol in solution was only tested with thiophenol and this was done in a mixture of acetonitrile and water, whereas the ferrocenyl hexane thiol was added to the electrodes in pure acetonitrile, so the addition of thiophenol in pure acetonitrile was tested (Scheme 4) for comparison.

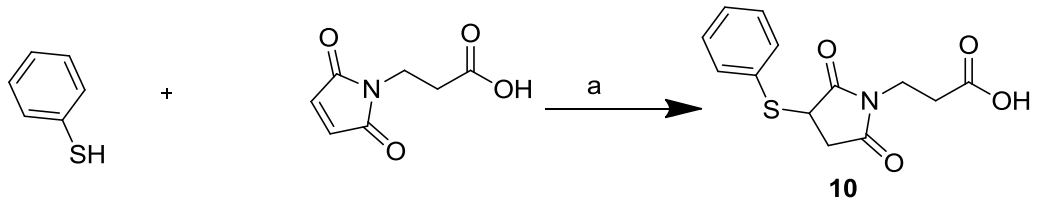

Scheme 4 – a) acetonitrile. Addition of thiophenol to 3-maleimidopropionic acid in acetonitrile

This reaction was found to take much longer, 48 hours to go to completion compared to 2 hours with water in the solution. On this basis the reaction time of the Michael addition of ferrocenyl hexane thiol was likely limiting surface coverage.

Model Synthesis

While keeping all the other conditions constant electrodes (**8,** Scheme 3) were prepared and immersed in the ferrocene for 2, 22, 27 and 48 hours (Scheme 5), with each electrode prepared in duplicate. The ferrocene electrodes (**11a-d,** Scheme 5) were then washed for half an hour in acetonitrile before electrochemical testing. The coverage was calculated as before, using the average of the integrated oxidation and reduction peaks from the 10th cycle (Figure 13).

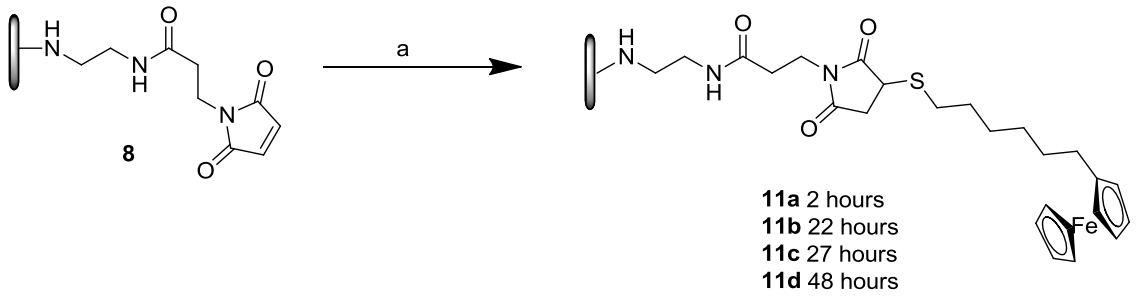

Scheme 5 – Variation of ferrocene addition time

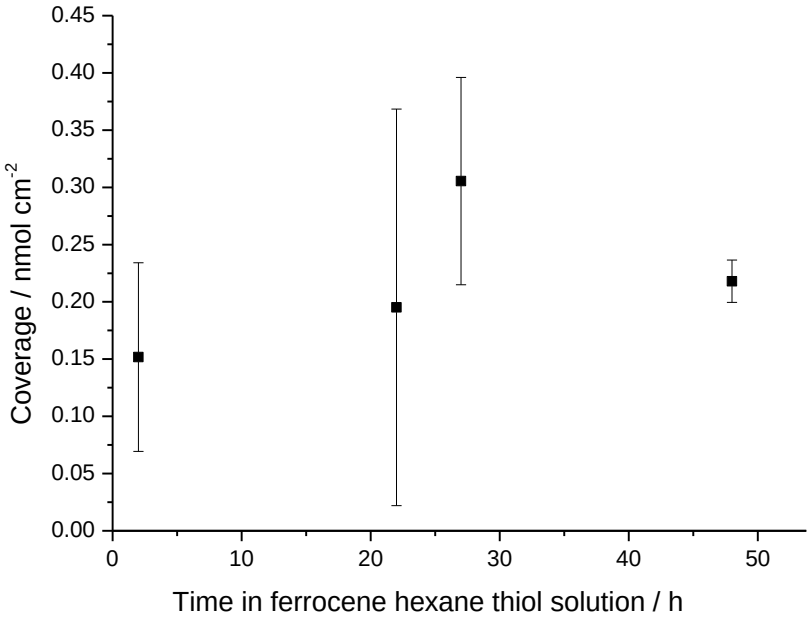

Figure 13 – Coverage from variation of times in ferrocene solution, average of 2 electrodes.

As shown in Figure 13 the results are not very consistent which makes it difficult to evaluate a true trend, although there does seem to be a general increase in the coverage following an increased time in the ferrocene thiol with

a maximum after 27 hours. However if the errors are taken into consideration the length of time does not appear to have much of an effect on the coverage. The maximum coverage obtained is only 3 x 10^{-10} mol cm^{-2} which is still only 66% coverage after 27 hours and dropped to 2.30 x 10^{-10} mol cm^{-2} after 48 hours suggesting there could still be other reasons for the limited coverage.

In addition to this the stability of the electrodes was also tested. After synthesis and initial testing the electrodes were put in a vial of acetonitrile and then re-tested after 24 hours in storage (Figure 14).

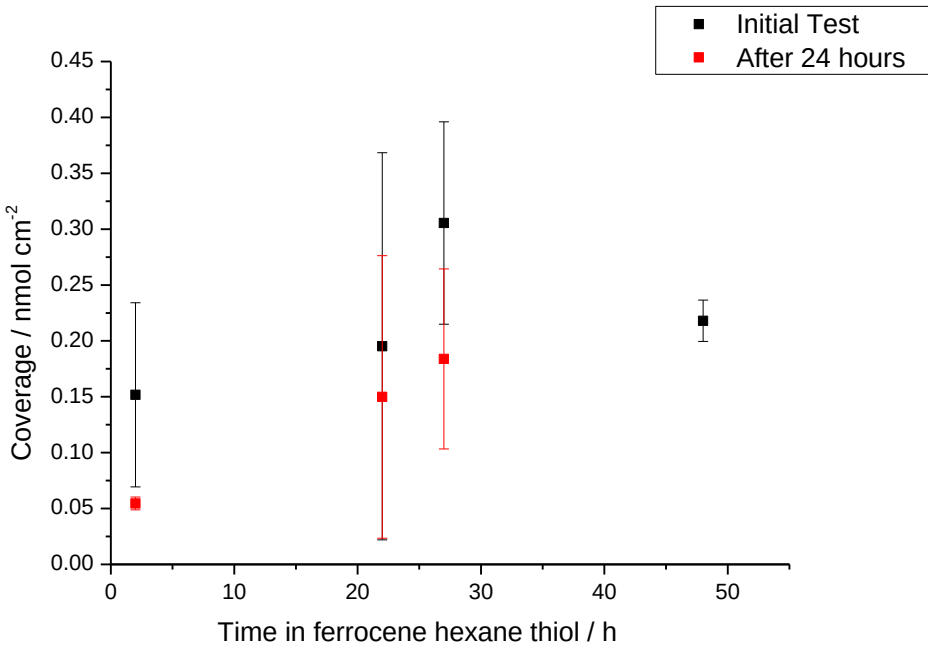

Figure 14 – Stability of ferrocene electrodes

As shown in Figure 14 the coverage decreased after storage, despite a stable CV during initial testing. The decrease could be due to the decomposition of the tether or the ferrocene itself. An alternative electroactive thiol would be needed to test this.

2.3.1 Analysis by X-Ray Photoelectron Spectroscopy (XPS)

In order to investigate the composition of the surface samples, were prepared on glassy carbon plate for analysis by X-Ray photoelectron spectroscopy. XPS allows the chemical composition of solid samples to be determined by irradiation of the sample with soft X-rays to emit electrons from the top few

atomic layers (1-10 μm) [68]. Analysis of the energy of the electrons emitted allows the elemental composition to be determined.

The kinetic energy (KE) of the emitted electrodes may be described as

$KE = h\nu - BE - ø$ (Equation 2)

where $h\nu$ is the energy of the photon BE is the binding energy of the atomic orbital which the electron originates from and ø is the spectrometer work function. The binding energy is the energy difference between the excited state and the original state of the photoelectron, which is within a range specific to the element the electron is from. Moreover the BE is dependent on the chemical environment of the element so may also be used to determine the presence of different functional groups[68].

Samples were prepared on GC plate (Sigradur G glassy carbon plates (HTW, Germany) polished on 1200 grade silicon carbide paper, and modified using the same synthesis as on the electrodes (Scheme 6). The change in surface composition was monitored using a sample of each synthetic step. Previous analysis had shown successful attachment and deprotection of a range of mono-Boc-protected diamines[41].

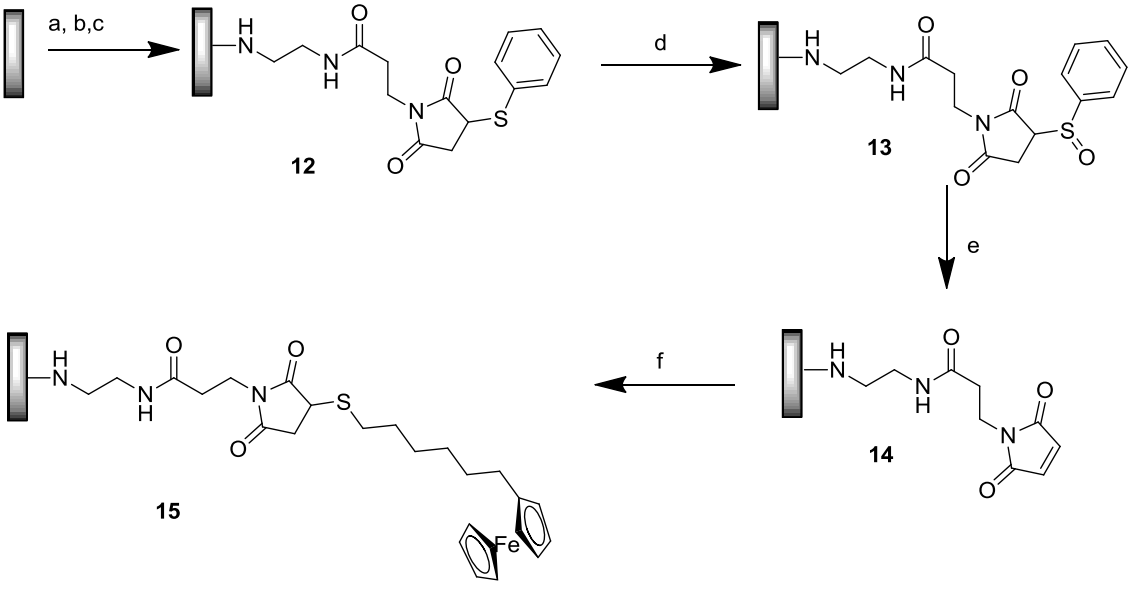

Scheme 6 – Preparation of XPS samples

Each sample had a survey scan (Figure 15) over a wide binding energy range to evaluate the overall composition and elements present in the sample followed

by narrow scans in the regions of interest: carbon (C1s), nitrogen (N1s), oxygen (O1s) and sulphur (S2p).

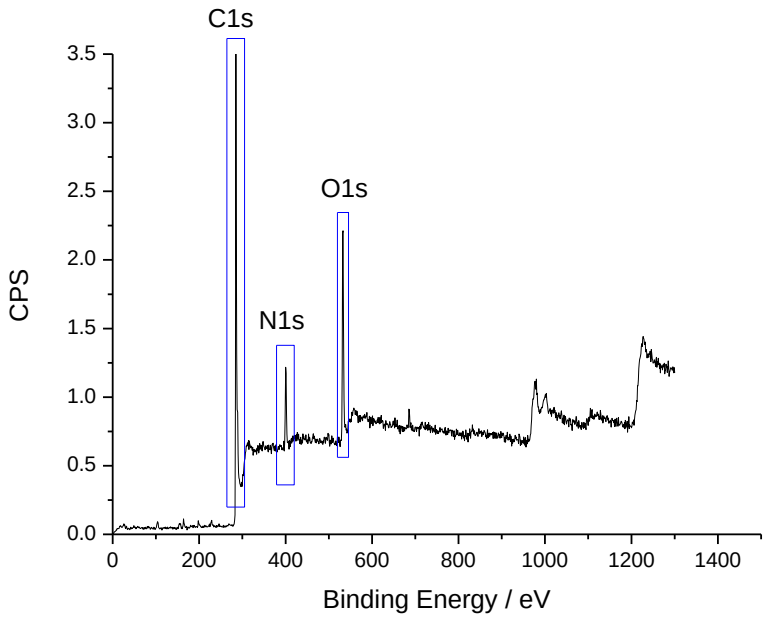

Figure 15 – Example Survey scan of **12 (**Scheme 6**)**

As the sample is prepared on glassy carbon plate is made up of tangled ribbons of carbon[69] with oxygen functionalities [70] such as hydroxyl and carbonyl groups, these elements (C, H and O) are only of limited use for the analysis of surface composition. The nitrogen and sulphur regions are the most important thing to compare between samples.

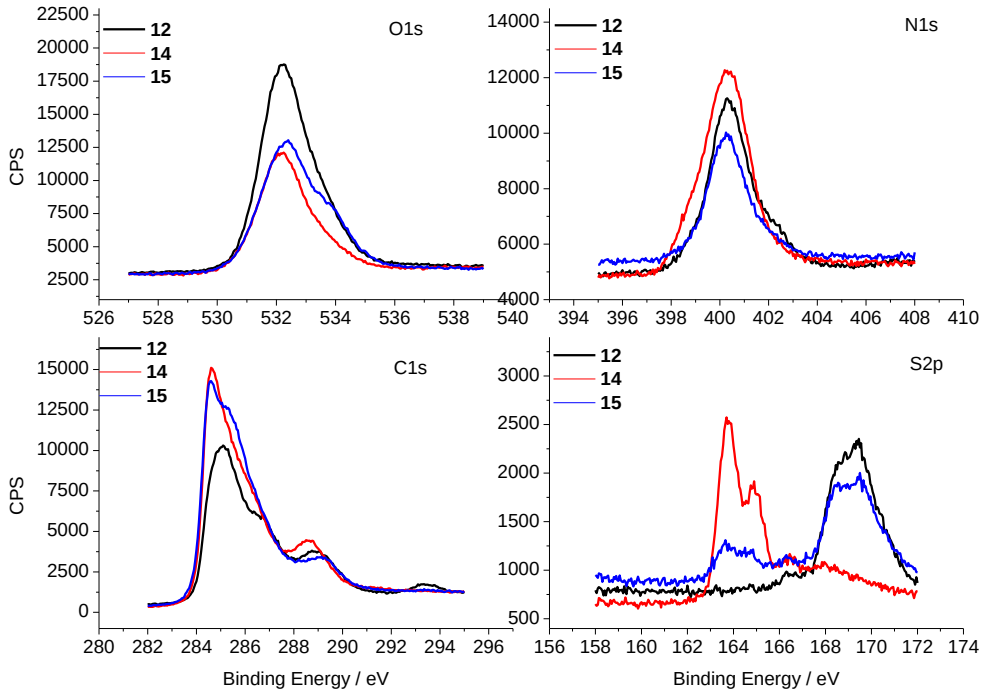

Figure 16 – Narrow range scans for XPS samples **12**, **14** and **15** (Scheme 6)

Sulphur is present in all of the samples (Figure 16), however the binding energy varies. The peak in sample **12** is at 165 eV, however sample **14** which has been oxidized and heated to try and remove the sulphur and re-form the maleimide has a higher binding energy for sulphur of 170 eV. This increase in binding energy is consistent with the sulphur being oxidized[71]. As there is no peak visible at 165 eV in sample **14** it can be assumed that all of the sulphur was oxidized, however the elimination step was not sufficient to remove all of the sulphoxide.

Sample **15** after the addition of ferrocene has a peak at 165 eV, consistent with the thiol on the ferrocene having successfully reacted with the maleimide to form a thioether. A second smaller peak at 170 eV is also seen, consistent with the previous sample which retained some sulphoxide.

The ratio of the elements on the surface can be determined, using the areas under the peaks and intensity factors. The relative amounts of sulphur and nitrogen may then be compared (Table 1).

Table 1 – XPS results percentage calculated using CasaXPS from an average of two samples.

Sample	Binding energy / eV	%S	%N	S/N
12	170	1.77	8.02	22 %
14	164	0.59	11.33	5 %
15	170 and 164	0.98	8.08	12 %

The ratio of sulphur/nitrogen on the surface reduced from 22% to 5% from sample **12**-**14**, indicating that the elimination of the sulphur worked partially but it was not complete in the time given. Upon addition of the ferrocene-thiol the amount of sulphur on the surface increased again, though it was not as high as it was to begin with, showing that the coverage of ferrocene was not as high has it might be. This is consistent with the coverage found from voltammetry, where the amount of ferrocene was less than a full monolayer.

Overall these results suggest that the elimination of the sulphoxide was the limiting step which prevents the formation of a full monolayer of ferrocene on the surface, as not all of the maleimide has been formed on the surface. In order to improve the coverage the length of heating of the sulphoxide sample would need to be increased.

2.3.2 Anthraquinone thiol

Anthraquinones are quinone derivatives with a range of applications, originally used as dyes[72] but with other uses including as a ligand for protein purification[73] and in medicine as anticancer and antitumor agents[74]. Anthraquinone has also been used as a catalyst for oxygen reduction[75].

Model Synthesis

Anthraquinone-2-carboxylic acid has been used as a model redox system by Bartlett, Kilburn *et al.* and successfully coupled to amine modified electrodes using different linkers and varying chemistry[41-43]. Due to the reversible and stable electrochemistry of anthraquinone it is a good alternative model redox compound, with a greater stability than ferrocene.

Anthraquinone thiol **16** was prepared according to literature procedure[76] in 36% yield (Scheme 7).

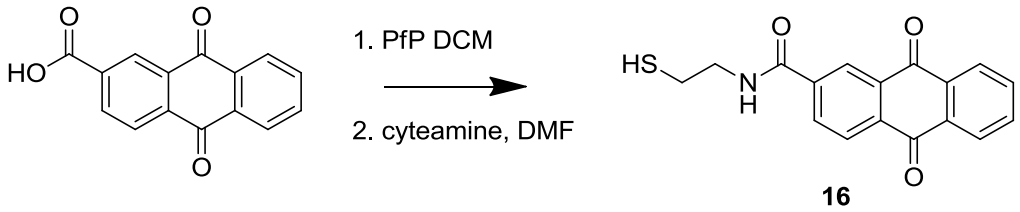

Scheme 7 –synthesis of anthraquinone-thiol

The anthraquinone thiol was used as an alternative model thiol, due to the increased stability in comparison to ferrocene hexane thiol. A sample of **6** (Scheme 3) was prepared and oxidized, following the XPS results the heating step was extended, followed by the addition of the anthraquinone (Scheme 8). Initially the heating time was increased from 1 h to 1.5 h and 2 h.

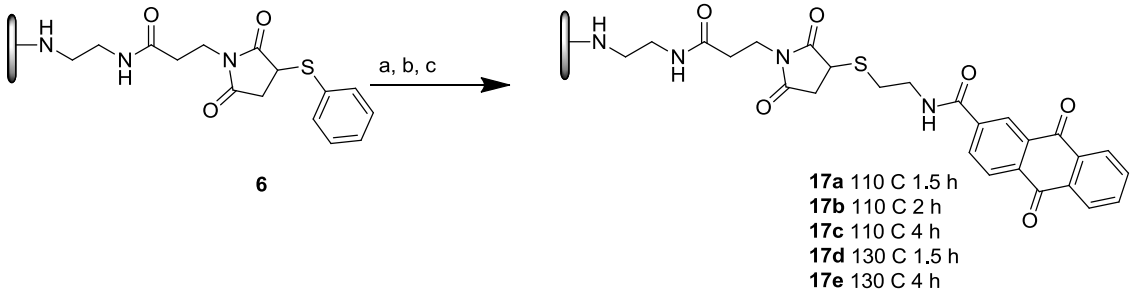

Scheme 8 - coupling of Anthraquinone thiol. a) mCPBA 0°C 1 h, b) Δ, c) **16** in DMF 16 h

The anthraquinone modified electrodes were studied by CV (Figure 19) giving redox peaks at the expected potential for anthraquinone (-0.47 V vs SCE)[41]. The anodic and cathodic peak currents also increase linearly with scan rate, consistent with a species immobilized on the surface (Figure 17).

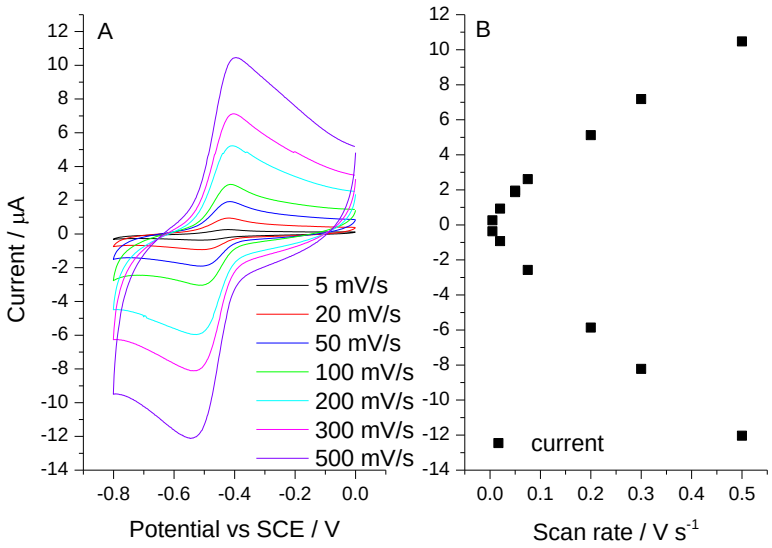

Figure 17 – a) Representative CV of **17** in 100 mM phosphate buffer, pH 7 with 100 mM TEATFB at varying scan rate. Geometrical electrode area 0.0707 cm^2 b) plot of anodic and cathodic peak current vs scan rate.

The coverage of anthraquinone on the surface was calculated from the 10th cycle of the CV using Faraday's law (Figure 18).

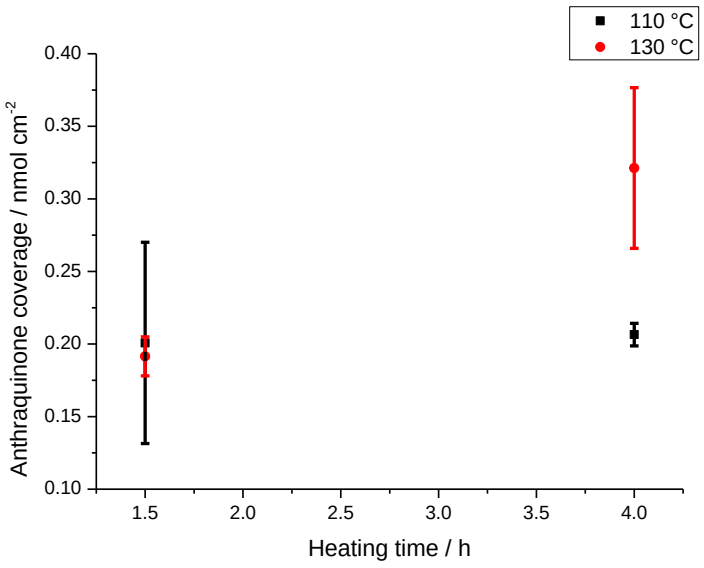

Figure 18 – Average coverage of anthraquinone on the surface after different time and temperature of heating (Scheme 8).

In addition to the heating time the temperature was varied, with DMF used as a higher boiling point solvent. The surface coverage appeared to increase when

the sulphoxide elimination step is carried out over a longer time, presumably due to the more complete removal of the sulphoxide. The anthraquinone coverage was determined to be 2.0 x 10^{-10} (±0.6 x 10^{-10}) mol cm^{-2} after 1.5 h, and 2.06 x 10^{-10} (±0.06 x 10^{-10}) mol cm^{-2} after 4.5 h heating at 110 ˚C and immersion in **16,** After heating at 130 ˚C the coverages were greater, 1.91 x 10^{-10} (±0.1 x 10^{-10}) mol cm^{-2} after 1.5 h, however the greatest coverage was after 4 hours at 130˚C with a coverage of 3.21 x 10^{-10} (±0.35 x 10^{-10}) mol cm^{-2}. These anthraquinone coverages are significantly greater than ferrocene coverage of 1.44 x 10^{-10} mol cm^{-2}**.** However due to the difference in structure and coupling conditions between ferrocene thiol and anthraquinone thiol the coverage is expected to be different, therefore direct comparison with ferrocene coverage is not possible. Anthraquinone appears to be a better choice of redox model as the CV was a lot more stable with cycling and the coverage was more consistent, shown by the smaller error.

The coverage did not significantly increase after further heating, with 4 hour coverage of 3.47 x 10^{-10} mol cm^{-2}, 8 hours 3.85 x 10^{-10} mol cm^{-2} and 4.11 x 10^{-10} mol cm^{-2} after 24 hours. The coverage of **16** as a SAM on gold has been calculated [76] to be 1.44 x 10^{-10} mol cm^{-2}. However as the present work is on carbon, a softer and rougher surface, the maximum coverage could be higher. In work done by Bartlett, Kilburn *et al.* a maximum coverage of anthraquinone carboxylic acid coupled to an ethylene diamine linker was as high as 1.22 x 10^{-9} cm^{-2} [41] after rough polishing of the glassy carbon electrode. Direct attachment of an anthraquinone diazonium salt by Sarapuu, Vaik *et al.*[75] gave a coverage of 4.3 x 10^{-10} mol cm^{-2} on glassy carbon polished on 0.3μm alumina as electrodes used here.

Although the greatest coverage obtained in this work, 3.21 x 10^{-10} mol cm^{-2} (Figure 18), is much lower than monolayer coverage 1.22 x 10^{-9} mol cm^{-2} [41]this work uses a number of synthetic steps and bulkier groups, whereas the higher coverage is obtained from the direct coupling of the anthraquinone carboxylic acid to an amine monolayer. In addition our coverage (Figure 18) is in agreement with the 4.3 x 10^{-10} mol cm^{-2} monolayer prepared from direct attachment of the diazonium salt by Sarapuu, Valik *et al.*[75].

2.3.3 XPS analysis

Samples of electrodes **17** were prepared in duplicate for XPS using the optimized conditions for sulphoxide elimination (4 h, 130°C) (Scheme 9) and coupled with anthraquinone thiol (**16**) and analysed by XPS.

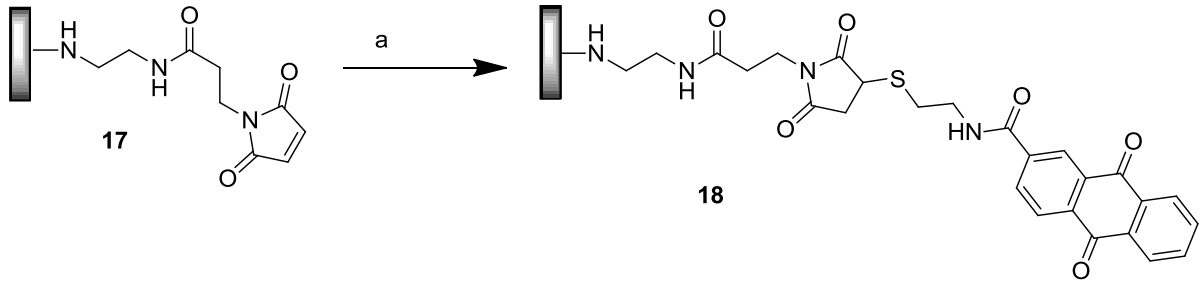

Scheme 9 – a) **16** in DMF, 16 h

The surface composition of the samples was then investigated using XPS and then compared with XPS samples **12** and **13** (Scheme 6).

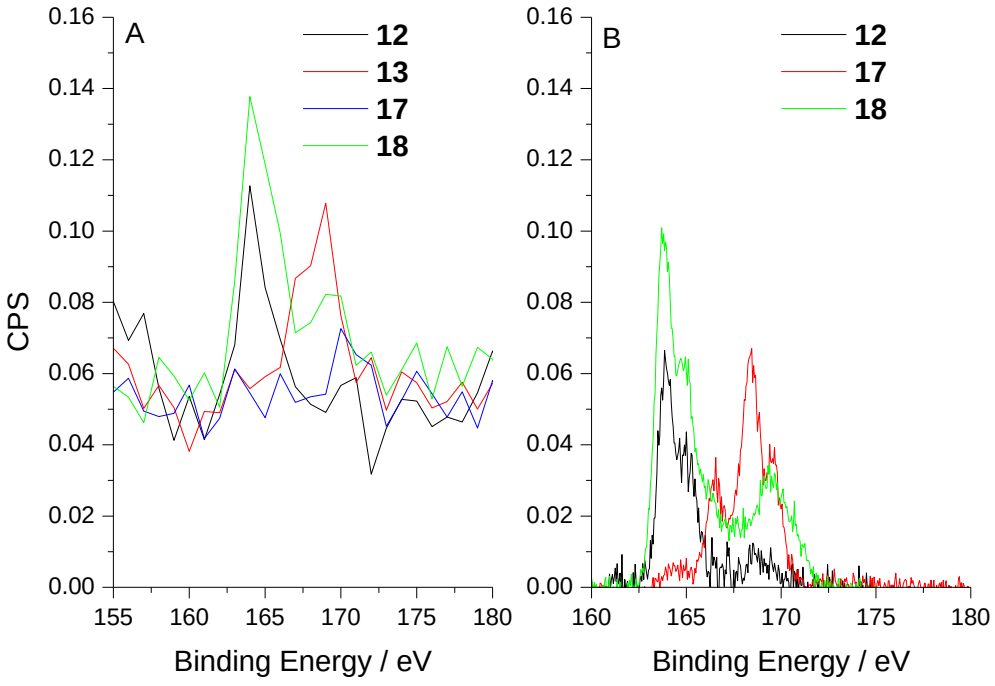

Figure 19 – a) Sulphur region from survey scan b) XPS scans in region for S2p.

The results (Figure 19) indicate that there is no residual sulphur in sample **17** which had been heated for 4 hours at 130°C, suggesting that the sulphoxide has been successfully eliminated after 4 hours, consistent with CV experiments. For sample **18** the addition of the anthraquinone thiol appears to successfully create a thioether bond, as shown by the peak at 165 eV.

2.4 Monolayer assembly on gold

A self-assembled monolayer (SAM) on gold was also prepared for anthraquinone thiol **16** (Scheme 10) for comparison to the work done on GC. Gold wire electrodes (1 mm diameter, sealed in glass) were polished successively on wet 1200 grade silicon carbide paper, 5 µm alumina lapping film and 1 µm and 0.3 µm alumina slurries. The electrodes were then washed with water and cycled in 1 M sulphuric acid for 10 cycles at 100 mV s^{-1} to further clean the surface. Electrodes were then immersed in a 1 mmol solution of the thiol in DMF, left for 4.5 h and 26 h.

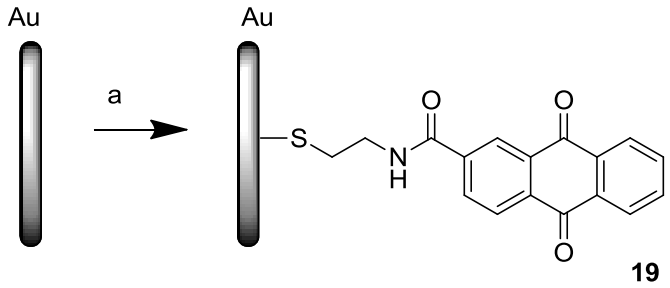

19

Scheme 10- a) 1 mmol **14** in DMF

The electrodes were then tested by CV (Figure 20) in buffer and the coverages were calculated from the 10th cycle. No significant difference in the coverages was seen, indicating that a full monolayer had assembled in 4 h or less.

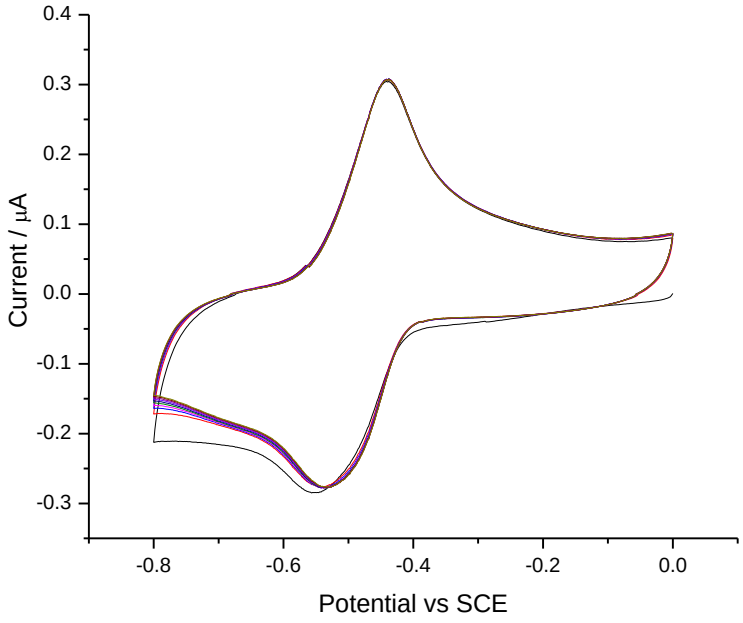

Figure 20 – CV of **19** at 100 mV/s in 100 mM phosphate buffer pH 7 with 100 mM TEATFB. Geometrical electrode area 0.023 cm^2.

The SAM appeared to be stable with cycling (Figure 20) and the coverage (Table 2) was calculated using Faraday's law using the geometric area and the real surface area calculated from the acid CV.

Table 2 – Coverage of **14** on gold. [a] calculated from last cycle of acid CV using conversion factor of 390 µC cm^{-2} [b] 0.023 cm^2

Area	**Coverage / mol cm^{-2}**
Real[a]	4.07 x 10^{-11} +/- 0.55
Geometric[b]	2.19 x 10-10+/- 0.11

The real surface area is significantly larger than the geometric area and the coverage is accordingly higher than the expected coverage of 1.44 x 10^{-10} mol cm^{-2} [76]. Although the polishing method used was the same as on carbon, gold is a much harder metal so the roughness of carbon could account for the larger than expected coverages on carbon.

2.5 Selenium chemistry

After a number of heating and cooling cycles, associated with the sulphoxide elimination step, considerable damage to electrode connections was found to be a problem. In light of this issue an alternative to the previously used sulphoxide elimination was investigated. Selenium has been used in the past to protect the double bond of a maleimide [77] and unlike the sulphur analogue the selenium is spontaneously eliminated at room temperature upon oxidation. As before a model synthesis in solution was completed to test the synthetic steps (Scheme 11).

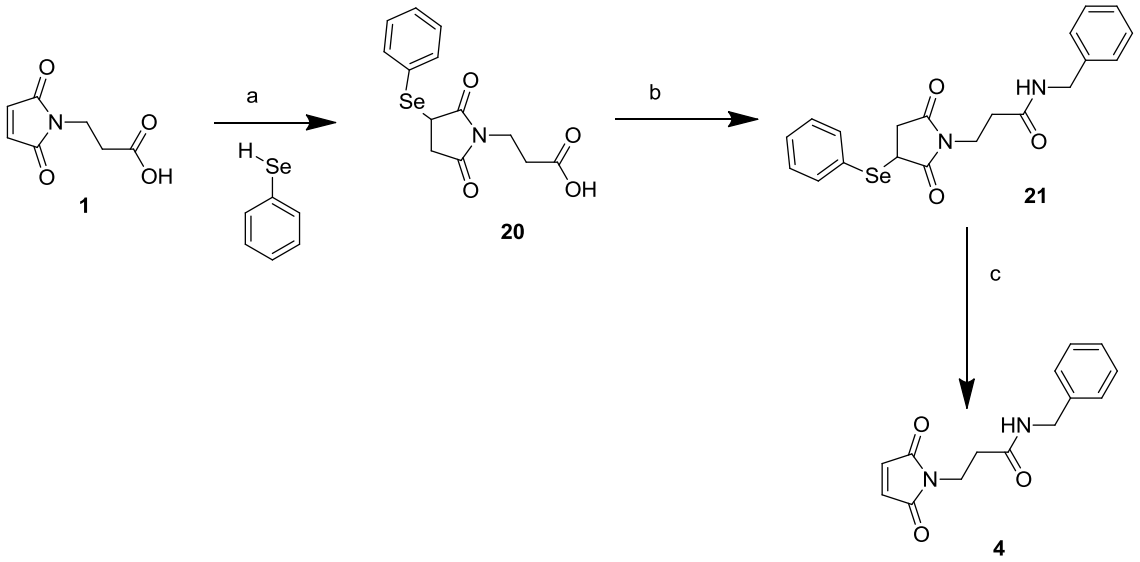

Scheme 11– Model synthesis using selenium. a) acetonitrile b) HBTU, DIEA, DMF 16 h c) mCPBA 0°C 1 h, 1 h rt

First phenylselenol was added to 3-maleimidopropionic acid in acetonitrile to give the selenyl protected **20**, following this the acid was coupled with benzylamine to act as an model for the amine modified GC surface, affording the amide **21**. The selenyl protection was then eliminated by oxidation with mCPBA to give **4** in a 38% yield.

After successful testing in solution the methods were tested on electrodes (Scheme 12) using the model system developed previously.

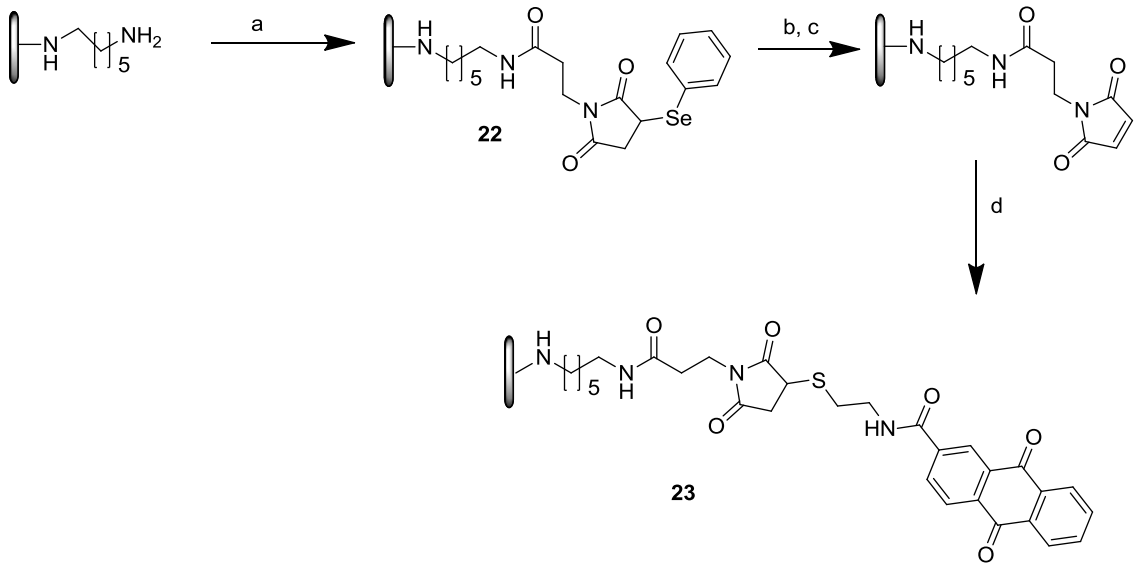

Scheme 12 – Model synthesis using selenium. a) **20**, HBTU, DIEA, DMF b) mCPBA in acetonitrile, 1 h 0°C, 1 h rt, c) 2 h in acetonitrile d) **16** in DMF 16 h

Electrodes were prepared (Scheme 12) and tested by CV (Figure 21), redox peaks at the expected potential for anthraquinone (-0.47 V vs SCE)[41] (Figure 21 A) were observed and peak currents increased linearly with scan rate (Figure 21 B), consistent with a species immobilized on the surface.

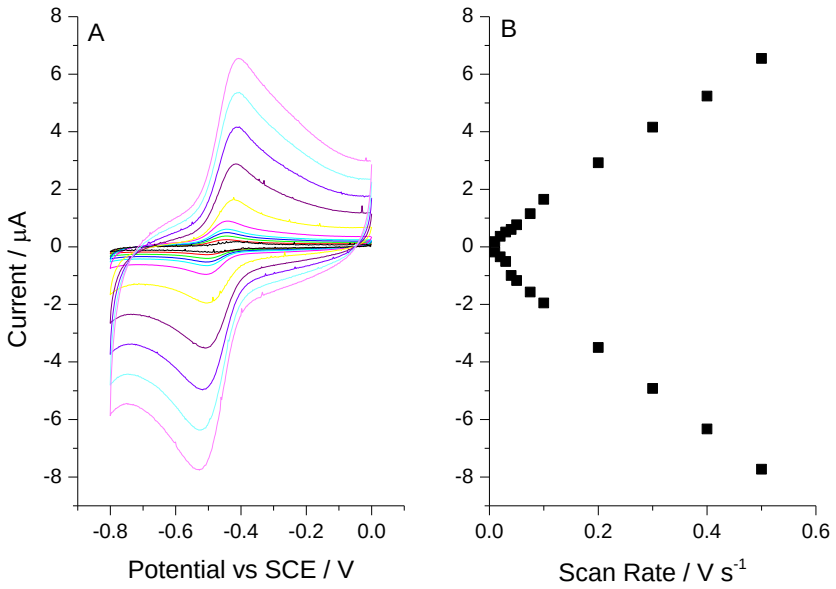

Figure 21 - a) Representative CV of **23** in 100 mM phosphate buffer, pH 7 with 100 mM TEATFB at varying scan rate. Geometrical electrode area 0.0707 cm² b) plot of anodic and cathodic peak current vs scan rate.

Coverage was calculated from the 10th cycle of the CV, 1.5 x 10^{-10} mol cm^{-2} (±0.15 x 10^{-10}). This coverage is close to the theoretical maximum of 1.44 x 10^{-10} mol cm^{-2}.

2.6 Conclusions

A novel method for the preparation of maleimide on the surface of glassy carbon electrodes has been developed. The method uses a combination of electrochemical and solid phase synthesis to build up the structure of a tether to bind thiols on the surface.

The system was first tested in solution: a maleimide carboxylic acid was protected with thiophenol to create a thioether and then coupled to benzylamine as a model for the surface. The maleimide was then re-created by oxidation of the thioether followed by heating to eliminate the sulphoxide.

The chemistry was then used on the surface with the thioether coupled to an amine functionalised electrode followed by reformation of the maleimide bond. Ferrocene and anthraquinone thiols were used as a model for the protein and the surfaces were analysed using voltammetry to calculate the coverage and XPS to evaluate the elemental composition of the surface.

Finally following problems with heating the electrodes to eliminate sulfoxides, selenols were chosen as an alternative to thiols to protect the maleimide bond. Once oxidised the selenide would eliminate at room temperature, removing the need for heating. A model system in solution proceeded as expected and this method would be used in the future.

This work aimed to create a monolayer on the surface; however as previously discussed it is very important to have control over the surface composition. Work on controlling the coverage is evaluated in Chapter 3.

3. Partial Coverage

3.1 Aims of the work

With enzyme attachment in mind it is important to consider the relative size of the biomolecule and the tether it is to be linked to. Enzymes range in size however even small proteins are much larger than the simple molecule tether on the electrode. It is also important to note that enzymes are not a regular shape, and if the target group for binding is buried in the enzyme structure it may be very difficult to interact with. Therefore if the tether is densely packed on the surface it could prevent the enzyme from binding to the reactive group used.

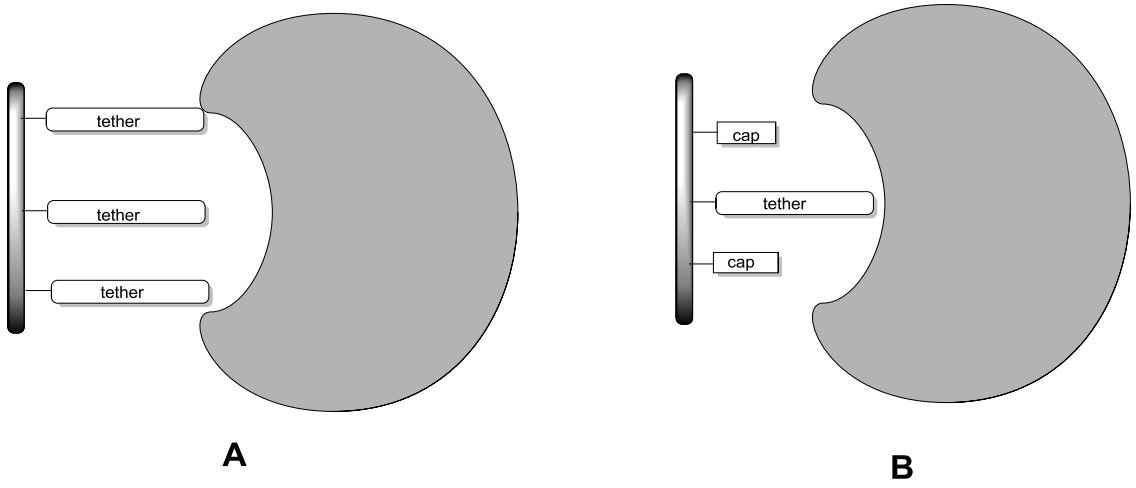

Figure 22 – Partial coverage concept. A – electrode functionalised with full monolayer of tether, B electrode modified with partial coverage of tether

As shown in (Figure 22) a partial coverage could help to pattern the surface to favour coupling with the enzyme. If a full monolayer of the functional group is present (A) then it may be difficult for this to couple with residues on the enzyme, however if a partial coverage of the functional group is there then only the functional group is protruding from the surface and the rest of the surface can be covered with a capping group. The capping group used may be small as to not interact with the enzyme (B) or large to try and prevent any interaction. In addition to this the capping group may be modified to change the electrostatic interactions between the enzyme and electrode surface.

Partial Coverage

This work aims to create a mixture on the electrode surface in order to create a partial coverage of the desired functional group. In particular this work aimed to create such procedures for a carbon surface.

3.2 Concentration

3.2.1 Previous work

Previous work by Bartlett, Kilburn *et al.* showed that the variation of the concentration of redox molecules as well as the coupling agent used affected the surface coverage obtained[43]. Building on this work was done on making bi- and tri- functionalised surfaces with multiple redox groups attached. Electrodes were prepared by simultaneous coupling of a mixture of two acyl chlorides to amine-functionalised surfaces, in addition sequential functionalization was attempted using a low concentration of the first acyl chloride coupled, followed by a second coupling reaction with another acyl chloride.

3.2.2 Control using a spacer

Following on from this work a low concentration of a spacer molecule could be used to increase the length of the tether and control the coverage simultaneously. Previous work[42] has shown successful use of both aromatic and aliphatic molecules as spacers to increase the length of the tether on the electrode.

3.2.2.1 Low concentration

Initially a 6 carbon spacer was used to increase the tether length. Previous work used low concentration acyl chlorides[42] to control the coverage, in this work both acyl chlorides and carboxylic acids were coupled for comparison (Scheme 13). Initially a full monolayer of EDA was prepared on the surface, followed by coupling of the acyl chloride or carboxylic acid. Following the removal of the Boc group two routes were followed, the direct attachment of anthraquinone carboxylic acid and the preparation of maleimide on the surface followed by attachment of anthraquinone thiol **16** (Scheme 13).

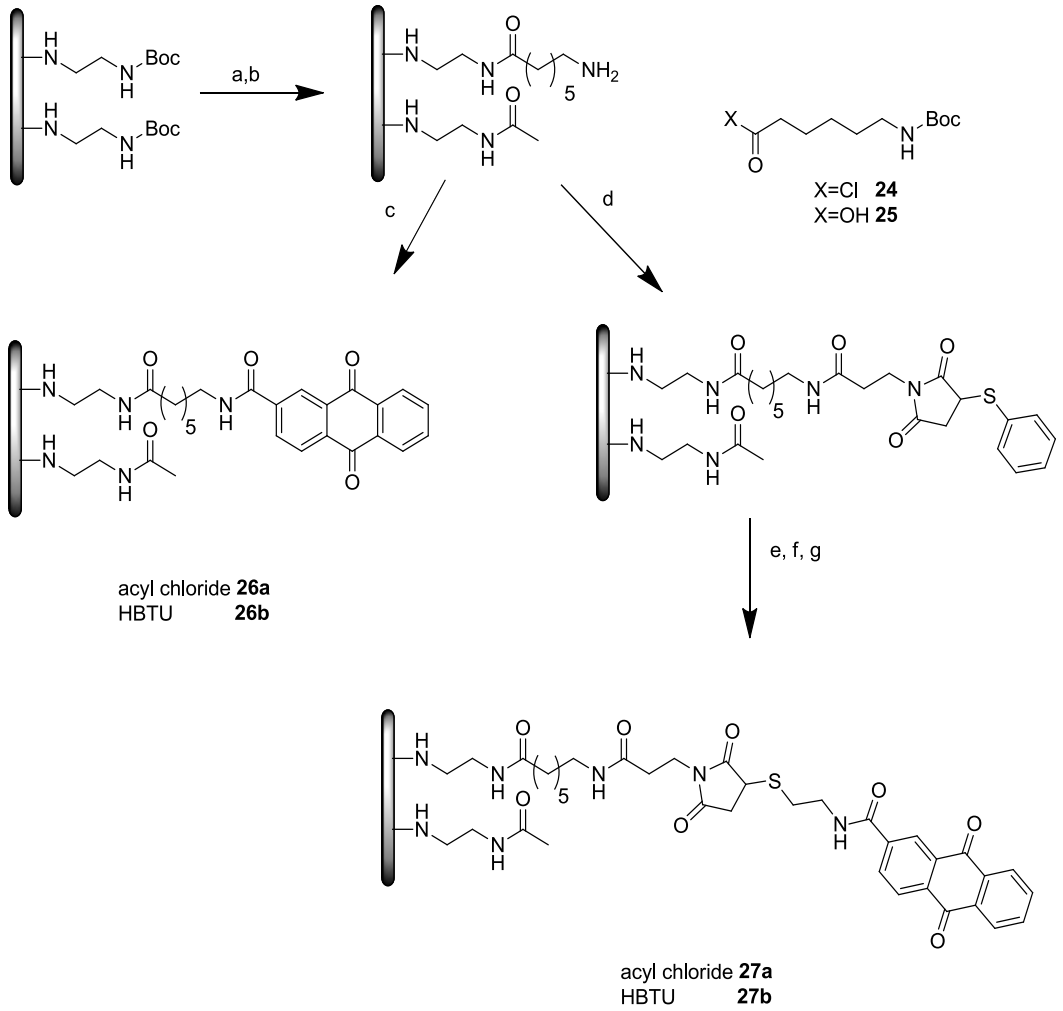

Scheme 13 – partial coverage from 1 mM spacer a) 4M HCl in dioxane, 1h b) **24**, Pyridine, DCM or **25**, HBTU, DIEA, DMF c) Anthraquinone-2-carboxylic acid, HBTU, DIEA, DMF d)**2**, HBTU, DIEA, DMF e) mCPBA in acetonitrile, 0 °C 1 h, f) DMF 130 °C, 4 h g) **16** in DMF, 16 h

Following the synthesis the electrodes were tested by Cyclic Voltammetry at 50 mV s^{-1} (Figure 23), coverage was calculated from the 5th cycle when the current was stable.

Partial Coverage

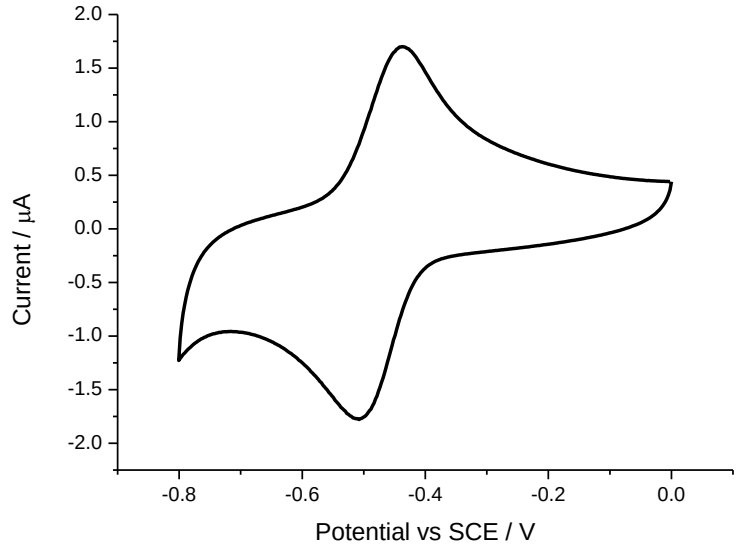

Figure 23 – CV of **27b** at 50 mV s^{-1} in 100 mM phosphate buffer pH7 with 100 mM TEATFB

The coverage for electrodes prepared using HBTU and acyl chloride showed very similar coverages of anthraquinone coupled directly to the amine surface The average coverage of anthraquinone, from electrodes prepared in duplicate, is shown in Figure 24. Error bars are shown in the graph but it should be noted that the standard deviation they represent has limited value when there are only two values it is calculated from and ideally there would be more values to compare.

The coverage of anthraquinone after preparation of maleimide on the surface (**27a, b**) is very similar to the coverage after coupling of anthraquinone carboxylic acid directly to the amine-modified surface (**26 a, b**). The coverage for the acyl chloride electrodes which had anthraquinone carboxylic acid directly coupled to amine-modified surface (**26a**) was the highest, 4.5 x 10^{-10} mol cm^{-2}, which is a very high coverage. This coverage is the same as for a full monolayer of anthraquinone thiol. From these results it appears that a full monolayer is obtained from a spacer concentration of 1 mM.

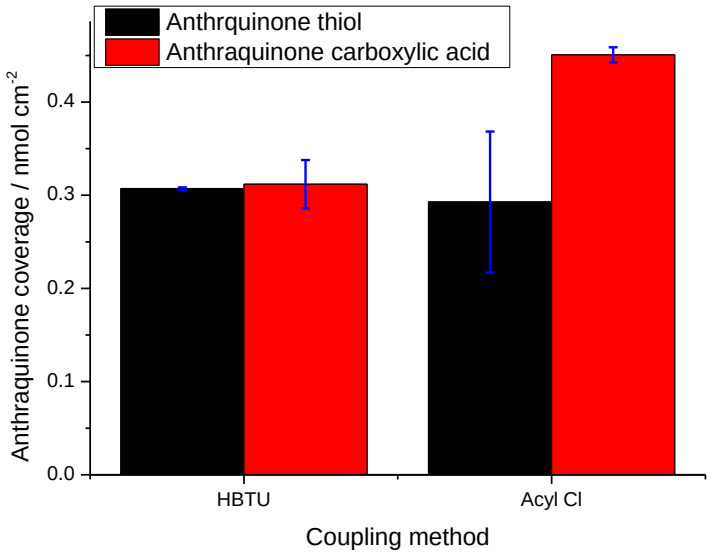

Figure 24 – Average coverage of anthraquinone after coupling of spacer at low concentration. Coupling conditions shown in Scheme 13. Each bar represents the mean of two replicate electrodes, with standard deviation shown as an error bar.

Following this lower concentrations of spacer were used (Scheme 14). Electrodes were prepared using the carboxylic acid of the spacer as little difference was seen between the HBTU and acyl chloride methods previously.

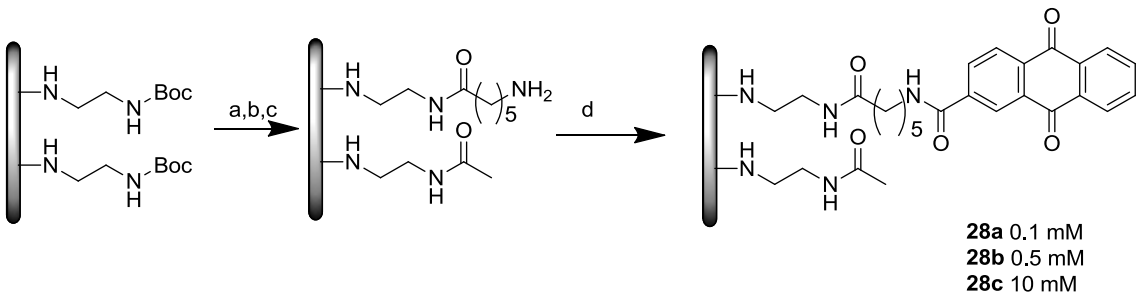

Scheme 14 – Partial coverage using low spacer concentrations. a) 4M HCl in dioxane, 1h b) **25**, HBTU, DIEA, DMF c) acetyl chloride, pyridine, DCM d) Anthraquinone-2-carboxylic acid, HBTU, DIEA, DMF.

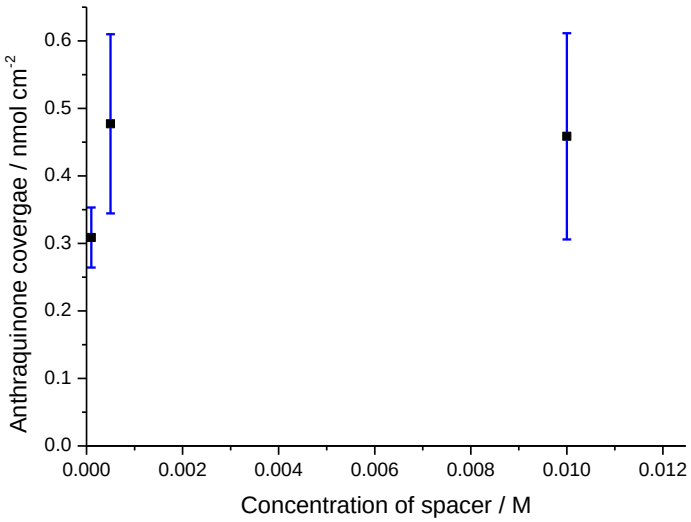

Figure 25 – Anthraquinone coverage of **28a-c** after using spacer concentration to control coverage. Coupling conditions shown in Scheme 14. Each point represents the mean of two replicate electrodes, with standard deviation shown as an error bar.

The coverage of anthraquinone does not appear to decrease greatly with a decreasing concentration of spacer. The coverages were still very high, as much, or greater than a full monolayer of anthraquinone. It was thought that even at low concentration the reaction time was sufficiently long that the reaction would go to completion.

3.2.2.2 Time in spacer

Following the low concentration results the effect of reaction time was investigated, initially the concentration of the spacer was kept at 1 mMol and electrodes were immersed in the spacer coupling solution for times between 10 minutes and 1 hour (Scheme 15).

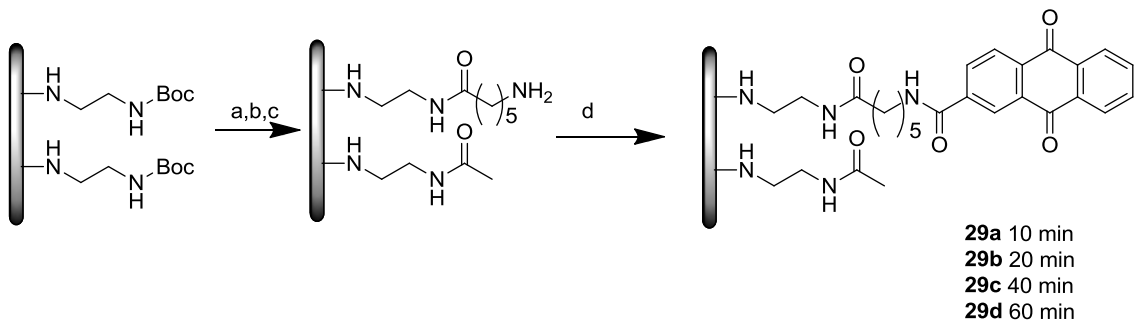

Scheme 15 – Effect of spacer coupling time on anthraquinone surface coverage. a) 4M HCl in dioxane, 1h b) **25**, HBTU, DIEA, DMF 10 to 60 min c) acetyl chloride, pyridine, DCM d) Anthraquinone-2-carboxylic acid, HBTU, DIEA, DMF.

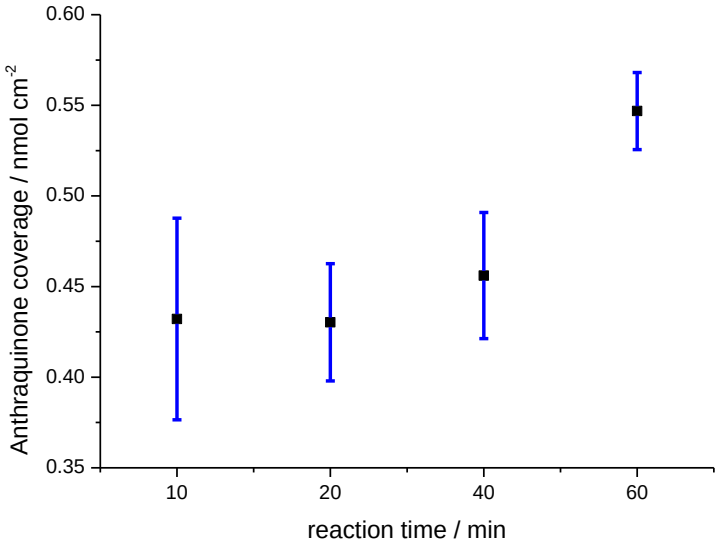

Figure 26 – Anthraquinone coverage after variation of time in spacer. Coupling procedure shown in Scheme 15. Each point represents the mean of two replicate electrodes, with standard deviation shown as an error bar.

The coverage of anthraquinone coupled to electrodes after short times in the spacer solution (Figure 26) were lower than the previous results when low concentrations of spacer were used and left overnight to couple, however results were still very high and with large errors. The greatest coverage was achieved after 60 minutes coupling time, and the lowest coverage after 10 minutes coupling time. However even the smaller coverage was 3.7×10^{-10} mol cm^{-2}, very close to a monolayer of anthraquinone thiol measured at 4×10^{-10} mol cm^{-2}.

Partial Coverage

The high coverages and large errors suggested that using the concentration to control coverage was not a reliable method. The coverage obtained was very close to a monolayer despite attempts to limit the amount of amines on the surface. This led to the conclusion that the anthraquinone could be sticking to the surface. In order to investigate the level of non-specific adsorption a number of control reactions were required.

3.3 Control reactions

3.3.1 Control electrodes

An amine-functionalised electrode was prepared and immersed in anthraquinone thiol (Scheme 16) using the same conditions as previously to investigate the level of non-specific adsorption.

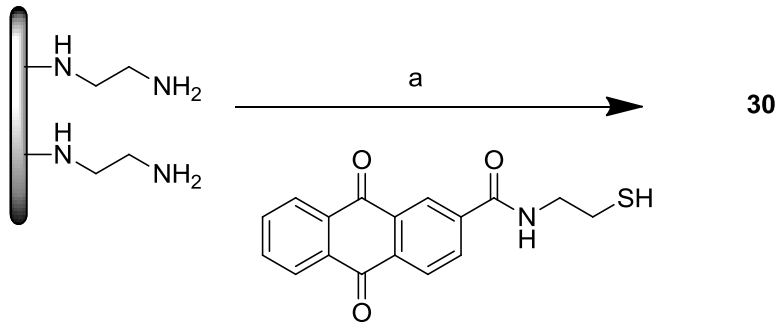

Scheme 16 – a) **16** in DMF, 16 h

The electrodes were tested immediately after synthesis and then sonicated to try and remove any non-specifically adsorbed anthraquinone thiol (Figure 27). At the same time a previously prepared maleimide electrode was treated under the same conditions for comparison (Figure 28).

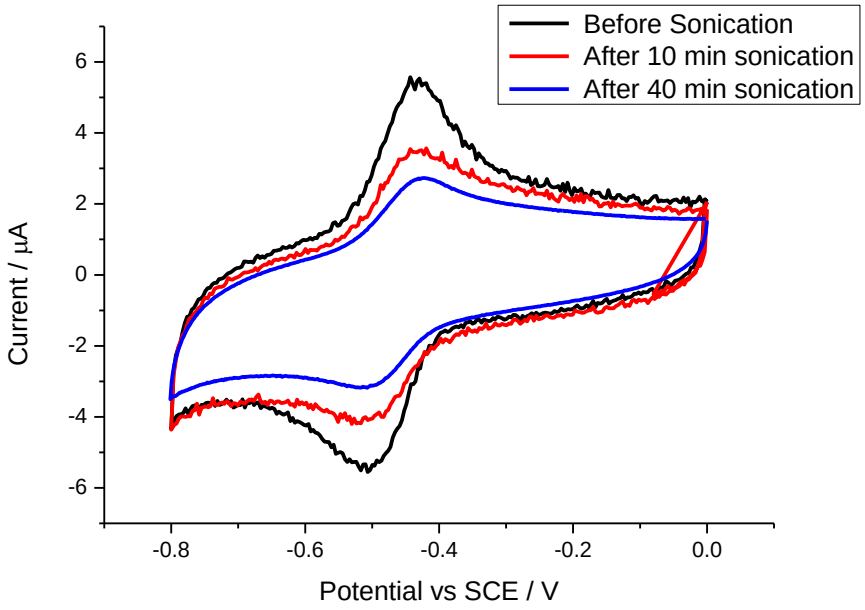

Figure 27 – Stability of anthraquinone thiol on an amine functionalised electrode **30** (Scheme 17) GC electrode area 0.0707 cm^2. CV at 100 mV s^{-1} in 100 mM phosphate buffer pH 7 with 100 mM TEATFB.

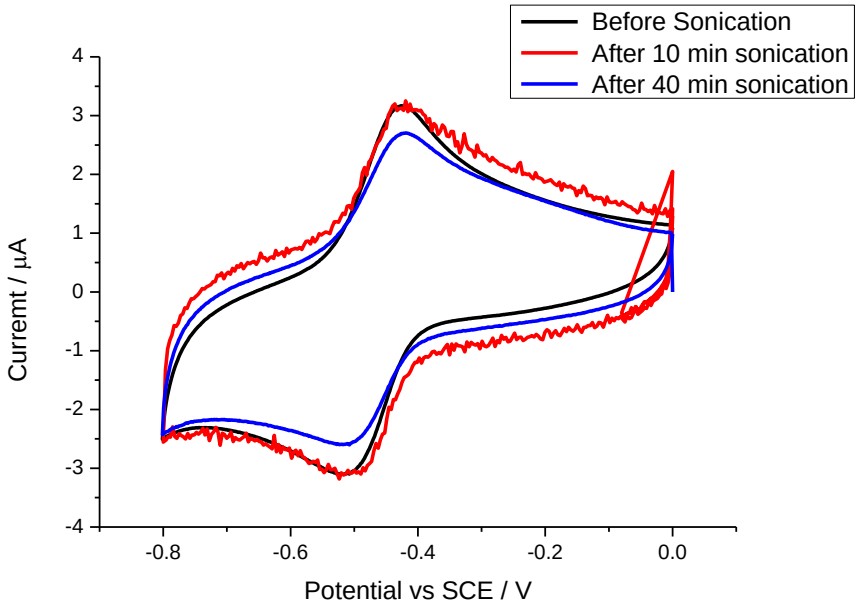

Figure 28 – Stability of maleimide-anthraquinone electrode (**17d**) GC electrode area 0.0707 cm^2CV at 100 mVs^{-1} in 100 mM phosphate buffer pH 7 with 100 mM TEATFB.

Partial Coverage

As seen immediately by CV (Figure 27, Figure 28) the peak current decreased on both the amine electrode (**30**) and the maleimide electrode (**17d**), however the current dropped less on the maleimide modified electrode. Coverage was calculated (Figure 29) from the CV before and after each stage of washing.

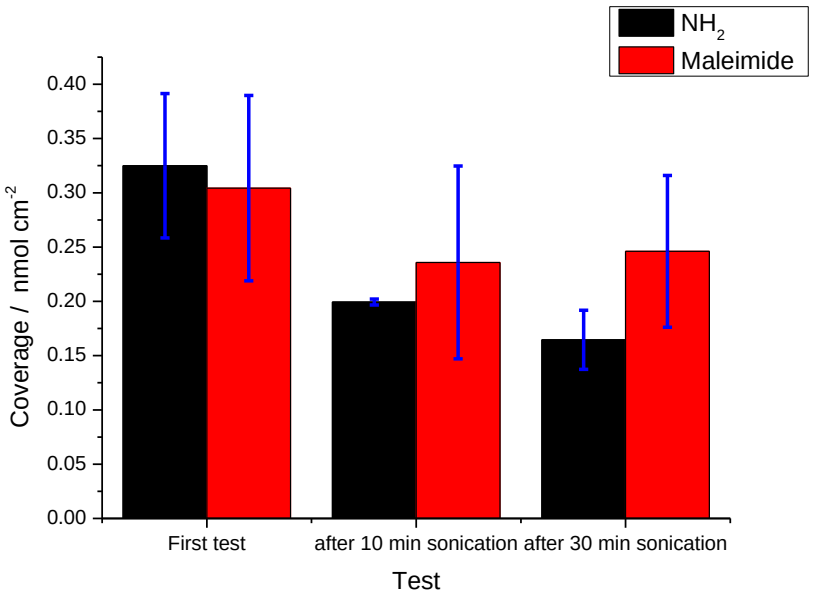

Figure 29 – Coverage of anthraquinone on amine (**30**) and maleimide (**17d**) functionalised electrodes. Coupling conditions shown in (Scheme 16) and (Scheme 8). Each bar represents the mean of two replicate electrodes, with standard deviation shown as an error bar.

Initially the EDA-functionalised electrode (**30**) had a greater surface coverage of anthraquinone. However after sonication the coverage dropped significantly and was less than the maleimide-modified electrode (**17d**). The maleimide-modified electrode was more stable, with a small initial drop in coverage followed by no further decrease after sonication, while coverage on the amine-functionalised electrode continued to decrease. This suggests that the anthraquinone thiol had successfully coupled with the maleimide functionalised electrodes and adsorbed non-specifically on the amine functionalised surface.

The oxidation of Boc-EDA was completed by CV, after the first cycle the current decreased dramatically and almost no current was seen after the fifth cycle, which showed that the surface had been blocked by EDA on the surface. However once the bulky Boc group had been removed there would have been a

space around the amine, allowing anthraquinone to adsorb onto the bare glassy carbon. Thiols have been previously shown to react with glassy carbon[78] and this could explain the remaining anthraquinone on the EDA modified electrode after prolonged sonication and washing. In addition the rings of the anthraquinone could be involved in π stacking with the surface of glassy carbon[79].

In order to investigate the amount of non-specific adsorption electrodes were prepared of each of the synthesis intermediates (Scheme 8) and immersed in a solution of anthraquinone-2-carboxylic acid without any coupling agent (Scheme 17).

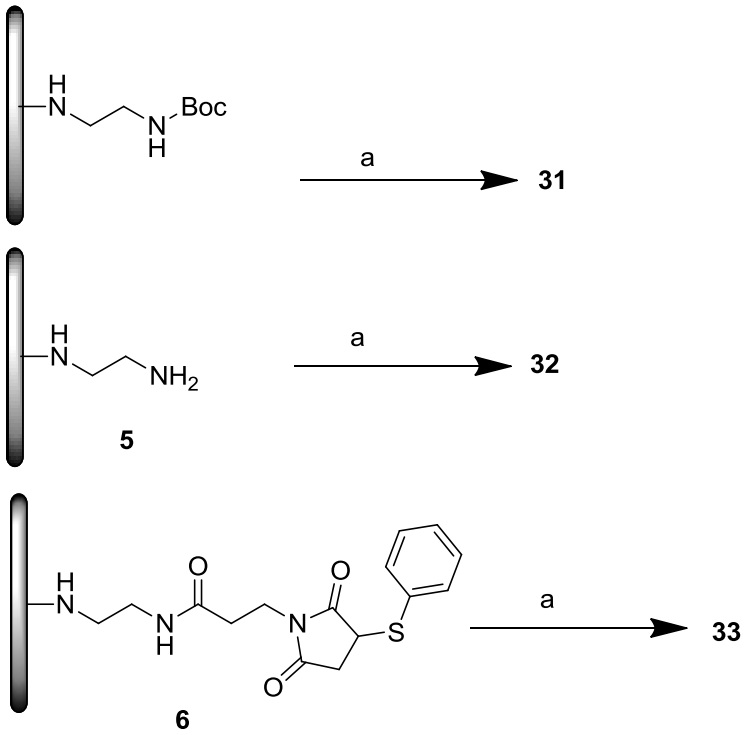

Scheme 17 – Control reactions a) Anthraquinone-2-carboxylic acid in DMF

Electrodes were then tested by cyclic voltammetry to evaluate the surface coverage (Figure 30).

Partial Coverage

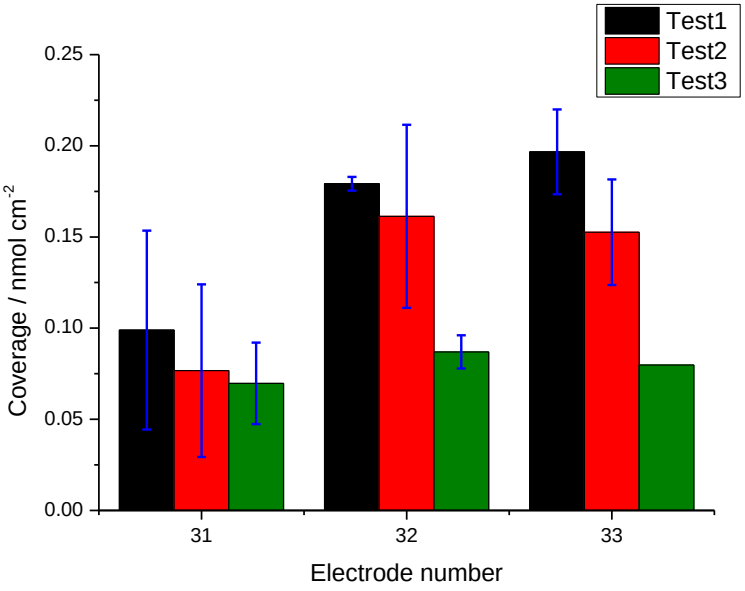

Figure 30 – Coverage of anthraquinone before and after sonication. Coupling procedure shown in Scheme 17. Test 1: first test after washing Test 2: after 10 min sonication, Test 3: After 40 minutes sonication. Each point represents the mean of two replicate electrodes, with standard deviation shown as an error bar.

As shown in Figure 30 the coverage of anthraquinone was dependant on the surface of the electrode, with the smallest coverage on the NHBoc surface which was the most blocked and the drop in coverage was very small after sonication. Following removal of the Boc group, the glassy carbon surface was more accessible and allowed hydrogen bonding to any oxygen functionalities on the surface. Due to the ambient conditions used there would not have been amide bond formation[80] however interactions through hydrogen bonding would have been possible between the amine and carboxylic acid groups. After sonication the coverage significantly dropped as adsorbed anthraquinone was removed, with the final coverage similar to the Boc-protected surface. The protected maleimide, though bulky has a longer chain than the Boc-EDA and would therefore be flexible and allow the anthraquinone to get to the GC surface. In addition the alkyl chains could act like a hydrophobic pocket for the anthraquinone to sit in.

In order to investigate the importance of the carboxyl group on the anthraquinone for interaction with the surfaces, a bare GC electrode was immersed in a solution of anthraquinone without further functional groups (Scheme 18).

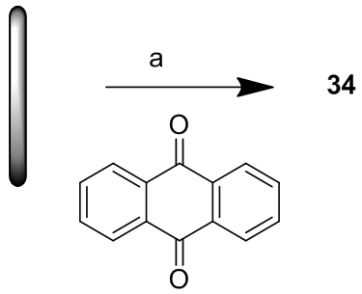

Scheme 18 – Control reaction of Bare GC with anthraquinone

The coverage of anthraquinone on bare GC (**34**) was found to be less than anthraquinone-2-carboxylic acid on any of the modified surfaces. The initial coverage was 7.9 x 10^{-11} mol cm^{-2}, which reduced to 3 x 10^{-11} mol cm^{-2} after sonication. In contrast the Boc-protected, blocked surface (**31**) had an average coverage of 7 x 10^{-11} mol cm^{-2} following sonication which is more than double the coverage of anthraquinone on bare GC (**34**). This result suggests the importance of the carboxylic acid in the affinity of anthraquinone to the surface. However, this also showed that even without coupling reagents or a carboxyl group anthraquinone would stick to a glassy carbon surface.

During partial coverage work acetyl chloride was used as a cap for free amines that remained after coupling the spacer; a capped surface was prepared to evaluate the adsorption of anthraquinone. A full monolayer of EDA was prepared and capped with acetyl chloride then immersed in anthraquinone-2-carboxylic acid coupling solution. For comparison bare glassy carbon electrodes were also immersed in the coupling solution (Scheme 19).

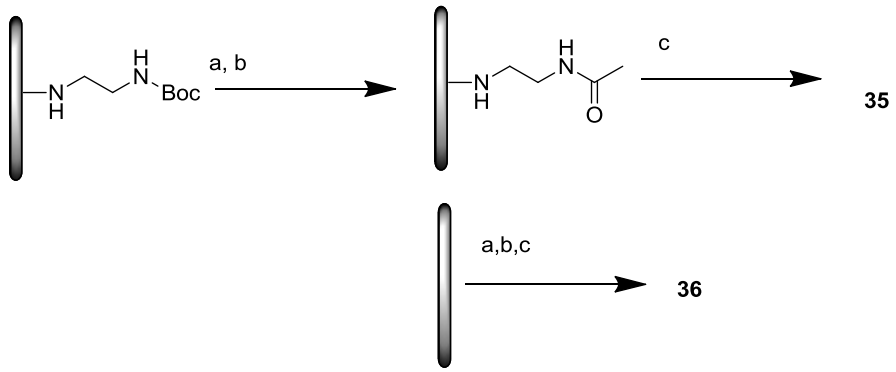

Scheme 19 – Control reactions for anthraquinone coupling on capped surfaces a) 4M HCl in dioxane, 1h b) acetyl chloride, pyridine, DCM c) Anthraquinone-2-carboxylic acid, HBTU, DIEA, DMF, 16 h

Partial Coverage

Electrodes were washed and sonicated until the CV was constant and coverage was calculated (Figure 31).

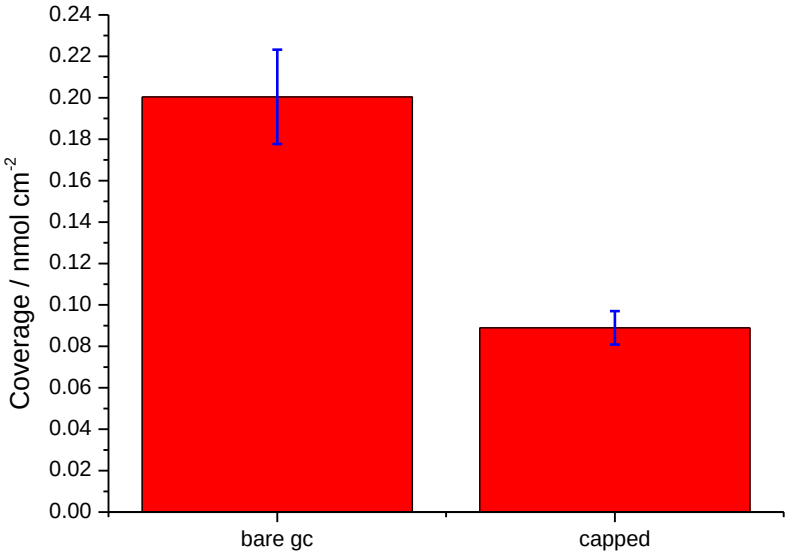

Figure 31 – Coverage of anthraquinone-2-carboxylic acid on bare glassy carbon (**35**) and capped (**36**) electrode surfaces (Scheme 19). Each bar represents the mean of two replicate electrodes, with standard deviation shown as an error bar.

The coverage of anthraquinone on bare glassy carbon was very high despite repeated washing and sonication. The capped surface had approximately half the coverage of anthraquinone compared to the bare glassy carbon, which showed that modification of the surface with different functional groups had an effect on the level of anthraquinone adsorption.

It is important to note that the glassy carbon surface used would have a range of oxygen functionalities on the surface such as carbonyl, hydroxyl and carboxylic acids. Historically these groups were also introduced intentionally to allow bridges to be formed to bond to desired substrates. To increase the amount of surface groups the electrode may be oxidised chemically using reagents such as $KMnO_4$[81] or NaOCl[82]. Oxygen treatment at high temperature[2] or plasma treatment[83] may also be used. An alternative to chemical treatment is anodic oxidation in solutions of H_2SO_4 or HNO_3[84]. The oxygen functionalities created may then be further treated to get the desired functional group on the

surface. Thionyl chloride and acetyl chloride are used as an activating agent[85] and carboxylic acids may be reduced to alcohols if necessary.

Due to the natural occurrence of oxygen on the surface the use of HBTU as a coupling agent could mean the anthraquinone reacted with the GC surface, explaining the anthraquinone that remained on the surface after repeated sonication and washing. Although the acetyl surface (**36**) was modified with Boc-EDA until the surface was 'blocked', when the amine was deprotected the GC surface would have been exposed once the bulky Boc group was removed. Bare GC after removal of the Boc group would be a problem in any work with small molecules; however this would not be a problem when an enzyme was used. Since, due to the size of the enzyme, it would be unable to access the GC surface. However the use of small molecules is important to quantify the surface coverage of linkers used. It was clear that control reactions were important, and the 'non-specific adsorption' was very dependent on the surface used.

3.4 Variation of anthraquinone concentration

Following control experiments the effect of anthraquinone concentration was investigated on amine-modified surfaces and bare glassy carbon electrodes prepared in parallel. Electrodes were immersed in solutions of varying concentration of anthraquinone was varied and HBTU was used as a coupling agent (Scheme 20).

Partial Coverage

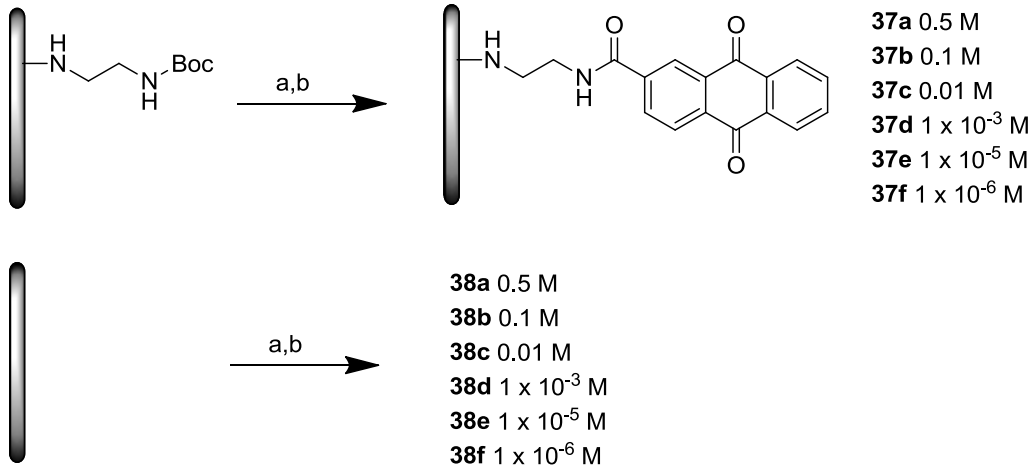

Scheme 20 – Coupling of anthraquinone at different concentrations a) 4M HCl in dioxane b) Anthraquinone 2-carboxylic acid, HBTU, DIEA, DMF.

Following modification the electrodes were extensively washed in DMF to remove as much of the non-specifically bound anthraquinone as possible before electrochemical testing. Electrodes were then tested by cyclic voltammetry at 100 mV/s for 20 cycles, during which time the current stabilised, and coverage was calculated from the 20th cycle when the response was constant. The results were then plotted (Figure 32).

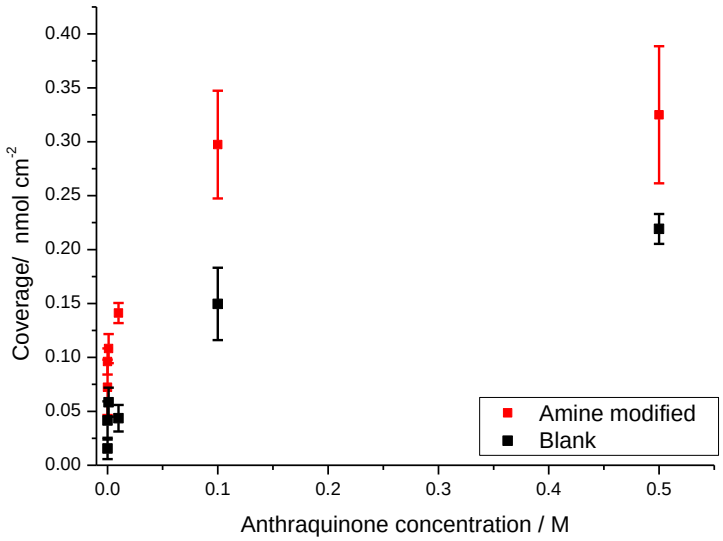

Figure 32 – Coverage after coupling with different concentrations of anthraquinone solution (Scheme 20). Each point represents the mean from 4 replicate electrodes, with standard deviation shown as an error bar.

Anthraquinone coverage was found to increase with the concentration of the anthraquinone in the coupling solution not only in the amine-modified electrodes but also in the control samples. The trend seems to plateau at between 0.1 M and 0.5 M solution, suggesting that the surface had been saturated at this concentration. The maximum coverage of anthraquinone was 3.25×10^{-10} mol cm^{-2} on the amine-modified surface and 2.19×10^{-10} mol cm^{-2} on bare GC. The coverage on the bare GC electrodes is very high, however the 'non-specific adsorption' on the electrode surface could be covalently bound anthraquinone that has reacted with oxygen functionalities on the surface as previously discussed. This effect would be very notable on a bare glassy carbon electrode as no linker such as EDA had been coupled to the surface and all of the GC was available for coupling. However in the functionalised surface only some bare GC would be available for this coupling. It is therefore very important to consider how the surface could be blocked to prevent this kind of effect.

3.5 Spontaneous addition of diazonium salt

A number of studies have shown that diazonium salts attach to the surface spontaneously[86]. This has been shown to be effective on a range of different materials including carbon black, carbon nanotubes[87] and other metals[88].

3.5.1 Anthraquinone

The spontaneous attachment could be used as an alternative method to control the surface coverage of linker. Polished GC electrodes were immersed into a solution of diazonium salt in acetonitrile for times between 2 and 10 minutes, and followed by Boc-deprotection and coupling to anthraquinone (Scheme 21).

Partial Coverage

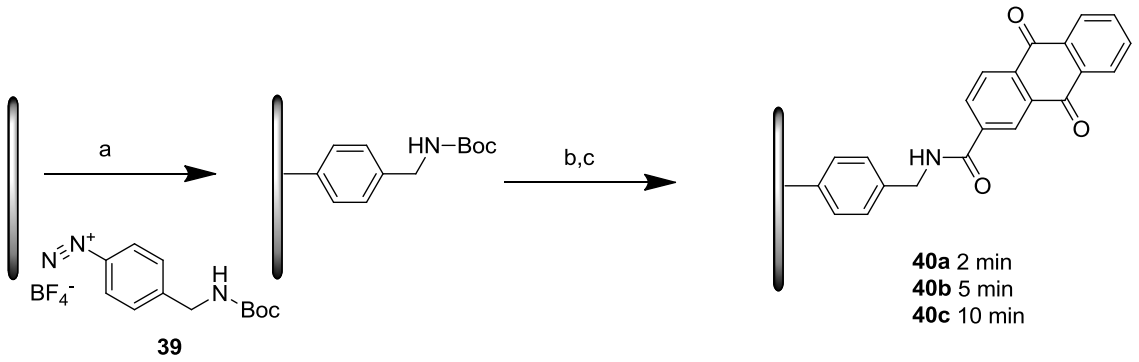

Scheme 21 – Spontaneous attachment of diazonium salt for varying durations followed by anthraquinone coupling. a) **39,** acetonitrile, TBATFB, 2-10 min, b) 4 M HCl in Dioxane, 1 h, c) Anthraquinone-2-carboxylic acid, HBTU, DIEA, DMF, 16 h.

Following washing and sonication electrodes were tested by CV and coverage was calculated from the 10th cycle.

Figure 33 – Anthraquinone coverage after spontaneous attachment of diazonium salt, coupling procedure shown in Scheme 21. Each point represents the mean of two replicate electrodes, with standard deviation shown as an error bar.

The coverage of anthraquinone was very high, presumably due to the high concentration used and the amount of bare glassy carbon available on surfaces with a low coverage of linker. If the 2 min result, with a very large error, was

ignored then the 5 minute and 10 minute results appear to fit a reasonable trend, however with only three points this is a very tentative conclusion. Electrodes immersed for two minutes would be expected to have the least linker on the surface, leaving a lot of bare glassy carbon for the anthraquinone to interact and react with, meaning that this electrode would have a high level of non-specific attachment as well as the desired coupling, which could contribute to the large error. Due to the large errors and non-specific attachment of anthraquinone on bare glassy carbon an alternative redox probe which does not interact with the surface would be preferable.

3.5.2 Dihydroxybenzene

Dimethoxybenzene was used in other work by Bartlett, Kilburn *et al.*[43, 45] and preliminary work suggested that it stuck to the surface less than anthraquinone and therefore it was investigated as an alternative redox probe. A number of electrodes were prepared by immersion in diazonium solution for 30 s – 10 min, then deprotected and coupled with dimethoxybenzene (Scheme 22). Following hydrolysis of the methoxy groups the electrodes were tested by CV and the coverage calculated.

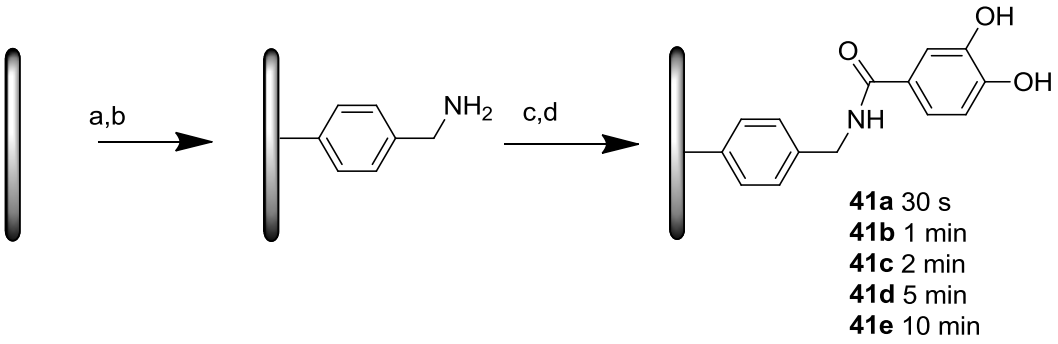

Scheme 22 – Modification of coverage by spontaneous addition of diazonium salt a) **39,** acetonitrile, TBATFB, 0.5-10 min , b) 4 M HCl in Dioxane, 1 h, c) 3,4-dimethoxybenzoic acid, HBTU, DIEA, DMF, 16 h, d) 1 M BBr_3 in DCM, 1 h.

Upon testing the current was found to constantly decrease on cycling and did not reach a stable current (Figure 34). In addition electrodes were re-tested by cyclic voltammetry after washing and found to have no remaining current, the dihydroxybenzene was found to be very unstable on the surface.

Partial Coverage

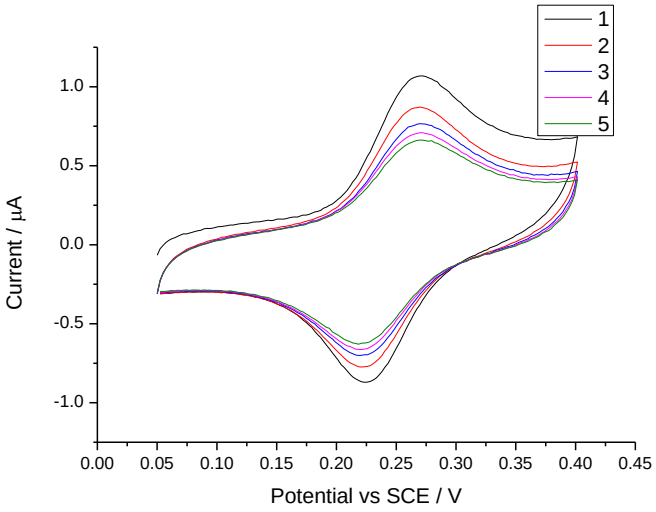

Figure 34 – First five cycles of CV of **41c** at 50 mV s^{-1} in 100 mM pH7 phosphate buffer with 100 mM TEATFB. Coupling procedure shown in Scheme 22.

Due to the instability electrodes were tested immediately after deprotection and both the first (Figure 36) and fifth cycles (Figure 35) were integrated for coverage calculations. In addition due to the inconsistency of the results the same experiment was repeated a number of times (i-v), each time duplicate electrodes were prepared in parallel for each of the durations in diazonium solution, and tested by cyclic voltammetry before calculation of the coverage.

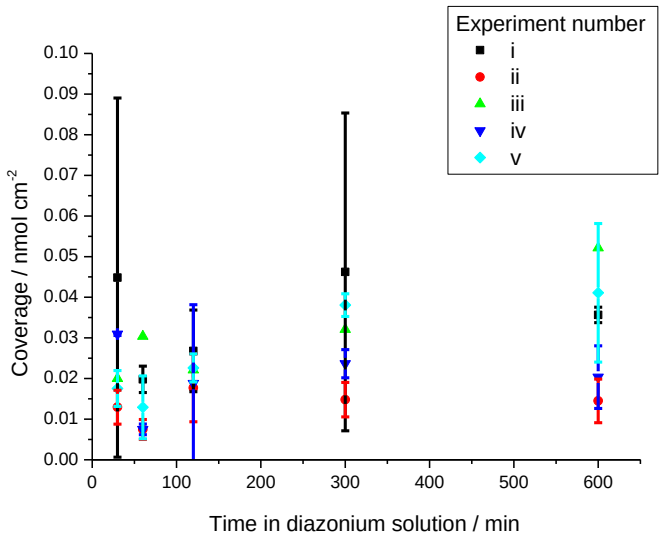

Figure 35 – Coverage of dihydroxybenzene on calculated from the 5th cycle of cyclic voltammetry on electrodes after immersion spontaneous addition of diazonium salt. Coupling procedure shown in Scheme 22. Each set of points (i-v) represents a separate

experiment done at a different time. Each point represents the mean coverage from two replicates, with the standard deviation shown as an error bar.

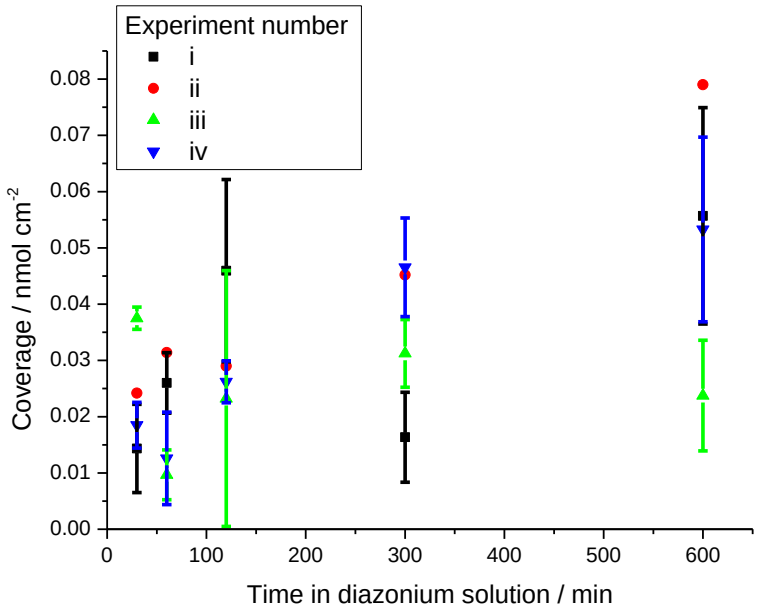

Figure 36 – Coverage of dihydroxybenzene calculated from the 1st cycle of CV on electrodes after immersion spontaneous addition of diazonium salt, coupling procedure shown in Scheme 22. Each set of points (i-iv) represents a separate experiment done at a different time. Each point represents the mean coverage from two replicates, with the standard deviation shown as an error bar.

Although there is a general trend of increasing coverage with increased time in diazonium solution the results are very inconsistent. The errors are large and the trend seems unclear from electrodes that were prepared in parallel. The same experiment was also done with a number of different concentrations (0.2 mM, 0.5 mM, 1 mM, 5 mM) of diazonium solution to see if that had any effect on the results (Figure 37).

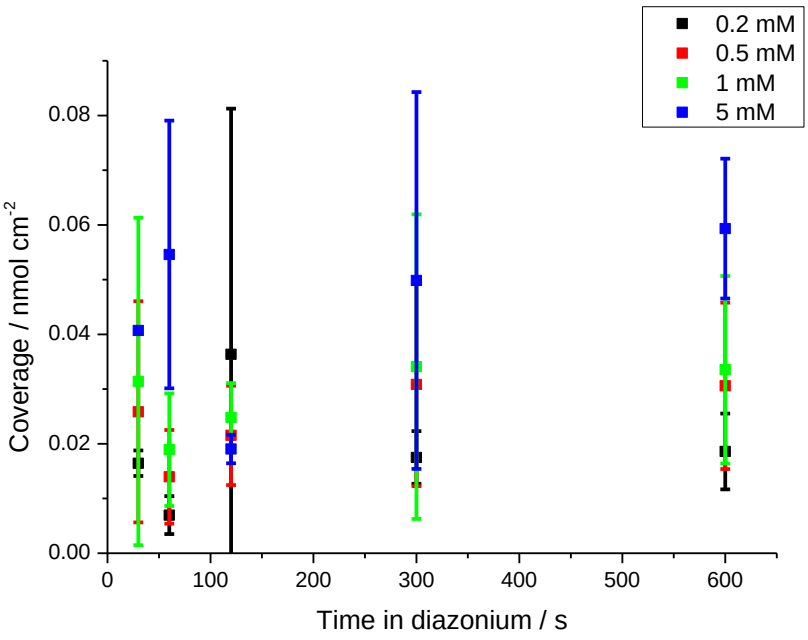

Figure 37 – Average results of anthraquinone coverage after variation of diazonium salt concentration and duration of attachment. Coupling procedure as Scheme 22. Each point represents the mean coverage from at least two replicates, with the standard deviation shown as an error bar.

Once all the results were plotted together it was clear that the spontaneous attachment of diazonium salt (**39**) was not a reliable method of controlling the surface coverage. Very large errors and scattered results were observed, possibly due to the relative instability of diazonium salts.

3.6 Short bursts of potential

While control of the concentration had an effect on the surface coverage of anthraquinone there were limitations to this method. The removal of the Boc group created gaps in the blocked surface and the coverage of free amines was not related to the desired surface coverage and free amines remained on the surface after anthraquinone coupling.

The control of coverage on the surface would be better done from the first modification step, this way the amount of free amines on the surface would reflect the desired surface coverage and no later capping or blocking of the

surface would be needed. In addition the amount of bare glassy carbon would be less as the Boc group would only be removed from the amines to be coupled, not the whole surface.

A full monolayer of amine on the electrode surface is often prepared by either oxidation of an amine or reduction of a diazonium salt, usually using cyclic voltammetry. Multiple cycles are used in a reasonably wide potential range in order to completely block the surface. However, if the potential of oxidation or reduction is used and held for a short time the radical could form and attach to the surface, but not block it.

3.6.1 Oxidation of amine

To create a full monolayer of EDA on the surface the potential was cycled from 0.8-2.1 V vs Ag/AgCl for 5 cycles, however the amine was oxidised at ~1.8 V vs Ag/AgCl and the surface was almost blocked after the first cycle. In order to reduce the coverage of linker the potential was stepped to 1.8 V vs Ag/AgCl and held for varying durations. Following this electrodes were washed with acetonitrile, to remove any unreacted amine, then the Boc group was removed and acetonitrile was coupled (Scheme 23). In addition, based on the work with concentration a low concentration of anthraquinone was used to avoid side reactions with any bare GC.

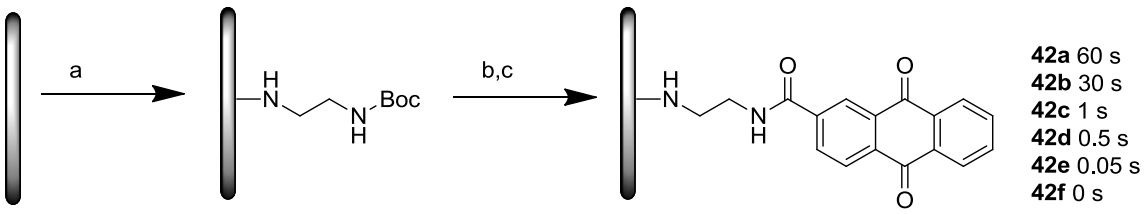

Scheme 23 – Attachment of EDA using potential steps of varying duration followed by coupling of anthraquinone. A) 1.8 V vs Ag/AgCl. Boc-EDA, Acetonitrile, TBATFB, b) 4 M HCl in Dioxane, 1 h, c) Anthraquinone-2-carboxylic acid, HBTU, DIEA, DMF, 16 h.

Following anthraquinone coupling electrodes were washed extensively with DMF before being tested by CV, after 20 cycles the current had stabilised and the coverage was then calculated from the 20th cycle (Figure 38).

Partial Coverage

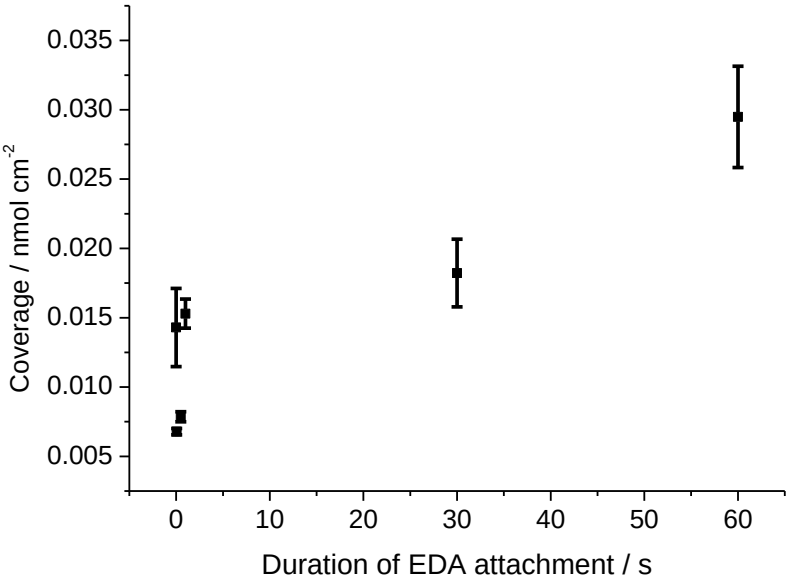

Figure 38 – Coverage of Anthraquinone after varying duration of linker attachment, average of 4 electrodes. (Scheme 23).

Anthraquinone coverage appears to be dependant on the duration the potential was held for, the greatest coverage, 2.9 x 10^{-11} mol cm^{-2} being achieved after a 60 s at 1.8 V vs Ag/AgCl in EDA solution. The previous work with a full monolayer of EDA using a 1 μM solution of anthraquinone gave a full monolayer coverage of 7.2 x 10^{-11} mol cm^{-2}, suggesting approximately a 40 % coverage is achieved after 60 s at 1.8 V vs Ag/AgCl. The lowest coverages were achieved with the low pulse durations, with a 9 % layer being achieved after 50 ms in EDA solution at 1.8 V vs Ag/AgCl.

The coverage of a bare GC electrode immersed in a 1 μM solution of anthraquinone was 1.4 x 10^{-11} mol cm^{-2}, very close to the coverage of electrodes held at 1.8 V vs Ag/AgCl for 1s and greater than electrodes held at 1.8 V vs Ag/AgCl for 500 ms or 50 ms, with coverages of 7.8 x 10^{-12} mol cm^{-2} and 6.8 x 10^{-12} mol cm^{-2} respectively. It is therefore very difficult to determine conclusively how much of the coverage on modified electrodes is down to undesirable side reactions and non-specific adsorption and how much is covalently bound in the desired orientation. However general trends are apparent at levels above non-specific adsorption.

The results from this work were promising; though it remained clear that blocking bare glassy carbon was very important and must be considered in future work.

3.7 Mixture of amines

Though there are a number of reliable procedures to create a close packed monolayer on the surface[12, 28, 89] there has been less research into mixed monolayers on carbon. However there has been a number of mixed monolayers of thiols on gold[11, 53, 90] reported. Mixed monolayers have been formed from mixtures disulphides and thiols, where a preference for adsorption of thiols over disulphides was observed[15b]. Whitesides *et al*. prepared a SAM resistant to non-specific protein adsorption[15c]. Carboxylic acid terminated thiols were adsorbed on gold, following activation with acetic anhydride, a range of amines were coupled to the surface to introduce disorder. This method allowed more variation in the surface than traditional methods involving the adsorption of ethylene glycol thiols on gold while successfully preventing non-specific adsorption of proteins.

Due to the mobility of thiols on the gold surface the layers formed are dynamic and can change if they are left in the deposition solution[11]. Long chains were favoured over the short chains and if gold was left in the deposition solution the longer chain component exchanged onto the surface[16], meaning the fraction of the two thiols in the deposition doesn't necessarily represent the percentage on the surface.

A mixture of long and short chain thiols was used to monitor the composition of mixed layers; the thickness of the layer was used to determine the relative concentration of the different components. The results showed that the most stable layers were long chain thiols, with short chain thiols being less stable and the least stable layers were mixtures, but also that the mixture separated into small islands of long or short chains on the surface[13]. It was later found that even very similar thiols separated into different phases on a nanometre scale[14-15] . The separation observed is possible on gold due to the mobile nature of the gold-sulphur bond; however a covalent bond to carbon would not have this problem.

Partial Coverage

The preparation of a mixed monolayer of diazonium salts has been investigated by a number of groups. Gooding *et al.* investigated the addition of a mixture of diazonium salts prepared *in situ* with a mixture of pre-prepared diazonium salts and found little difference between the two sets of results. The surface coverage of the diazonium salts were measured using XPS which showed that the ratio on the surface was not exactly as in solution. The more easily reduced diazonium salt had a greater surface coverage than the initial concentration in the reduction solution, however a mixture on the surface was formed[38c].

A mixed layer of 4-carboxyphenyl and phenyl diazonium salts was formed on glassy carbon electrodes and Ferrocenemethylamine was coupled to the carboxylic acid-functionalised surface. The mixed layer was formed by reduction of a mixture of the diazonium salts and confirmed by XPS analysis[22a]. When the results were compared to a mixed layer of thiols on gold, it was discovered that the electron transfer on gold was faster; suggesting that multilayers had formed on the mixed diazonium salt layer.

Mixed layers have also previously been prepared for protein electrochemistry. Mixed poly-ethylene glycol (PEG) layers were prepared by reduction of a mixture of PEG and oligo(phenylethynylene)-based diazonium salts onto glassy carbon electrodes. PEG was used as a group to stop the non-specific adsorption of proteins onto the electrode and ferrocene methylamine and horseradish peroxidise were coupled to the other group, allowing direct electron transfer[91].

While the use of diazonium salts has been widely reported there are a number of disadvantages such as limited stability and formation of multilayers[39]. However the use of mono-Boc-protected diamines has avoided these problems and has been successfully used to create stable monolayers of carbon.

The oxidation of a mixture of two amines was investigated. A mixture of a mono-Boc-protected diamine and a ‘capping group’ was prepared in solution and then oxidised onto the glassy carbon surface. The use of different ratios of the amines in solution was proposed to create mixtures of amines on the surface proportional to the ratio of amines in solution (Scheme 24).

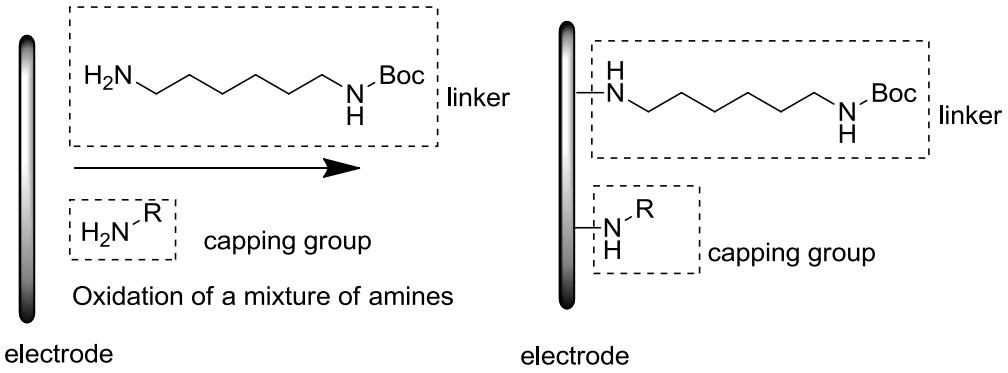

Scheme 24 – Attachment from a mixture of amines

The purpose of the capping group initially was just to space out the amine on the surface. Therefore, in order to optimise coupling to the amine, the capping group would need to be a small molecule shorter in length than the amine. Initially propylamine was chosen as it is a small amine with a short chain. However upon investigation by CV the surface was not easily blocked by the small molecule and after 15 cycles current was still seen. The attachment of propylamine may have be proceeding well, but the small nature of the molecule means that the passage of the current is not blocked well, unlike the bulky Boc group which will quickly block the surface. In addition to this propylamine is much more volatile, and due to this the ratio of the mixture may not be reliable. Therefore for this application propylamine is not suitable as a blocking group. Benzylamine was then chosen as an alternative capping group and *N*-Boc-1,4-butanediamine (Boc-BDA) was chosen as the diamine.

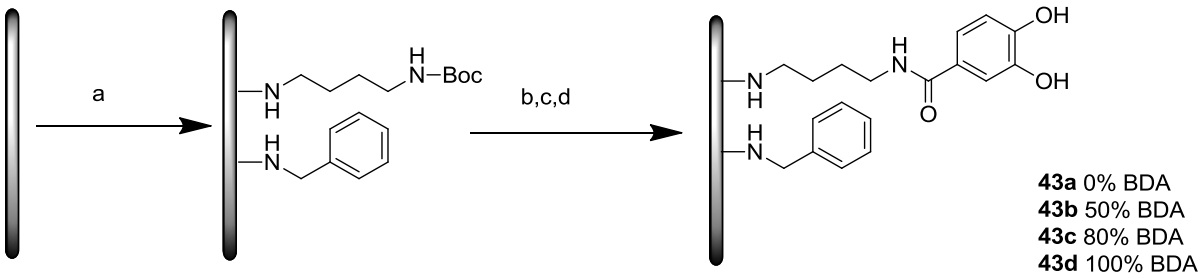

Scheme 25- Attachment from a mixture of *N*-Boc-1,4-butanediamine (Boc-BDA) and benzylamine a) Oxidation of a mixture of amines (0-100 % Boc-BDA, 0-100% benzylamine) 2.1 V vs Ag/AgCl 180 s or 0.8-2.1 V vs Ag/AgCl b) 4M HCl in dioxane, 1 h c) 3,4,dimethoxybenzoic acid, HBTU, DIEA, DMF d) 1 M BBr_3 in DCM.

Partial Coverage

The mixture was attached by both CV (Figure 39) and holding the potential at 2.1 V vs Ag/AgCl (Figure 40), a potential that both amines would be oxidised at immediately.

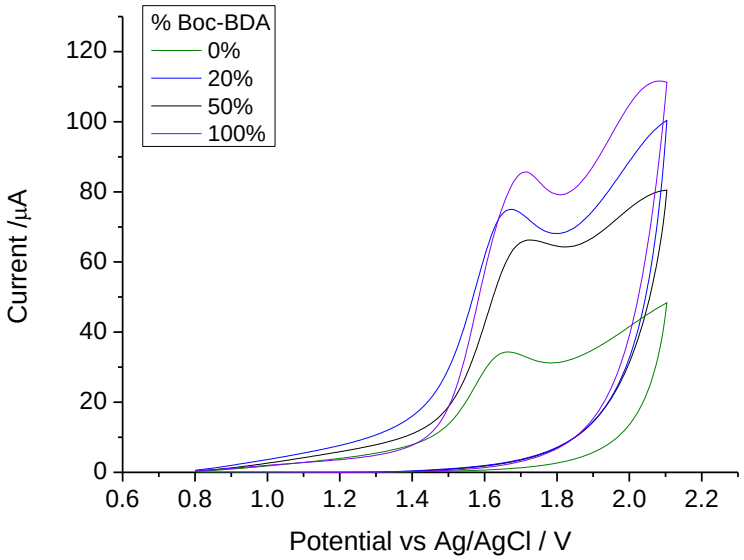

Figure 39 – Oxidation of a mixture of Boc-BDA and Benzylamine (Scheme 25) by CV at 75 mV/s 0.8-2.1 vs Ag/AgCl, argon saturated solution. First cycle shown.

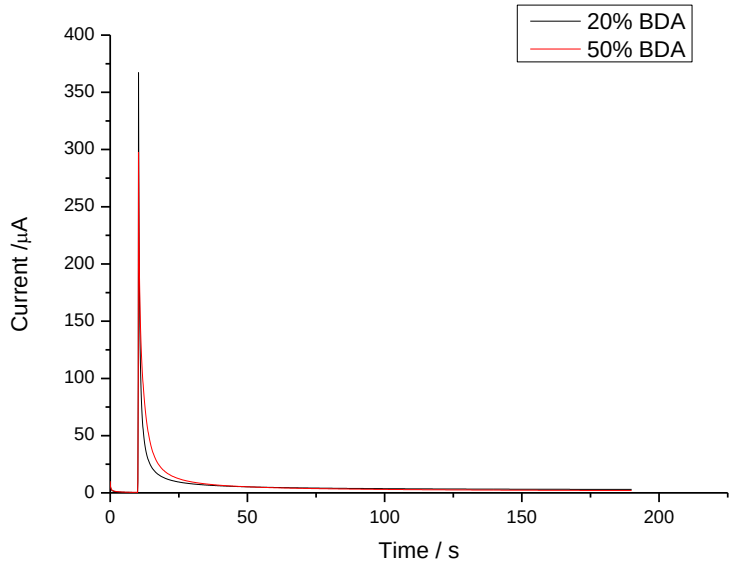

Figure 40 – Attachment from a mixture of BDA and Benzylamine (0-80% Benzylamine, 20- 50% Boc-BDA) total amine concentration 10 mM. Potential stepped to 2.1 V vs Ag/AgCl for 180 s.

From the cyclic voltammetry it is seen that the potential the amines were oxidised at was slightly different, which could mean that the amine oxidised at a lower potential would be present at a higher concentration on the surface. Therefore the better approach is chronoamperometry as both amines are easily oxidised at 2.1 V vs Ag/AgCl. Following the attachment of the mixture to the surface the Boc group was removed and dimethoxybenzene was then coupled to the free amine on the surface. After treatment with BBr_3 the electrodes were tested electrochemically for the presence of dihydroxybenzene and the surface coverage was calculated from the resulting cyclic voltammetry.

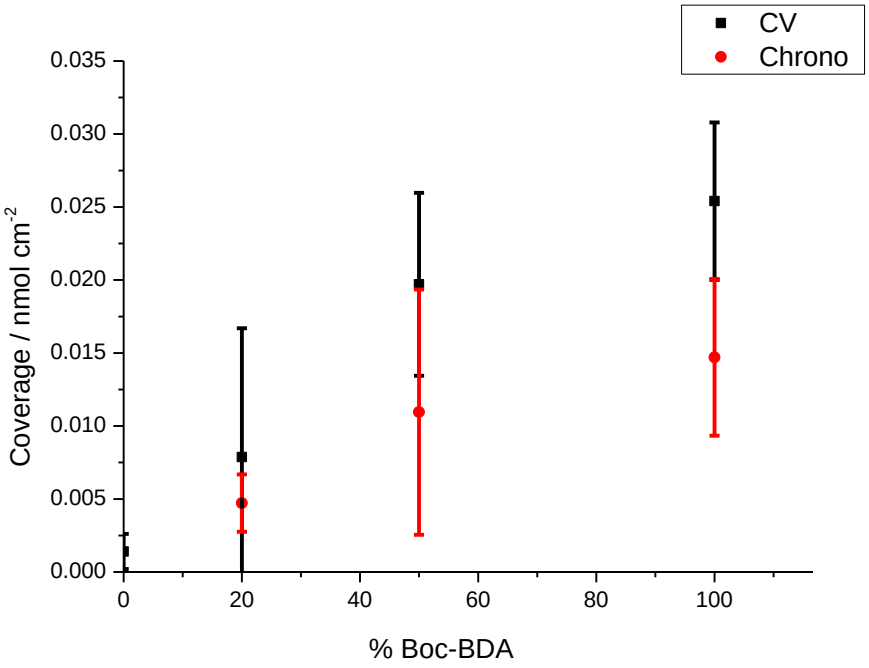

Figure 41 – Coverage of dihydroxybenzene from a mixture of BDA and benzylamine. Coupling procedure shown in Scheme 25. Each point represents the mean value from two replicates with standard deviation shown by the error bar.

The coverage for electrodes prepared by cyclic voltammetry and chronoamperometry both show the same trend (Figure 41), the coverage increases as expected with increasing the Boc-BDA solution concentration. The coverage also appears to be greater for the electrodes prepared using cyclic voltammetry; this is likely to be due to the potential being cycled for a greater time. The control electrode prepared with just benzylamine shows some non-specific adsorption of dimethoxybenzene (1.4×10^{-12} mol cm^{-2}). However this is

Partial Coverage

only 5% of the full monolayer coverage (2.5 x 10^{-11} mol cm^{-2}) achieved by cyclic voltammetry.

The aromatic structure of benzylamine on the surface is similar to the surface of GC, and it is possible that an amine radical would attack it, leading to undesirable multilayers on the surface. Due to this benzylamine is not a good capping group and an alternative was needed.

In section 3.3 EDA was coupled to the surface and capped with acetyl chloride, this surface was shown to have the least non-specific adsorption of anthraquinone. For this reason *N*-(2-aminoethyl)acetamide was chosen as a capping group. In addition the chain length of the mono-Boc protected diamine was lengthened by two carbons, using *N*-Boc-1,6-hexanediamine (Boc-HDA), to ensure that the amide coupling was not hindered.

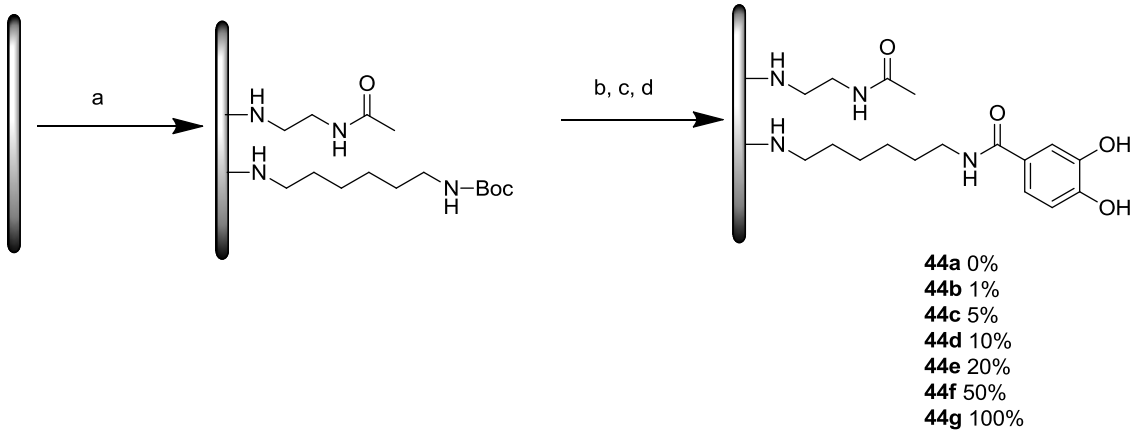

Scheme 26 – Attachment from a mixture of Boc-HDA and N-(2-aminoethyl)acetamide a) Oxidation of a mixture of amines (0-100 % Boc HAD, 0-100% benzylamine) in acetonitrile, 2.1 V vs Ag/AgCl 180 s or 0.8-2.1 V vs Ag/AgCl b) 4M HCl in dioxane, 1 h c) 3,4,dimethoxybenzoic acid, HBTU, DIEA, DMF d) 1 M BBr_3 in DCM.

Mixtures of Boc-HDA and aminoethylacetamide were prepared and oxidised onto the surface by stepping the potential to 2.1 V vs Ag/AgCl for 180 s (Scheme 26). The Boc group was then removed and dimethoxybenzene was coupled to the free amine, following demethylation with BBr_3. The electrodes were tested by cyclic voltammetry and coverage was calculated (Figure 42).

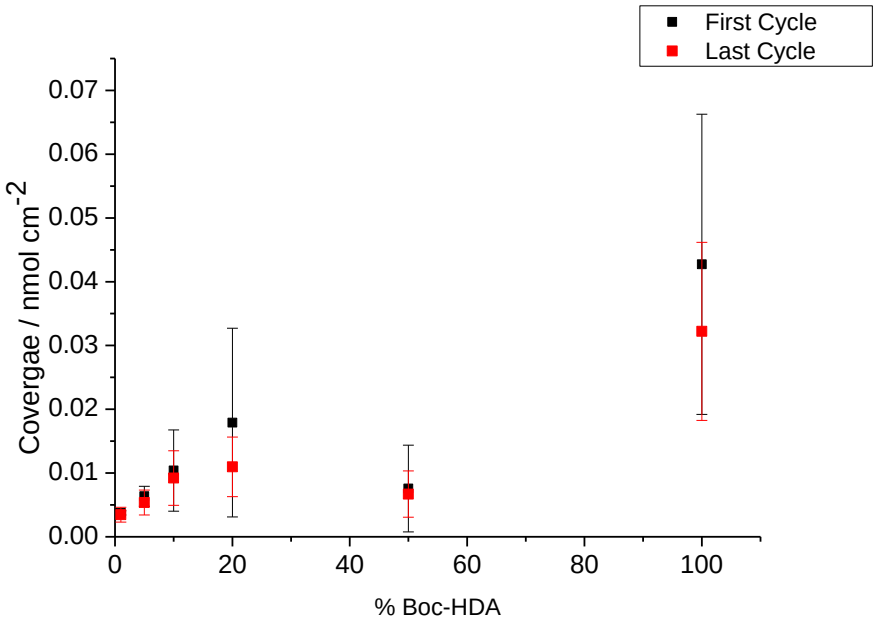

Figure 42– Variation of the coverage of dihydroxybenzene resulting from different concentration of HDA. Coupling procedure shown in Scheme 26. Each point represents the mean of three replicate electrodes, with the standard deviation shown in an error bar.

The coverage of dihydroxybenzene (Figure 42) on the surface appeared to be directly proportional to the concentration of the Boc-HDA present in the starting mixture. There was however a drop at 50% coverage, which did not fit with the general trend, presumably due to an error. In addition both the first cycle and the last cycle were shown and a clear decrease in coverage with cycling is evident with every example. As previously discussed the decrease in coverage is due to the instability of dihydroxybenzene on the surface.

To ensure the consistency of the method the experiment was repeated using high throughput methods. Both dihydroxybenzene and anthraquinone were used as electroactive groups to test the coverage. Electrodes were prepared in parallel and modified with the amine mixtures prepared from mixing stock solutions in different proportions. Following the removal of the Boc group the amines were then coupled to either anthraquinone-2-carboxylic acid or 3,4-dimethoxybenzoic acid (Scheme 27).

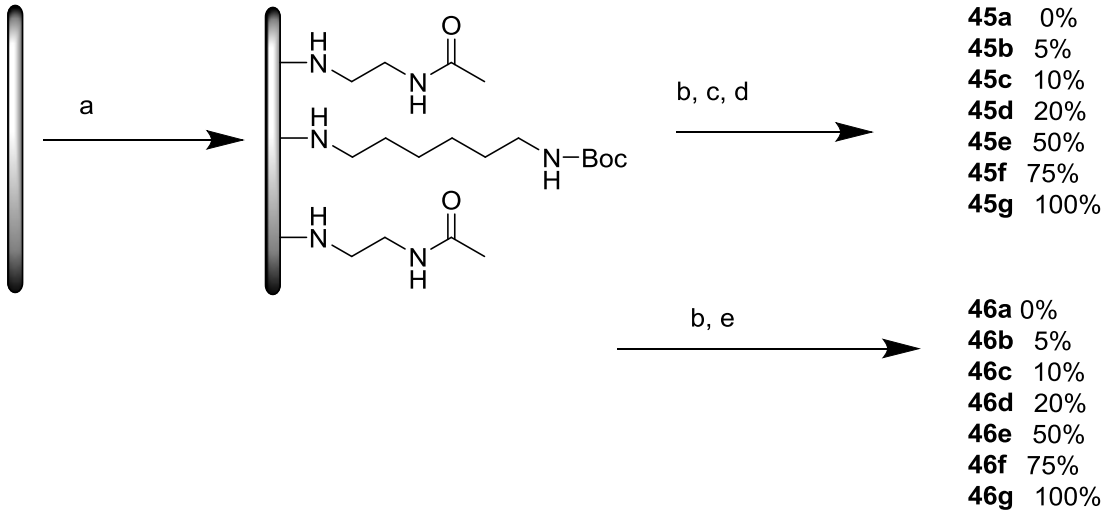

Scheme 27 – Partial coverage from a mixture of amines. a) Oxidation of a mixture of amines (0-100 % Boc HDA, 0-100% aminoethylacetamide, total amine concentration 10 mM) in acetonitrile 2.1 V vs Ag/AgCl 180 s or 0.8-2.1 V vs Ag/AgCl b) 4M HCl in dioxane, 1 h c) 3,4,dimethoxybenzoic acid, HBTU, DIEA, DMF d) 1 M BBr_3 in DCM e) anthraquinone-2-carboxylic acid, HBTU, DIEA, DMF, 16 h.

As shown in Figure 43 and Figure 44 there is a clear relationship between the proportion of Boc-HDA and the amount of either dihydroxybenzene (Figure 44) or anthraquinone (Figure 43) on the surface.

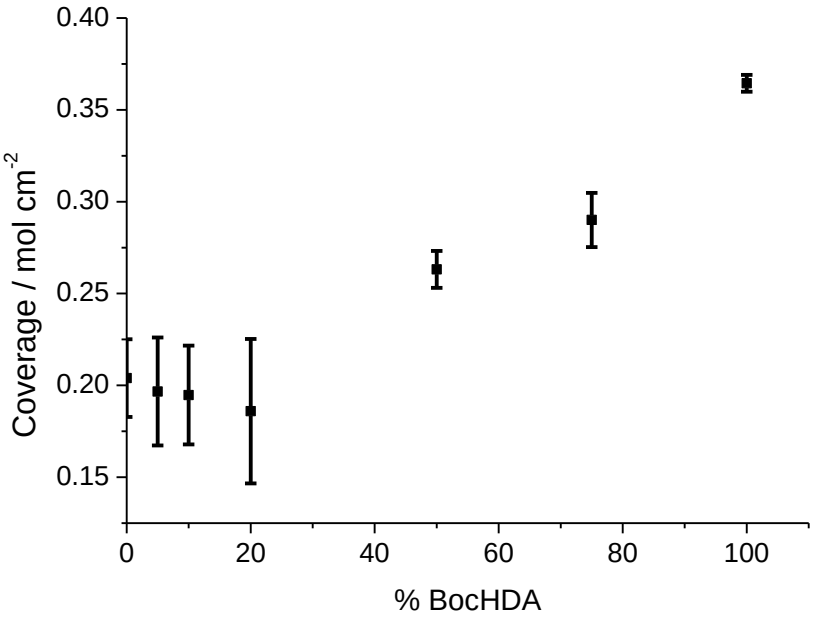

Figure 43 – Coverage of Anthraquinone with varying concentration of Boc-HDA. Coupling procedure shown in Scheme 27**.** . Each point represents the mean of three replicate electrodes, with the standard deviation shown in an error bar.

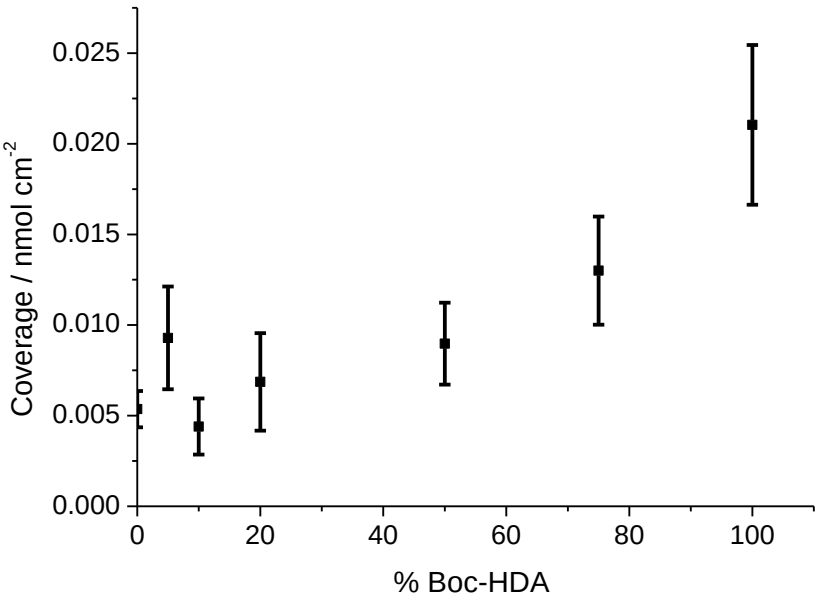

Figure 44 – Coverage of dihydroxybenzene with varying concentration of Boc-HDA. Coupling procedure shown in Scheme 27. Each point represents the mean of three replicate electrodes, with the standard deviation shown in an error bar.

This trend is clear for the high concentrations but below 20% the coverage found is very close to the amount which will bind to the surface non-specifically as shown by the coverage at 0% Boc-HDA. This shows how it is very difficult to quantify any low surface coverage due to the quantity of redox groups sticking to the surface. In addition to this at low concentrations the amount of anthraquinone on the surface has a larger error, reflecting the non-specific aspect of the binding.

3.8 Conclusions

A number of methods to create a partial coverage on electrodes were attempted. It was discovered that the reporter groups used would also stick non-specifically to bare GC as well as couple with amines on the surface. This created problems in determining the coverage of linker on the surface.

The use of varying oxidation time for EDA attachment appeared to have an effect on anthraquinone coverage; however this method left a lot of bare GC, in particular for the lower coverages which would need to be later filled with a capping group to prevent non-specific adsorption of other molecules.

It has been shown using two different reporter groups, anthraquinone and dihydroxybenzene, that a coverage proportional to the amount of Boc-protected amine in the oxidation solution may be achieved at concentrations above 20%. An alternative method of analysis is required to resolve concentrations lower than 20% due to the amount the reporting groups stick to the surface.

This mixture method may be used to attach enzymes and have different groups surrounding them, to see the effect on enzyme activity and binding. This is explored in Chapters 4 and 5.

4. Cytochrome C – a model protein

4.1 Aims of the work

Following the successful preparation of electrodes with maleimide functionality on the surface and subsequent attachment of simple molecules via a thiol linkage, the next logical step was to use the maleimide linkage to couple biomolecules. Proteins often denature in the organic solvents which we used for coupling the simple thiols so the coupling would need to be tested in aqueous buffers. As engineered proteins take some time to prepare and are often available only in small amounts a widely available model protein was used initially. Cytochrome C (Figure 45) is a commercially available redox protein, and Cytochrome C from bovine heart has a cysteine residue (highlighted in yellow, Fig 1) near the haem, so was considered to be a suitable model for coupling to our maleimide functionalised electrodes. The active site of the redox protein has a haem group which allows it to be detected electrochemically.

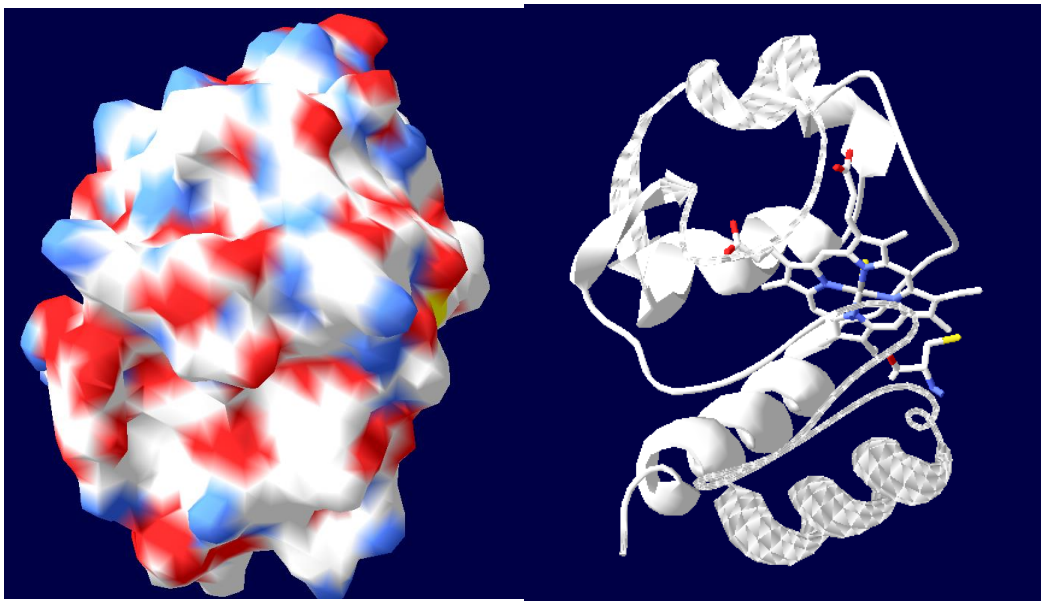

Figure 45 – Structure of Cytochrome C drawn from PDB file '2B4Z'. Left: surface of Cytochrome C. Right: ribbon structure with haem and cysteine (yellow) shown.

Cytochrome C was the first redox-active protein in which DET (direct electron transfer) was studied[92]. The first examples of DET between Cytochrome C and an electrode were described in 1977 by Yeh *et al.*[93] at a tin-doped indium oxide

electrode and Hill *et al.* at a gold electrode using 4,4'-bipyridyl as a promoter in the solution[94]. Diffusion controlled voltammetry was observed in both examples, indicating a one electron transfer process. The electron transfer is believed to be enabled by a transient mechanism similar to the binding of Cytochrome C *in vivo*. Lysine groups near the haem are aligned to the electrode surface by electrostatic interactions with anionic groups on the surface. *In vivo* the same attraction between positively charged lysines and anionic groups on another protein surface allow protein-protein interactions by hydrogen bonding or salt bridges[95].

A whole range of modifiers have since been investigated. Hill *et al.* used a bifunctional strategy with X-Y modifiers, X to bind to the electrode surface using a thiol or disulphide, and Y to bind to Cytochrome C using anionic groups such as phosphate and carboxylate[56c, 95a]. This method was advantageous as it followed the same mechanism used in nature, preventing denaturation of the protein[96]. Other groups have prepared other carboxylic acid terminated[56b, 97] and pyridine/imidazole terminated[98] SAMs and successfully orientated and bound Cytochrome C to electrode surfaces.

The covalent attachment of Cytochrome C has also been demonstrated using carboxylic acid terminated SAM of thiols on gold[56b, 99], and later from diazonium salts[100] and on polymers[101]. After adsorption of Cyctochrome C onto the carboxylic acid monolayer, EDC coupling was used to covalently bind lysine residues on the protein to the carboxylic acid layer on the electrode surface. More recently vertically aligned carbon nanofibres have been modified with a range of functional groups, including carboxylic acids to bind Cytochrome C[102].

Mixed monolayers have also been prepared to bind Cytochrome C,[97c, 103]. In addition to a reactive group to bind the Cytochrome C, a diluent, not designed to bind to the protein, was used to space out the reactive group on the electrode surface. The use of a diluent was shown to have an effect on the electron transfer rate, with the fastest electron transfer rate constant on the surfaces diluted with hydroxyl[104] or methyl-terminated[103b] thiols.

Yue *et al.* found that diluting the amount of carboxylic acid or pyridine on the electrode surface increased the rate constant for electron transfer[103c]. The diluents were thought to provide an alternative electron transfer pathway, shortening the distance the electron must travel. However if the diluent used

has a repulsive effect then binding and electron transfer could be hindered. Whitesides *et al.* used alkane thiols terminated with sulphonate groups as a diluent which was found to cause the Cytochrome C to orientate differently on the electrode, preventing fast electron transfer.[105]

4.2 Purification of Cytochrome C

Commercially sourced Cytochrome C is often insufficiently pure for electrochemical use and is usually re-purified before use, most commonly by ion exchange chromatography[106]. There are a number of reports about the extraction and purification of Cytochrome C[107].

Initially the electrochemical activity of the Cytochrome C (Sigma-Aldrich, Cytochrome C Bovine heart BioChemika ≥95%) was investigated using the procedure of Hill *et al.*[108] to determine if the purity was sufficient for further work. The Cytochrome C was tested by CV using gold electrodes, with and without 4,4'-bipyridyl in solution, however no redox peaks or change in electrochemistry was seen, indicating that the Cytochrome C was insufficiently pure. Following the poor electrochemical results the sample was analysed by gel electrophoresis (Figure 46).

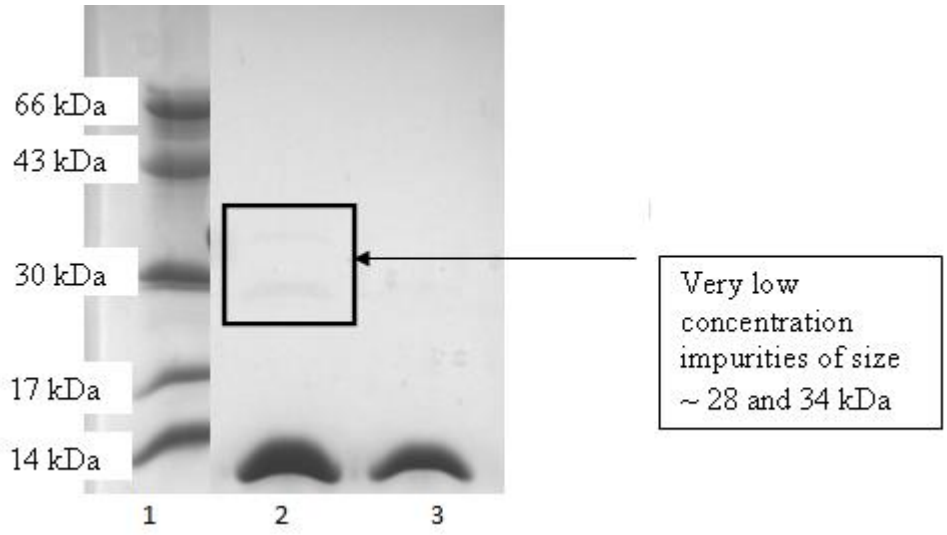

Figure 46 –15% SDS PAGE of Cytochrome C from bovine heart (Sigma-Aldrich, BioChemika ≥95%) , lane **1** – MW marker (kDa), **2** – 1 mg/mL, **3** – 0.5 mg/mL

Two samples of Cytochrome C, at different concentrations, were prepared in phosphate buffer, for analysis. The more concentrated sample (**1,** 1 mg/mL) of Cytochrome C (12.3 kDa) shows small impurities at 28 and 34 kDa (Figure 46)

that are not clear in the less concentrated sample. On the basis of these results the Cytochrome C required purification. The ion exchange purification outlined by Margoliash *et al.*[107b] was followed with a few changes. Instead of the Amberlite IRC-50 ion exchange column an SP-Sepharose column was used. However due to the stronger binding of the Cytochrome C to this column, the concentration of the sodium chloride used by Margoliash[107b] was not great enough to displace the Cytochrome C so a second gradient from 0.5 M to 1M NaCl had to be used. Following the ion exchange purification the eluted fractions were analysed by gel electrophoresis but the purity had not changed significantly, with the impurities at 28 kDa and 24 kDa still present (Figure 47).

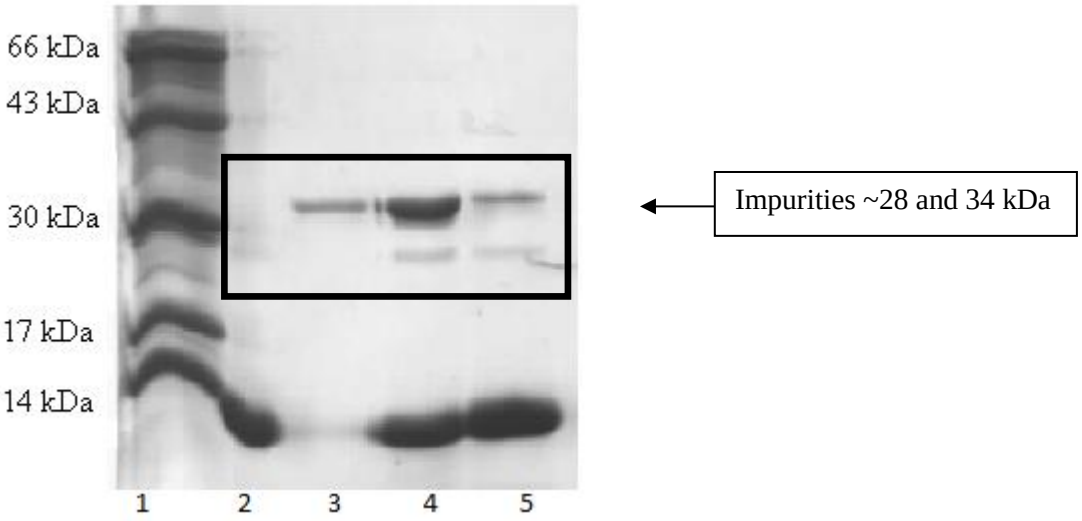

Figure 47 – 15% SDS PAGE after purification, lane **1** – MW marker (kDa), **2** – commercial Cytochrome C (0.5 mg/mL), **3** – F47 (0 mg/mL), **4**- F46 (0.97 mg/mL), **5** –F45 (0.75 mg/mL)

Eluted fractions 45 and 46 were combined and concentrated from ~24 mL to 3.5 mL and further purified using S75 gel filtration column in order to remove the higher molecular weight impurities and to exchange the buffer to a buffer suitable for further work. The protein containing fractions were then analysed by gel electrophoresis and no impurities were seen (Figure 48).

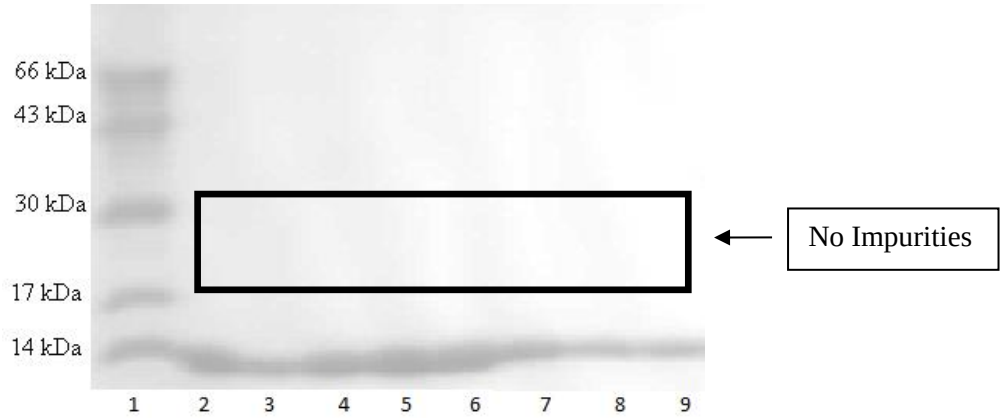

Figure 48 – 15% SDS PAGE combined fractions 45-46 after purification by S75 gel filtration, lane **1** – MW marker (kDa), 2 commercial Cytochrome C (0.5 mg/mL) **3** –**9** fractions after gel filtration, concentrations from Bradford Assay: **3** (0.33 mg/mL) **4** (0.61 mg/mL), **5** (0.65 mg/mL), **6** (0.65 mg/mL), **7** (0.64 mg/mL), **8** (0.60 mg/mL), **9** (0.50 mg/mL).

The purity of the combined fractions were then re-tested electrochemically using the method by Hill et al [94] (Scheme 28).

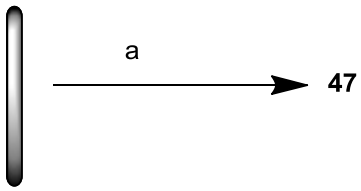

Scheme 28 – Electochemical testing of Cytochrome C. a) 2 mM Cytochrome C in 100 mM phosphate buffer (pH7) with 100 mM sodium perchlorate and 5 mM 4,4'-bipyridyl.

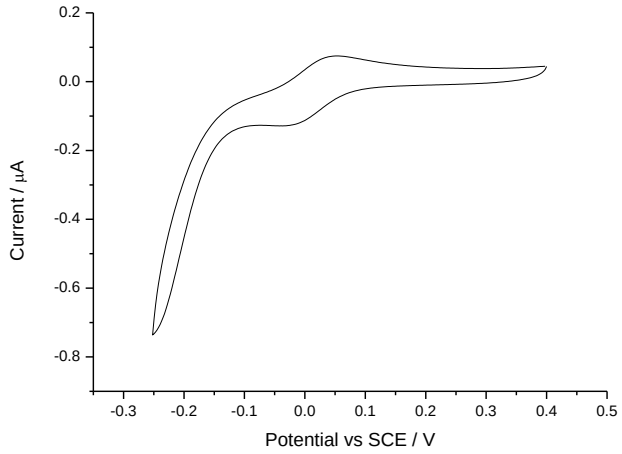

Figure 49 – Cytochrome C (2 mM) in pH 7 phosphate buffer (100 mM) with 4,4-bipyridyl (5 mM), gold electrode area: 0.03 cm2, scan rate 10 mV/s.

Cytochrome C

Following purification the Cytochrome C was pure enough to show electrochemical activity (Figure 49) and could be used as a model for the enzyme on maleimide-functionalised electrodes.

4.3 Attachment of Cytochrome C

Using the chemistry described in Chapters 2 and 3, GC electrodes could be modified in a number of ways to create surfaces with different concentrations of the tether on the surface. In order to evaluate the best surface modification for Cytochrome C a library approach was taken. The use of small libraries of electrodes allows a quick screen of a range of surface modifications to be tested and evaluated, a method which is becoming increasingly popular[26].

4.3.1 Full monolayer

4.3.1.1 Use of spacers

The structure of the surface was known to be important, and in addition to the partial coverage methods developed in Chapter 3, the effect of tether length was also investigated by the introduction of a spacer (Figure 50).

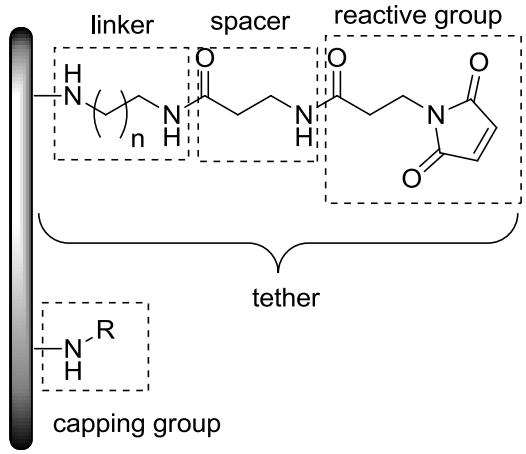

Figure 50 – Strategy for building up the structure on the surface.

The spacers used were Boc-Gly, 4-((tert-butoxycarbonyl)amino)butanoic acid and 6-((tert-butoxycarbonyl)amino)hexanoic acid which were synthesised according to a literature procedure[109].

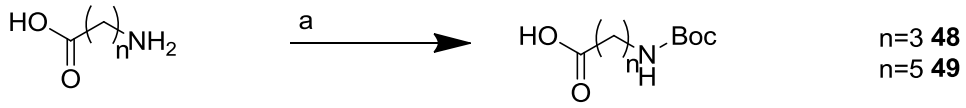

Scheme 29 – Synthesis of spacers[109] a) Boc_2O, dioxane, water

Initially a full monolayer of the tether was prepared on the electrode surface (Scheme 30) and different spacers were used to evaluate the effect of tether length

A monolayer of linker was prepared on GC electrodes using Boc-HDA, which had been used in the partial coverage work in Chapter 3. Following attachment of the linker onto the surface by electrochemical oxidation the Boc-amine was deprotected and coupled with spacers of increasing length. Maleimide functionality was then introduced on the surface using the methodology described in Chapter 2 and Cytochrome C was coupled (Scheme 30). A capped surface was also prepared as a control to quantify the amount of non-specific binding of Cytochrome C (Scheme 31).

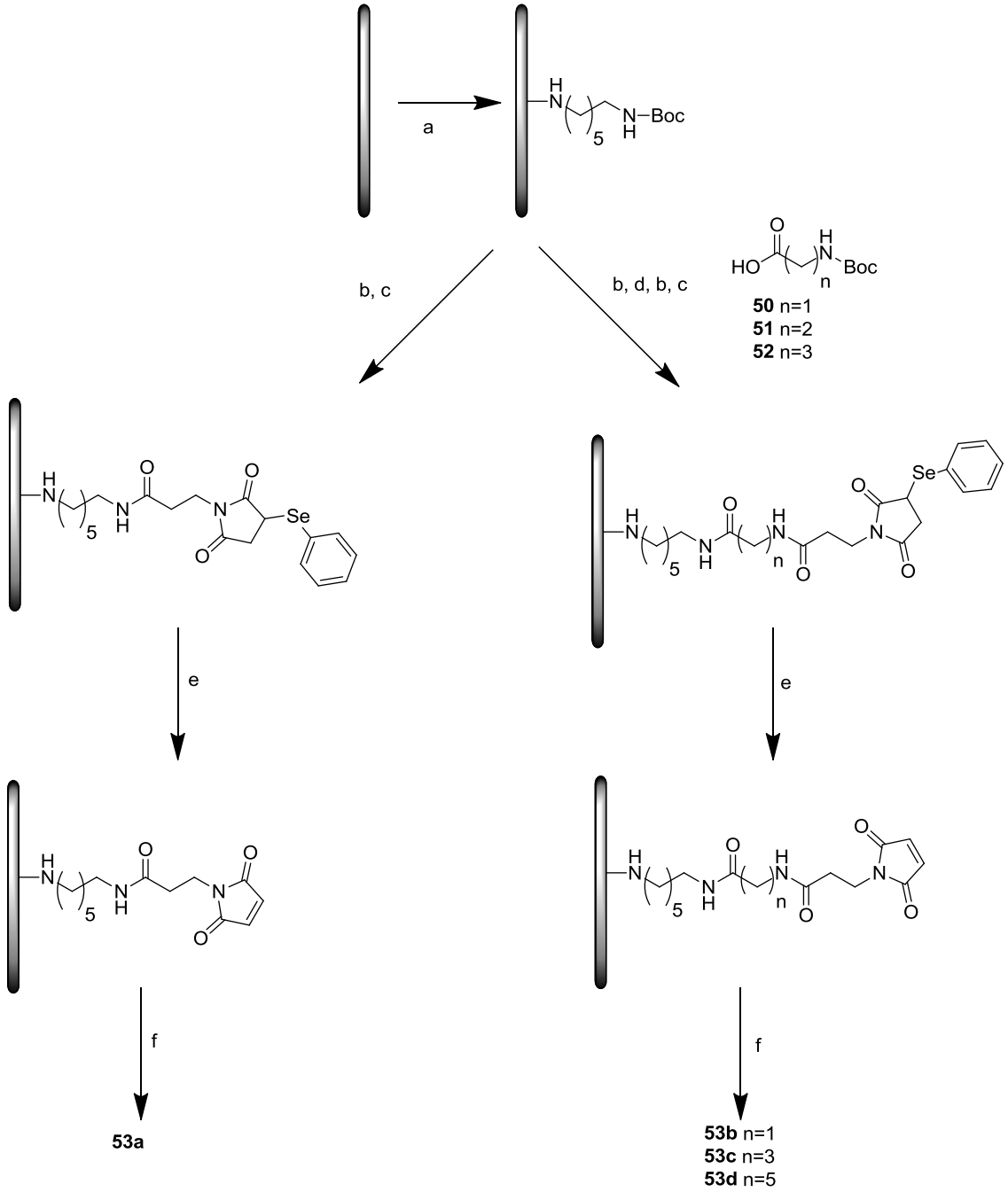

Scheme 30 – Preparation (**53a-d**) a full monolayer of linker with varying length of spacer and reactive group. a) Boc-HDA (10 mM), TBATFB (150 mM), acetonitrile 2.1 V vs Ag/AgCl, 180s, b) 4M HCl in dioxane 1 h, c) **27**, HBTU, DIEA, DMF 16 h, d) **51** or **52** or **53**, HBTU, DIEA, DMF, e) *m*CPBA in acetonitrile, 1 h at 0°C, 1 h at room temperature, f) Cytochrome C in 20 mM pH 7 phosphate buffer, 16 h 4°C

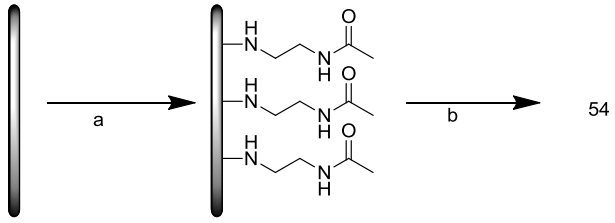

Scheme 31 – Preparation of a capped surface (**54**) as control sample. a) electrochemical oxidation of aminoethylacetamide, b) Cytochrome C in 20 mM pH7 phosphate buffer 16 h 4°C

Electrodes **53a-d** and **54,** (Scheme 30**,** Scheme 31) were then tested individually by CV at 20 mV s^{-1} (Figure 51). A monolayer of Cytochrome C on a maleimide layer was reported by Wilner *et al.*[106d] to be ~8 x 10^{-12} mol cm^{-2}. With such a low coverage visual observation of redox peaks by cyclic voltammetry above the background current could be difficult. It was therefore necessary to subtract the background current and a baseline was drawn by anchoring points either side of the expected redox peak and then subtracting this to give the baseline subtracted current.

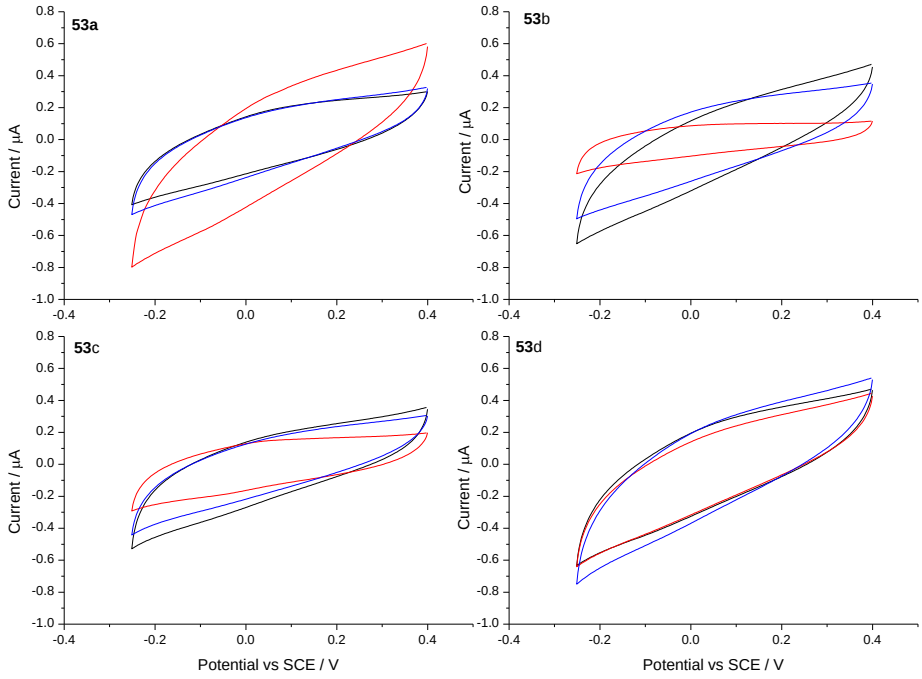

Figure 51 – Cyclic voltammetry of electrodes **53a-d** (Scheme 30). Cyclic voltammetry at 20 mV/s in 20 mM pH 7 phosphate buffer with 100 mM sodium perchlorate. Geometrical electrode area of 0.0707 cm^2

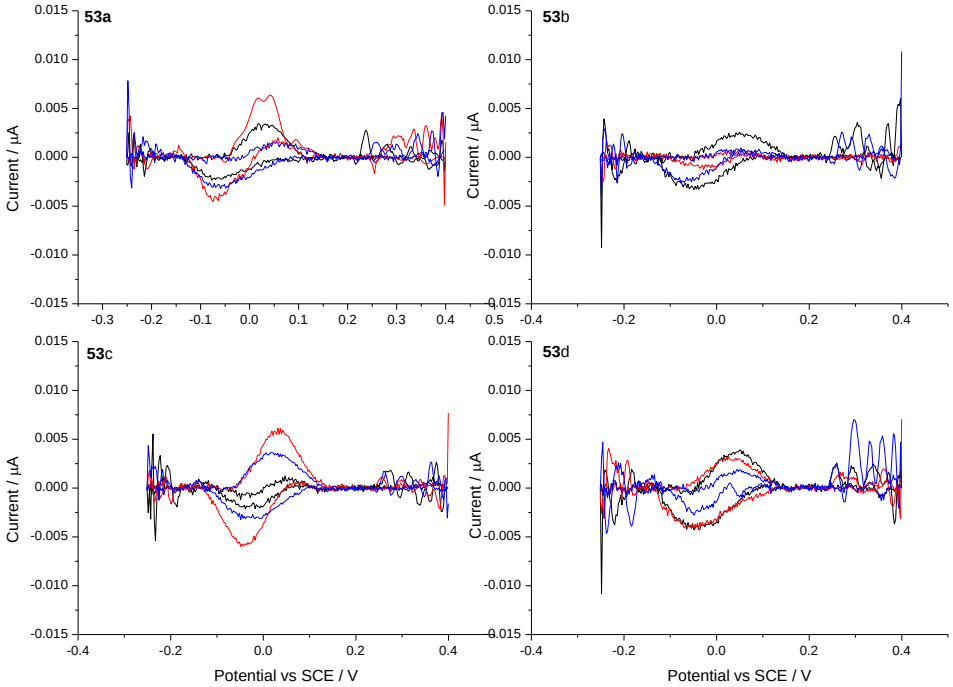

Figure 52 – Background subtracted cyclic voltammetry from Figure 51 of electrodes **53a-d** (Scheme 30).

After background subtraction small peaks could be clearly seen (Figure 52). The peaks were integrated and coverage was calculated (Figure 54) using Faraday's law, and the same was done with the capped layer (Figure 53).

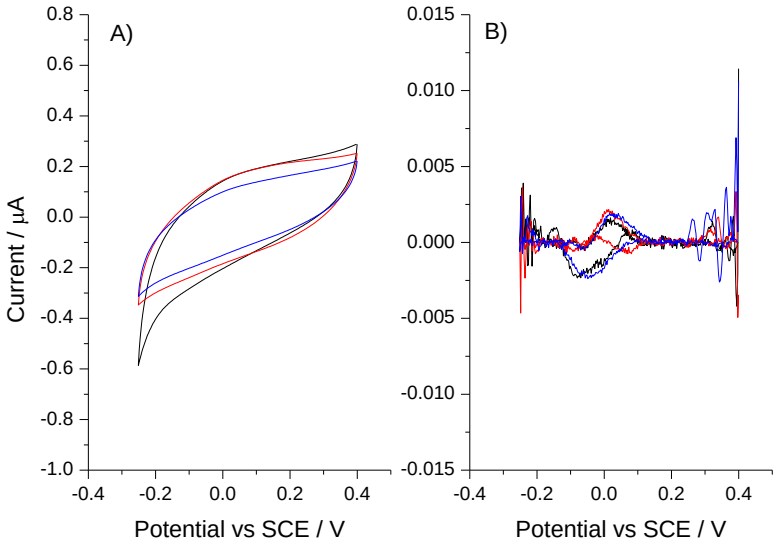

Figure 53 – A) CV of **54** at 20 mV/s in 20 mM phosphate buffer, pH 7 with 100 mM sodium perchlorate, B) Background subtracted CV

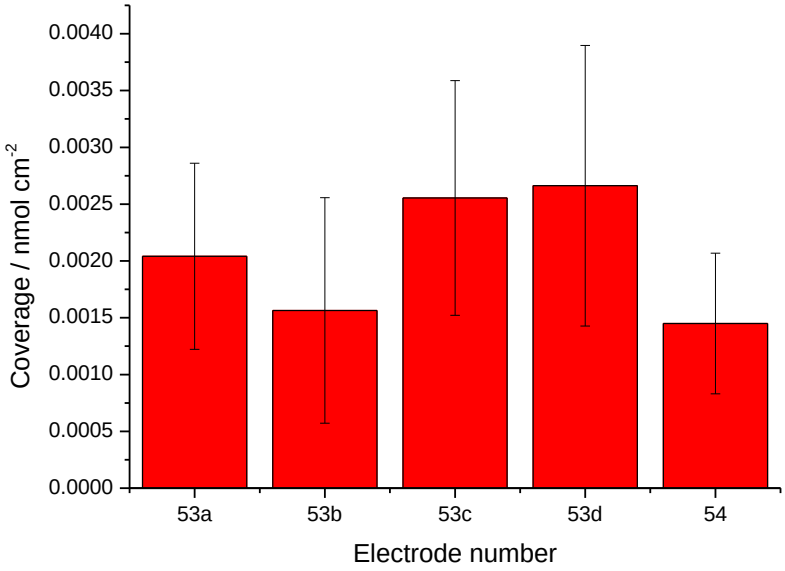

Figure 54 - Coverage of Cytochrome C electrodes **53a-d** and **54** (Scheme 30 and Scheme 31) following addition of spacer. Each bar shows the mean coverage from 3 electrodes and standard deviation.

The coverage of Cytochrome C was found to be inconsistent, with large error bars (Figure 54). In addition, the coverage was very low with a maximum of 2.66 x 10^{-12} mol cm^{-2}, not much higher than 1.44 x 10^{-12} mol cm^{-2} seen in the

capped layer (**54**). This combined with the large errors suggested that only non-specific adsorption had taken place on these electrodes.

4.3.1.2 Background subtraction

In order to test the baseline procedure a polished glassy carbon electrode was used as control sample and tested under the same conditions (Figure 55, A). The background was then subtracted (Figure 55, B) using a baseline created in Origin (version 8). The baseline was created separately for each half of the voltammogram using 100 points automatically placed on the curve across the potential range, points were then removed from the potential range of the peak, -0.16 to 0.14 and -0.10 to 0.20 V *vs* SCE for cathodic and anodic peaks, respectively. The remaining points were interpolated using B-spline function to produce the baseline.

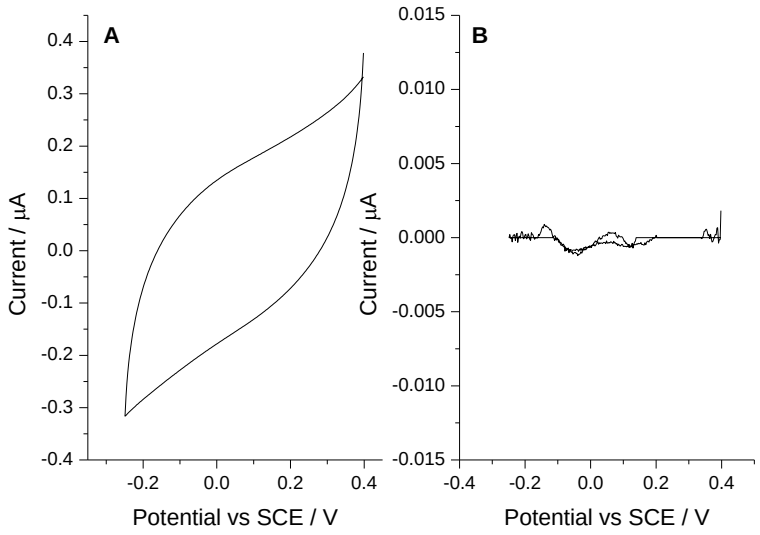

Figure 55 – Background subtraction sample, polished glassy carbon electrode A) Cyclic voltammetry at 20 mV/s in 20 mM pH 7 phosphate buffer with 100 mM sodium perchlorate. Geometrical electrode area of 0.0707 cm^2 B) background subtracted data

The background subtracted current for the control sample was predominantly noise, with no clear peaks, unlike the electrodes which had been treated with Cytochrome C which had clear peaks after background subtraction.

4.3.2 Partial Coverage

Following unsuccessful coupling to a full monolayer it was thought that the coverage of the maleimide reactive group on the surface was too high. As shown by the cartoon (Figure 56) if the layer is too compact it is difficult for the enzyme to bind to the reactive group as it is not be uniform in shape.

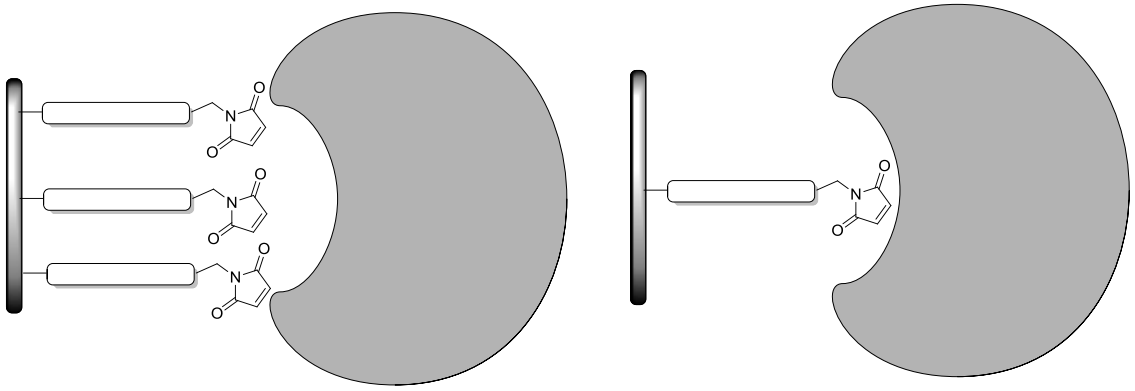

Figure 56 – Schematic of the partial coverage hypothesis (not to scale).

It should be noted that Figure 56 is a cartoon and in reality the surface is not that smooth, the roughness of the electrodes would have a large influence on how much the tether protrudes from the electrode surface. In this work the electrodes are polished with 0.3 μm alumina, to get a relatively smooth surface, however this is far from atomically smooth. In reality it is likely that some of the tether chains would be lost in the surface defects. However there would be many chains still protruding well from the surface and the partial coverage would allow the tether to protrude clearly from the higher part of the surface.

In order to test this idea the partial coverage methods developed in Chapter 3 were applied. Boc-HDA and the diluent capping group (aminoethylacetamide) were attached to the surface simultaneously by electrochemical oxidation of different mixtures of the two amines, allowing variation of the linker coverage. Following this the tether was lengthened by the addition of a spacer, Boc-Gly, and then the maleimide prepared on the surface, and Cytochrome C was coupled (Scheme 32).

Cytochrome C

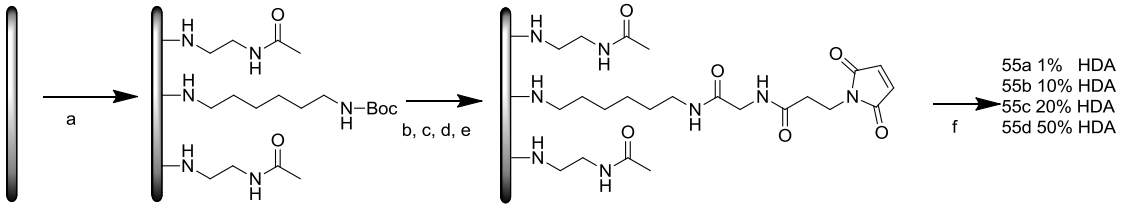

Scheme 32 - Preparation of a mixed monolayer on the surface to vary coverage**.** a) electrochemical oxidation of a mixture of amines (1-50% Boc-HDA and 50-99% aminoethylacetamide) in acetonitrile, 2.1 V vs Ag/AgCl, 180 s b) 4M HCl in dioxane, 1h c) Boc-Gly, HBTU, DIEA, DMF d) **27**, HBTU, DIEA, DMF 16 h e) *m*CPBA in MeCN 1h 0°C, 1h room temperature, f) Cytochrome C in pH 7 phosphate buffer (20 mM) 16 h 4°C

Electrodes, prepared in triplicate, were tested by CV at 20 mV s^{-1} and the second cycle had the background subtracted (Figure 58). Coverage was calculated by integration of the peaks obtained.

In addition to cyclic voltammetry the electrodes were evaluated by differential pulse voltammetry (DPV) (Figure 57) to clearly observe the peaks without the background subtraction. However due to difficulties transforming the charge from DPV into coverage the background subtraction procedure was used to calculate the charge and coverage of Cytochrome C on the prepared electrodes.

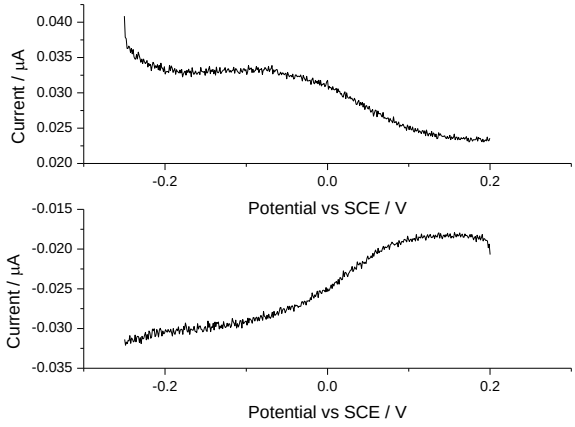

Figure 57- Differential pulse voltammetry of **55b** in 20 mM pH 7 phosphate buffer with 100 mM sodium perchlorate. Geometrical electrode area of 0.0707 cm^2.

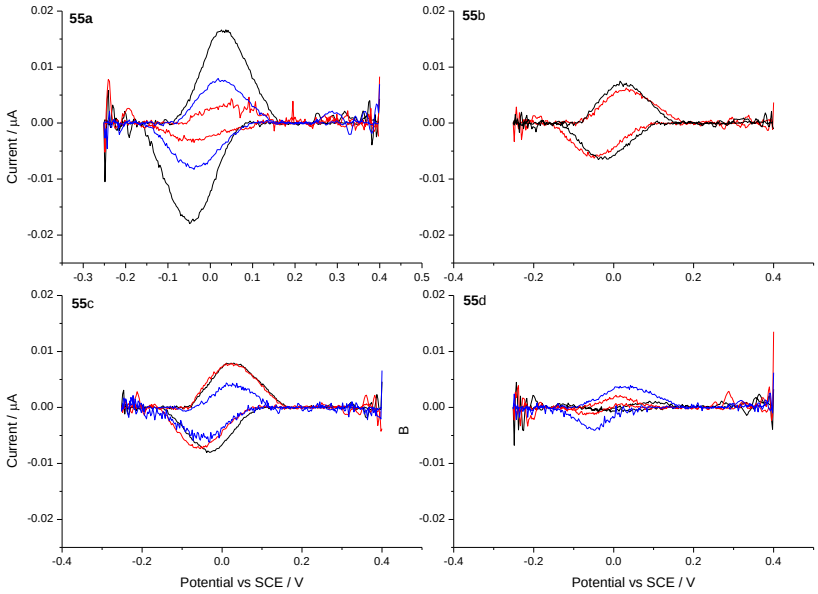

Figure 58 – Background subtracted current of electrodes **55a-d (**Scheme 32**)** after Cyclic voltammetry at 20 mV/s in 20 mM pH 7 phosphate buffer with 100 mM sodium perchlorate. Geometrical electrode area of 0.0707 cm².

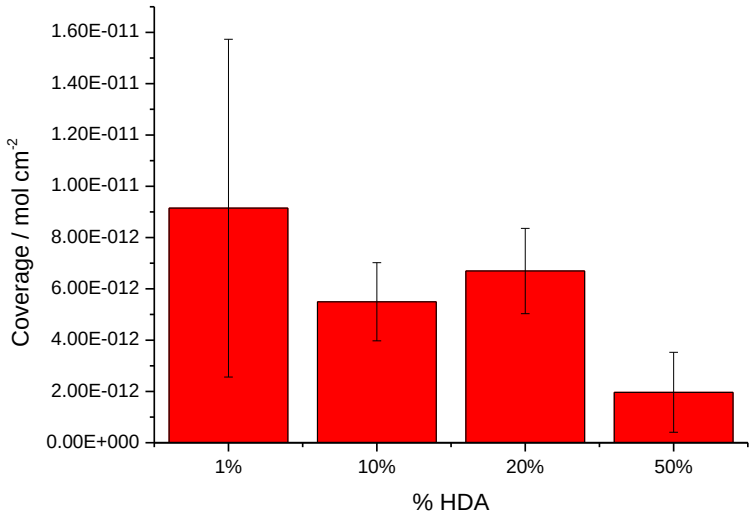

Figure 59 – Coverage of Cytochrome C on electrodes **55a-d** (Scheme 32) following variation of coverage. Each bar shows the mean value from 3 electrodes and standard deviation.

The coverage of electrodes with a partial coverage of linker is greater (Figure 59) than for the full monolayer electrodes (Figure 54), with exception of the 1%

layer of linker the error is also much less than for a full monolayer, suggesting that this binding is more specific and more reproducible. In the 1 % layer the problem could be that not enough of the linker is on the surface. The exact quantification of the amount of linker on the surface is problematic due to non-specific adsorption of reporter molecules such as anthraquinone on the surface, with approximately 20% coverage being non-specific. With only 1% linker and 99% capping group in the oxidation solution if the rate of addition of the capping group was much faster than the linker then the amount of linker attached to the electrode surface could be very low, allowing a high level of non-specific adsorption which is suggested by the large error.

In contrast the 10 % layer has only a small error bar and average coverage of Cytochrome C was 5.49 $x10^{-12}$ mol cm^{-2}, suggesting that a low coverage of the tether does increase the amount of Cytochrome C on the surface. This is supported by the fact that the 50% layer has the lowest coverage of Cytochrome C with only 1.96 $x10^{-12}$ mol cm^{-2}.

4.3.2.1 Effect of Spacer Length

Using the most consistent result with greatest coverage of Cytochrome C, a 10% layer of linker, another small library was prepared to investigate the effect of spacer length (Scheme 33). Thus a 10 % layer of linker was prepared on the electrode surface followed by coupling of spacers (**50-52)** with varying chain length then introduction of maleimide and coupling of Cytochrome C.

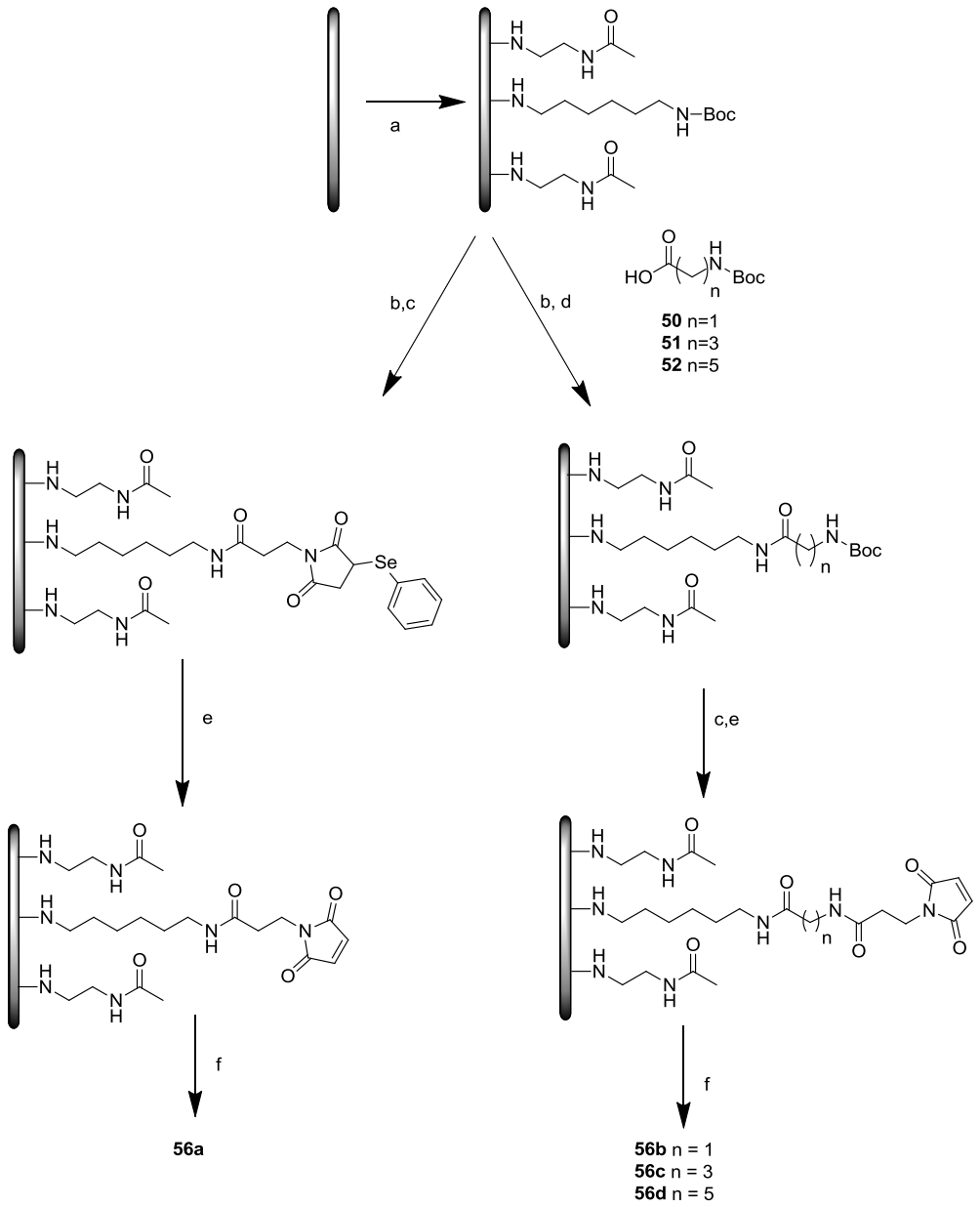

Scheme 33 – Preparation of **56a-d**. a) Boc -HDA (1 mM) aminoethylacetamide (9 mM), acetonitrile, TBATFB (150 mM) b) 4M HCl in dioxane, 1 h, c) **27**, HBTU, DIEA, DMF 16 h, d) **50** or **51** or **52**, HBTU, DIEA, DMF, e) *m*CPBA in acetonitrile, 1 h at 0 °C, 1 h at room temperature, f) Cytochrome C in 20 mM pH 7 phosphate buffer, 4°C

Electrodes, prepared in triplicate, were tested individually by cyclic voltammetry at 20 mV s^{-1} in 20 mM pH 7 phosphate buffer with 20 mM sodium perchlorate. The background was subtracted as described previously (Figure 61). Coverage was calculated from integration of the baseline-subtracted current using Faraday's law as previously described.

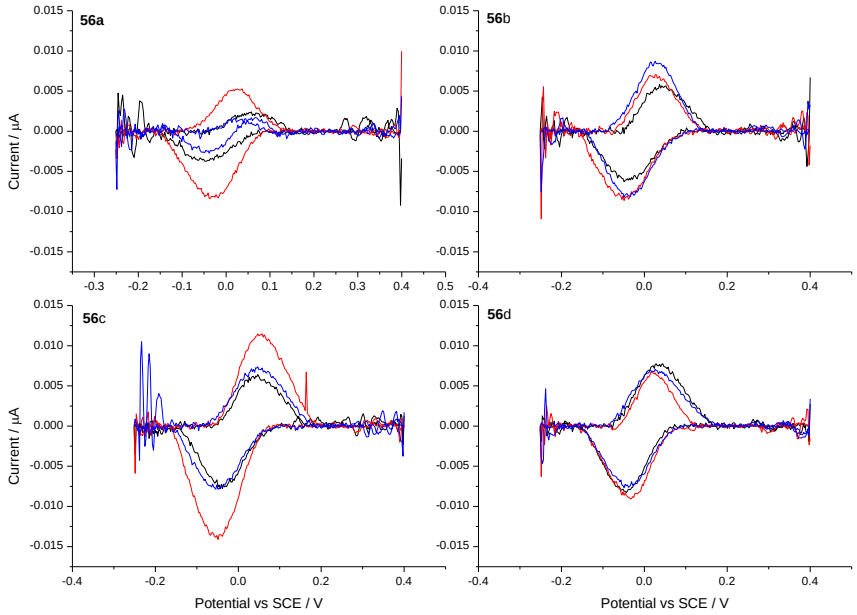

Figure 60 – Baseline-subtracted CVs of **56a-d** after after Cyclic voltammetry at 20 mV/s in 20 mM pH 7 phosphate buffer with 100 mM sodium perchlorate. Geometrical electrode area of 0.0707 cm².

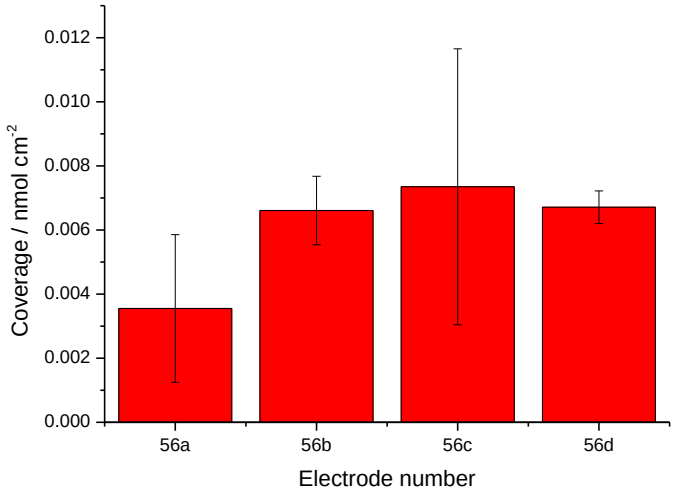

Figure 61 – Coverage of Cytochrome C on electrodes **56a-d** with 10% tether layer and increasing spacer length (Scheme 33). Each bar shows the mean value from 3 electrodes and standard deviation.

The Cytochrome C coverage increases with the use of a spacer (Figure 63). Electrodes prepared without a spacer (**56a**) have a smaller coverage and larger

error suggesting more non-specific adsorption in these samples. Increased coverage is seen with a spacer of at least two carbon atoms in length, with electrodes **56b-d** having an average coverage of 7 x 10^{-12} mol cm^{-2}, very close to the full monolayer coverage of 8 x 10^{-12} mol cm^{-2}. These results suggest that the best coverage is obtained with a partial coverage of 10% and spacer of at least two carbon atoms in length, and in this case a 6 carbon spacer had the least error.

4.3.3 Combined results

The results of the Cytochrome C experiments have been presented as they were carried out, in three separate libraries; however the results from the libraries and other individual experiments may be usefully compared.

The first thing to consider was the coverage of the linker used, comparing the increments between 0% and 100% (Figure 62).

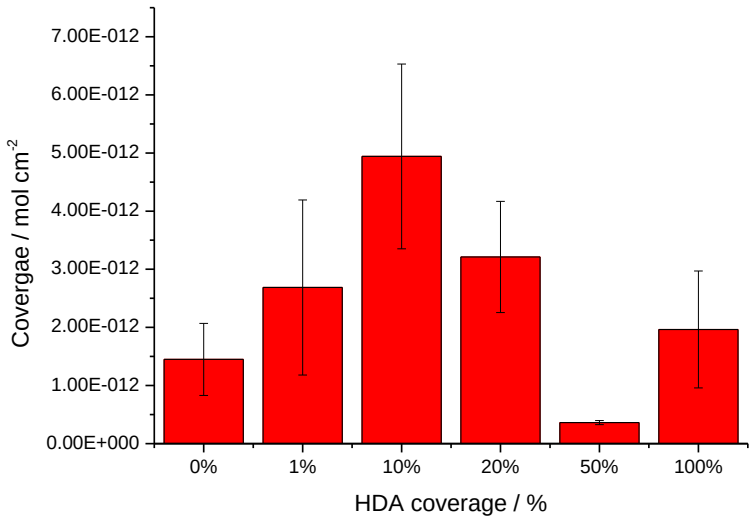

Figure 62 – Variation of tether coverage, each bar represents the mean coverage, from at least 3 electrodes, with the standard deviation shown as an error bar.

The results (Figure 62) suggest that the coverage increases to a maximum of 5 x 10^{-12} mol cm^{-2} at 10% linker coverage then reduces down to 2 x 10^{-12} mol cm^{-2} for a 100% coverage and 1.5 x 10^{-12} mol cm^{-2} for non-specific coverage on a fully capped layer. The result obtained using 50 % of the linker does not fit

with this trend and may well be an anomaly due to experimental error as only one set of electrodes was used in that case.

In addition, the effect of spacer length on both a full monolayer (Figure 54) and 10% layer of linker (Figure 61) was investigated and the comparison of these results (Figure 62) shows the significance of linker coverage.

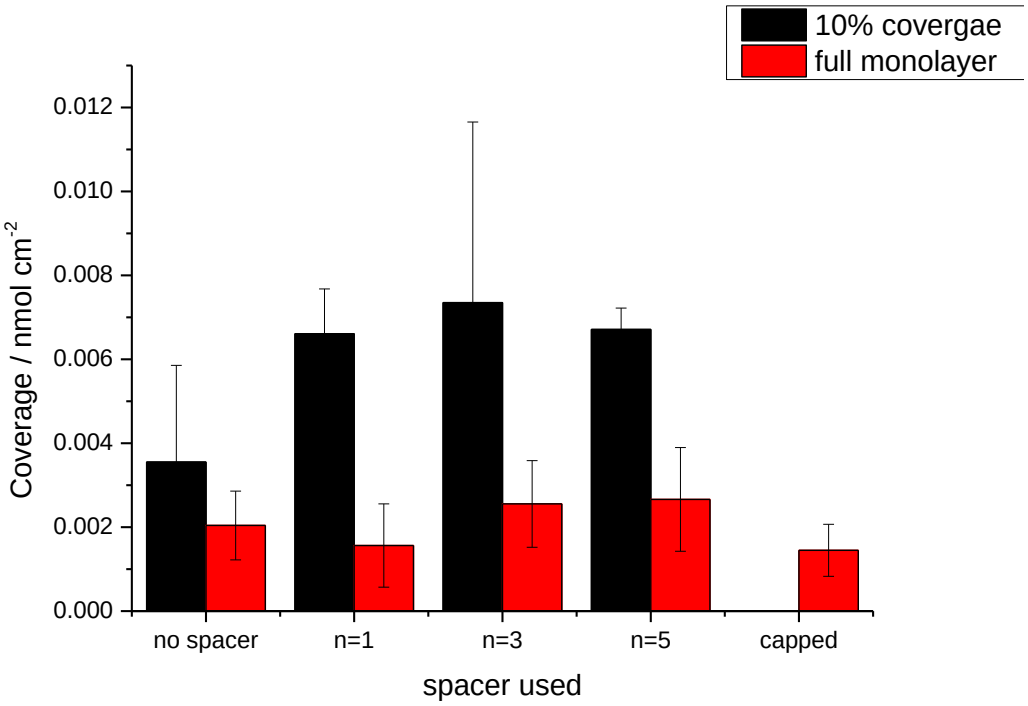

Figure 63 - Coverage of Cytochrome C on a full monolayer or 10% layer of linker with spacers of varying length. Coupling procedure shown in Scheme 33. Coverage calculated from CV at 20 mV s^{-1} followed by background subtraction and integration of the peak. Each bar shows the mean value from at least 3 electrodes and standard deviation.

The coverage of Cytochrome C on a full monolayer of linker does not significantly change with an increase in spacer length and the coverage is all ~ 2 x 10^{-12} mol cm^{-2}, very similar to that seen for the capped layer at 1.44 x 10^{-12} mol cm^{-2}. However if a 10 % layer of linker is prepared on the surface, a clear change in coverage is seen with increasing spacer length (Figure 63). A notable coverage of Cytochrome C is possible after a spacer of at least two carbons is added, however without a spacer the coverage is, within error, the same as a capped layer which has only non-specific adsorption. The coverage is very similar between n=1 and n=3 carbons at 4.94 x 10^{-12} mol cm^{-2} and 4.98 x 10^{-12} mol cm^{-2} respectively. However a further increase is seen to 6.71 x 10^{-12}

mol cm^{-2} with the longest (n=5) spacer. These results suggest that not only is the partial coverage important but that the length of the tether has a significant effect on the coupling of Cytochrome C.

4.4 Modelling of Cytochrome C

In order to judge the length of the spacer required for coupling of Cytochrome C and other engineered enzymes some approximate modelling was done of Cytochrome C and linkers. The modelling was carried out using the pdb file (2B4Z) from the RCSB protein data bank of Cytochrome C from Bovine Heart, and a file of the linkers created in ChemDraw3D. As the surface is proposed to have a mixed structure it is likely that the underlying capped layer limits the accessibility of the linker as shown in Figure 64.

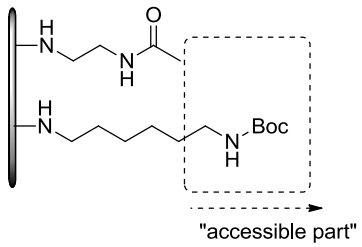

Figure 64 – "accessible part" of the linker

The "accessible parts" were drawn for each of the different spacers used, then each was put into Swiss PDB Viewer along with the pdb file for Cytochrome C. The protein was rotated and the maleimide functionalised linker was aligned visually next to the thiol group of cysteine. The manipulation of the protein and linker structures was continued until the maleimide was in a position to bond to the thiol. Once the two were aligned the surface was applied to the image of Cytochrome C, showing the amount the linker would protrude.

Cytochrome C

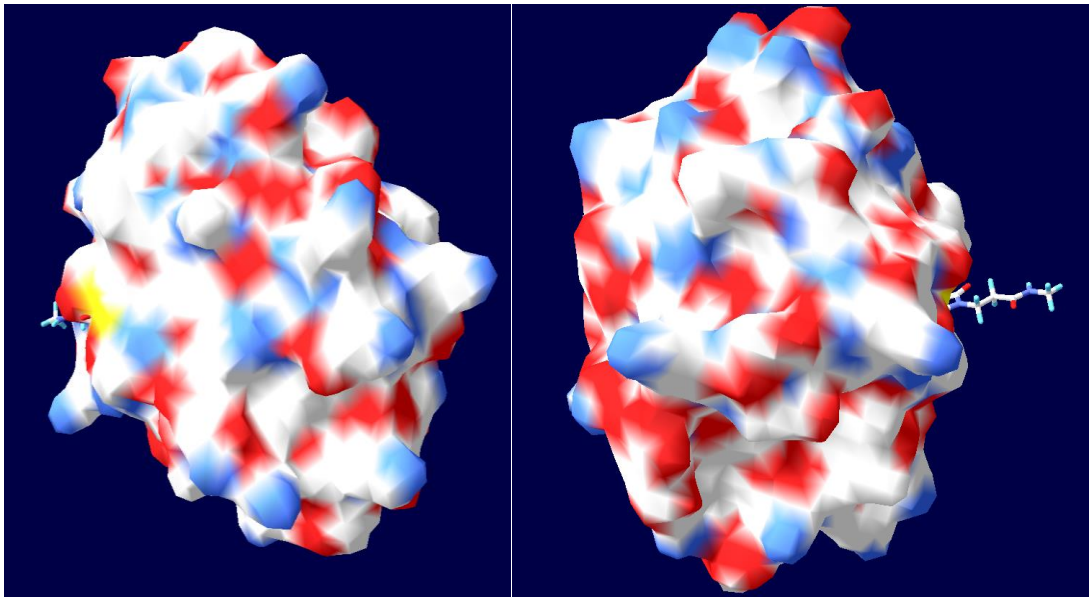

Figure 65 – Cytochrome C surface with 'accessible' linkers shown. Left: 0C spacer, Right: 2 C spacer

When no spacer (Figure 65 left) is added to the electrode surface the chain is not sufficiently long to bind well to the enzyme as some other groups on the surface of the protein protrude further out than the cysteine. However when a two carbon spacer, (Figure 65 right) is added, the chain appears to be lengthened enough to allow simple binding of the maleimide on the electrode to the thiol in the protein. This ties in well with the experimental results obtained.

Figure 65 also gives a good representation of the size of the protein in comparison to the linkers used and gives a good idea of why having the tether diluted on the surface could be important. As the protein is not completely spherical and the cysteine isn't on a protruding part of the protein surface the reactive group of the tether on the electrode needs to be able to get in to the crevice of the protein and spacing out the tether on the electrode would make the coupling easier.

4.5 Conclusions

Cytochrome C has been used as a model protein for testing attachment onto the electrode surface. Initially a full monolayer of the tether was prepared on the electrode surface; however the coverage of Cytochrome C on the electrodes

was not significantly different to the coverage on a capped layer where only non-specific adsorption was possible.

Previously developed methods to make a partial coverage on the surface were then used to make surfaces with 0-100 % linker coverage and a two carbon spacer was used to ensure that the tether was sufficiently long to bind the Cytochrome C. The coverage of the linker had a significant effect on the coverage of Cytochrome C, with clear increase in Cytochrome C coverage when a low coverage of tether was used. The best results were when a 10 % coverage of linker was used and the lowest coverage was from a full monolayer.

A final experiment was carried out with 10 % linker coverage and varying length of spacer, this showed a 10 % coverage with a spacer of at least two carbons gave a coverage significantly higher than the capped layer with only non-specific adsorption. The best coverage was obtained from a 10 % layer with 6 carbon spacer, 6.71×10^{-12} mol cm^{-2} which is close to the 8×10^{-12} mol cm^{-2} monolayer coverage suggested.

It is known[110] that the rate of electron transfer decays exponentially as the distance between the two centres, the electrode and active site of the enzyme, increases, for this reason spacer lengths greater than 6 carbons were not investigated. It has been reported that electron-transfer rates drop by $\sim 10^4$ when the distance between the electrode and active site is increased from 8 to 17 Å[111]. The critical distance was reported to be 20 Å for laccase by Yarapolov[112] and 18 Å for horseradish peroxidase by Kulys.

The combined results indicate that there are two key factors to consider in the covalent binding of proteins to electrode surfaces: the surface coverage and the length of the tether used. It is important to consider the nature of the protein being used, in particular the size (diameter) and position of the targeted attachment site.

With these promising results the engineered enzymes could now be investigated as discussed in Chapter 5

5. Enzyme attachment – Glucose Dehydrogenase

5.1 Glucose Dehydrogenase (GDH)

The discovery of FAD-dependant glucose dehydrogenase was made as early as 1951[113]. However it was not until the use of GDH in glucose biosensors in the 1990s[114] when a thermostable GDH was found. Since then a number of variants have been located and isolated.

A new variant of GDH was found in a pathogenic plant fungus *Glomerella cingulate*[115]. The glycosylated enzyme was found to have a high specificity for D-glucose and D-xylose. Sequence analysis showed that *Gc*GDH was structurally in the family of glucose–methanol–choline (GMC) oxidoreductases, the same family as GOx. The biological function of *Gc*GDH is not yet known, however it has been proposed to be involved in the fungal attack pathway; the reduction of quinones and phenoxy radicals allows GDH to neutralise the attack on fungus by laccases and peroxidases[115].

Like GOx, *c*GDH oxidises glucose at the C1 position, allowing only the β glucose to be oxidised. The oxidation of β- D-glucose by GDH is achieved by the following reaction in which $2H^+$ and $2e^-$ are transferred from glucose to the FAD centre in *GcGDH*[116].

β -D-glucose + GDH_{FAD} → gluconolactone + GDH_{FADH2}

The hydrolysis of gluconolactone has been supported by a steady drop in pH after glucose conversion is complete[115]. In nature quinones would be the favoured electron acceptors, however iron complexes and redox dyes such as dichloroindophenol (DCIP) have been effectively used as alternatives[115].

The oxidation of a range of carbohydrates by *GcGDH* was investigated[115] using DCIP as an electrode acceptor, a strong preference for glucose as observed, with xylose having only ~31 % activity, maltose and cellobiose had much lower rates with only 2.3 % and 1.6 % relative activity respectively, lactose was not converted at all.

Glucose Dehydrogenase

The use of an FAD-dependent GDH as an alternative to GOx in biosensors allows a faster turnover rate[116] and greater stability. In addition the enzyme is unaffected by oxygen, whereas in GOx-based biosensors the oxygen turnover reduces the electron yield and produces H_2O_2 which degrades the biocatalyst. FAD dependent GDH has already been used in biosensors by both Abbott and Bayer[117].

5.2 Electron Transfer between Proteins and Electrodes

There are 2 mechanisms of electron transfer between the electrode and bioelement, direct electron transfer (DET) and mediated electron transfer (MET). While mediated systems are well studied and commonly show initial high activity, the long term stability is not good. It is thought that DET would not have the same problems with stability; the main requirements for DET are that the redox centre of the enzyme is orientated correctly and is within electron tunnelling distance from the electrode[118]. In order to achieve this it is necessary to have a highly controlled method of electrode modification.

5.2.1 Direct Electron Transfer (DET)

Direct electrochemistry has been seen with less than 10% of known redox enzymes[87a], one of the key reasons for this is the fact that the active centre of the enzyme is often buried deep in the protein structure. Beyond the critical distance of 3 Å the rate of electron transfer decays exponentially[119].

Redox enzymes may be divided into two types, intrinsic or extrinsic enzymes[120]. Intrinsic enzymes have one area where the reaction between the substrate and redox active sites of the enzyme occurs. As there is no natural requirement for an electron pathway to the surface of the enzyme DET is not favoured and is very difficult to achieve[92]. An example of a well-studied intrinsic enzyme is GOx (Glucose Oxidase), which reduces oxygen to hydrogen peroxide in nature, working as an anti-fungal agent. Despite the difficulty of electron transfer, due to the interest of GOx for glucose sensing applications there is still research in this area[53].

Extrinsic proteins naturally bind to another protein for electron transfer, therefore there is both an electron pathway to the surface and groups on the surface for another protein to bind to, making them an ideal choice for DET. Examples of extrinsic proteins include Cytochrome C Oxidase and CDHs (cellobiose dehydrogenase). In CDH electrons are transferred internally from the catalytically active flavin domain to the haem domain which can then reduce Cytochrome C or communicate with electrodes.

Another key consideration is the orientation of the protein, if the enzyme is orientated with the redox centre not facing the electrode the pathway for electron transfer is not simple and the distance for electron transfer may be too great.

5.2.2 Mediated Electron Transfer (MET)

Due to difficulties in electron transfer, an alternative to the use of DET is MET – mediated electron transfer. Mediators act as intermediates and diffuse between the active site and electrode, being oxidised and reduced, acting as a redox shuttle[47]. Mediators must be soluble in both the oxidised and reduced forms to allow a rapid diffusion between the enzyme and electrode, in addition the reaction between the mediator and enzyme must be fast to avoid blocking of the active site. The mediator must then be easily reoxidised at the electrode surface at a low over potential and unaffected by pH. Common mediators include ferrocene and quinone derivatives[67b, 121] and metal complexes based on Fe, Os, Ru and Ni due to the reversible nature of the redox behaviour of transition metals.

Mediators may also be incorporated into the structure of the linker used to attach the enzyme to the electrode surface or enzymes may be modified to have mediators incorporated into their structure[40]. The efficiency of electron transfer is dependent on the transport properties of the mediator as well as the electron transfer steps in the assembly used. The mediator would ideally be incorporated near to the active site of the enzyme, allowing the electron to transfer quickly from the redox centre to the mediator. Enzymes confined on a surface would be ideally orientated with the active site facing towards the electrode surface[47].

5.3 Aims

Following on from the success of attaching Cytochrome C, the main aim was to bind engineered enzymes to the modified surface. Following successful attachment the aim would be to optimize the enzyme activity and stability on the surface.

5.4 Engineered GDH

Two variants of glucose dehydrogenase (GDH) were provided by the University of Natural Resources and Life Sciences, BOKU, in Vienna. Each variant had a single cysteine residue introduced near the active site but accessible from the surface. A third variant with the cysteine site near the active site was engineered, however the mutation so close to the active site introduced too great a structural change and the enzyme lost all activity. It is therefore important to note that if the enzyme structure is disrupted too much by modification then this would have an effect on the activity.

The two variants of *Gc*GDH (Figure 66) provided had the cysteine at varying distances from the surface, variant A (T343C) had the cysteine very close the surface and variant B (K423C) had the cysteine closer to the active site.

Figure 66- GDH ribbon structure with FAD shown in Yellow, Cysteine introduced in cyan (T343C) and pink (K423C). Drawn from PDB structure provided by BOKU in Swiss PDB viewer.

5.5 Electrochemical Evaluation of GDH in Solution

Many functional aspects of enzymes can be investigated using electroanalytical techniques; in particular the chemistry of the active site may be investigated by following the biocatalytic process. Factors such as interfacial and intramolecular electron transfer, dependence on pH, substrate transport and inhibitors may also be shown.

Michaelis and Menten proposed a mechanism for enzyme reactions back in 1913.

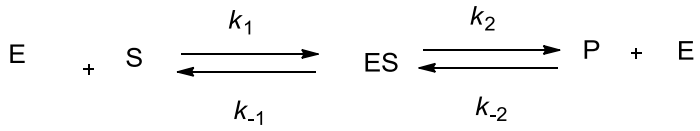

Figure 67 – Mechanism for enzyme reactions

Here E is the free enzyme, S is the substrate, P is the product of the reaction and ES is an enzyme-substrate complex. k_n's are the rate constants for the forward and backward reactions. As the rate is usually studied at the start of the reaction the backward arrow may be omitted, and k_2 rate constant may be re-named k_{cat}, the catalytic rate constant for conversion of the enzyme-substrate complex into the free enzyme (E) and product of the reaction (P).

The Michaelis-Menten equation assumes the study of the initial velocity of the reaction and is:

$$V_o = (V_{max}[S])/(K_m+[S])$$

where V_o is the initial reaction velocity, V_{max} is the maximum (theoretical) velocity of the reaction ($V_{max}=k_2[E_o]$, where E_o is the total enzyme concentration), [S] is the substrate concentration and k_m is the Michaelis-Menten constant ($K_m = (k_{-1} + k_{cat})/k_1$).

K_m may be estimated from a plot of reaction rate vs substrate concentration, using the substrate concentration at which the rate is half of the V_{max} value. It is important as it shows the strength of binding between the enzyme and substrate.

If the substrate concentration is less than k_m then the velocity of the reaction is known to increase linearly with substrate concentration, and most enzyme and substrate is free, meaning that the rate of the reaction is dependent on the rate of the substrate binding at a given concentration. When the concentration of substrate is equal to K_m the initial reaction velocity is half of V_{max}. At high concentrations above K_m, the system can become saturated and the rate of reaction is independent of substrate concentration, the velocity has reached V_{max}.

In order to develop an electrochemical testing procedure the wild type enzyme was first evaluated in solution, using 2,6-dichloroindophenol (DCIP) as a mediator.

DCIP (2,6-dichloroindophenol) works efficiently as an electron shuttle as it is a quinone, quinones are one of the natural electron acceptors of glucose dehydrogenase and work well as they accept two electrons (Scheme 34).

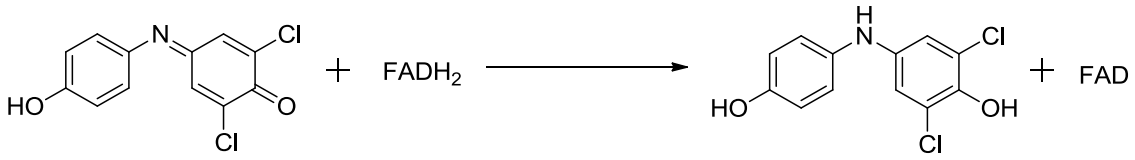

Scheme 34 – Reaction of DCIP with $FADH_2$, as it would be in the active site of GDH.

5.5.1 Dichloroindophenol as a mediator

The electrochemistry of the mediator was evaluated first by cyclic voltammetry without addition of enzyme (Figure 68). A solution of DCIP was prepared in citrate buffer, using the same pH and concentration as was used in spectrophotometric activity tests which were performed in BOKU, so that the activity could be compared.

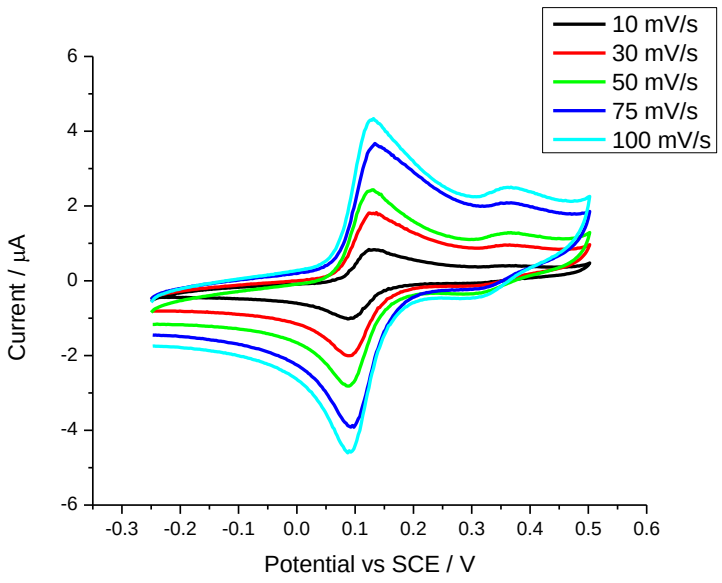

Figure 68 – Cyclic Voltammetry at a range of scan rates, solution of 0.5 mM DCIP, 50 mM citrate buffer pH 5.5. GC electrode used, electrode area: 0.0707 cm^2.

The voltammetry of the mediator alone should follow the Randles-Sevčik equation[122]

$$I_p = 2.69 \times 10^5 \; n^{3/2} \; A \; [M] \; D^{1/2} \; \nu^{1/2}$$

where I_p is the peak current in amps, n is the number of electrons transferred (2 in this case), A is the area of the electrode in cm^2, [M] is the concentration of the mediator ([DCIP] = 0.5×10^{-6} mol cm^{-3}), D is the diffusion coefficient of the mediator in cm^2 s^{-1} and ν is the sweep rate in V s^{-1}.

The peak current was plotted against the square root of scan rate (Figure 69), the relationship was linear as expected, showing that the reaction was reversible. However the cyclic voltammetry was not ideal in this case due to a second peak in the voltammogram at ~0.35 V vs SCE which is more prominent at high scan rates. For this reason the shape of the voltammogram at 0.1 V vs SCE is distorted and it is difficult to accurately calculate the peak current. Therefore the intercept of the liner fitted lines are not at the origin as they should be, causing an inaccuracy in the plot.

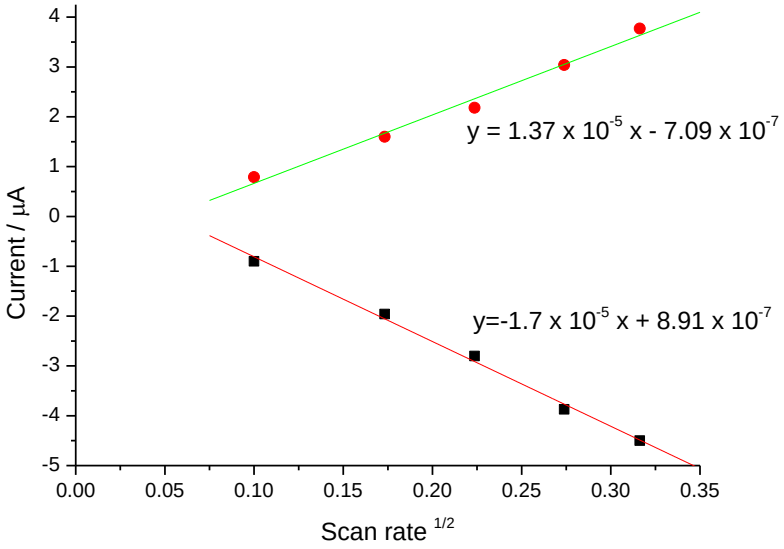

Figure 69 – Plot of peak current vs square root of the scan rate for DCIP. Calculated from cyclic voltammetry in 0.5 mM DCIP, 50 mM citrate buffer pH 5.5 (Figure 68). GC electrode area: 0.0707 cm^2.

The diffusion coefficient was estimated from the gradient,

$D = (\text{gradient}/2.69 \times 10^{-5} \times n^{3/2} \times A \times [\text{DCIP}])^2$

$D = (1.7 \times 10^{-5} / 2.69 \times 10^{5} \times 1.58 \times 0.0707 \times 0.5 \times 10^{-6})^2$

$D = 1.2 \times 10^{-6}\ cm^2\ s^{-1}$.

Following the mediator evaluation *Gc*GDH (wild type) was added to the solution and cyclic voltammetry was repeated at 10 mV/s. Following this aliquots of D(+)-glucose were added to the solution and mixed. After each addition the cyclic voltammetry was repeated (Figure 70).

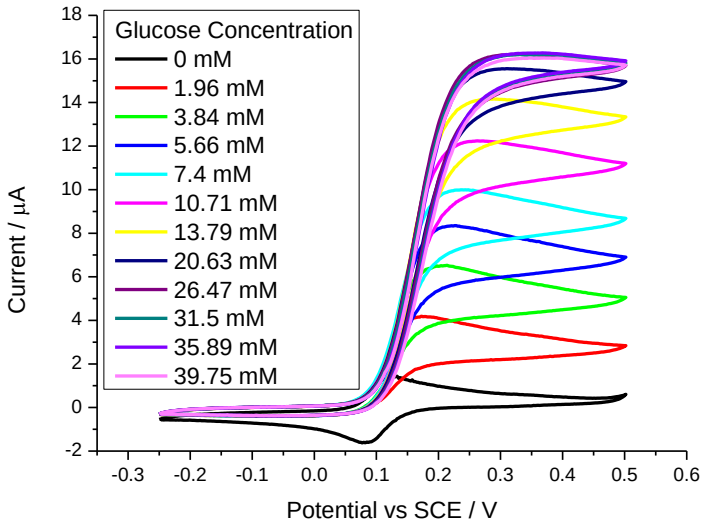

Figure 70 – Cyclic Voltammetry at 10 mV s^{-1} in solution of 0.5 mM DCIP, 50 mM citrate buffer pH 5.5, 3 nM *Gc*GDH following addition of glucose. GC working electrode area 0.0707 cm^2.

The observed current increased upon each addition of glucose until a saturation point around 35 mM of glucose. The voltammetry showed the classic behaviour for MET, increased current was only observed for the oxidation of DCIP, and no reduction wave was seen, due to the reduction of the DCIP by GDH. DCIP is oxidized by the electrode, however in the presence of GDH the oxidized DCIP is converted back to the reduced form before the reverse reaction occurs by cyclic voltammetry. The relationship between the mediator (M), GDH and glucose is shown (Figure 71).

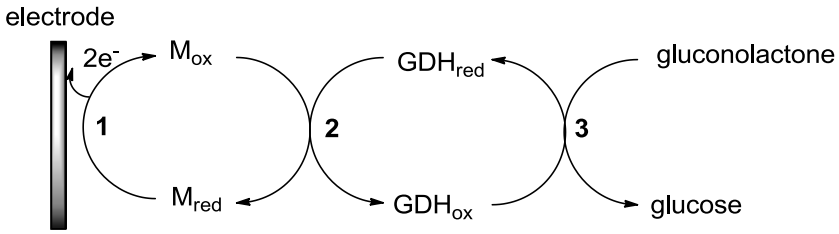

Figure 71 – Relationship between mediator (M), GDH and glucose.

Glucose dehydrogenase naturally oxidises glucose to gluconolactone and during this reaction the enzyme is reduced. GDH then needs to be re-oxidised before it can oxidize glucose again and DCIP can be used for this, it acts as a final electron acceptor. For this reason current is only seen for the oxidation of

Glucose Dehydrogenase

DCIP, GDH converts the oxidized form to the reduced form before the reduction potential is reached.

Initially the rate of these conversions is dependent on the concentration of glucose as the current increases, the rate limiting step is the reaction of glucose and the enzyme. However at high concentration, when the current has stopped increasing the limiting factor is either the reaction of DCIP with the enzyme (**2,** Figure 71) or the reaction of the enzyme and glucose (**3,** Figure 71).

The increase in current showed that the enzyme was working well to oxidise glucose and DCIP was working reasonably as a mediator. The current was extrapolated from the cyclic voltammetry and plotted against the glucose concentration (Figure 72).

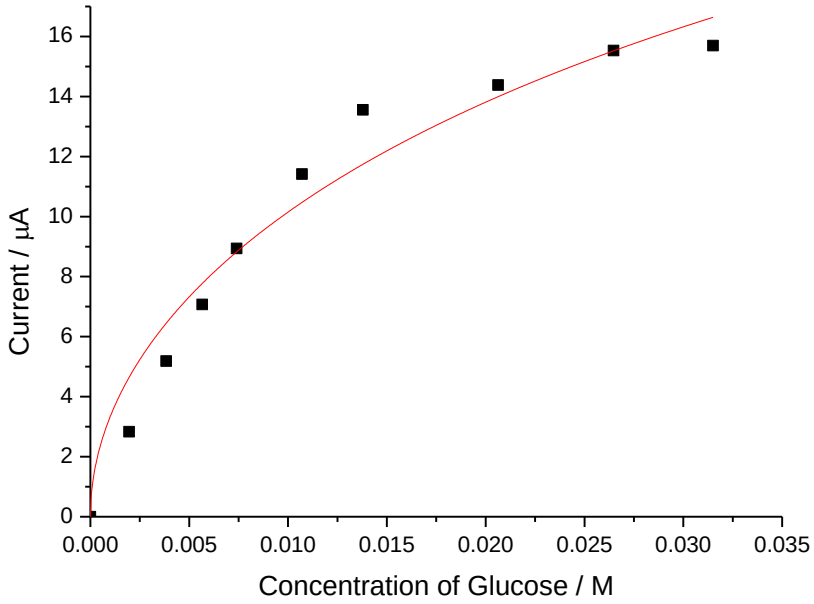

Figure 72 –Plot of current vs glucose concentration, from cyclic voltammetry at 10 mV s^{-1} in solution of 0.5 mM DCIP, 50 mM citrate buffer pH 5.5, 2 µM *Gc*GDH following addition of glucose. GC working electrode area 0.0707 cm^2.

In homogeneous mediated enzyme kinetics there are a number of possible scenarios[123] for the kinetics of the reaction of mediator and enzyme.

In **Case II** the current is determined by the reaction of mediator with the enzyme, the kinetics are dependent on the rate of the reaction between the enzyme and the mediator:

$$i = nFA\ (D\ k\ [\mathrm{Ez}])^{1/2}\ [\mathrm{M}]$$

Where *i* is current, *D* is diffusion coefficient for the mediator, *k* is the rate constant for the enzyme mediator reaction, [Ez] is the concentration of enzyme. And [M] is the concentration of mediator.

In **case III** the concentration of substrate is low and the current is determined by the reaction of the enzyme with the substrate.

$$i = nFA\left(\frac{D\ k_{cat}\ [\mathrm{Ez}]\ [S][M]}{k_m}\right)^{1/2}$$

Where [S] is substrate concentration, k_m and k_{cat} are enzyme-substrate kinetics

In **case IV** the current is determined by saturated enzyme kinetics, the concentration of substrate is greater than the K_m.

$$i = nFA\ (D\ k_{cat}\ [\mathrm{Ez}][\mathrm{M}])^{1/2}$$

In all three equations the square root applies to the kinetic terms, the reason for this is that the reactions occur within a layer at the electrode surface. The reaction layer is set up as the mediator reacts at the electrode surface then diffuses away into the bulk solution and then reacts with the enzyme.

It is also noted that as the concentration of substrate is increased the situation changes, varying between the possible scenarios for kinetics. At low concentration of substrate the case will be **case III**, then as the concentration of substrate gets high the situation will change to either **case II** or **IV**.

If the situation changes from case III to IV then this is “Michaelis-Menten” type behaviour.

Glucose Dehydrogenase

If the situation is going **case III-II** then:

$$i = nFA\,(D\,k_{cat}\,[\mathrm{Ez}][\mathrm{M}])^{1/2}\left(\frac{[S]}{[S]+\frac{k_{m'}\,k\,[M]}{k_{cat}}}\right)^{1/2}$$

Which gives apparent values for Vmax' and Km'

$k_{m'} = (k_m\,k\,[\mathrm{M}] / k_{cat})$

$V_{max'} = nFA\,(D\,[\mathrm{Ez}][\mathrm{M}])^{½}$

If the situation changes from **case III-IV** then:

$$i = nFA\,(D\,k_{cat}\,[Ez][M])^{1/2}\left(\frac{[S]}{[S]+k_m}\right)^{1/2}$$

Therefore the experimental data may be fitted to

$$\mathrm{i} = V_{max'}\left(\frac{[\mathrm{S}]}{[\mathrm{S}]+k_m''}\right)^{1/2}$$

In all cases and the V_{max} may be used to clarify the results.

$$\frac{V_{max'}}{k_{m'}} = \frac{V_{max}}{k_m} = nFA\left(\frac{D\,kcat\,[Ez][M]}{k_m}\right)^{1/2}$$

In the mediated reaction with the enzyme in homogeneous solution the appropriate form of the Michaelis-Menten equation [123] is:

$$i = V''_{\max}\left(\frac{[\mathrm{S}]}{[\mathrm{S}]+K''_{\mathrm{M}}}\right)^{1/2}$$

The equation contains a square root which arises due to the reaction layer formed by the diffusion of redox species from the electrode surface[123] V''_{max} and K''_{Mapp} are the apparent values of V_{max} and K_M derived from the fitting.

The data in Figure 72 was fitted to the model for the homogeneous enzyme mediator, using Origin v8 to draw a curve and V''_{max} was calculated to be 3.6 x 10^{-5} A and the K''_m value 11 mM, close to the literature value[117] of 10.2 mM.

Using this, the value of k_{cat}/K_M may be calculated.

$$\frac{V''_{\max}}{K''_{\mathrm{M}}{}^{1/2}} = \frac{V_{\max}}{K_{\mathrm{M}}{}^{1/2}} = nFA\left(\frac{\mathrm{D}k_{\mathrm{cat}}[\mathrm{Ez}][\mathrm{M}]}{K_{\mathrm{M}}}\right)^{1/2}$$

$V''_{max}/(K''_{M})^{1/2}$ = 1.1 x 10^{-4} A $M^{-1/2}$

1.1 x 10^{-4} A $M^{-1/2}$ = nFA (D k_{cat} [Ez][M] / K_M)$^{1/2}$

k_{cat}/K_M = 2.0 x 10^4 dm^3 mol^{-1} s^{-1}

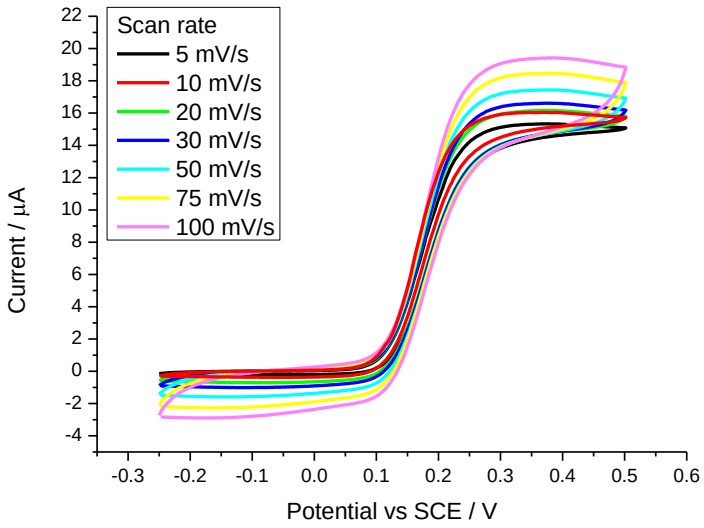

Figure 73 – Variation of Scan rate, solution of 0.5 mM DCIP, 50 mM citrate buffer pH 5.5, 2 µM *Gc*GDH, 39.75 mM of glucose.

As expected the CV with glucose is not very scan-rate dependent for efficient mediation of the reaction.

5.6 Electrochemistry on the Surface

5.6.1 'Direct Electrochemistry'

Direct electrochemistry is notoriously difficult to achieve, however it is highly desirable for electrochemists interested in next generation biosensors and biofuel cells. As discussed DET is dependent on the ability for electron transfer between the attached enzyme or redox protein. The capacity for electron transfer would require a good connection between the electrode and enzyme with the correct orientation and favourable distance.

Glucose Dehydrogenase

5.6.1.1 Variant 1 (T343C)

Initially the enzyme with the cysteine near the surface was investigated, as the attachment to the electrode surface would be simplified by the proximity of the cysteine to the enzyme surface. As the cysteine was not buried it was anticipated that no spacer would be needed, however electrodes were prepared both with and without (Scheme 35) a two carbon spacer for comparison. In addition to this, as a control sample, electrodes were prepared with maleimide and no enzyme.

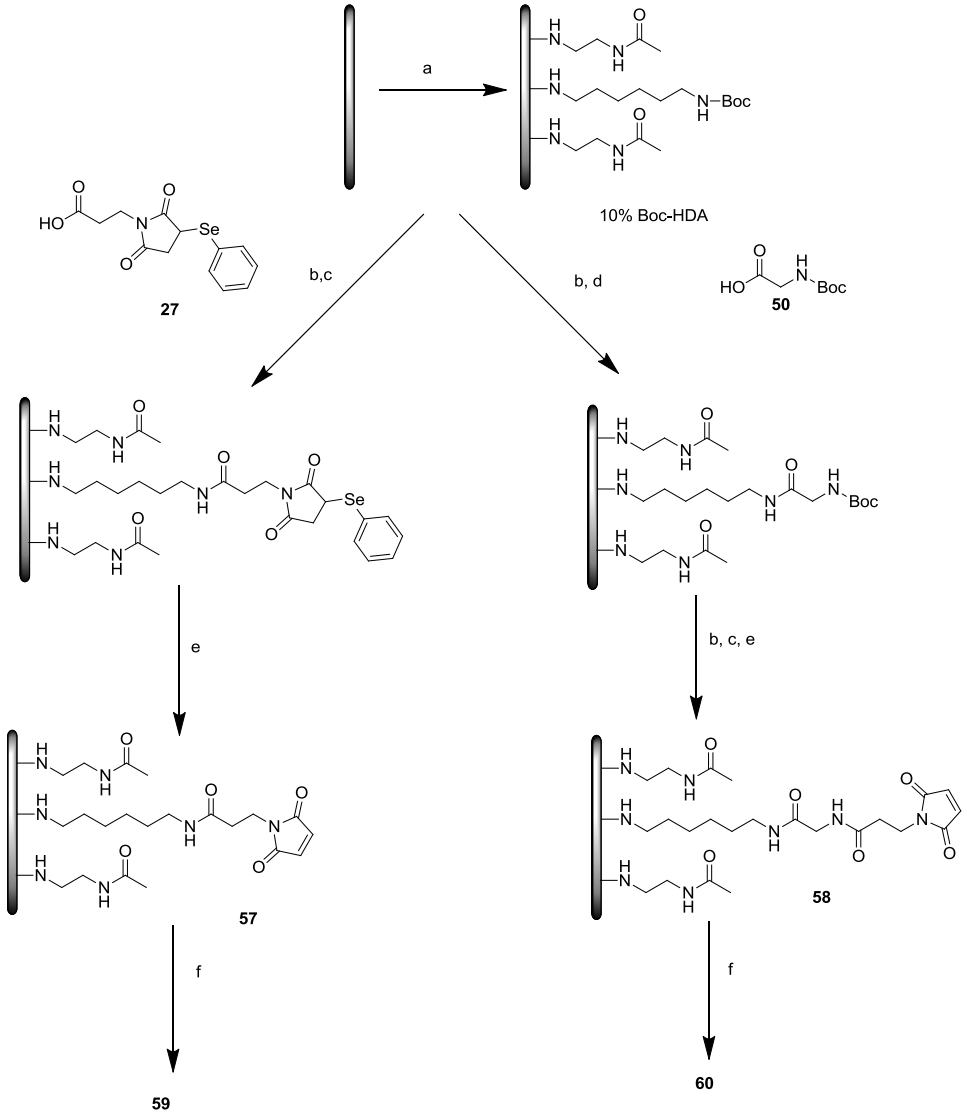

Scheme 35 – Synthesis of GDH electrodes **57** and **58.** a) Boc -HDA (1 mM) aminoethylacetamide (9 mM), acetonitrile, TBATFB (150 mM). 180 s at 2.1 V vs Ag/AgCl b) 4M HCl in dioxane, 1 h, c) **27**, HBTU, DIEA, DMF 16 h, d) **50**, HBTU,

DIEA, DMF, e) *m*CPBA in acetonitrile, 1 h at 0 °C, 1 h at room temperature, f) *Gc*GDH (T343C), in 20 mM phosphate buffer pH 7, 4°C

The electrodes were tested for DET by cyclic voltammetry using a wide scan range in pH 5.5 citrate buffer without the addition of any mediator. Voltammetry was done at 2 mV/s and then glucose solution was added.

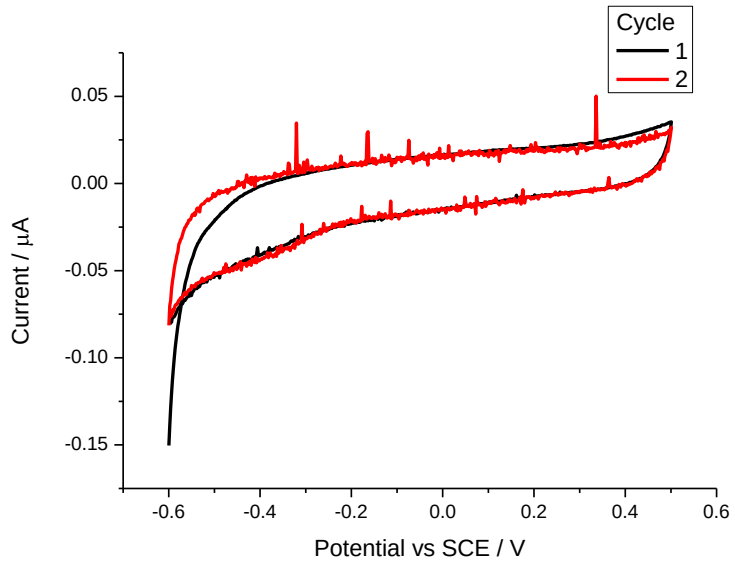

Figure 74 – CV of **57** (Scheme 35) in Ar saturated pH 5.5 citrate buffer (100 mM) with 100 mM TEATFB at 2 mV/s

The control sample showed no clear peaks by cyclic voltammetry (Figure 74), suggesting that any peaks in the cyclic voltammetry of *Gc*GDH modified electrode might be derived from the enzyme itself.

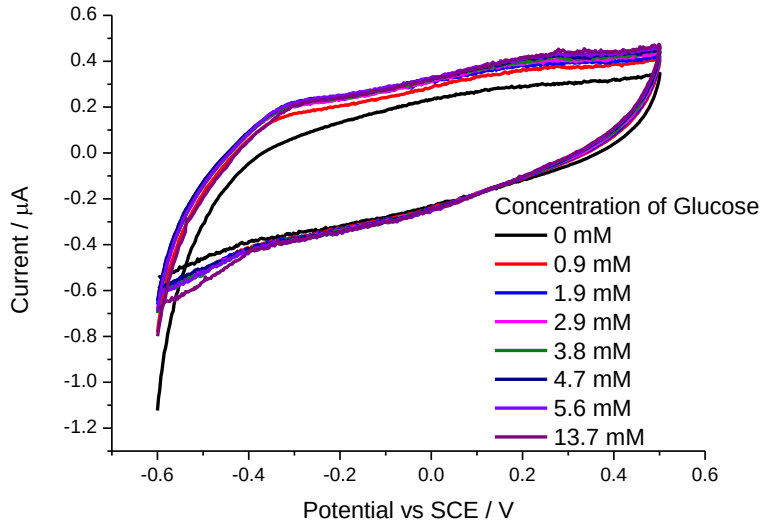

Figure 75 - CV of **59** (Scheme 35) at 2 mV/s in Ar Saturated pH 5.5 citrate buffer (100 mM) with 100 mM TEATFB, following addition of glucose, first cycles shown.

Upon testing of *Gc*GDH modified electrode **59** by cyclic voltammetry under the same conditions a small peak was observed at about -0.35 V vs SCE (Figure 75), upon the addition of glucose the current increased from this point. The same experiment was performed on the *Gc*GDH modified electrode (**60**) with a two carbon spacer (Figure 76). Similar features were also seen, however the observed peak and current increase were greater, suggesting more enzyme could be on the surface.

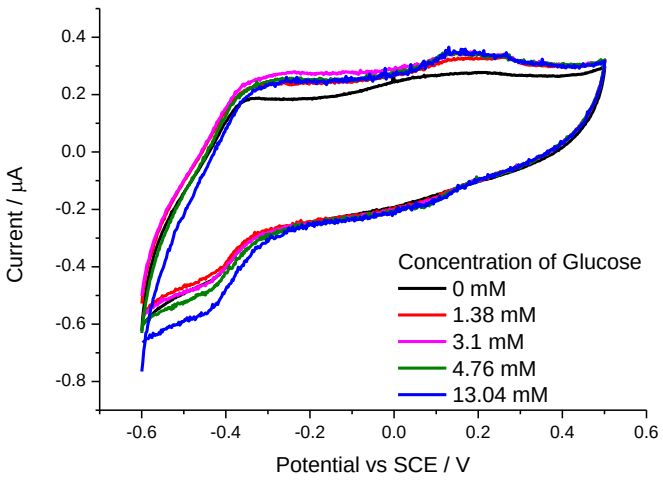

Figure 76 – CV of **60** (2 carbon spacer with T343C mutant, Scheme 35) at 2 mV/s in Ar Saturated pH 5.5 citrate buffer (100 mM) with 100 mM TEATFB. First cycle shown.

In addition to the peak at around -0.35 V a reversible feature was observed at 0.2 V vs SCE, this is most likely an impurity or a quinone on the surface of the glassy carbon. The feature is consistently seen in CVs within this potential range.

5.6.1.2 K423C

Following successful attachment of the GDH the other mutant with the more buried cysteine was investigated. In this case because the cysteine is much further from the surface a 6 carbon spacer was introduced before coupling (Scheme 36).

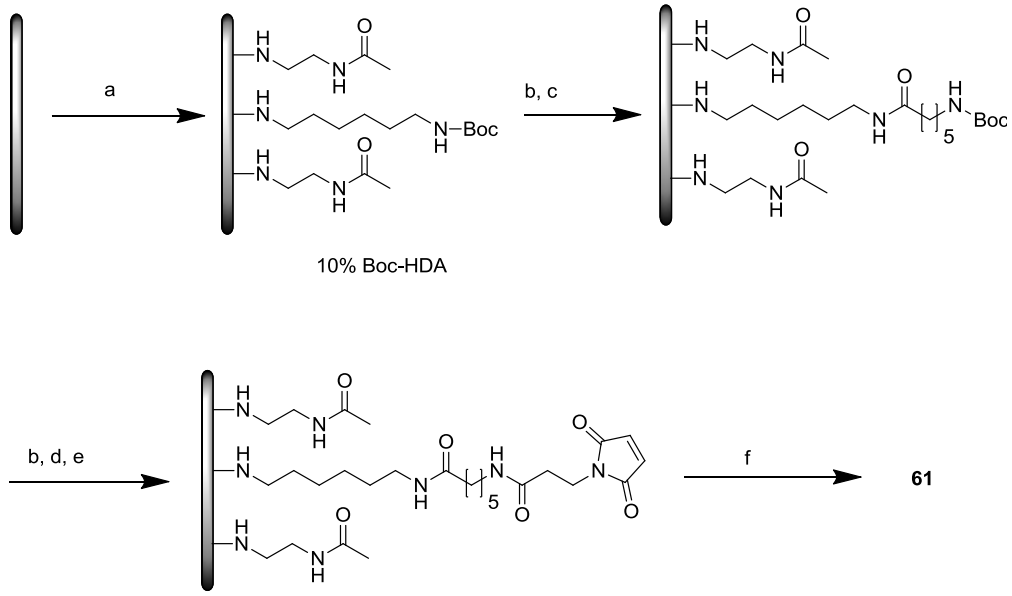

Scheme 36 – Attachment of K423C using a 6C spacer a) Boc -HDA (1 mM) aminoethylacetamide (9 mM), acetonitrile, TBATFB (150 mM). 180 s at 2.1 V vs Ag/AgCl b) 4M HCl in dioxane, 1 h, c) **52**, HBTU, DIEA, DMF, 16 h d) **27**, HBTU, DIEA, DMF 16 h e) *m*CPBA in acetonitrile, 1 h at 0 °C, 1 h at room temperature, f) *Gc*GDH (T343C), in 20 mM phosphate buffer pH 7, 4°C

Electrodes were tested by cyclic voltammetry in pH 5.5 citrate buffer at (10 mV/s) and aliquots of glucose were added (Figure 77). The observed voltammetry was similar to the other mutant, with features around -0.35 V vs SCE and a smaller, broader peak around 0.1 V vs SCE. Upon addition of glucose the current increased from the potential of -0.35 V vs SCE, as before.

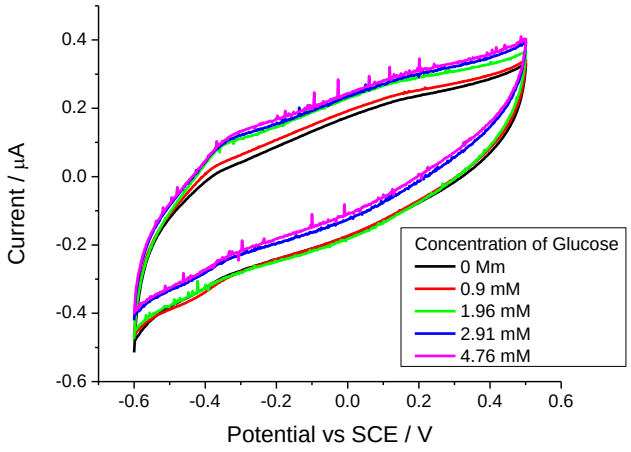

Figure 77 – CV of **61** (6C spacer, K423C attached, Scheme 36) in pH 5.5 citrate buffer, with 100 mM TEATFB. Second cycle shown.

The same electrode was tested after 24 hour storage in the same buffer at 4 ˚C. No increase in current was seen, suggesting that the enzyme activity had been lost upon storage (Figure 78).

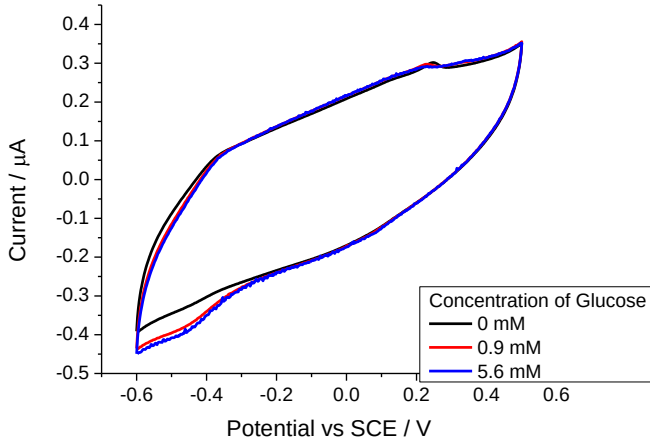

Figure 78 – Cyclic voltammetry of 5 (6C spacer, K423C attached, Scheme 36) after 24 hours storage at 4 °C. Voltammetry in pH 5.5 citrate buffer, with 100 mM TEATFB. Second cycle shown.

As it is notoriously difficult to achieve DET the procedure was repeated, however this time the electrode was tested without glucose in the solution twice, each time two cycles were completed and then the experiment was stopped. Aliquots of glucose were then added as before (Figure 79).

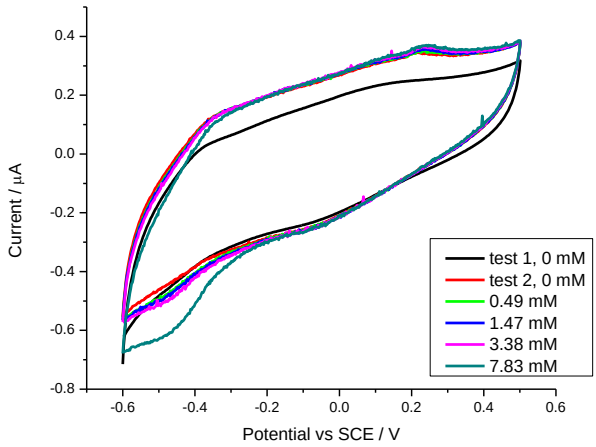

Figure 79 – CV of **61** at 10 mV/s in pH 5.5 citrate buffer with 100 mM TEATFB, D-glucose added in aliquots. Second cycle shown. Electrode area 0.0707cm^2.

The cyclic voltammetry (Figure 79) observed after the second cycle showed an increase in current similar to the phenomenon seen when 'direct electrochemistry' had been seen, however the increase was seen without the addition of glucose.

The first cyclic voltammetry (black line) was done before the electrode was held at - 0.35 V for 30 min, and then a second cyclic voltammogram was done without glucose (red), this showed an increase in current only in the oxidation half, there was no shift in the reduction current, so the reason for the increased current is not clear.

As a control to rule out DET, the experiment was repeated using L-glucose and D-glucose. L-Glucose is not oxidised by *GcGDH* so this should not cause any increase in current, however if the current were to be due to DET then addition of D-glucose would cause an increase in current. The results may be seen below in Figure 80.

Glucose Dehydrogenase

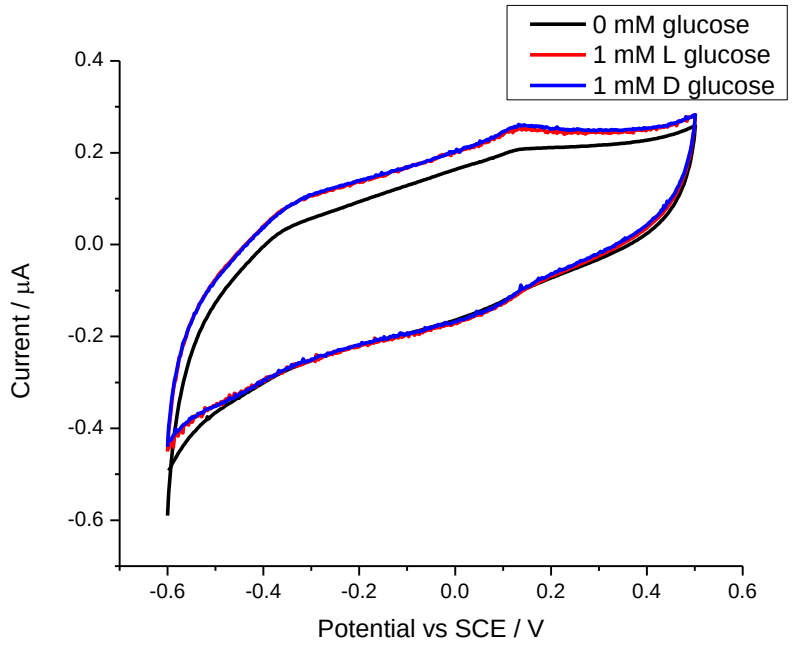

Figure 80 – 'DET' test of **61** at 10 mV/s in pH 5.5 citrate buffer (50 mM) with 100 mM TEATFB.

The increase in current was seen with the addition of L glucose and again the shift is only in the oxidation part of the CV. Each cycle was stopped at -0.6 V vs SCE before the addition of glucose and mixing, so once again the electrode was held at a negative potential, however the duration was much less than 30 minutes. It is still not clear what the increase in current is caused by, there are no peaks in the reduction part of the CV which are slowly oxidised. It is possible that the increase in current is simply due to a change in the capacitance of the electrode, after a change in potential the surface has changed. This change in capacitance could be due to adsorption or desorption of something from the surface or changes in how the surface is arranged due to the oxidation of the electrode.

The key outcome of the control experiment was that direct electron transfer was ruled out, as the increase in current was seen on addition of L-Glucose, which is not oxidised by GDH. It is important to note that in many literature examples of 'DET' the evidence is not convincing as there are insufficient controls reported.

5.6.1.3 5.6.1.3 FAD Control Sample

In order to try and determine if the peak observed at -0.35 V vs SCE was related to the flavin in the GDH, a control sample was prepared with maleimide and FAD was added to the surface (Scheme 37).

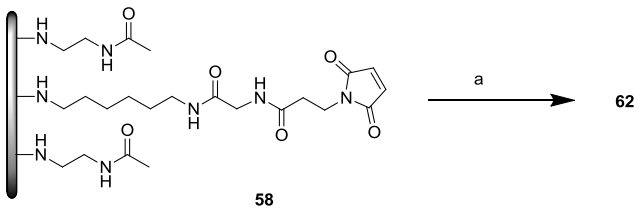

Scheme 37 – Preparation of **62**, control sample with non-specific attachment of FAD. A) Flavin adenine dinucleotide disodium salt hydrate in phosphate buffer pH 7.

As shown in Figure 81 the flavin appears to adsorb onto the surface, as new features appear at -0.35 V together with a smaller broad feature at 0.1 V vs SCE. The previous control electrodes (Figure 74) showed no peaks at all in this region, suggesting that these features come from the FAD. The features are similar to the features seen when the enzyme has been attached.

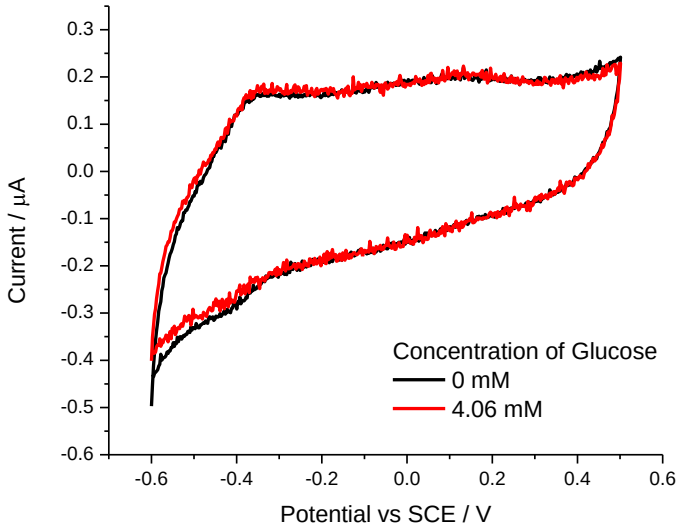

Figure 81 – Cyclic voltammetry of **62** (FAD control, Scheme 37) in pH 5.5 citrate buffer with 100 mM TEATFB, 2nd cycle shown. Electrode area 0.0707 cm².

Glucose Dehydrogenase

This suggests that the peak at -0.35 V vs SCE could be from free flavin that has come out of the GDH as it is not covalently bound to the enzyme. It is assumed that the potential for the flavin may differ when it is in the enzyme, compared to free flavin simply adsorbed, however the actual potential for the flavin in *Gc*-GDH is unknown[124]. Integration of the peak from the cyclic voltammetry gives an approximate coverage of 3.29×10^{-11} mol cm^{-2}.

5.6.2 Mediated Electrochemistry

Following the unsuccessful attempt at direct electrochemistry the focus was switched to the mediated electrochemistry of the electrodes.

5.6.2.1 T343C

In addition to the test for DET, **59** was also tested for mediated electron transfer (MET) using cyclic voltammetry at 2 mV/s (Figure 82) in citrate buffer with DCIP as a mediator.

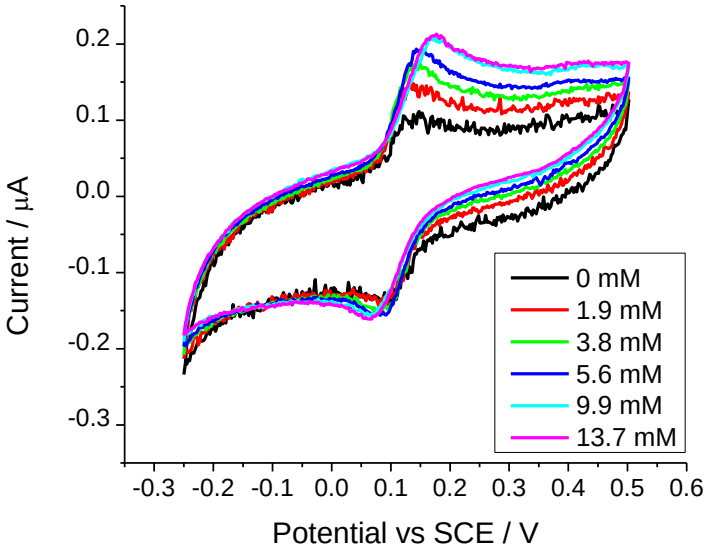

Figure 82 - Representative cyclic voltammetry of **59** at 2 mV/s in 100 mM pH 5.5 citrate buffer, 100 µM DCIP with 100 mM TEATFB. Synthesis procedure shown in Scheme 35, electrode area 0.0707 cm^2. First cycle shown.

Although a catalytic current is seen the reduction peak does not disappear as you would expect to see at high concentrations of glucose, and was observed in solution (Figure 70). Here (Figure 82) the reduction peak is clearly observed,

this is due to the much lower concentration of GDH on the surface. At such a low concentration of GDH it is not possible for the DCIP to be reduced by the enzyme faster than the change in potential.

The catalytic current was plotted against the concentration of glucose (Figure 83) and used to estimate the K_M value.

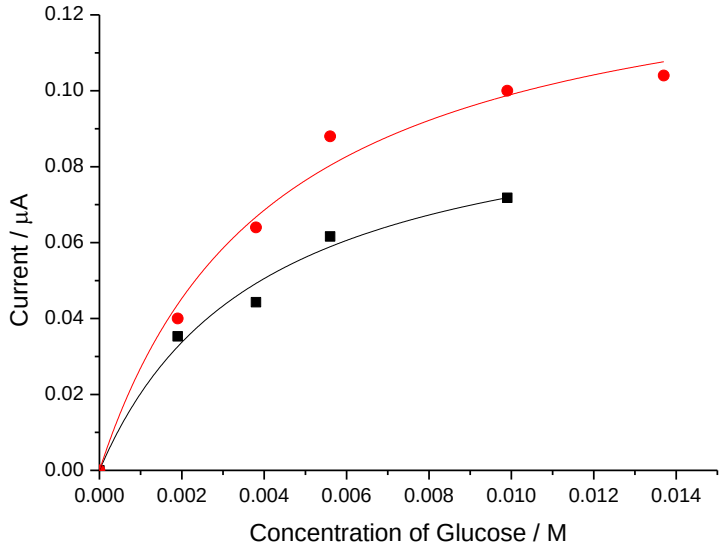

Figure 83 – Plot of current vs concentration of glucose for duplicate electrodes **59** prepared from Scheme 35. Data extrapolated from cyclic voltammetry at 2 mV/s in pH 5.5 citrate buffer (50 mM) with 100 mM TEATFB and 100 µM DCIP. Electrode area 0.0707 cm^2.

The duplicate electrodes followed a very similar curve, despite the current being different, suggesting that the Km was consistent, while the increased current in one of the electrodes suggests that the concentration of enzyme on the two electrodes was not the same. The apparent K_m value was determined to be 3.96 mM and 4.21 mM for the two electrodes prepared, consistent values within experimental error. Despite the variation in concentration, as Km is a measure of the affinity between an enzyme and substrate, a factor independent of concentration, this was expected.

Electrodes prepared with a two carbon spacer were also tested by cyclic voltammetry (Figure 84) and the current was extrapolated and plotted against glucose concentration to calculate K_m (Figure 85).

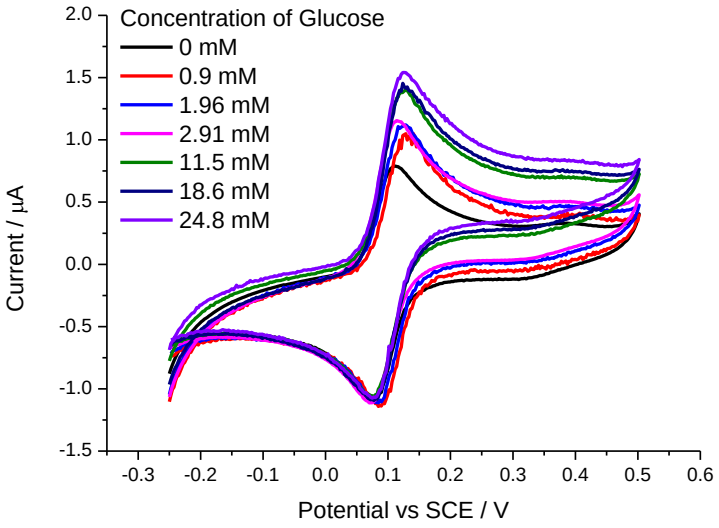

Figure 84 – Representative cyclic voltammetry of **60** at 2 mV/s in 100 mM pH 5.5 citrate buffer, 100 µM DCIP with 100 mM TEATFB. First cycle shown. Synthesis procedure shown in Scheme 35, electrode area 0.0707 cm².

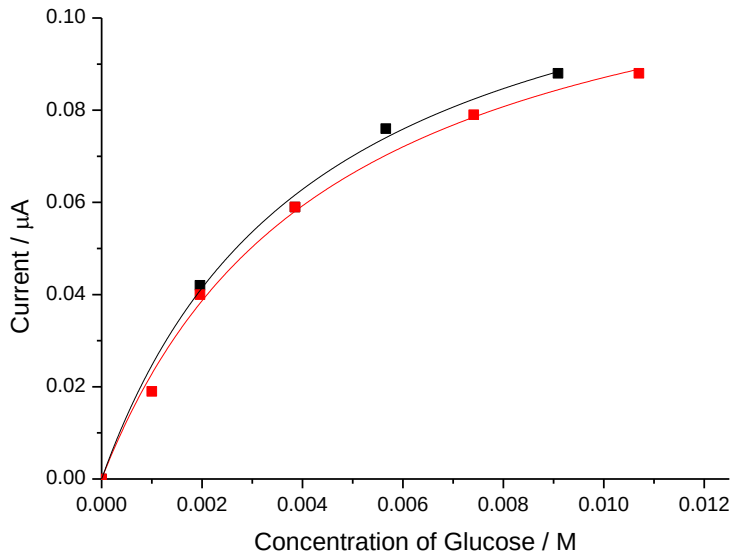

Figure 85 – Plot of current vs concentration of glucose for duplicate electrodes **60** prepared from Scheme 35. Data extrapolated from cyclic voltammetry at 2 mV/s in pH 5.5 citrate buffer (50 mM) with 100 mM TEATFB and 100 µM DCIP. Electrode area 0.0707 cm².

The two electrodes were very consistent with similar currents and curves, the estimated k_m values were calculated to be very consistent at 4.5 mM and 4.3 mM.

In order to demonstrate that the enzyme was still active and specific after attachment to electrodes, freshly synthesized electrodes **60** were tested for MET using cyclic voltammetry (

Figure 86), using the addition of aliquots both L-and D-glucose. As *Gc*GDH is specific to D-glucose the current was only expected to increase when D-glucose was added, as shown in (Figure 87).

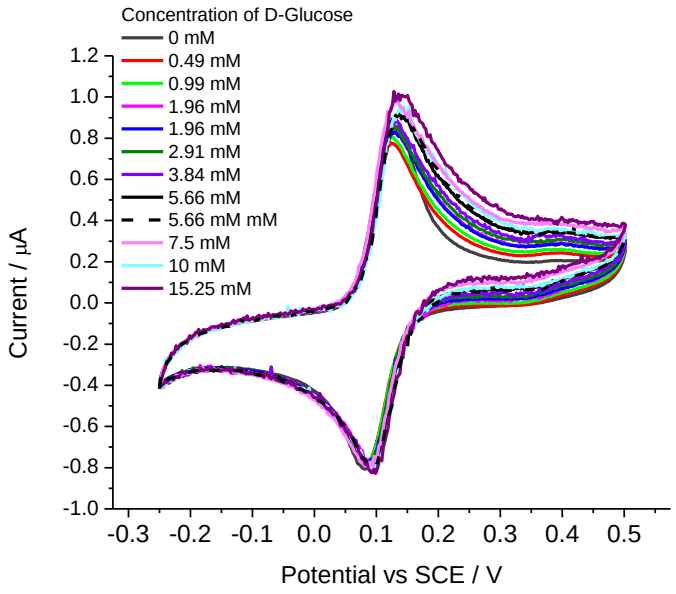

Figure 86 – Cyclic voltammetry of **60** (Scheme 35) at 10 mV/s following the addition of D- and L-Glucose in 100 mM pH 5.5 citrate buffer, 100 µM DCIP with 100 mM TEATFB. First cycle shown. Electrode area 0.0707 cm^2.

Glucose Dehydrogenase

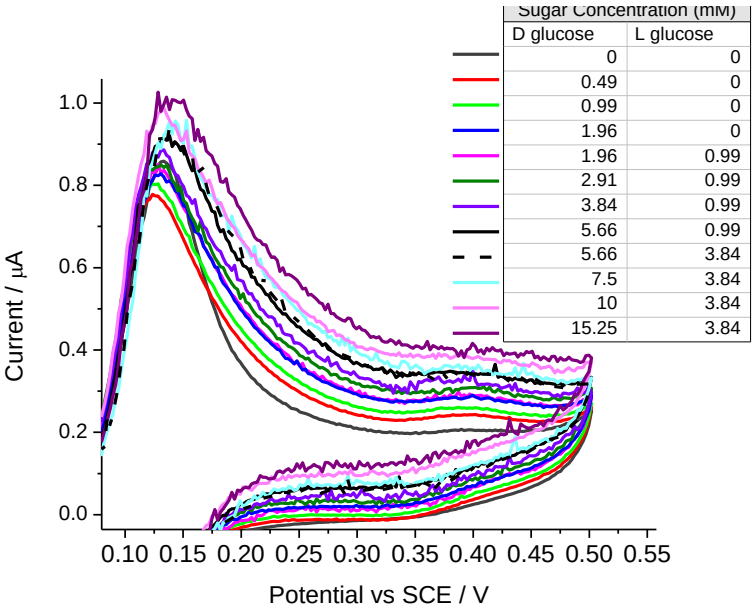

Figure 87 – Oxidation part of cyclic voltammetry of **60** (Scheme 35) at 10 mV/s to show the catalytic current following the addition of D- and L-Glucose in 100 mM pH 5.5 citrate buffer, 100 µM DCIP with 100 mM TEATFB. First cycle shown. Electrode area 0.0707 cm^2.

As shown in

Figure 86 the current consistently increased upon the addition of D-Glucose, however it did not increase upon addition of L-Glucose, showing the increase in current was due to the specific oxidation of D-Glucose. The current was plotted against concentration of glucose (Figure 88) for comparison of the duplicates prepared and to estimate the k_m value.

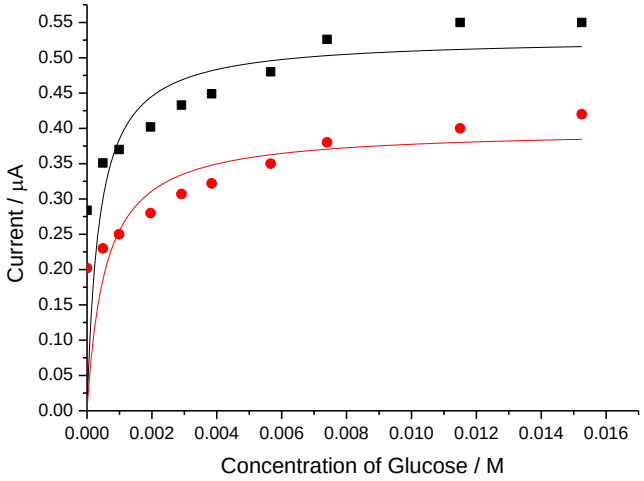

Figure 88 – Plot of current vs glucose concentration for **60** (Scheme 35). Data extrapolated from cyclic voltammetry at 10 mV/s in pH 5.5 citrate buffer (50 mM) with 100 mM TEATFB and 100 µM DCIP. First cycle shown. Electrode area 0.0707 cm².

The duplicates prepared have a different current; however the shape of the graph and K_m values are similar for both electrodes prepared. The K_m value is 0.37 mM and 0.56 mM for the electrodes. This suggests that the amount of enzyme on the electrodes is different; however the efficiency of the enzyme is the same. The shape of the calculated curve and the points on it do not fit well, in addition the K_m values are very low, and this is most likely due to the amount of L-Glucose in the testing solution.

5.6.2.2 Duration of Enzyme Attachment

Following successful attachment of variant 1, the second variant was investigated; In addition the enzyme coupling conditions were also investigated. The initial conditions used were the same as Cytochrome C, which had been left to couple with the electrode surface in the fridge for at least 16 hours. Electrodes were prepared as before (Scheme 36) but with varying duration for the final reaction (Scheme 38), electrodes were left with enzyme for 2, 4 and 24 hours and then tested for mediated electron transfer.

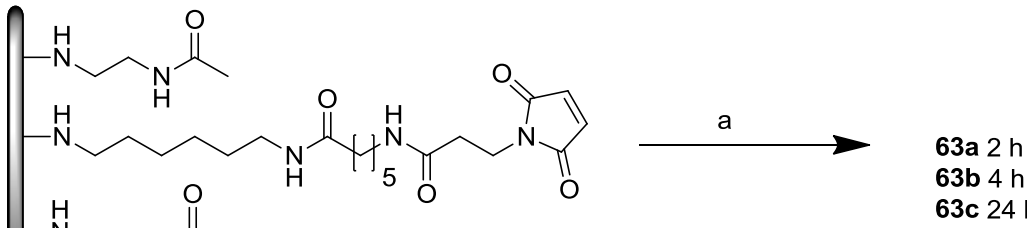

Scheme 38 – Variation of enzyme coupling time. A) *Gc*GDH K423C in phosphate buffer, pH 7 at 4 °C 2h, 4, or 24 h.

The prepared electrodes were then tested by cyclic voltammetry as before, at 10 mV s^{-1} in pH 5.5 citrate buffer (50 mM) with mediator (DCIP). The results may be seen in Figure 89 (2 h), Figure 90 (4 h) and Figure 91 (24 h).

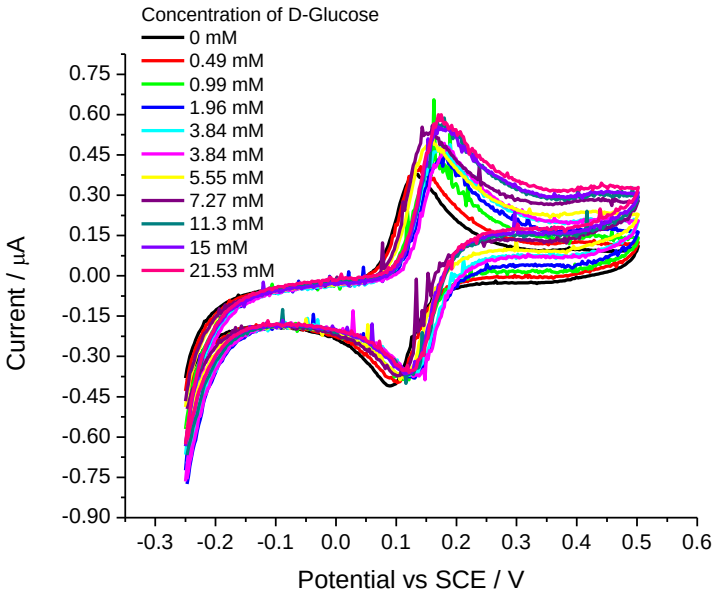

Figure 89 – CV of **63a** (after 2 hours with T423C) in 50 mM citrate buffer pH 5.5 with 100 mM TEATFB and 100 µM DCIP, 10 mV/s

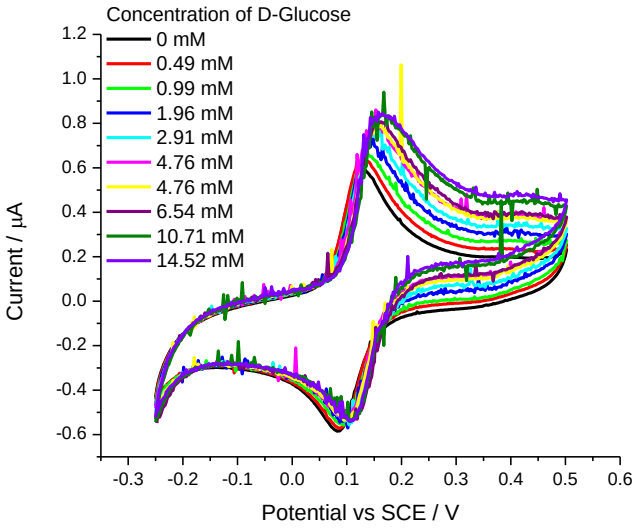

Figure 90 – CV of **63b** (after 4hr coupling with T423C) in 50 mM citrate buffer pH 5.5 with 100 mM TEATFB and 100 µM DCIP, 10 mV/s

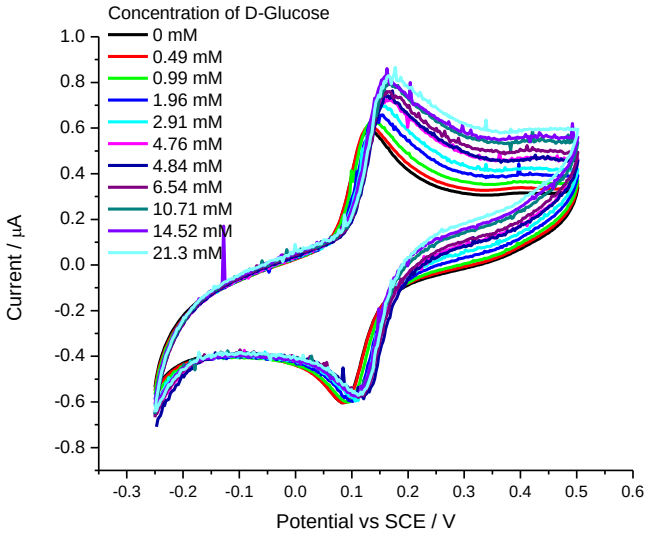

Figure 91 – CV of **63c** (after 24hr coupling with T423C) in 50 mM citrate buffer pH 5.5 with 100 mM TEATFB and 100 µM DCIP, 10 mV/s

From these results it was clear that the enzyme had successfully reacted with the surface after just 2 hours. Each electrode was prepared in duplicate and the currents were plotted against glucose concentration (Figure 92).

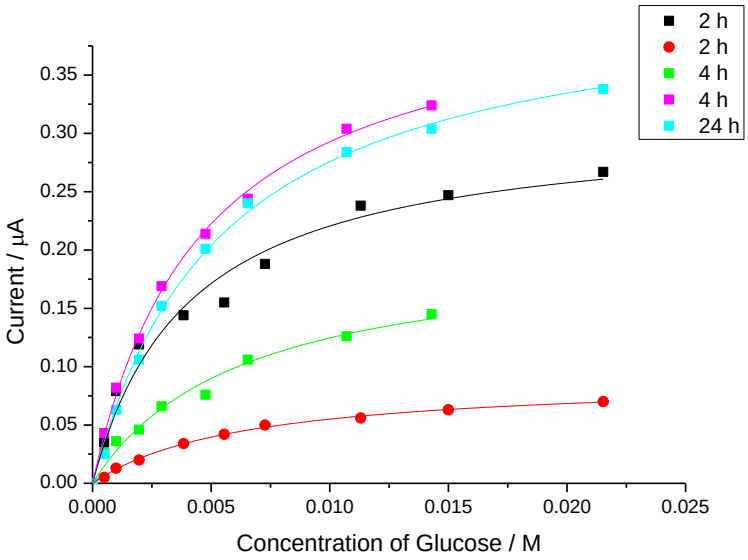

Figure 92 – Plot of current vs concentration of glucose after variation of reaction time. Extrapolated from cyclic voltammetry at 10 mV/s in 50 mM citrate buffer pH 5.5 with 100 mM TEATFB and 100 µM DCIP, 10 mV/s. Electrode area 0.0707 cm^2.

The results of the duplicates were not very consistent, and showed that the coupling had been achieved in as little as two hours. The results for 24 hours coupling time were similar to the results for two hours coupling time, suggesting that the enzyme activity was unaffected by the coupling conditions in pH 7 buffer.

The electrodes were all prepared at the same time, so it is assumed that the structure on the surface is the same, however the currents are variable, suggesting that the amount of enzyme on the surface is not the same. This error may be due to an experimental error when coupling the enzyme, as a small drop of enzyme solution was put on the surface of each electrode individually. If the drop used did not stay on the electrode surface and leaked away then the loading would not be the same.

The electrodes were then stored for 24 hours in pH 5.5 buffer, without DCIP or glucose, at 4 ˚C and then retested. After storage the activity of the enzyme had decreased, there was only a minimal increase in current upon glucose addition on retesting (Figure 93).

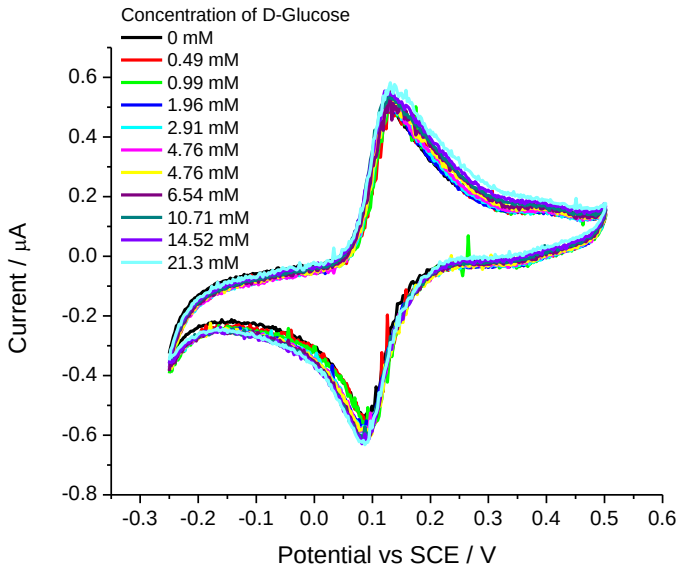

Figure 93 – **63a** after 24 hours storage. Cyclic voltammetry at 10 mV/s in 50 mM citrate buffer pH 5.5 with 100 mM TEATFB and 100 µM DCIP. Electrode area 0.07007 cm^2.

This loss in activity is likely to be due to the storage conditions which would need to be modified. Over the course of the testing there was no decrease in current and this was done at room temperature, so the enzyme appears relatively stable. However the use of glucose and mediator in the testing solution may improve the stability. In addition the coupling is done at pH 7, and the enzyme also appears stable in this solution, so the electrodes may also be stored in pH 7 buffer. A screening process of buffer would be needed to find the best conditions for enzyme storage.

As the reaction was complete in 2 h a shorter reaction time of 1.5 hours was also investigated. Electrodes were tested by cyclic voltammetry and from this a plot of current vs glucose concentration was drawn (Figure 94).

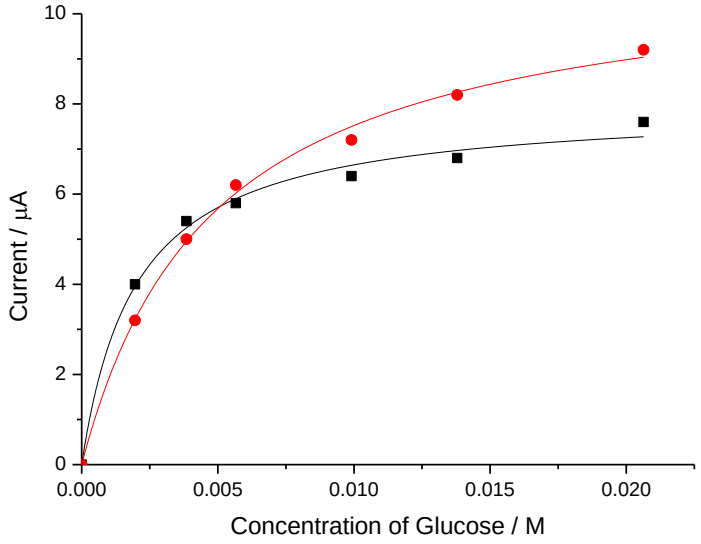

Figure 94 – Plot of Plot of current vs concentration of glucose after variation of reaction time. Extrapolated from cyclic voltammetry at 10 mV/s in 50 mM citrate buffer pH 5.5 with 100 mM TEATFB and 100 µM DCIP, 10 mV/s. Electrode area 0.0707 cm^2.

The reaction was successful in 1.5 hours, with a clear increase in current and the duplicate electrodes appear more consistent in this case, however the total current was much lower than the previous results, suggesting that there was not as much enzyme on the surface. This suggests that the reaction may not be complete in 1.5 hours, and requires a greater reaction time of at least 2 hours to achieve more current.

5.7 Alternative Mediators

The mediator used for the experiments, DCIP, was found to not be ideal as it was found to stick to some of the electrodes, shown by an increase in peak current without addition of glucose, for this reason ferrocene carboxylic acid was investigated as an alternative mediator.

5.7.1 Ferrocene Carboxylic Acid

The solution electrochemistry of ferrocene carboxylic acid was investigated (Figure 95) first and then it was used as a mediator for the recombinant wild type *Gc*GDH in solution, using the same buffer and pH as with DCIP.

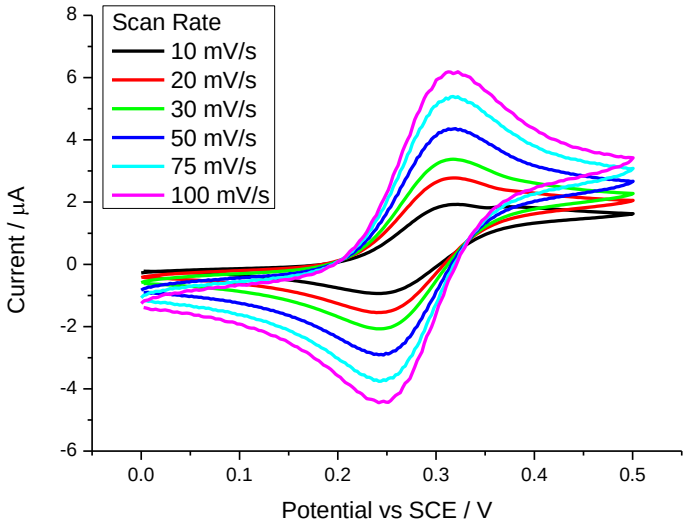

Figure 95 – Cyclic voltammetry of ferrocene carboxylic acid (0.5 mM) at varying scan rates in 50 mM citrate buffer with 100 mM TEATFB.

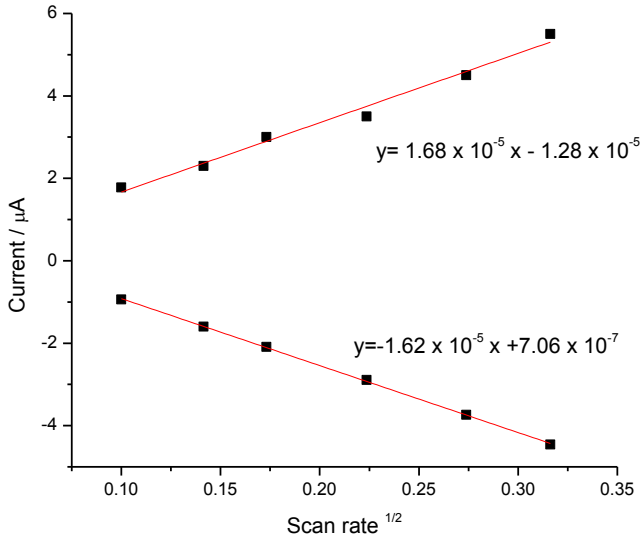

Figure 96 – Plot of current vs square root of scan rate for solution of ferrocene carboxylic acid (0.5 mM) in 50 mM citrate buffer with 100 mM TEATFB.

The relationship between √scan rate and peak current was shown to be linear, showing that the process was indeed revisable. As before the diffusion coefficient was calculated using the Randles-Sevick equation, *D* was calculated to be 2.9 x 10^{-6} cm^2 s^{-1}.

Glucose Dehydrogenase

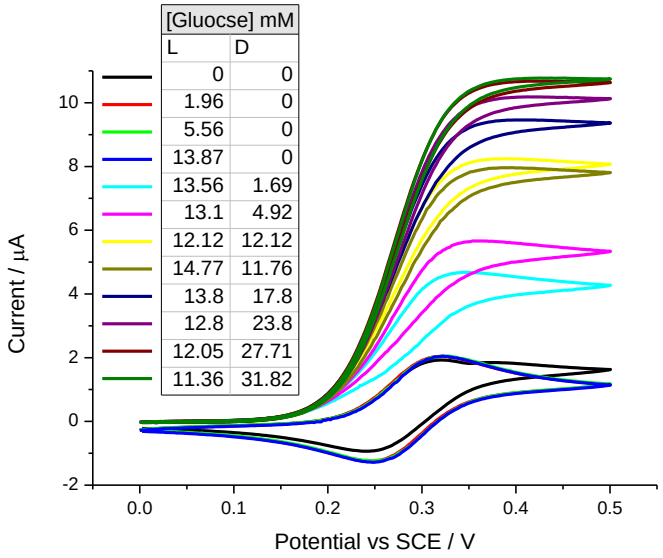

Figure 97 - Cyclic voltammetry at 10 mV/s glucose in 100 mM pH 5.5 citrate buffer, Ferrocene carboxylic acid (0.5 mM) with 100 mM TEATFB and *rGc*GDH (0.15µM) following the addition of D- and L-Glucose. First cycle shown. Electrode area 0.0707 cm².

As on the surface both D- and L-Glucose were used to show that the enzyme was specific to the oxidation of D-Glucose, and no current increase was seen on addition of L-Glucose (Figure 97). The current and concentrations of D-Glucose were plotted, in order to estimate k_m (Figure 98).

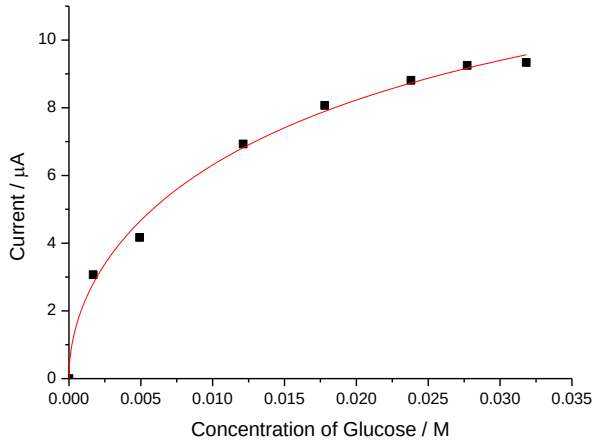

Figure 98 – Plot of current vs concentration of glucose after addition of glucose. Extrapolated from cyclic voltammetry at 10 mV/s in 50 mM citrate buffer pH 5.5 with 100 mM TEATFB and Ferrocene carboxylic acid (0.5 mM) and GDH (2µM), 10 mV/s. Electrode area 0.0707 cm².

The data was fitted to the modified Michaelis-Menten equation:

$$i = V''_{\max}\left(\frac{[S]}{[S] + K''_{Mapp}}\right)^{1/2}$$

The values were calculated as follows, K''_m = 47 mM and V''_{max} = 1.5 x 10^{-5} A

$V''_{max}/(K''_M)^{1/2}$ = 6.9 x 10^{-5} A $M^{-1/2}$

By comparison to the data in Figure 72, with DCIP as a mediator, the observed currents are smaller with ferrocene. This suggests that the current is not limited by the enzyme/substrate reaction and suggest that the reaction is limited by step 3, the reaction of mediator with the enzyme therefore:

$V_{max} = nFA\,(D\,k\,[Ez])^{1/2}\,[M]$

This gives a value for k of 8.3 x 10^5 dm^3 mol^{-1} s^{-1}

For this case $K''_M = \frac{K_M k[M]}{k_{cat}}$

Therefore k_{cat}/K_M = 3.5 x 10^4 dm^3 mol^{-1} s^{-1}.

The plateau was reached at 27 mM glucose, and the variation of scan rates was repeated at the high concentration (Figure 99).

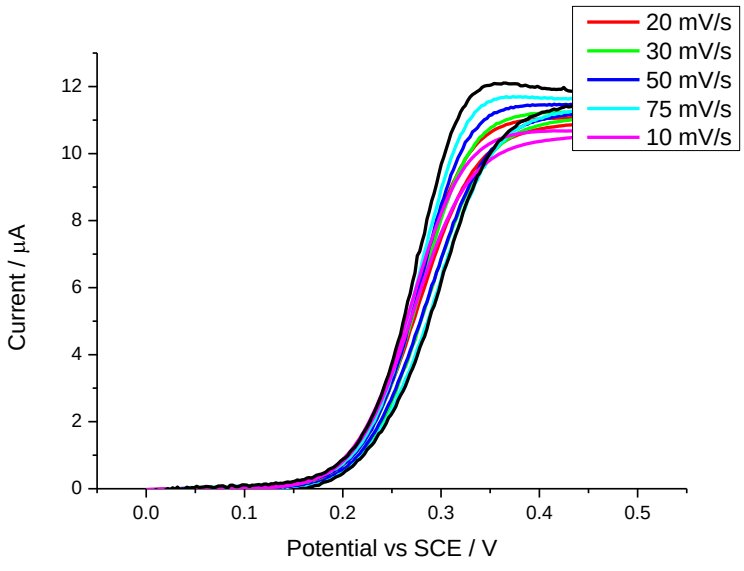

Figure 99- Cyclic voltammetry of ferrocene carboxylic acid (0.5 mM) at varying scan rates in 50 mM citrate buffer with 100 mM TEATFB, 2 µM *Gc*GDH and glucose.

Glucose Dehydrogenase

Ferrocene carboxylic acid was shown to have good reversible electrochemistry and worked well as a mediator for GDH.

5.8 Oxidation of Alternative Sugars

L-Glucose is a good way to show that the GDH is still active and specific to D-Glucose, an alternative method of demonstrating the enzyme activity and specificity would be the use of other sugars. Although the other sugars differ from glucose some are still oxidised, though at a slower rate.

5.8.1 Xylose

The activity of GDH with xylose was investigated, as a possible alternative to L-glucose. Xylose has been shown to react with GDH previously but at a much lower rate (33% activity) than glucose.

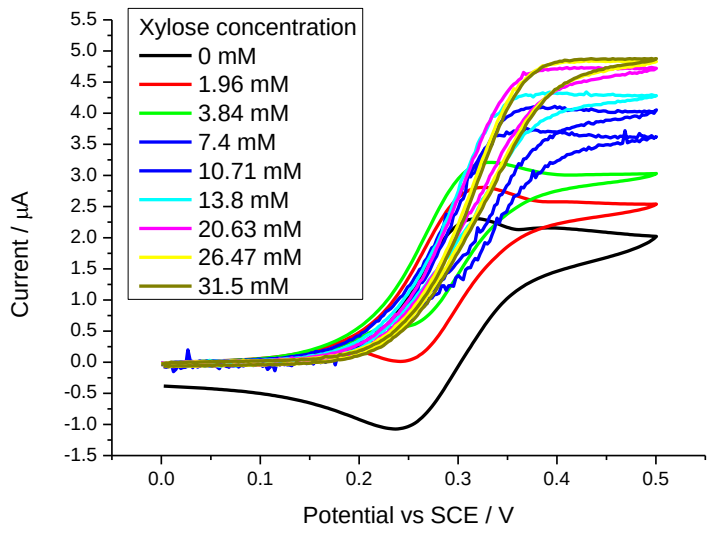

Figure 100 – Cyclic voltammetry of ferrocene carboxylic acid (0.5 mM) in 50 mM citrate buffer pH 5.5 with 100 mM TEATFB and GDH 5.81 µM following addition of xylose.

Upon the addition of xylose the current is initially seen to increase, in addition at a low concentration (1.96 mM) of xylose the reduction peak is also seen, showing the reaction of xylose with GDH is sufficiently slow so that ferrocene is not re-oxidised by GDH quickly enough to consume it all in the timescale. However at higher concentrations the reverse peak disappeared. The current

increase on the whole is much smaller than with glucose and V_{max} was achieved at 20 mM xylose.

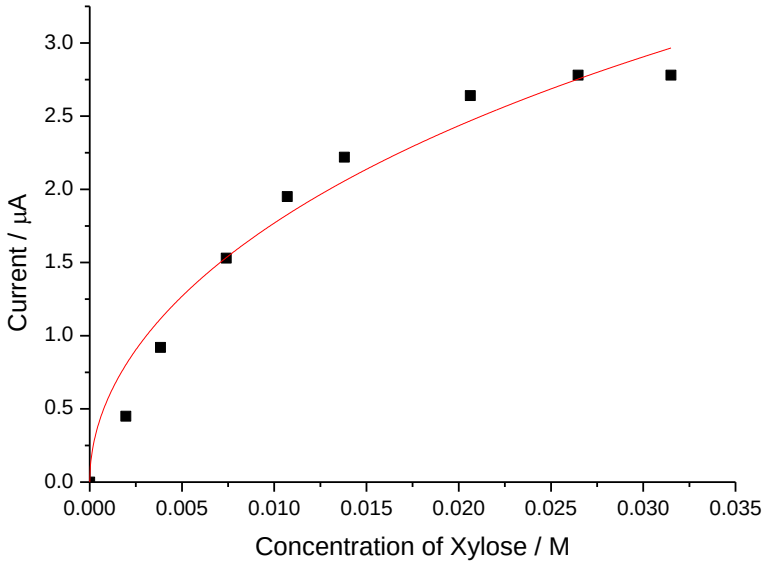

Figure 101 – Plot peak current vs concentration of Xylose. Data extrapolated from cyclic voltammetry (Figure 100) of ferrocene carboxylic acid (0.5 mM) in 50 mM citrate buffer pH 5.5 with 100 mM TEATFB and GDH (2 µM) following addition of xylose.

The results were fitted to the modified Michaelis-Menten equation, for the mediated reaction of enzyme in homogeneous solution, and the apparent values of V_{max} *and* K_M were calculated. K''_m = 170 mM and V''_{max} = 7.4 x 10^{-6} A.

$V''_{max}/(K''_M)^{1/2}$ = 1.8 x 10^{-5} A $M^{-1/2}$

In the case of xylose the current is limited by the saturated enzyme kinetics, as the currents are not as large as with glucose, despite the same enzyme and mediator concentrations. Therefore the relevant form of the equation is:

$V_{max} = nFA(D\, k_{cat}[Ez][M])^{1/2}$

$K_{cat} = (V_{max} / nFA)^2\ 1/D[Ez][M]$

Therefore K_M for xylose is 170 mM and k_{cat} = 100 s^{-1}

The scan rate experiment was repeated at the high concentration of xylose (Figure 102). At slow scan rates the current remains catalytic and there is no

reduction peak, however at fast scan rates the change in potential is faster than the reaction between ferrocene and GDH.

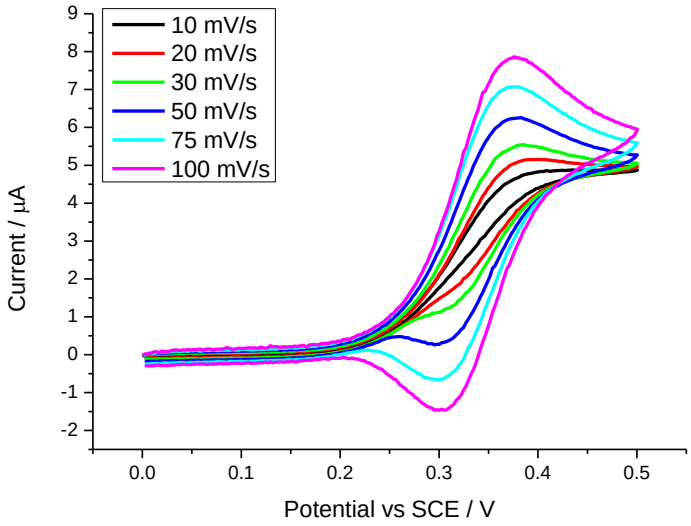

Figure 102 – Cyclic voltammetry of ferrocene carboxylic acid (0.5 mM) in 50 mM citrate buffer pH 5.5 with 100 mM TEATFB and 2 µM GDH with 31.5 mM xylose.

5.8.2 Galactose

Galactose was investigated as an alternative sugar, with the same experiment repeated using galactose (Figure 103).

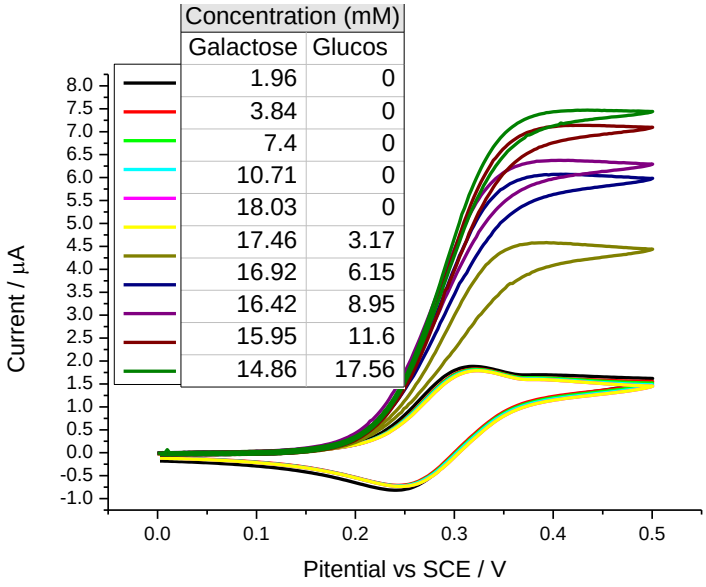

Figure 103 - Cyclic voltammetry of ferrocene carboxylic acid (0.5 mM) in 50 mM citrate buffer pH 5.5 with 100 mM TEATFB and 2µM GDH following addition of galactose and glucose

Following no increase in current at all on addition of galactose, to a concentration of 18 mM, glucose was added to the solution in order to test the activity of the enzyme. Upon addition of D-Glucose there was an increase in the current, showing that the enzyme was active and that galactose was not oxidized by GDH. For this reason galactose would be good alternative to L-Glucose to show the enzyme specificity.

5.9 GDH Variants in Solution

5.9.1 T343 C in solution

Finally the solution electrochemistry of the two GDH variants was investigated, using ferrocene as a mediator and both D- and L-Glucose to ensure the enzyme specificity.

*Gc*GDH-(T343C) was investigated by CV, initially L-Glucose was added to the solution and no increase in current was seen, following this D-Glucose was added and the current increased as expected (Figure 104).

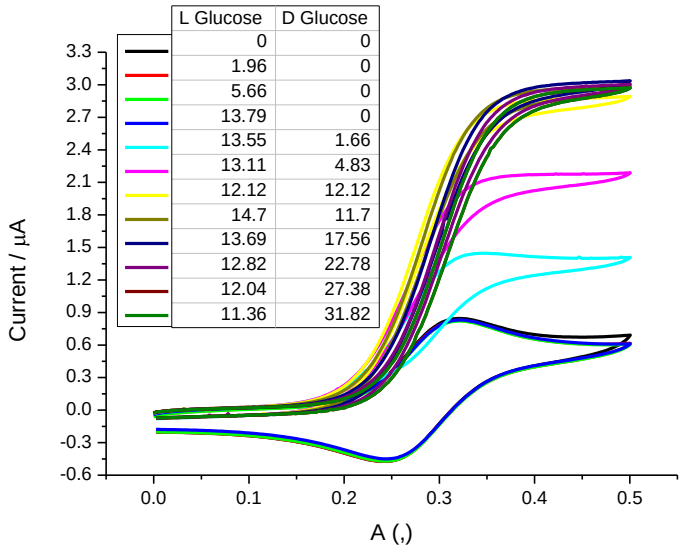

Figure 104 - Cyclic voltammetry at 10 mV s^{-1} in ferrocene carboxylic acid (0.5 mM) in 50 mM citrate buffer pH 5.5 with 100 mM TEATFB and 1µM *Gc*GDH T343C following addition of glucose

The current increase was plotted against the concentration of D-Glucose (Figure 104).

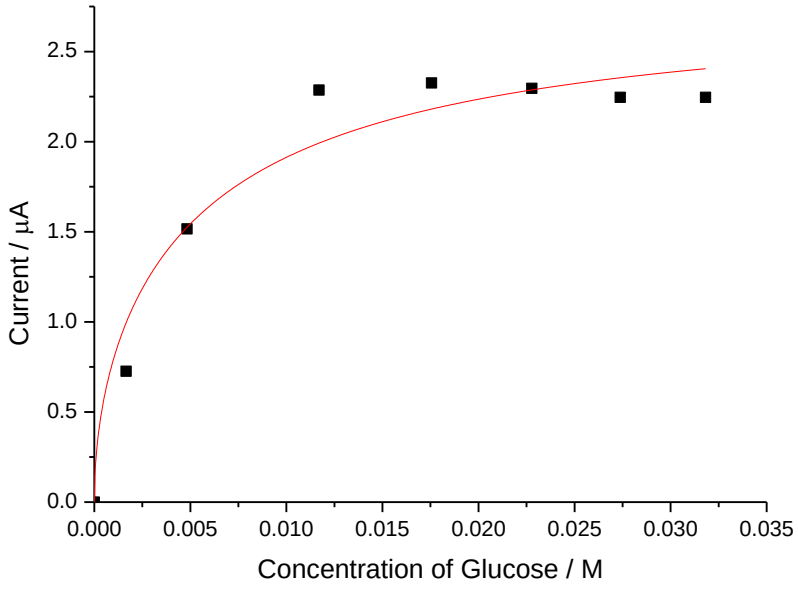

Figure 105 – Plot of peak current vs the concentration of glucose for *Gc*GDH(T343C). Extrapolated from cyclic voltammetry at 10 mV s^{-1} in ferrocene carboxylic acid (0.5

mM) in 50 mM citrate buffer pH 5.5 with 100 mM TEATFB and 1 μM *Gc*GDH T343C following addition of glucose

The data was fitted using the modified equation for the homogeneous, mediated reaction of GDH. The apparent values of K_m *and* V_{max} were found to be 12 mM and 2.9 μA respectively. $V''_{max}/(K''_M)^{1/2} = 2.6 \times 10^{-5}$ A $M^{-1/2}$

The current reached a plateau at approximately 27 mM and the scan rates were repeated at high concentration of glucose in order to calculate the rate constants for the reaction between the GDH and glucose.

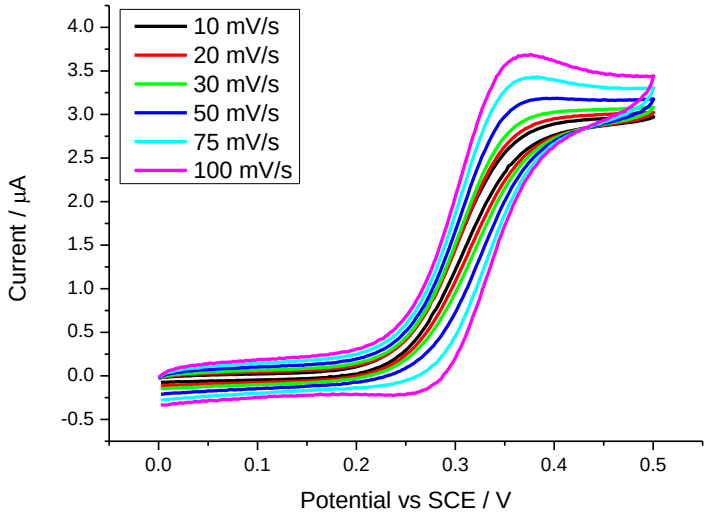

Figure 106 - Cyclic voltammetry at varying scan rate in of ferrocene carboxylic acid (0.5 mM) in 50 mM citrate buffer pH 5.5 with 100 mM TEATFB and 1 μM *Gc*GDH T343C and 12.04 mM L-Glucose and 31.46 mM D-Glucose.

5.9.2 K423C in solution

The electrochemistry of the second variant, K423C, was also investigated in solution, using ferrocene as a mediator and D- and L-Glucose to show that the enzyme was specific (Figure 107).

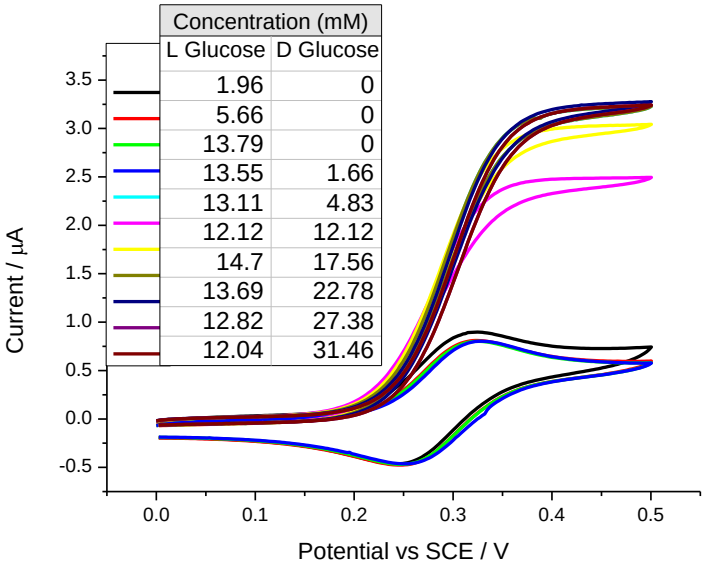

Figure 107 - Cyclic voltammetry at 10 mV s^{-1} in ferrocene carboxylic acid (0.5 mM) in 50 mM citrate buffer pH 5.5 with 100 mM TEATFB and 0.15 µM *Gc*GDHK423C following addition of glucose

The currents were then extrapolated and plotted against glucose concentration (Figure 108).

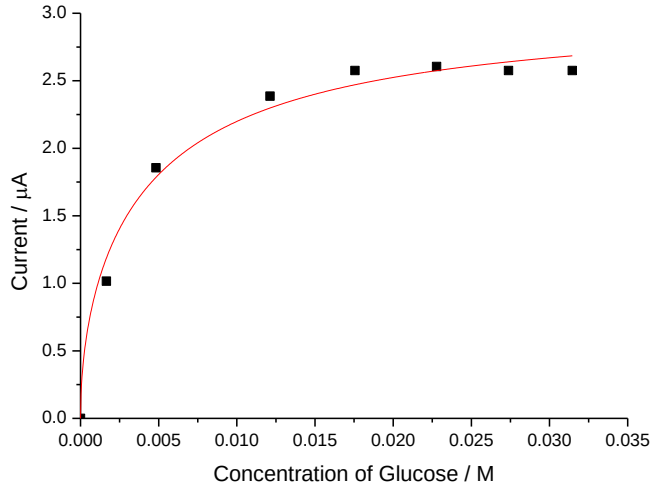

Figure 108 – Plot of current vs concentration of glucose for *Gc*GDH K423C. Extrapolated from cyclic voltammetry at 10 mV s^{-1} in ferrocene carboxylic acid (0.5 mM) in 50 mM citrate buffer pH 5.5 with 100 mM TEATFB and 1.5 µM *Gc*GDH K423C following addition of glucose

The plotted data was fitted to a curve using the modified equation for the homogeneous, mediated reaction of GDH. The apparent values of *Km* and *Vmax* were found as: K''_M = 9.3 mM and V''_{max} = 3.1 μA. It should be noted that these values may be affected by inhibition by L-glucose in the solution.

$V''_{max}/(K''_M)^{1/2} = 3.2 \times 10^{-5}$ A $M^{-1/2}$

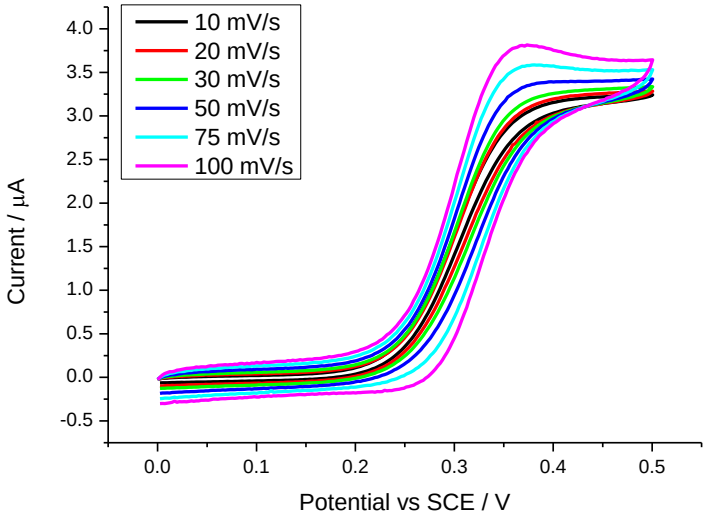

Figure 109 - Cyclic voltammetry at varying scan rate in of ferrocene carboxylic acid (0.5 mM) in 50 mM citrate buffer pH 5.5 with 100 mM TEATFB and 1.5 μM *Gc*GDHK423C and 12.04 mM L- glucose and 31.46 mM D glucose.

The data for both mutants of GDH (Figure 108) and (Figure 104) show very similar kinetics. For the cysteine near the surface (T343C) the value of K^{123}_{cat}/K_M was 1.3 x 10^3 dm^3 mol^{-1} s^{-1} and for the cysteine nearer the active site was 1.9 x 10^4 dm^3 mol^{-1} s^{-1}. However both have much lower values than the native enzyme where K_{cat}/K_M =3.5 x 10^4 dm^3 mol^{-1} s^{-1}. It is not clear if the difference in kinetics of the enzyme were due to the mutation or alteration of the mediator kinetics.

5.10 Conclusions

The successful attachment of two varients of *Gc*GDH has been demonstrated using GC electrodes modified with maleimide. Initially modified electrodes showed some features which looked like possible DET, however control reactions ruled out this phenomenon. The mediated ET of both variants of *Gc*GDH was investigated both on modified electrode surfaces and in solution.

Glucose Dehydrogenase

The use of D(+) and L (-) glucose has proven the activity of the enzyme to remain specific to D (+) glucose when immobilized on the surface. In addition to D- and L-Glucose xylose and galactose were investigated as alternative sugars for comparison. Both sugars behaved as expected and galactose was shown to be a possible alternative to L-Glucose to show the enzyme was specific.

The duration of enzyme coupling was also tested using K423C, using times of 1.5-24 hours, and it was found the reaction was very fast with attachment complete in approximately 2 hours. In all the experiments done on the surface the k_m value of *Gc*GDH for glucose was found to be approximately 2.5 mM. While the k_m value was consistent, the amount of enzyme on the surface was found to vary slightly with experiment, and this would need to be improved in the future. In addition though the initial results were good the enzyme was shown to lose activity on the surface within 24 hours and this would need improvement.

6. Conclusions

The work completed in this thesis has developed a novel method for the modification of electrode surfaces for enzyme immobilisation. A novel method for the preparation of maleimide on the surface of glassy carbon electrodes was developed utilising a combination of electrochemical and solid phase synthesis to build up the structure. The method was first tested in solution; a maleimide carboxylic acid was protected with thiophenol to create a thioether. Benzylamine was then used as a model for amine modified surface and coupled to the acid. Maleimide was then regenerated by oxidation of the thioether followed by sulphoxide elimination.

The chemistry was then tested on the surface, the thioether being coupled to an amine-functionalised electrode followed by reformation of the maleimide. Ferrocene and anthraquinone thiols were used as models for the protein and the surfaces were analysed using voltammetry and XPS to evaluate the surface composition and elemental composition respectively.

Following problems with heating the electrodes, selenols were used as an alternative to thiols to protect the maleimide bond. On oxidation the selenide did not require heat and eliminated at room temperature. A model system in solution proceeded as expected and the method was used for the following work.

Initial work focused on the preparation of a monolayer on the electrode surface however, as previously discussed, it is important to have control over the surface composition for a range of applications and therefore work was done on the preparation of partially covered surfaces. A number of methods to create a partial coverage on electrodes were investigated.

During partial coverage work it was discovered that the reporter groups used to determine surface coverage bound non-specifically to bare GC in addition to coupling with amines on the surface as desired. This created problems in determining the coverage of linker on the surface, particularly at layers modified with less than 20% of linker.

Variation of the duration of oxidation for Boc-EDA attachment appeared to have an effect on anthraquinone coverage and increased oxidation time led to

an increase in anthraquinone coverage. However the method left a lot of bare GC, in particular for the lower coverage. In order to avoid non-specific adsorption of other molecules the bare GC would need to later be filled, requiring an additional step in the synthesis.

An alternative method was investigated, using a mixture of the Boc-Amine and an amine-functionalised 'capping group'. The ratios of the two groups were varied and electrodes oxidised in the mixtures. Two different reporter groups, anthraquinone and dihydroxybenzene, were used for the work and it was found that a coverage proportional to the amount of Boc-protected amine in the oxidation solution was achieved at concentrations above 20%. An alternative method of analysis would be required to resolve concentrations lower than 20% due to the non-specific binding of reporting groups on bare glassy carbon.

Following the successful attachment of simple thiols and development of partial coverage methods the attachment of a simple biomolecule, Cytochrome C, was investigated. Initially a full monolayer of the tether was prepared on the electrode surface; however the coverage of Cytochrome C on the electrodes was not significantly different to the coverage on a capped layer where only non-specific adsorption was possible.

The oxidation of a mixture of amines was then used to make surfaces with 0-100% linker coverage and a two carbon spacer was used to ensure that the tether was sufficiently long to bind the Cytochrome C. From these results it appeared that the best results were when a 10% coverage of linker was used.

An investigation of the tether length was then completed, using spacers to increase the chain length. A 10% linker coverage was used with the varying length of spacer, this showed that a 10% coverage with a spacer of at least two carbons gave a coverage significantly higher than a capped layer with only non-specific adsorption. The best coverage was obtained from a 10% layer with 6 carbon spacer, 6.71×10^{-12} mol cm^{-2} , close to the 8×10^{-12} mol cm^{-2} monolayer coverage reported by Wilner.

Following the successful attachment of Cytochrome C, work was done with engineered varients of Glucose Dehydrogenase from *Glomerella cingulate*. The

enzyme had been engineered to have a single cysteine residue for binding to maleimide-modified surfaces.

The successful attachment of two varients of *gc*GDH was demonstrated on electrodes modified with a 10% layer of linker and maleimide. Initially the electrodes showed some features by cyclic voltammetry which looked like possible DET, however control reactions ruled out this phenomenon. The mediated ET of both variants of G*c*GDH was investigated both on modified electrode surfaces and in solution.

The use of D(+) and L (-) glucose showed the activity of the enzyme remained specific after immobilisation on the surface. In addition to D (+) and L (-) glucose xylose and galactose were investigated as alternative sugars for comparison. Xylose was shown to react with the enzyme while galactose did not, as expected.

The duration of enzyme coupling was also tested, coupling times of 1.5-24 hours were used and it was found the reaction was complete in approximately 2 hours. In all the experiments done on the electrode surface the K_m value of *Gc*GDH for glucose was found to be approximately 2.5 mM.

While the K_m value was consistent the amount of enzyme on the surface was found to vary slightly with experiment, and this would need to be improved in the future. In addition though the initial results were good the enzyme was shown to lose activity on the surface within 24 hours and this would need improvement.

6.1 Further work

The work is of relevance to a range of applications such as biofuel cells and biosensors. However further development would be required for these applications. A range of enzymes could be attached using this method, allowing adaptation of the electrodes to varying applications such as fuel cell cathodes or anodes depending on the enzyme used.

The stability of the enzyme on the surface would need improvement for applications such as this, it is not clear why the enzyme is not stable on the

surface, it is possible that the storage conditions needed modification or it could be due to the binding of the enzyme. There are a number of things that could be investigated to improve stability, including the modification of storage conditions or the use of a polymer film on top of the enzyme.

The method of attachment could also be investigated, with different options such as click chemistry or NTA binding which may both also be targeted, Click chemistry using azide/alkyne modified proteins and NTA using histidine tagged proteins.

In addition the partial coverage methods developed may be utilized to introduce a range of different functional groups as the ‘capping group’, allowing the nature of the electrode surface to be designed. This modification may aid binding of the biomolecule, by the creation of favourable interactions such as hydrogen bonding and electrostatic interactions which may be tuned depending on the target for binding.

While there are a number of areas which may be further investigated, the successful attachment of GDH onto a maleimide-modified electrode surface has been achieved using novel methods for creating a partial coverage of maleimide on the surface of electrodes.

7. Experimental

6.2 Synthesis

6.2.1 General

All chemicals were reagent grade and used as received unless otherwise stated. Reactions were done under air unless a dry atmosphere was required in which case reactions were done in oven dried glassware with dry solvents under nitrogen. Dichloromethane was distilled over $CaCl_2$. TLC was done on foil backed sheets of silica gel (0.25 mm) with fluorescent indicator UV254. Column chromatography was performed on Sorbsil C60, 40–60 mesh silica. 3-(2,5-dioxo-2,5-dihydro-1H-pyrrol-1-yl)propanoic acid[125] and N-(2-mercaptoethyl)-9,10-dioxo-9,10-dihydroanthracene-2-carboxamide[76] were prepared according to literature procedures.

6.2.2 Instrumentation

^{1}H and ^{13}C NMR spectra were recorded on a Bruker AV300 spectrometer at 300 MHz and 75.5 MHz respectively. Spectra were referenced with respect to the residual peak for the deuterated solvent. Chemical shifts (δ) are reported in ppm and coupling constants (J) are given in Hz. The following abbreviations are used singlet (s), doublet (d), triplet (t), quartet (q), broad (b) and multiplet (m). Distortionless enhancement by phase transfer (DEPT) spectral editing technique was used to elucidate the carbon multiplicities, (C) (CH) (CH_2), (CH_3). Low resolution mass spectra were recorded on a Waters ZMD mass spectrometer, single quadrupole, 2700 autosampler in methanol or acetonitrile, high resolution mass specta were recorded on a Brukner MaXis in acetonitrile. Infrared spectra were recorded either as neat solids or oils on a Bio-Rad Golden Gate ATR FT-IR spectrometer fitted with an ATR accessory. Melting points were determined in open capillary tubes using a Gallenkamp Electrothermal melting point apparatus and are uncorrected.

6.2.3 Synthesis of 2 3-(2,5-dioxo-3-(phenylthio)pyrrolidin-1-yl)propanoic acid

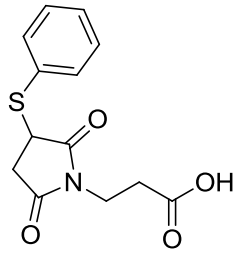

0.75 g 3-maleimidopropionic acid (4.43 mmol, 1 eq) was dissolved in 50 mL acetonitrile and 8 mL water, 0.42 mL thiophenol (3.54 mmol, 0.8 eq) was added. The mixture was stirred at room temperature for 5 hours and then the solvent was reduced to half and the product was filtered. 98%, pale yellow solid. ^{1}H NMR (300 MHz, DMSO-d_6)δ ppm 2.33 (t, *J*=7.54 Hz, 2 H) 2.62 (d, J=3.77 Hz, 1 H) 3.23 (dd, J=18.27 Hz, 1 H) 3.50 (t, *J*=7.72 Hz, 2 H) 4.40 (dd, J=9.1 Hz 1 H) 7.26 - 7.41 (m, 3 H) 7.44 - 7.64 (m, 2 H). [ESI-] 278.1: [M-H]. MP: 143-145 ˚C, in agreement with other literature values [143-145 ˚C].[126]

6.2.4 Synthesis of 3 N-benzyl-3-(2,5-dioxo-3-(phenylthio)pyrrolidin-1-yl)propanamide

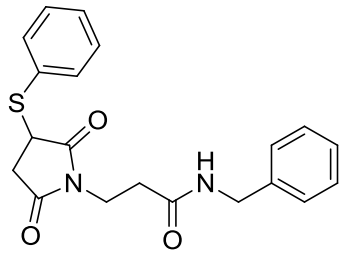

2 (0.21 g, 7.5 x 10^{-4} mol, 1 eq) and HBTU (0.302 g, 7.96 x 10^{-4} mol, 1.1 eq) were dissolved in 3 mL DMF, DIEA (0.68 mL, 3.04 mmol, 4.2 eq) and benzylamine (0.1 mL, 7.5 x 10^{-4} mol, 1 eq) were added. The solution was stirred for 16 hours and then DMF was evaporated. Crude product was dissolved in 20 mL ethyl acetate and washed with 2 M HCl (10 mL) and *sat*$NaHCO_3$ solution (10 mL). Organic layers were then combined and dried with $MgSO_4$ and evaporated. Column was done 3% MeOH in DCM and product was re-crystallised in ethanol. White solid, 150 mg, 54%. ^{1}H NMR (300 MHz, CHLOROFORM-*d*) δ ppm 2.27 (t, *J*=7.32 Hz, 2 H) 2.61 (dd, *J*=19.03, 3.29 Hz, 1

H) 3.03 (dd, *J*=19.03, 9.15 Hz, 1 H) 3.55 (t, *J*=6.95 Hz, 2 H) 3.90 (dd, *J*=8.97, 3.11 Hz, 1 H) 4.27 (d, *J*=5.49 Hz, 2 H) 6.28 (br. s., 1 H) 7.00 - 7.38 (m, 8 H) 7.49 (dd, *J*=8.23, 1.28 Hz, 2 H) **^{13}C NMR** (100MHz, CD_3CN) δ ppm 32.99 (**C**H_2), 35.21 (**C**H_2), 35.84 (**C**H_2), 42.49 (**C**H_2), 43.45 (**C**H), 126.88(**C**H), 127.32 (**C**H), 128.32 (**C**H), 128.66 (**C**H), 129.22 (**C**H), 131.45, 133.14 (**C**H), 169.19 (**C**), 169.34 (**C**), 174.34 (**C**), 175.5 (**C**). **[ESI]$^+$:** 391.1: [M + Na^+], 759.1: [2M + Na^+]. **HRMS [ESI]$^+$:** calculated 391.1087 [M + Na^+] , 391.1091 observed [M + Na^+] **MP:** 118-120 ˚C

IR: 3323, 2359, 1771, 1692, 1641, 1544, 1495, 1439, 1427, 1402, 1336, 1234, 1145, 1096, 1072, 1022, 964, 949, 769, 730, 690, 605, 605, 567, 507, 482, 446.

6.2.5 Synthesis of 4 N-benzyl-3-(2,5-dioxo-2,5-dihydro-1H-pyrrol-1-yl)propanamide

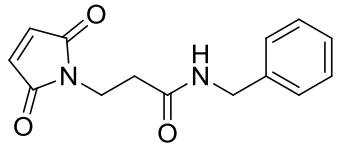

Method A from thioether: **3** (0.1 g, 2.7 x1 0^{-4} mol) was dissolved in DCM (3 mL) and *m*CPBA (0.051 g, 2.97 x1 0^{-4} mol, 1.1 eq) was added, the resulting solution was cooled to 0 ˚C and stirred for 1 hour, then allowed to warm to room temperature for 1 hour. DCM (12 mL) was added and the solution was washed with $NaHCO_3$ (7.5 mL) and brine (7.5 mL) the dried with $MgSO_4$. Toluene (3 mL) was then added and the mixture was heated to 110 ˚C for 2 h, the solvent was then evaporated. The crude product was purified by column chromatography, 10% MeOH in DCM. 35 mg, 49%. **NMR** ^{1}H NMR (400 MHz, ACETONITRILE-d_3) δ ppm 2.49 (t, *J*=7.3 Hz, 2 H) 3.74 (t, *J*=7.07 Hz, 2 H) 4.31 (d, *J*=6.06 Hz, 2 H) 6.76 (s, 2 H) 7.10 - 7.48 (m, 5 H)
^{13}C NMR (100 MHz, ACETONITRILE-d_3) δ ppm 32.6 (**C**H_2), 34.58 (**C**H_2), 34.77 (**C**H), 36.25 (**C**H_2), 42.07 (**C**H_2), 126.46 (**C**H), 126.9 (**C**H), 127.9 (**C**H), 128.66 (**C**H), 128.87 (**C**H), 135.35 (**C**H), 168.92 (**C**), 174.31 (**C**), 176.03 (**C**). LRMS [ESI^+] 281: [M + Na^+]. **HRMS:** [ESI^+] calculated 281.0897: [M + Na^+], observed 281.0899 **MP**: 164-166 ˚C

Method B from selenide: **28** (160mg, 3.8 x10 $^{-4}$ mol) and *m*CPBA (100 mg, 6.09 x10 $^{-4}$ mol, 1.6 eq) were dissolved in MeCN (10 mL), the mixture was cooled to 0 ˚C and stirred for 1 hour then allowed to warm to room temperature and stirred for 1 h. The solvent was the evaporated and the crude product was purified by column chromatography with 0-3% MeOH in DCM. The product was then recrystallized in hot ethanol. 70 mg (71%) pale yellow solid. Characterisation as above.

6.2.6 Synthesis of 27 3-(2,5-dioxo-3-(phenylselanyl)pyrrolidin-1-yl)propanoic acid

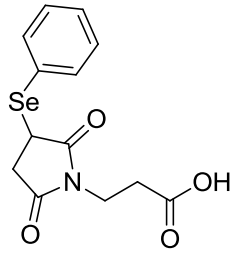

1 (1.7g, 10 mmol) was dissolved in MeCN (15 mL) and phenylselenol (0.9 mL, 8.4 mmol) was added , after 5 hours the resulting precipitate was filtered and washed with acetonitrile to afford white solid, 1.34 g, 48%. **^{1}H NMR** (300 MHz, ACETONITRILE-d_3)δ ppm 2.35 (2H, t, J = 7.7 Hz), 2.65 (1H, dd, J = 18.9, 3.3 Hz), 3.20 (1H, dd, J =18.9, 9.1 Hz), 3.50 (2H, t, J = 7.7 Hz), 4.15 (1H, dd, J = 9.1, 3.3 Hz), 7.30 – 7.45 (3H, m), 7.60 (2H, d, J = 6.6 Hz), 9.07 (1H, s, broad) ppm **^{13}C NMR** (75 MHz, ACETONITRILE-d_3)δ ppm 30.479 (**C**H$_2$), 33.905 (**C**H$_2$), 34.943 (**C**H), 36.441 (**C**H$_2$), 125.523 (**C**), 128.904 (**C**H), 129.077 (**C**H), 135.636 (**C**H), 170.937(**C**), 174.942 (**C**), 176.170(**C**). [ESI$^-$] 325: [M – H]. **HRMS:** 349.9904 obtained [M+Na$^+$], 349.9903 expected [M+Na$^+$]. **MP:** 118-121 ˚C. **IR:** cm^{-1}2958, 2637, 1773, 1694, 1437, 1399, 1370, 1348, 1302, 1278, 1260, 1223, 1158, 1137, 1068, 1019, 990, 964, 911, 753, 737, 692, 671, 609, 516, 468

6.2.7 Synthesis of 28 N-benzyl-3-(2,5-dioxo-3-(phenylselanyl)pyrrolidin-1-yl)propanamide

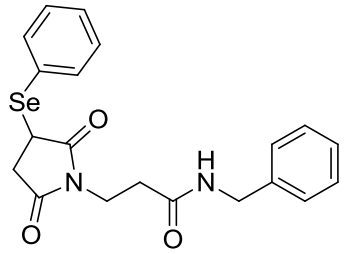

3 (0.3 g , 9.17 x 10^{-4} mol, 1 eq) and HBTU (0.4169 g, 1.1 mmol, 1.2 eq) were dissolved DMF (3 mL) and DIEA (0.67 mL, 3.85 mmol, 4.2 eq) and benzylamine (0.1 mL, 9.17 x 10^{-4} mol, 1eq) were added. The resulting solution was stirred for 16 h. DMF was then evaporated and the crude product was purified by column chromatography,2% MeOH in DCM. White solid, 50 mg, 13%. ^{1}H NMR (300 MHz, CHLOROFORM-*d*) δ ppm 2.43 (td, *J*=7.23, 1.65 Hz, 2 H) 2.68 (dd, *J*=18.84, 3.84 Hz, 1 H) 3.11 (dd, *J*=19.03, 9.15 Hz, 1 H) 3.75 (t, *J*=7.14 Hz, 2 H) 3.98 (dd, *J*=9.15, 4.03 Hz, 1 H) 4.40 (d, *J*=5.49 Hz, 2 H) 6.06 (br. s., 1 H) 7.16 - 7.42 (m, 8 H) 7.46 - 7.65 (m, 2 H) ^{13}C NMR (100 MHz, ACETONITRILE-d_3) δ ppm 32.6 (**C**H_2), 34.58 (**C**H_2), 34.77 (**C**H), 36.25 (**C**H_2), 42.07 (**C**H_2), 126.46 (**C**H), 126.9 (**C**H), 127.9 (**C**H), 128.66 (**C**H), 128.87 (**C**H), 135.35 (**C**H), 168.92 (**C**), 174.31 (**C**), 176.03 (**C**). **LRMS** [ESI^+]: 439: [M + Na^+], 855: [2M + Na^+]. **HRMS** [ESI^+]: calculated 439.0532 [M + Na^+] , 439.0536 observed [M + Na^+]

6.3 Electrochemical and Solid Phase Synthesis

6.3.1 Instrumentation

Glassy carbon (GC) working electrodes were 3 mm diameter glassy carbon rods (HTW, Germany) sealed in glass and connected to copper wires using indium (Aldrich).

GC electrodes were polished on silicon carbide paper (1200 grade, 3M) followed by alumina lapping film (5 μm) and finally alumina slurries (1.0 and 0.3 μm, Buehler) on polishing cloths (Buehler) before surface modification. Platinum gauze was used as a counter electrode and saturated calomel electrode (SCE) or Silver/Silver Chloride (Ag/AgCl -0.045 vs SCE) were used as

reference electrodes. XPS samples were prepared on Sigradur G glassy carbon plates (HTW, Germany), which were polished only using silicon carbide paper (1200 grade, 3M). XPS analysis was performed on a Scienta ESCA300 photoelectron spectrometer with AlKα X-ray source at Daresbury Laboratory, UK.

All electrochemical solutions were prepared with reagent grade water (18 MΩ cm) from a Purite purification system. Pureshield argon (BOC) was used to purge electrochemical solutions as stated. Electrochemical measurements were performed in glass cells in a standard three electrode arrangement using either a μAutolab type III or an Autolab PGSTAT 302 (Ecochemie, Netherlands) equipped with a frequency response analyzer module. Buffer solutions were made by mixing stock solutions to the correct pH using Hanna HI 1131 pH meter.

6.3.2 Reagents

Boc-Glycine, *N*-Boc-ethylenediamine, *N*-Boc-butanediamine, *N*-Boc-hexanediamine, tetrabutylammonium tetrafluoroborate, Aminoethyl acetamide, maleic anhydride, β-alanine, were purchased from Sigma-Aldrich. Phenylselenol was purchased from Acros. Acetonitrile used for electrochemical solutions was sourced from Rathburn. HPLC grade acetonitrile (Fisher) was used for all other solutions. Lab reagent grade acetone (Fisher) and analytical grade ethanol (Fisher) were used for washing electrodes.

Glucose dehydrogenases (GDH) from Glomerella Cingulata were kindly supplied by the University of Natural Resources and Life Sciences, Vienna, Austria. The wild type GDH was supplied in 50 mM pH 5.5 citrate buffer at a concentration of 39.5mg/mL (Bradford assay) and an activity (DCIP assay, pH 5.5, 30oC) =22330 U/mL. The recombinant GDH T343C was supplied in 50 mM pH 5.5 citrate buffer at a concentration of 3.5 mg/mL(Bradford assay), and an activity (DCIP assay, pH 5.5, 30°C) = 2200 U/mL. The recombinant GDH K432C was supplied in 50 mM pH 5.5 citrate buffer with concentration of 4.3 mg/mL (Bradford assay), with activity (DCIP assay, pH 5.5, 30oC) = 2700 U/mL.

Citric acid (BDH AnalaR, 97%), sodium citrate tribasic dihydrate (Sigma-Aldrich, ACS reagent, ≥99.0%), D(+) glucose (BDH) L(+) glucose (Sigma) DCIP (Sigma) Flavin adenine dinucleotide disodium salt hydrate ≥95% (HPLC), powder, sigma were all used as received.

4-(N-Boc-aminomethyl)benzene diazonium tetrafluoroborate [127], 4-((tert-butoxycarbonyl)amino)butanoic acid [128], 6-((tert-butoxycarbonyl)amino)hexanoic acid [109] were prepared according to literature procedures.

6.3.2.1 Purification of Cytochrome C

Cytochrome C was purchased from Sigma Aldrich (Bovine heart BioChemika ≥95%) and purified according to literature procedure[129] with small modifications, SP-sepharose, 14 cm column, 1.6 cm diameter, 28 mL volume, Capacity: 0.18 - 0.25 mmol/mL was used for ion exchange with 20 mM phosphate buffer pH 8 on a gradient to 0.5 M NaCl in 20 mM sodium phosphate buffer. Cytochrome C (30 mg in 21 mL) was loaded and few drops 1 M $K_3Fe(CN)_6$ was added, the column was run at 4 mL/min for 6 column volumes, then gradient was set up over 200 mL to 0.5 M NaCl, a further 3 column volumes were run to elute the protein. Bradford assay was used to detect the protein containing fractions and SDS-PAGE was done, desired fractions were combined and concentrated to 3-4 mL and gel filtration was done on S75 column, using 100 mM phosphate buffer. Bradford assay was used to determine protein fractions and SDS page used to confirm purity.

Electrochemical testing of Cytochrome C

Cytochrome C (2 mM) in 100 mM phosphate buffer pH7 with 100 mM sodium perchlorate was degassed with argon, a gold electrode was immersed and CV was done 0.4 - -0.15 V vs SCE at 10 mV/s. 5 mM 4,4'-bipyridyl was added to the solution and the CV repeated.

6.3.3 Electrochemical Modification

General method of amine oxidation:

Experimental

A solution of *N*Boc-Diamine linker (10 mM) in acetonitrile with 0.1 M TBATFB was prepared and degassed with argon, individual electrodes were immersed and cycled 0.8-2.1 V vs Ag/AgCl at 50 mV/s for 5 cycles.

General method of mixed amine oxidation:

Stock solutions of 10 mM Boc-HDA and 10 mM aminoethylacetamide were prepared. TBATFB (150 mM) and acetonitrile (50 mL) were added to volumetric flask and aminoethylacetamide (48 µL, 10 mM) was added to make capping solution. TBATFB (0.269g, 7.5 mmol, 150 mM) and acetonitrile (50 mL) were added to volumetric flask and Boc-HDA (112 µL, 10mM) was added to make Boc-HDA solution. Stock solutions were mixed in different proportions (Table 3) to give different percentages of HDA (total concentration of amine 10 mM, total volume 10 mL). Solutions were degassed with argon, electrodes were immersed and held at 2.1 V vs Ag/AgCl for three minutes then washed with acetonitrile.

Table 3 – Preparation of mixed amine solutions

"%Boc-HDA"	Boc-HDA solution	Capping solution
1%	0.1 mL	9.9 mL
10%	1 mL	9 mL
20%	2 mL	8 mL
30%	3 mL	7 mL
50%	5 mL	5 mL
75%	7.5 mL	2.5 mL
100%	10 mL	0 mL
0%	0	10 mL

Reduction of diazonium salt

4-NBoc aminophenyl diazonium tetrafluoroborate (0.002 g) was dissolved in 10 mL acetonitrile and 0.329 g TBATFB was added. The solution was degassed

with argon for 10 minutes and electrodes were cycled 0.6- -0.9 V vs Ag/AgCl for 5 cycles then washed with acetonitrile.

6.3.4 Solid Phase Synthesis

General method for deprotection of Boc-Group

Electrodes were then deprotected in 4M HCl in dioxane for 1 hour and then washed with acetone, ethanol and dried.

General method for coupling anthraquinone

Anthraquinone-2-carboxylic acid (2.01 g, 8 mmol) was combined with HBTU (3.64g, 9.6 mmol) and dissolved in 16 mL DMF, 6 mL DIEA was added and electrodes were immersed for 16 hours. Electrodes were washed in stirred DMF for 1 hour then washed with acetone, ethanol and dried.

General method for coupling dimethoxybenzene:

Electrodes were then deprotected in 4M HCl in dioxane for 1 hour and then washed with acetone, ethanol and dried. 0.450 g (1.1810^{-3} mol) HBTU, 0.150 g (8.24×10^{-4} mol) 3,4-dimethoxybenzoic acid and 4 mL DMF were combined and stirred, 0.75 mL DIEA was then added. Electrodes were then immersed in this solution for 16 hr and then washed with acetone and ethanol. They were then deprotected in 1M BBr_3 in DCM for 1 hour before testing.

General method for hydrolysis of dimethoxybenzene

Electrodes were deprotected with 1 M BBr_3 in DCM (3 mL) for 1 hour, under Ar then washed with ethanol and dried.

General method for coupling of ferrocene-thiol

6-(ferrocenyl)hexanethiol (0.08 g) was dissolved in acetonitrile (12 mL) electrodes were then immersed in this solution for 16 h.

General method for addition of protected maleimide

27 (0.1635 g, 0.5 mmol) was combined with HBTU (0.22 g, 0.6 mmol) and dissolved in 2 mL DMF, DIEA (0.36 mL, 2.1 mmol) was then added and electrodes immersed. After 16 hours electrodes were washed with acetone and ethanol.

Experimental

General method for regeneration of maleimide

mCPBA (0.119 g) was dissolved in 3 mL acetonitrile and cooled to 0˚C and electrodes were immersed for 1 hour, after this the solution was allowed to warm to room temperature and electrodes were left 1 hour. Electrodes were then washed with acetone and then put in stirred acetonitrile for 2 hours then washed with acetone and water and dried under argon.

General method of coupling 2C spacer:

Electrodes were then deprotected in 4 M HCl in dioxane for 1 hour then washed with acetone and ethanol. Boc-Gly (2 mmol) and HBTU (0.909 g, 1.2 mmol) were dissolved in 4 mL DMF and DIEA (1.46 mL, 8.4 mmol) was added, electrodes were then immersed for 16 hours and then washed with acetone and ethanol.

General method of Cytochrome C addition

20 µL of Cytochrome C in phosphate buffer (20 mM, pH 7) was put on the surface of electrode which was then covered and stored in the fridge (4˚C) overnight, electrodes were then washed with 20 mM phosphate buffer, but not allowed to dry, before testing.

General method of GDH addition

The GDH buffer was exchanged from pH 5.5 citrate buffer (50 mM) to 20 mM pH7 phosphate buffer for coupling. This was done using mini dialysis devices (Fisher Scientific) with 10 K cut off. The dialysis devices were put in gently stirred phosphate buffer (20 mM, pH7, 500 mL) for 10 minutes, fresh buffer was then put in (500 mL) and the dialysis units were immersed for 20 minutes, the dialysis units were then put in a final 500 mL of buffer in the fridge for 1.5 hours.

20 µL of G*c*GDH in phosphate buffer (20 mM, pH 7) was put on the surface of electrode which was then covered and stored in the fridge (4˚C) overnight, electrodes were then washed with 20 mM phosphate buffer, but not allowed to dry, before testing.

6.3.5 Electrochemical Characterisation

Electrochemical testing of ferrocene electrodes

The testing for ferrocene was done in TBATFB in acetonitrile, 0.1 M and scanned from 0-1.1 V vs Ag/AgCl at different scan rates.

Electrochemical testing of anthraquinone electrodes

The anthraquinone electrodes were tested using 0.1 M phosphate buffer at pH 7 in 0.1 M TEATFB. They were scanned at 0 - -0.8 vs SCE.

Electrochemical testing of Dihydroxybenzene modified electrodes

Dihydroxybenzene modified electrodes were tested in 0.1 M phosphate buffer at pH 7 in 0.1 M TEATFB, electrodes were cycled from 0.05 – 0.4 V vs SCE.

Electrochemical testing of Cytochrome C modified electrodes

Cytochrome C modified electrodes were tested in 20 mM phosphate buffer at pH 7 with 0.1 M sodium perchlorate, electrodes were cycled from -0.25 - 0.4 V vs SCE.

Electrochemical testing of GDH modified electrodes

Glucose dehydrogenase modified electrodes were tested in 100 mM citrate buffer at pH 5.5 with 0.1 M TBATFB, electrodes were cycled in a degassed solution from -0.6 - 0.6 V vs SCE for direct electrochemical testing.

Electrodes were tested for mediated electrochemistry using DCIP by cycling -0.25 – 0.5 V vs SCE in a solution of 100 mM pH 5.5 citrate buffer, 100 µM DCIP with 100 mM TEATFB. Aliquots of 100 mM D-glucose or L-glucose in 100 mM pH 5.5 citrate buffer, 100 µM DCIP with 100 mM TEATFB were added before repeating the CV.

Electrodes were tested for mediated electrochemistry using ferrocene carboxylic acid by cycling 0 – 0.5 V vs SCE in pH 5.5 citrate buffer (100 mM) with 100 mM TBATFB and 0.5 mM ferrocene carboxylic acid. Aliquots of sugars (100 mM) in pH 5.5 citrate buffer (100 mM) with 100 mM TBATFB and 0.5 mM ferrocene carboxylic acid were added and CV repeated after each addition.

List of References

1. Lane, R. F.; Hubbard, A. T., Electrochemistry of chemisorbed molecules. I. Reactants connected to electrodes through olefinic substituents. *J Phys Chem-US* **1973,** *77* (11), 1401-1410.
2. Watkins, B. F.; Behling, J. R.; Kariv, E.; Miller, L. L., Chiral electrode. *J. Am. Chem. Soc.* **1975,** *97* (12), 3549-3550.
3. Elliott, C. M.; Murray, R. W., Chemically modified carbon electrodes. *Anal. Chem.* **1976,** *48* (8), 1247-1254.
4. Ronkainen, N. J.; Halsall, H. B.; Heineman, W. R., Electrochemical biosensors. *Chem. Soc. Rev.* **2010,** *39* (5), 1747-1763.
5. Cahen, D.; Hodes, G., Molecules and Electronic Materials. *Adv. Mater.* **2002,** *14* (11), 789-798.
6. Barendrecht, E., Chemically and physically modified electrodes: some new developments. *J. Appl. Electrochem.* **1990,** *20* (2), 175-185.
7. Bullen, R. A.; Arnot, T. C.; Lakeman, J. B.; Walsh, F. C., Biofuel cells and their development. *Biosens. Bioelectron.* **2006,** *21* (11), 2015-2045.
8. (a) Farneth, W. E.; Diner, B. A.; Gierke, T. D.; D'Amore, M. B., Current densities from electrocatalytic oxygen reduction in laccase/ABTS solutions. *J. Electroanal. Chem.* **2005,** *581* (2), 190-196; (b) Blanford, C.; Foster, C.; Heath, R.; Armstrong, F., Efficient electrocatalytic oxygen reduction by the blue copper oxidase, laccase, directly attached to chemically modified carbons. *Faraday Discuss.* **2009,** *140*, 319 - 335; (c) Calabrese Barton, S.; Gallaway, J.; Atanassov, P. Y., Enzymatic Biofuel Cells for Implantable and Microscale Devices. *Chem. Rev.* **2004,** *104*, 4867-4886; (d) Willner, I.; Yan, Y. M.; Willner, B.; Tel-Vered, R., Integrated Enzyme-Based Biofuel Cells-A Review. *Fuel Cells* **2009,** *9* (1), 7-24; (e) Boland, S.; Barriere, F.; Leech, D., Designing stable redox-active surfaces: Chemical attachment of an osmium complex to glassy carbon electrodes prefunctionalized by electrochemical reduction of an in situ-generated aryldiazonium cation. *Langmuir* **2008,** *24* (12), 6351-6358; (f) Kundu, A.; Jang, J. H.; Gil, J. H.; Jung, C. R.; Lee, H. R.; Kim, S. H.; Ku, B.; Oh, Y. S., Micro-fuel cells - Current development and applications. *J. Power Sources* **2007,** *170* (1), 67-78.
9. Wieckowski A., *Interfacial Electrochemistry: Theory: Experiment, and Applications*. CRC Press: 1999.
10. Kissinger P., *Laboratory Techniques in Electroanalytical Chemistry*. Second edition ed.; CRC Press: 1996.
11. Brown, A. P.; Anson, F. C., Cyclic and differential pulse voltammetric behavior of reactants confined to the electrode surface. *Anal. Chem.* **1977,** *49* (11), 1589-1595.
12. Gooding, J. J.; Mearns, F.; Yang, W.; Liu, J., Self-Assembled Monolayers into the 21st Century: Recent Advances and Applications. *Electroanal* **2003,** *15* (2), 81-96.
13. Bain, C. D.; Troughton, E. B.; Tao, Y. T.; Evall, J.; Whitesides, G. M.; Nuzzo, R. G., Formation of monolayer films by the spontaneous assembly of organic thiols from solution onto gold. *J. Am. Chem. Soc.* **1989,** *111* (1), 321-335.
14. (a) Dubois, L. H.; Nuzzo, R. G., Synthesis, Structure, and Properties of Model Organic Surfaces. *Annu. Rev. Phys. Chem.* **1992,** *43* (1), 437-463; (b) Ulman, A., Formation and Structure of Self-Assembled Monolayers. *Chem. Rev.* **1996,** *96* (4), 1533-1554.

15. (a) Laibinis, P. E.; Whitesides, G. M.; Allara, D. L.; Tao, Y. T.; Parikh, A. N.; Nuzzo, R. G., Comparison of the structures and wetting properties of self-assembled monolayers of n-alkanethiols on the coinage metal surfaces, copper, silver, and gold. *J. Am. Chem. Soc.* **1991,** *113* (19), 7152-7167; (b) Walczak, M. M.; Chung, C.; Stole, S. M.; Widrig, C. A.; Porter, M. D., Structure and interfacial properties of spontaneously adsorbed n-alkanethiolate monolayers on evaporated silver surfaces. *J. Am. Chem. Soc.* **1991,** *113* (7), 2370-2378; (c) Ihs, A.; Liedberg, B., Infrared Study of Ethyl and Octyl Xanthate Ions Adsorbed on Metallic and Sulfidized Copper and Silver Surfaces. *Langmuir* **1994,** *10* (3), 734-740.
16. Laibinis, P. E.; Whitesides, G. M., Self-assembled monolayers of n-alkanethiolates on copper are barrier films that protect the metal against oxidation by air. *J. Am. Chem. Soc.* **1992,** *114* (23), 9022-9028.
17. (a) Volmer, M.; Stratmann, M.; Viefhaus, H., Electrochemical and electron spectroscopic investigations of iron surfaces modified with thiols. *Surf. Interface Anal.* **1990,** *16* (1-12), 278-282; (b) Stratmann, M., Chemically modified metal surfaces—a new class of composite materials. *Adv. Mater.* **1990,** *2* (4), 191-195.
18. Shimazu, K.; Sato, Y.; Yagi, I.; Uosaki, K., Packing state and stability of self-assembled monolayers of 11-ferrocenyl-1-undecanethiol on platinum electrodes. *Bull. Chem. Soc. Jpn.* **1994,** *67* (3), 863-865.
19. Nuzzo, R. G.; Allara, D. L., Adsorption of bifunctional organic disulfides on gold surfaces. *J. Am. Chem. Soc.* **1983,** *105* (13), 4481-4483.
20. Gooding, J. J., Advances in interfacial design sensors: Aryl diazonium salts for electrochemical biosensors and for modifying carbon and metal electrodes. *Electroanal* **2008,** *20* (6), 573-582.
21. Murray, R. W., Chemically modified electrodes. *Acc. Chem. Res.* **1980,** *13* (5), 135-141.
22. (a) Netzer, L.; Sagiv, J., A new approach to construction of artificial monolayer assemblies. *J. Am. Chem. Soc.* **1983,** *105* (3), 674-676; (b) Lee, H.; Kepley, L. J.; Hong, H. G.; Mallouk, T. E., Inorganic analogs of Langmuir-Blodgett films: adsorption of ordered zirconium 1,10-decanebisphosphonate multilayers on silicon surfaces. *J. Am. Chem. Soc.* **1988,** *110* (2), 618-620.
23. Merz, A.; Bard, A. J., A stable surface modified platinum electrode prepared by coating with electroactive polymer. *J. Am. Chem. Soc.* **1978,** *100* (10), 3222-3223.
24. Van de Mark, M. R.; Miller, L. L., A poly-p-nitrostyrene electrode surface. Potential dependent conductivity and electrocatalytic properties. *J. Am. Chem. Soc.* **1978,** *100* (10), 3223-3225.
25. Abruna, H. D.; Denisevich, P.; Umana, M.; Meyer, T. J.; Murray, R. W., Rectifying interfaces using two-layer films of electrochemically polymerized vinylpyridine and vinylbipyridine complexes of ruthenium and iron on electrodes. *J. Am. Chem. Soc.* **1981,** *103* (1), 1-5.
26. Szentirmay, M. N.; Martin, C. R., Ion-exchange selectivity of Nafion films on electrode surfaces. *Anal. Chem.* **1984,** *56* (11), 1898-1902.
27. McCreery, R. L., Advanced carbon electrode materials for molecular electrochemistry. *Chem. Rev.* **2008,** *108* (7), 2646-2687.
28. Downard, A. J., Electrochemically assisted covalent modification of carbon electrodes. *Electroanalysis* **2000,** *12* (14), 1085-1096.
29. Barbier, B.; Pinson, J.; Sanchez, G. D. a. M., Electrochemical Bonding of Amines to Carbon Fiber Surfaces. *J. Electrochem. Soc.* **1990,** *137*, 1757-1764.

30. Deinhammer, R. S.; Ho, M.; Anderegg, J. W.; Porter, M. D., Electrochemical oxidation of amine containing compounds - a route to the surface modification of glassy-carbon electrodes. *Langmuir* **1994,** *10* (4), 1306-1313.
31. Adenier, A.; Chehimi, M. M.; Gallardo, I.; Pinson, J.; Vilà, N., Electrochemical Oxidation of Aliphatic Amines and Their Attachment to Carbon and Metal Surfaces. *Langmuir* **2004,** *20* (19), 8243-8253.
32. Delamar, M.; Hitmi, R.; Pinson, J.; Saveant, J. M., Covalent modification of carbon surfaces by grafting of functionalized aryl radicals produced from electrochemical reduction of diazonium salts. *J. Am. Chem. Soc.* **1992,** *114* (14), 5883-5884.
33. Philippe Allongue, M. D., Bernard Desbat, Olivier Fagebaume, Rachid Hitmi; Pinson, J.; Savaent, J.-M., Covalent Modification of Carbon Surfaces by Aryl Radicals Generated from the Electrochemical Reduction of Diazonium Salts *J. Am. Chem. Soc.* **1997,** *119*, 201-207.
34. Allongue, P.; Delamar, M.; Desbat, B.; Fagebaume, O.; Hitmi, R.; Pinson, J.; Saveant, J. M., Covalent modification of carbon surfaces by aryl radicals generated from the electrochemical reduction of diazonium salts. *J. Am. Chem. Soc.* **1997,** *119* (1), 201-207.
35. Delamar, M.; Désarmot, G.; Fagebaume, O.; Hitmi, R.; Pinsonc, J.; Savéant, J. M., Modification of carbon fiber surfaces by electrochemical reduction of aryl diazonium salts: Application to carbon epoxy composites. *Carbon* **1997,** *35* (6), 801-807.
36. (a) de Villeneuve, C. H.; Pinson, J.; Bernard, M. C.; Allongue, P., Electrochemical Formation of Close-Packed Phenyl Layers on Si(111). *The J. Phys Chem B* **1997,** *101* (14), 2415-2420; (b) Kariuki, J. K.; McDermott, M. T., Formation of Multilayers on Glassy Carbon Electrodes via the Reduction of Diazonium Salts. *Langmuir* **2001,** *17* (19), 5947-5951.
37. Dyke, C. A.; Tour, J. M., Unbundled and Highly Functionalized Carbon Nanotubes from Aqueous Reactions. *Nano Lett.* **2003,** *3* (9), 1215-1218.
38. (a) Adenier, A.; Bernard, M.-C.; Chehimi, M. M.; Cabet-Deliry, E.; Desbat, B.; Fagebaume, O.; Pinson, J.; Podvorica, F., Covalent Modification of Iron Surfaces by Electrochemical Reduction of Aryldiazonium Salts. *J. Am. Chem. Soc.* **2001,** *123* (19), 4541-4549; (b) Liu, G.; Böcking, T.; Gooding, J. J., Diazonium salts: Stable monolayers on gold electrodes for sensing applications. *J. Electroanal. Chem.* **2007,** *600* (2), 335-344; (c) Liu, G.; Chockalingham, M.; Khor, S. M.; Gui, A. L.; Gooding, J. J., A Comparative Study of the Modification of Gold and Glassy Carbon Surfaces with Mixed Layers of In Situ Generated Aryl Diazonium Compounds. *Electroanal* **2010,** *22* (9), 918-926.
39. Pinson, J.; Podvorica, F., Attachment of organic layers to conductive or semiconductive surfaces by reduction of diazonium salts. *Chem. Soc. Rev.* **2005,** *34* (5), 429-439.
40. Baranton, S.; Bélanger, D., Electrochemical Derivatization of Carbon Surface by Reduction of in Situ Generated Diazonium Cations. *J Phys Chem B* **2005,** *109* (51), 24401-24410.
41. Ghanem, M. A.; Chretien, J. M.; Pinczewska, A.; Kilburn, J. D.; Bartlett, P. N., Covalent modification of glassy carbon surface with organic redox probes through diamine linkers using electrochemical and solid-phase synthesis methodologies. *J. Mater. Chem.* **2008,** *18* (41), 4917-4927.
42. Chretien, J. M.; Ghanem, M. A.; Bartlett, P. N.; Kilburn, J. D., Covalent tethering of organic functionality to the surface of glassy carbon electrodes by using electrochemical and solid-phase synthesis methodologies. *Chem Eur J* **2008,** *14* (8), 2548-2556.

43. Chretien, J. M.; Ghanem, M. A.; Bartlett, P. N.; Kilburn, J. D., Covalent Modification of Glassy Carbon Surfaces by Using Electrochemical and Solid-Phase Synthetic Methodologies: Application to Bi- and Trifunctionalisation with Different Redox Centres. *Chem. Eur. J.* **2009,** *15* (44), 11928-11936.
44. (a) Sosna, M.; Stoica, L.; Wright, E.; Kilburn, J. D.; Schuhmann, W.; Bartlett, P. N., Mass transport controlled oxygen reduction at anthraquinone modified 3D-CNT electrodes with immobilized Trametes hirsuta laccase. *PCCP* **2012,** *14* (34), 11882-11885; (b) Sosna, M.; Chretien, J.-M.; Kilburn, J. D.; Bartlett, P. N., Monolayer anthracene and anthraquinone modified electrodes as platforms for Trametes hirsuta laccase immobilisation. *PCCP* **2010,** *12* (34), 10018-10026.
45. Ghanem, M. A.; Chretien, J. M.; Kilburn, J. D.; Bartlett, P. N., Electrochemical and solid-phase synthetic modification of glassy carbon electrodes with dihydroxybenzene compounds and the electrocatalytic oxidation of NADH. *Bioelectrochemistry* **2009,** *76* (1-2), 115-125.
46. Pinczewska, A.; Sosna, M.; Bloodworth, S.; Kilburn, J. D.; Bartlett, P. N., High-Throughput Synthesis and Electrochemical Screening of a Library of Modified Electrodes for NADH Oxidation. *J. Am. Chem. Soc.* **2012,** *134* (43), 18022-18033.
47. Sarma, A. K.; Vatsyayan, P.; Goswami, P.; Minteer, S. D., Recent advances in material science for developing enzyme electrodes. *Biosens. Bioelectron.* **2009,** *24* (8), 2313-2322.
48. Rusling, J. F., *Biomolecular Films: Design, Function, and Applications. Surfactant Science Series Volume 111.* Marcel Dekker, Inc.: New York, Basel. 2003.
49. Blanford, C., Foster, C., Heath, R., Armstrong, F., Efficient electrocatalytic oxygen reduction by the blue copper oxidase, laccase, directly attached to chemically modified carbons. *Faraday Discuss.* **2009,** *140*, 319 - 335.
50. Farneth, W. E.; Diner, B. A.; Gierke, T. D.; Dâmore, M. B., Current densities from electrocatalytic oxygen reduction in laccase/ABTS solutions. *J. Electroanal. Chem. 581*.
51. Glykys, D. J.; Banta, S., Metabolic Control Analysis of an Enzymatic Biofuel Cell. *Biotechnol. Bioeng.* **2009,** *102* (6), 1624-1635.
52. Samanta, D.; Sarkar, A., Immobilization of bio-macromolecules on self-assembled monolayers: methods and sensor applications. *Chem. Soc. Rev.* **2011,** *40* (5), 2567-2592.
53. Heller, A.; Feldman, B., Electrochemical Glucose Sensors and Their Applications in Diabetes Management. *Chem. Rev.* **2008,** *108* (7), 2482-2505.
54. Gooding, J. J.; Hibbert, D. B., The application of alkanethiol self-assembled monolayers to enzyme electrodes. *Trends Anal. Chem.* **1999,** *18* (8), 525-533.
55. Scouten, W. H.; Luong, J. H. T.; Stephen Brown, R., Enzyme or protein immobilization techniques for applications in biosensor design. *Trends Biotechnol.* **1995,** *13* (5), 178-185.
56. (a) Tarlov, M. J.; Bowden, E. F., Electron-transfer reaction of cytochrome c adsorbed on carboxylic acid terminated alkanethiol monolayer electrodes. *J. Am. Chem. Soc.* **1991,** *113* (5), 1847-1849; (b) Collinson, M.; Bowden, E. F.; Tarlov, M. J., Voltammetry of covalently immobilized cytochrome c on self-assembled monolayer electrodes. *Langmuir* **1992,** *8* (5), 1247-1250; (c) Ion, A.; Banica, F., Direct electrochemistry of bovine heart cytochrome c facilitated by cysteine derivatives and analogues. Some effects of facilitator structure. *J. Solid State Electrochem.* **2001,** *5* (6), 431-436.
57. Piletsky, S.; Piletska, E.; Bossi, A.; Turner, N.; Turner, A., Surface functionalization of porous polypropylene membranes with polyaniline for protein immobilization. *Biotechnol. Bioeng.* **2003,** *82* (1), 86-92.

58. Barlett, P. N.; Cooper, J. M., A review of the immobilization of enzymes in electropolymerized films. *J. Electroanal. Chem.* **1993,** *362* (1-2), 1-12.
59. Schmid, E. L.; Keller, T. A.; Dienes, Z.; Vogel, H., Reversible Oriented Surface Immobilization of Functional Proteins on Oxide Surfaces. *Anal. Chem.* **1997,** *69* (11), 1979-1985.
60. Hermanson, G. T., *Bioconjugate techniques*. 1996.
61. Nagel, B.; Warsinke, A.; Katterle, M., Enzyme Activity Control by Responsive Redoxpolymers. *Langmuir* **2007,** *23* (12), 6807-6811.
62. Brinkley, M., A brief survey of methods for preparing protein conjugates with dyes, haptens and cross-linking reagents. *Bioconjugate Chem.* **1992,** *3* (1), 2-13.
63. (a) Uchiyama, S.; Tomita, R.; Sekioka, N.; Imaizumi, E.; Hamana, H.; Hagiwara, T., Application of polymaleimidostyrene as a convenient immobilization reagent of enzyme in biosensor. *Bioelectrochemistry* **2006,** *68* (2), 119-125; (b) Billah, M. M.; Hodges, C. S.; Hays, H. C. W.; Millner, P. A., Directed immobilization of reduced antibody fragments onto a novel SAM on gold for myoglobin impedance immunosensing. *Bioelectrochemistry* **2010,** *80* (1), 49-54; (c) Zhang, X.; Sun, G.; Hovestädt, M.; Syritski, V.; Esser, N.; Volkmer, R.; Janietz, S.; Rappich, J.; Hinrichs, K., A new strategy for the preparation of maleimide-functionalised gold surfaces. *Electrochem. Commun.* **2010,** *12* (10), 1403-1406; (d) Lee, C.-Y.; Nguyen, P.-C. T.; Grainger, D. W.; Gamble, L. J.; Castner, D. G., Structure and DNA Hybridization Properties of Mixed Nucleic Acid/Maleimide−Ethylene Glycol Monolayers. *Anal. Chem.* **2007,** *79* (12), 4390-4400; (e) Heggli, M.; Tirelli, N.; Zisch, A.; Hubbell, J. A., Michael-Type Addition as a Tool for Surface Functionalization. *Bioconjugate Chem.* **2003,** *14* (5), 967-973; (f) Ferrero, V. E. V.; Andolfi, L.; Di Nardo, G.; Sadeghi, S. J.; Fantuzzi, A.; Cannistraro, S.; Gilardi, G., Protein and Electrode Engineering for the Covalent Immobilization of P450 BMP on Gold. *Anal. Chem.* **2008,** *80* (22), 8438-8446; (g) Holland, J. T.; Lau, C.; Brozik, S.; Atanassov, P.; Banta, S., Engineering of Glucose Oxidase for Direct Electron Transfer via Site-Specific Gold Nanoparticle Conjugation. *J. Am. Chem. Soc.* **2011,** *133* (48), 19262-19265.
64. (a) Ghosh, S. S.; Kao, P. M.; McCue, A. W.; Chappelle, H. L., Use of maleimide-thiol coupling chemistry for efficient syntheses of oligonucleotide-enzyme conjugate hybridization probes. *Bioconjugate Chem.* **1990,** *1* (1), 71-76; (b) Riederer, I. M.; Herrero, R. M.; Leuba, G.; Riederer, B. M., Serial protein labeling with infrared maleimide dyes to identify cysteine modifications. *J. Proteomics* **2008,** *71* (2), 222-230.
65. (a) Brault, L.; Denance, M.; Banaszak, E.; El Maadidi, S.; Battaglia, E.; Bagrel, D.; Samadi, M., Synthesis and biological evaluation of dialkylsubstituted maleic anhydrides as novel inhibitors of Cdc25 dual specificity phosphatases. *Eur. J. Med. Chem.* **2007,** *42* (2), 243-247; (b) Subasinghe, N.; Schulte, M.; Roon, R. J.; Koerner, J. F.; Johnson, R. L., Quisqualic acid analogs: synthesis of beta-heterocyclic 2-aminopropanoic acid derivatives and their activity at a novel quisqualate-sensitized site. *J. Med. Chem.* **1992,** *35* (24), 4602-4607.
66. Jaegfeldt, H.; Kuwana, T.; Johansson, G., Electrochemical stability of catechols with a pyrene side chain strongly adsorbed on graphite electrodes for catalytic oxidation of dihydronicotinamide adenine dinucleotide. *J. Am. Chem. Soc.* **1983,** *105* (7), 1805-1814.
67. (a) Chidsey, C. E. D.; Bertozzi, C. R.; Putvinski, T. M.; Mujsce, A. M., Coadsorption of ferrocene-terminated and unsubstituted alkanethiols on gold: electroactive self-assembled monolayers. *J. Am. Chem. Soc.* **1990,** *112* (11), 4301-4306; (b) Harper, J. C.; Polsky, R.; Wheeler, D. R.; Brozik, S. M.,

Maleimide-activated aryl diazonium salts for electrode surface functionalization with biological and redox-active molecules. *Langmuir* **2008,** *24* (5), 2206-2211.
68. J. Moulder, W. F. S., P. E. Sobol, and K.D. Bomben, *Handbook of X-ray Photoelectron Spectroscopy*. Perkin Elmer Corporation (Physical Electronics): 1992.
69. Gunasingham, H.; Fleet, B., Comparative study of glassy carbon as an electrode material. *Analyst* **1982,** *107* (1277), 896-902.
70. Wildgoose, G. G.; Abiman, P.; Compton, R. G., Characterising chemical functionality on carbon surfaces. *J. Mater. Chem.* **2009,** *19* (28), 4875-4886.
71. John F. Moulder; Stickle, W. F.; Sobol, P. E.; Bomben, K. D., *Handbook of X-ray Photoelectron Spectroscopy*. Perkin-Elmer Corporation, Physical Electronics Division, Minnesota, USA: 1992.
72. Matsui, M.; Sedyohutomo, A.; Satoh, M.; Abe, Y.; Funabiki, K.; Muramatsu, H.; Shibata, K., Solubility and decomposition temperature of 1,4-bis(arylamino)anthraquinone dyes. *Dyes Pigments* **1999,** *40* (1), 21-26.
73. Boháčová, V.; Dočolomanský, P.; Breier, A.; Gemeiner, P.; Ziegelhöffer, A., Interaction of lactate dehydrogenase with anthraquinone dyes: characterization of ligands for dye–ligand chromatography. *J. Chroma. B* **1998,** *715* (1), 273-281.
74. Routier, S.; Bernier, J. L.; Catteau, J. P.; Riou, J. F.; Bailly, C., Synthesis, DNA binding, topoisomerase II inhibition and cytotoxicity of two guanidine-containing anthracene-9,10-diones. *Anticancer Drug Des* **1998,** *13* (5), 407-15.
75. Sarapuu, A.; Vaik, K.; Schiffrin, D. J.; Tammeveski, K., Electrochemical reduction of oxygen on anthraquinone-modified glassy carbon electrodes in alkaline solution. *J. Electroanal. Chem.* **2003,** *541* (0), 23-29.
76. Kertesz, V.; Whittemore, N. A.; Chambers, J. Q.; McKinney, M. S.; Baker, D. C., Surface titration of DNA-modified gold electrodes with a thiol-tethered anthraquinone. *J. Electroanal. Chem.* **2000,** *493* (1-2), 28-36.
77. (a) Sharpless, K. B.; Lauer, R. F.; Teranishi, A. Y., Electrophilic and nucleophilic organoselenium reagents. New routes to .alpha.,.beta.-unsaturated carbonyl compounds. *J. Am. Chem. Soc.* **1973,** *95* (18), 6137-6139; (b) Numao, N.; Hemmi, H.; Naujokaitis, S. A.; Rabinovitz, M.; Beisler, J. A., Showdomycin analogs: synthesis and antitumor evaluation. *J. Med. Chem.* **1981,** *24* (5), 515-520.
78. Médard, C.; Morin, M., Chemisorption of aromatic thiols onto a glassy carbon surface. *J. Electroanal. Chem.* **2009,** *632* (1-2), 120-126.
79. Jaegfeldt, H.; Torstensson, A. B. C.; Gorton, L. G. O.; Johansson, G., Catalytic oxidation of reduced nicotinamide adenine dinucleotide by graphite electrodes modified with adsorbed aromatics containing catechol functionalities. *Anal. Chem.* **1981,** *53* (13), 1979-1982.
80. Valeur, E.; Bradley, M., Amide bond formation: beyond the myth of coupling reagents. *Chem. Soc. Rev.* **2009,** *38* (2), 606-631.
81. Dreyer, D. R.; Park, S.; Bielawski, C. W.; Ruoff, R. S., The chemistry of graphene oxide. *Chem. Soc. Rev.* **2010,** *39* (1), 228-240.
82. Boehm, H. P.; Diehl, E.; Heck, W.; Sappok, R., Surface Oxides of Carbon. Angew. Chem. Int. Edit. **1964,** *3* (10), 669-677.
83. Evans, J. F.; Kuwana, T., Radiofrequency oxygen plasma treatment of pyrolytic graphite electrode surfaces. *Anal. Chem.* **1977,** *49* (11), 1632-1635.
84. Besenhard, J. O.; Fritz, H. P., The Electrochemistry of Black Carbons. Angew. Chem. Int. Edit **1983,** *22* (12), 950-975.
85. Rocklin, R. D.; Murray, R. W., Chemically modified carbon electrodes: Part XVII. Metallation of immobilized tetra(aminophenyl)porphyrin with manganese,

iron, cobalt, nickel, copper and zinc, and electrochemistry of diprotonated tetraphenylporphyrin. *J.Electroanal. Chem.* **1979,** *100* (1–2), 271-282.
86. Khoshroo, M.; Rostami, A., Electrochemical and impedance spectroscopy studies of various diazonium salts on a glassy carbon electrode. *Monatsh. Chem.* **2010,** *141* (8), 841-846.
87. (a) Léger, C.; Bertrand, P., Direct Electrochemistry of Redox Enzymes as a Tool for Mechanistic Studies. *Chem. Rev.* **2008,** *108* (7), 2379-2438; (b) Strano, M. S.; Dyke, C. A.; Usrey, M. L.; Barone, P. W.; Allen, M. J.; Shan, H.; Kittrell, C.; Hauge, R. H.; Tour, J. M.; Smalley, R. E., Electronic Structure Control of Single-Walled Carbon Nanotube Functionalization. *Science* **2003,** *301* (5639), 1519-1522.
88. (a) Adenier, A.; Cabet-Deliry, E.; Chaussé, A.; Griveau, S.; Mercier, F.; Pinson, J.; Vautrin-Ul, C., Grafting of Nitrophenyl Groups on Carbon and Metallic Surfaces without Electrochemical Induction. *Chem. Mater.* **2005,** *17* (3), 491-501; (b) Barriere, F.; Downard, A. J., Covalent modification of graphitic carbon substrates by non-electrochemical methods. *J. Solid State Electrochem.* **2008,** *12* (10), 1231-1244.
89. Chaki, N. K.; Vijayamohanan, K., Self-assembled monolayers as a tunable platform for biosensor applications. *Biosens. Bioelectron.* **2002,** *17* (1-2), 1-12.
90. Li, J.; Wang, Y.-B.; Qiu, J.-D.; Sun, D.-c.; Xia, X.-H., Biocomposites of covalently linked glucose oxidase on carbon nanotubes for glucose biosensor. *Anal. Bioanal. Chem.* **2005,** *383* (6), 918-922.
91. Liu; Gooding, J. J., An Interface Comprising Molecular Wires and Poly(ethylene glycol) Spacer Units Self-Assembled on Carbon Electrodes for Studies of Protein Electrochemistry. *Langmuir* **2006,** *22* (17), 7421-7430.
92. Noll, T.; Noll, G., Strategies for "wiring" redox-active proteins to electrodes and applications in biosensors, biofuel cells, and nanotechnology. *Chem. Soc. Rev.* **2011,** *40* (7), 3564-3576.
93. Yeh, P.; Kuwana, T., Reversible electrode reaction for cyctochrome c. *Chem. Lett.* **1977,** *6* (10), 1145-1148.
94. Eddowes, M. J.; Hill, H. A. O., Novel method for the investigation of the electrochemistry of metalloproteins: cytochrome c. *J. Chem. Soc., Chem. Commun.* **1977,** (21), 771b-772.
95. (a) Allen, P. M.; Allen, H.; Hill, O.; Walton, N. J., Surface modifiers for the promotion of direct electrochemistry of cytochrome c. *J. Electroanal.Chem.* **1984,** *178* (1), 69-86; (b) Eddowes, M. J.; Hill, H. A. O.; Uosaki, K., Electrochemistry of cytochrome c. Comparison of the electron transfer at a surface-modified gold electrode with that to cytochrome oxidase. *J. Am. Chem. Soc.* **1979,** *101* (23), 7113-7114.
96. Maeda, Y.; Yamamoto, H.; Kitano, H., Self-Assembled Monolayers as Novel Biomembrane Mimetics. 1. Characterization of Cytochrome c Bound to Self-Assembled Monolayers on Silver by Surface-Enhanced Resonance Raman Spectroscopy. *J.Phys. Chem.-US* **1995,** *99* (13), 4837-4841.
97. (a) Niki, K.; Hardy, W. R.; Hill, M. G.; Li, H.; Sprinkle, J. R.; Margoliash, E.; Fujita, K.; Tanimura, R.; Nakamura, N.; Ohno, H.; Richards, J. H.; Gray, H. B., Coupling to Lysine-13 Promotes Electron Tunneling through Carboxylate-Terminated Alkanethiol Self-Assembled Monolayers to Cytochrome c. *The J. Phys. Chem. B* **2003,** *107* (37), 9947-9949; (b) Leopold, M. C.; Bowden, E. F., Influence of Gold Substrate Topography on the Voltammetry of Cytochrome c Adsorbed on Carboxylic Acid Terminated Self-Assembled Monolayers. *Langmuir* **2002,** *18* (6), 2239-2245; (c) El Kasmi, A.; Wallace, J. M.; Bowden, E. F.; Binet, S. M.; Linderman, R. J., Controlling Interfacial Electron-Transfer

Kinetics of Cytochrome c with Mixed Self-Assembled Monolayers. *J. Am. Chem. Soc.* **1998,** *120* (1), 225-226.
98. (a) Wei, J.; Liu, H.; Dick, A. R.; Yamamoto, H.; He, Y.; Waldeck, D. H., Direct Wiring of Cytochrome c's Heme Unit to an Electrode: Electrochemical Studies. *J. Am. Chem. Soc.* **2002,** *124* (32), 9591-9599; (b) Wei, J. J.; Liu, H.; Niki, K.; Margoliash, E.; Waldeck, D. H., Probing Electron Tunneling Pathways Electrochemical Study of Rat Heart Cytochrome c and Its Mutant on Pyridine-Terminated SAMs. *J.Phys.Chem. B* **2004,** *108* (43), 16912-16917; (c) Wei, J.; Liu, H.; Khoshtariya, D. E.; Yamamoto, H.; Dick, A.; Waldeck, D. H., Electron-Transfer Dynamics of Cytochrome C: A Change in the Reaction Mechanism with Distance. *Angew. Chem. Int. Ed.* **2002,** *41* (24), 4700-4703.
99. Nakano, K.; Yoshitake, T.; Yamashita, Y.; Bowden, E. F., Cytochrome c Self-Assembly on Alkanethiol Monolayer Electrodes as Characterized by AFM, IR, QCM, and Direct Electrochemistry. *Langmuir* **2007,** *23* (11), 6270-6275.
100. Liu, M.; Qi, Y.; Zhao, G., Carboxyphenyl Covalent Immobilization of Heme Proteins and its Favorable Biocompatible Electrochemical and Electrocatalytic Characteristics. *Electroanalysis* **2008,** *20* (8), 900-906.
101. (a) Bartlett, P. N.; Farington, J., The electrochemistry of cytochrome c at a conducting polymer electrode. *J. Electroanal. Chem.* **1989,** *261* (2B), 471-475; (b) Kim, H.-J.; Lee, K.-S.; Won, M.-S.; Shim, Y.-B., Characterization of protein-attached conducting polymer monolayer. *Langmuir* **2008,** *24* (3), 1087-1093.
102. Baker, S. E.; Colavita, P. E.; Tse, K.-Y.; Hamers, R. J., Functionalized Vertically Aligned Carbon Nanofibers as Scaffolds for Immobilization and Electrochemical Detection of Redox-Active Proteins. *Chem. Mater.* **2006,** *18* (18), 4415-4422.
103. (a) Dolidze, T. D.; Rondinini, S.; Vertova, A.; Waldeck, D. H.; Khoshtariya, D. E., Impact of self-assembly composition on the alternate interfacial electron transfer for electrostatically immobilized cytochrome c. *Biopolymers* **2007,** *87* (1), 68-73; (b) Arnold, S.; Feng, Z. Q.; Kakiuchi, T.; Knoll, W.; Niki, K., Investigation of the electrode reaction of cytochrome c through mixed self-assembled monolayers of alkanethiols on gold(111) surfaces. *J. Electroanal. Chem.* **1997,** *438* (12), 91-97; (c) Yue, H.; Waldeck, D. H.; Schrock, K.; Kirby, D.; Knorr, K.; Switzer, S.; Rosmus, J.; Clark, R. A., Multiple Sites for Electron Tunneling between Cytochrome c and Mixed Self-Assembled Monolayers. *The J. Phys. Chem. C* **2008,** *112* (7), 2514-2521.
104. Ge, B.; Lisdat, F., Superoxide sensor based on cytochrome c immobilized on mixed-thiol SAM with a new calibration method. *Anal. Chim. Acta* **2002,** *454* (1), 53-64.
105. Chen, X.; Ferrigno, R.; Yang, J.; Whitesides, G. M., Redox Properties of Cytochrome c Adsorbed on Self-Assembled Monolayers: A Probe for Protein Conformation and Orientation. *Langmuir* **2002,** *18* (18), 7009-7015.
106. (a) Allen, P. M.; Hill, H. A. O.; Walton, N. J., Surface modifiers for the promotion of direct electrochemistry of cytochrome c. *J. Electroanal. Chem.* **1984,** *178* (1), 69-86; (b) Ion, A.; Banica, F. G., Direct electrochemistry of bovine heart cytochrome c facilitated by cysteine derivatives and analogues. Some effects of facilitator structure. *J. Solid State Electr.* **2001,** *5* (6), 431-436; (c) Eddowes, M. J.; Hill, H. A. O., Electrochemistry of horse heart cytochrome c. *J. Am. Chem.Soc.* **1979,** *101* (16), 4461-4464; (d) Pardo-Yissar, V.; Katz, E.; Willner, I.; Kotlyar, A. B.; Sanders, C.; Lill, H., Biomaterial engineered electrodes for bioelectronics. *Faraday Discuss.* **2000,** *116*, 119-134.
107. (a) Hunnes, C. H., Isolation, purification, and characterization of bovine heart and yeast cytochromes c - An integrated biochemistry laboratory experience. *Biochem. Mol. Biol. Educ.* **2003,** *31* (4), 242-248; (b) Margoliash, E.;

Walasek, O. F., [61] Cytochrome c from vertebrate and invertebrate sources. In *Methods in Enzymology*, Ronald W. Estabrook, M. E. P., Ed. Academic Press: 1967; Vol. Volume 10, pp 339-348; (c) Brautigan, D. L.; Ferguson-Miller, S.; Margoliash, E., [18] Mitochondrial cytochrome c: Preparation and activity of native and chemically modified cytochromes c. In *Methods in Enzymology*, Sidney, F.; Lester, P., Eds. Academic Press: 1978; Vol. Volume 53, pp 128-164; (d) Mirkin, N.; Jaconcic, J.; Stojanoff, V.; Moreno, A., High resolution X-ray crystallographic structure of bovine heart cytochrome c and its application to the design of an electron transfer biosensor. *Proteins* **2008,** *70* (1), 83-92.
108. Eddowes, M. J.; Hill, H. A. O., Novel method of electrochemistry of metalloproteins - cytochrome c. *J. Chem. Soc.-Chem. Commun.* **1977,** (21), 771-772.
109. Quelever, G.; Kachidian, P.; Melon, C.; Garino, C.; Laras, Y.; Pietrancosta, N.; Sheha, M.; Louis Kraus, J., Enhanced delivery of [gamma]-secretase inhibitor DAPT into the brain via an ascorbic acid mediated strategy. *Org. Biomol. Chem.* **2005,** *3* (13), 2450-2457.
110. Degani, Y.; Heller, A., Direct electrical communication between chemically modified enzymes and metal electrodes. I. Electron transfer from glucose oxidase to metal electrodes via electron relays, bound covalently to the enzyme. *J.Phys. Chem.* **1987,** *91* (6), 1285-1289.
111. Mayo, S.; Ellis, W.; Crutchley, R.; Gray, H., Long-range electron transfer in heme proteins. *Science* **1986,** *233* (4767), 948-952.
112. (a) Yaropolov AI, S. T., Karyakin AA, Varfolomeev SD, Berezin IV, Possibility of electron tunneling transfer during enzymic catalysis of electrode processes. *Dokl Akad Nauk SSSR* **1981,** *260*, 1192-1195; (b) Kulys, J. J.; Samalius, A. S., Dependence of the efficiency of bioelectrocatalytic processes on the electrode surface state. *Bioelectrochem. Bioenerg.* **1984,** *13* (1-3), 163-169.
113. Ogura, Y., Studies on the glucose dehydrogenase of aspergillus oryzae. *J. Biochem.* **1951,** *38* (1), 75-84.
114. Sode, K.; Tsugawa, W.; Yamazaki, T.; Watanabe, M.; Ogasawara, N.; Tanaka, M., A novel thermostable glucose dehydrogenase varying temperature properties by altering its quaternary structures. *Enzyme Microb. Technol.* **1996,** *19* (2), 82-85.
115. Sygmund, C.; Klausberger, M.; Felice, A. K.; Ludwig, R., Reduction of quinones and phenoxy radicals by extracellular glucose dehydrogenase from Glomerella cingulata suggests a role in plant pathogenicity. *Microbiology-Sgm* **2011,** *157*, 3203-3212.
116. Zafar, M.; Beden, N.; Leech, D.; Sygmund, C.; Ludwig, R.; Gorton, L., Characterization of different FAD-dependent glucose dehydrogenases for possible use in glucose-based biosensors and biofuel cells. *Anal. Bioanal. Chem.* **2012,** *402* (6), 2069-2077.
117. Sygmund, C.; Staudigl, P.; Klausberger, M.; Pinotsis, N.; Djinovic-Carugo, K.; Gorton, L.; Haltrich, D.; Ludwig, R., Heterologous overexpression of Glomerella cingulata FAD-dependent glucose dehydrogenase in Escherichia coli and Pichia pastoris. *Microb. Cell Fact.* **2011,** *10*.
118. Wang, S. C.; Yang, F.; Silva, M.; Zarow, A.; Wang, Y. B.; Iqbal, Z., Membrane-less and mediator-free enzymatic biofuel cell using carbon nanotube/porous silicon electrodes. *Electrochem. Comm.* **2009,** *11* (1), 34-37.
119. Heller, A., Electrical wiring of redox enzymes. *Acc. Chem. Res.* **1990,** *23* (5), 128-134.

120. Guo, L.-H.; Allen, H.; Hill, O., Direct Electrochemistry of Proteins and Enzymes. In *Adv. Inorg. Chem.*, Sykes, A. G., Ed. Academic Press: 1991; Vol. Volume 36, pp 341-375.
121. Willner, I.; Katz, E., Integration of Layered Redox Proteins and Conductive Supports for Bioelectronic Applications. *Angew. Chem. Int. Ed.* **2000,** *39* (7), 1180-1218.
122. Bard, A. J. F., L.R. , *Electrochemical Methods: Fundamentals and Applications.* . John Wiley and Sons: New York, 1980.
123. Bartlett, P., *Bioelectrochemistry: Fundamentals, Experimental Techniques and Applications*. Wiley: Chichester, 2008.
124. Zafar, M. N.; Wang, X. J.; Sygmund, C.; Ludwig, R.; Leech, D.; Gorton, L., Electron-Transfer Studies with a New Flavin Adenine Dinucleotide Dependent Glucose Dehydrogenase and Osmium Polymers of Different Redox Potentials. *Anal. Chem.* **2012,** *84* (1), 334-341.
125. Pearson, R. J.; Kassianidis, E.; Slawin, A. M. Z.; Philp, D., Self-replication vs. reactive binary complexes - manipulating recognition-mediated cycloadditions by simple structural modifications. *Org. Biomol. Chem.* **2004,** *2* (23), 3434-3441.
126. Cowie, R. M.; Turega, S. M.; Philp, D., Probing the limits of rate acceleration mediated by hydrogen bonds. *Org. Lett.* **2006,** *8*, 5179-5182.
127. Lee, J.; Lee, J.; Kang, M.; Shin, M.; Kim, J.-M.; Kang, S.-U.; Lim, J.-O.; Choi, H.-K.; Suh, Y.-G.; Park, H.-G.; Oh, U.; Kim, H.-D.; Park, Y.-H.; Ha, H.-J.; Kim, Y.-H.; Toth, A.; Wang, Y.; Tran, R.; Pearce, L. V.; Lundberg, D. J.; Blumberg, P. M., N-(3-Acyloxy-2-benzylpropyl)-N'-[4-(methylsulfonylamino)benzyl]thiourea Analogues: Novel Potent and High Affinity Antagonists and Partial Antagonists of the Vanilloid Receptor. *J. Med. Chem.* **2003,** *46* (14), 3116-3126.
128. Buchini, S.; Buschiazzo, A.; Withers, S. G., A New Generation of Specific Trypanosoma cruzi trans-Sialidase Inhibitors. *Angew. Chem. Int. Ed.* **2008,** *47* (14), 2700-2703.
129. Hunnes, C. H., Isolation, purification, and characterization of bovine heart and yeast cytochromes c: An integrated biochemistry laboratory experience. *Biochem. Mol. Bio. Edu.* **2003,** *31* (4), 242-248.